AD NUMBER

ADB308065

LIMITATION CHANGES

TO:

Approved for public release; distribution is unlimited.

FROM:

Distribution authorized to DoD and DoD contractors only; Administrative/Operational Use; NOV 2004. Other requests shall be referred to US Army Engineer Research and Development Center, Cold Regions Research and Engineering Laboratory, 72 Lyme Road, Hanover, NH 03755-1290.

AUTHORITY

ERDC/COE/CRREL ltr dtd 3 Mar 2015

ERDC/CRREL TR-04-23

Cold Regions Research and Engineering Laboratory

US Army Corps of Engineers®
Engineer Research and Development Center

Underground UXO: Are They a Significant Source of Explosives in Soil Compared to Low- and High-Order Detonations?

Susan Taylor, James Lever, Michael Walsh, Marianne E. Walsh, Benjamin Bostick, and Bonnie Packer

December 2004

ERDC/CRREL TR-04-23
December 2004

Underground UXO: Are They a Significant Source of Explosives in Soil Compared to Low- and High-Order Detonations?

Susan Taylor, James Lever, Michael Walsh, Marianne E. Walsh

Cold Regions Research and Engineering Laboratory
U.S. Army Engineer Research and Development Center
72 Lyme Road
Hanover, NH 03755

Benjamin Bostick

Earth Science Department
Dartmouth College
Hanover, New Hampshire 03755

Bonnie Packer

U.S. Army Environmental Center
Aberdeen Proving Ground, Maryland 20101-5401

Final report

Prepared for U.S. Army Environmental Center

ABSTRACT

Are the amounts of explosives leaking from UXO significant compared to other sources? To answer this question, data were compiled on the contamination released by above ground detonations of different order and by the rupture or corrosion of UXO. The results indicate that low-order detonations, be they from malfunctioning munitions or sympathetic detonations, are currently the largest contributors to range contamination. Also, dissolution of the explosive charge from heavily corroded UXO is significant and will increase in importance with time. Unfortunately, only order-of-magnitude estimates are possible due to shortage of data on the actual fates experienced by different types of munitions. However, the framework used here for compiling and ranking the explosive sources can help guide policy-making and future research activity to reduce range contamination.

CONTENTS

ILLUSTRATIONS

TABLES

CONVERSION FACTORS, NON-SI TO SI UNITS OF MEASUREMENT

Non-SI units of measurement used in this report can be converted to SI units as follows:

Multiply	By	To obtain
acres	4,046.873	square meters
acres	0.4046873	hectare (10,000 m^2)
feet	0.3048	meters
feet per second	0.3048	meters per second
inches	0.0254	meters
pounds (mass)	0.4535924	kilograms

PREFACE

This report was prepared by Dr. Susan Taylor, Research Physical Scientist, Environmental Sciences Branch, Dr. James Lever, Mechanical Engineer, Applied Military Engineering Branch, Michael Walsh, Mechanical Engineer, Engineering Resources Branch, Marianne E. Walsh, Chemical Engineer, Environmental Sciences Branch, Cold Regions Research and Engineering Laboratory, Benjamin Bostick, Assistant Professor, Earth Science Department, Dartmouth College, and Bonnie Packer, Research Scientist, U.S. Army Environmental Center.

The authors thank the U.S. Army Environmental Center for funding this work. To help us determine the relative importance of UXO as a contaminant source, we obtained important information from Jay Clausen (AMEC), Roger Young (USACE, Huntsville), Travis Boyer (CTC), Lisa Greenfeld (AEC), Philip Thorne (ARA) and Peter Keene, Dr. Thomas Jenkins and Alan Hewitt (CRREL). We thank them for their contribution to this report. We thank Dr. David Ringelberg and Laura Perovich, from CRREL for helpful comments on the manuscript and Dr. Clarence Grant, Philip Thorne and Martin Stutz for reviewing and suggesting improvements to this document. We also thank Jane Mason and Mark Hardenberg for their help illustrating and editing the report.

This report was prepared under the general supervision of Dr. J-C. Tatinclaux, Chief, Environmental Sciences Branch; Dr. Lance Hansen, Deputy Director, and James Wuebben, Acting Director, CRREL.

The Commander and Executive Director of the Engineer Research and Development Center is COL James R. Rowen, EN. The Director is Dr. James R. Houston.

EXECUTIVE SUMMARY

A fired munition will experience one of many possible fates. Generally, it will detonate as intended. However, it is also possible that it will go low-order or be a dud. A dud might penetrate the ground or come to rest on the surface. Whether on the surface or underground, unexploded ordnance (UXO) will suffer one of the following fates: it can be intentionally blown-in-place, a round exploding nearby could detonate it sympathetically, the casing might be split during the initial impact or by nearby detonations, or the shell can remain intact and corrode over time. UXO pose two types of risk: the risk of detonation if the round is moved or stepped on, and the risk of leaking explosives into the environment if the round is not removed and disposed of properly. This report focuses on the environmental hazard.

The physical and chemical breakdown of UXO is a potentially important source of explosives to the environment. The rate, extent, and hazard potential of UXO breakdown depend in part on how the casings corrode in soil. It is, therefore, important to understand the mechanism by which corrosion occurs in soil systems. Here, we present an overview of metal corrosion with special focus on the corrosion of UXO related materials. Overall, we find that corrosion of low-carbon steel, the most commonly used steel in UXO, probably occurs at about 0.025 mm per year. Interestingly, variations in corrosion rate attributable to soil chemical conditions and the casing alloy are within a factor of 5. This suggests that most UXO, which have a minimum wall thickness between 2 and 10 mm, will corrode within 80 to 400 years under normal aerated soil conditions. Under reducing conditions similar to those encountered in wetlands and other anaerobic and flooded environments, sulfide production accelerates corrosion by about a factor of 10 (with considerable variability), resulting in perforation of the round after approximately 10–40 years. Pit corrosion is also common in soil environments and often results in much deeper, though much smaller, surface corrosion. Further refinement of the rate of UXO corrosion is not possible given the variability in soil chemical parameters, including pH, dissolved solute concentration, and biological activity. Nevertheless, these data suggest that corrosion has already caused some leakage of explosives from munitions and that leakage will increase significantly over the next 100 years.

Are the amounts of explosives leaking from UXO significant compared to other sources? To answer this question, we compiled data on the contamination released by above-ground detonations of different order and by the rupture or corrosion of UXO. The results indicate that low-order detonations, be they from malfunctioning munitions or sympathetic detonations, are currently the largest contributors to range contamination. Also, dissolution of the explosive charge

from heavily corroded UXO is significant and will increase in importance with time. Unfortunately, only order-of-magnitude estimates are possible owing to a shortage of data on the actual fates experienced by different types of munitions. However, the framework used here for compiling and ranking the explosive sources can help guide policy-making and future research activity to reduce range contamination.

LIST OF ABBREVIATIONS AND DEFINITIONS

AEC	U.S. Army Environmental Center.
ASRP	Ammunition Stockpile Reliability Program.
BIP	Blow-in-Place, an operation where EOD personnel destroyed one or more munitions. Munitions are blown-in-place when they have been damaged, are out of date, or are UXO that are dangerous to move. Generally, a block of C4 is strapped to the round and initiated electronically.
BRAC	Base Realignment and Closure Act.
C4	Mixture of 90% RDX (cyclonite, cyclotrimethylene trinitramine) and a binder (often polyisobutylene or dioctyl adipate), a plasticizer [di(2-ethylhexyl) or dioctyl sebacate], and petroleum oil.
Composition A5	Wax-coated, granular explosive consisting of RDX and plasticizing wax, mixed with 1.5% stearic acid.
Composition B	60–39 mixture of RDX and TNT that contains ~1% wax.
CRREL	Cold Regions Research and Engineering Laboratory.
DoD	Department of Defense.
DODIC Number	Department of Defense identification code designation for the munition type.
Dud (UXO)	Round that is fired but which completely fails to detonate at the target. Upon impact a dud can penetrate the ground or come to rest on the soil surface. During this process it either remains intact or breaks open.
EOD	Explosive ordnance disposal.
ERF	Eagle River Flats, a salt water marsh that is the impact area for Fort Richardson, Alaska.
ESTCP	Environmental Security Technology Certification Program.
HE	High explosive.
High-order	(HO) detonation: a term that refers to a munition that has high yield—the explosive filler generated a shock wave that travels at supersonic velocities.
HUTA	High use training area at MMR.
Frag.	Contraction for ordnance fragment.
FUDS	Formerly Used Defense Sites.
HMX	High explosive, octahydro-1,3,5,7-tetranitro-1,3,5,7-tetrazocine, used in octol (a 70–30,TNT–HMX mixture) often found as a bi-product of RDX production.

Live Fire	Tactically detonated munition, one that was detonated via the designed detonation chain: fuze, booster, main HE round.
Low-order	(LO) detonation (partial detonation): one where only a part of the explosive detonates. Generally, large fragments of shell casing and particles of explosives are scattered close to where the shell detonated. Some of the original explosive charge might remain in the shell.
MIDAS	Munitions Items Disposition Action System database.
MMR	Massachusetts Military Reservation.
NG	Nitroglycerine.
Octol	High explosive made of 70% HMX and 30% TNT, used mainly in rockets.
Passivation	Blocking of the metal surface by a non-reactive species, often through the formation of an insoluble metal oxide film that protects the metal surface from oxidants in solution.
ppm	Parts per million, mg/L, mg/kg.
ppb	Parts per billion, µg/L, µg/kg.
Propellants	Explosive charge used for propelling a projectile:
Single base	Nitrocellulose.
Double base	Nitrocellulose with nitroglycerine.
Triple base	Nitrocellulose, nitroglycerine and nitroguanidine.
RDX	High energy explosive, Hexahydro-1,3,5- trinitro-1,3,5-triazine.
SERDP	Strategic Environmental Research and Development Program.
TNT	2,4,6-trinitrotoluene, a high energy explosive.
UXO	Unexploded Explosive Ordnance, defined as an “explosive ordnance which has been primed, fuzed, armed, or otherwise prepared for action, and which has been fired, dropped, launched, projected, or placed in such a manner as to constitute a hazard to operations, installations, personnel, or materiel, and remains unexploded either by malfunction or design or for any other cause” (GPO 1989).
2,4-DNT/2,6-DNT	2,4- and 2,6-dinitrotoluene; two of six possible dinitrotoluenes, impurities in the making of TNT. The DNTs are used as propellants.
2A-DNT/4A -DNT	two different amino dinitrotoluenes that are breakdown products of TNT.

Underground UXO: Are They a Significant Source of Explosives in Soil Compared to Low- and High-Order Detonations?

SUSAN TAYLOR, JAMES LEVER, MICHAEL WALSH, MARIANNE E. WALSH, BENJAMIN BOSTICK, AND BONNIE PACKER

1 INTRODUCTION

The 1998 Defense Science Board report estimated that 1500 different sites, encompassing 15 million acres of land, contain Department of Defense (DoD) Unexploded Ordinance (UXO) (Foster 1998). Unexploded Ordnance (UXO) pose two types of risk: the risk of detonation if the round is moved or stepped on, and the risk of leaking explosives into the environment if the round is not removed and disposed of properly. Here, we address the second risk, environmental contamination.

UXO are composed of high explosives (e.g., RDX, TNT, HMX, Tetryl), a metallic casing, and lesser quantities of fuze materials. While the metallic casing is not hazardous to human health, the fill components each have their own characteristic toxicity, temperature-dependant solubility, and propensity for sorption, and, thus, differing potentials to impact surface water and groundwater quality.

Corrosion of the casing exposes the high explosive (HE) in UXO to dissolution by water moving through the soil. Previous studies have found that UXO buried in soil corrode at rates that depend on site- and munition-specific factors, including soil type and composition of the casing. Estimates for corrosion breakthrough vary from 10 years to several thousand years. The rates of corrosion are needed to predict the time scales over which HE will be released into the environment.

In this report we evaluate the rate of high explosive released from corroded UXO in comparison to that released by detonations or ruptured rounds. We begin by briefly summarizing UXO and explosive-contamination issues on training ranges and describe the properties of the most commonly manufactured munitions. Because UXO in the U.S. results primarily from live-fire testing and train-

ing, we focused on Army impact ranges. The plethora of different munitions and changes in munitions through time also necessitated that we focus our attention on types with production rates exceeding half a million rounds a year: 40-mm grenades, 60-mm, 81-mm, 4.2-in. and 120-mm mortars, 105-mm, 155-mm and 8-in. howitzer rounds.

The report then describes what is known about the fate of a round after it is fired. Generally, a round will detonate as intended. However, it might also undergo a low-order (incomplete) detonation or be a dud. These duds can penetrate the ground to some depth or come to rest on the surface. Whether on the surface or underground, the resulting UXO might be blown-in-place, detonated sympathetically, split open or left to corrode. The rate of HE released into the environment depends on the fate. Because the majority of UXO corrode in place, we have summarized what is known about corrosion in soil and its dependence on soil properties and climate. As dissolution of explosives precedes transport, we then summarize what is known about the dissolution of different HE particle masses. Using estimates of the HE contamination released from a munition experiencing a particular fate, the probability that it will experience that fate, and its dissolution rate, we have made order-of-magnitude estimates of which fates release the most HE into the environment. Although only order-of-magnitude estimates are possible, the framework used here for compiling and ranking the explosive sources can help guide policy-making and future research activity to reduce range contamination.

Lack of data necessitated that we focus on estimating average HE release rates across all U.S. Army training sites. Consequently, this report does not address site-specific range-management issues or the release rates of specific HE, such as TNT and Comp B. We also did not address HE transport processes or releases from heavy metals in UXO.

2 TRAINING RANGES

Training ranges provide soldiers the opportunity to practice using a variety of weapons and munitions. However, as a result of training, explosive residues from high-order detonations (HO), low-order detonations (LO—where a significant fraction of the explosive remains undetonated), and UXO may contaminate the soil and the groundwater, and consequently pose environmental and human health risks. The amount of explosive remaining after a detonation depends on the type of munition, its HE fill, its casing, and how the detonation was initiated and proceeded.

According to the data compiled by the Army Environmental Center (AEC) in their Active/Inactive Range Inventory, there are 66 active Army installations, which together cover 16.7 million acres of land (Fig. 1 and Table 1). The impact areas at these installations cover 1.36 million acres (Table 1). These data do not include impact areas on closed Army installations or those belonging to the other service branches. The impact areas vary in terms of their size, the intensity and types of training conducted on them, their climate, soil type, and underlying geology. UXO are generally found in the impact areas but have also been found outside these areas.

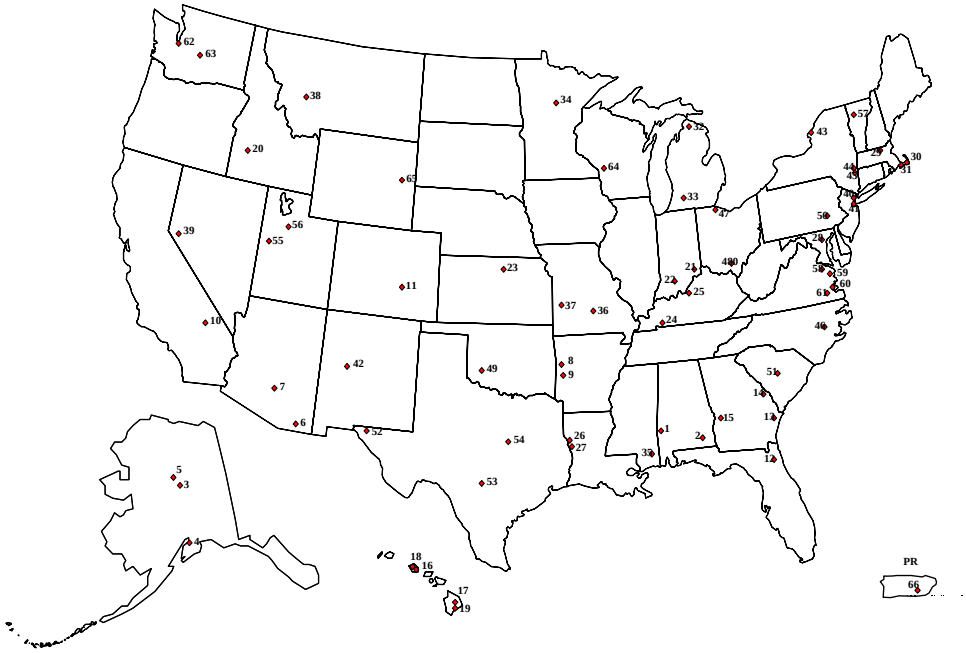

Figure 1. Locations of Army installations in the U.S.

Table 1. Army Installations (Army, National Guard, Army Reserve) that have impact areas. The states of Connecticut, Delaware, Illinois, Iowa, Maine, Nebraska, New Hampshire, Oregon, Rhode Island, South Dakota, Tennessee, West Virginia, and the District of Columbia have no listed impact areas.

State	Map number	Installation type	Size (ha)	Size (acres)	Number dud areas	Dud areas (ha)	Dud areas (acres)
Alabama	1	A	8,961	22142	2	1,514	3,741
	2	A	23,571	58244	1	1,219	3,013
Alaska	3	A	255,622	631642	4	25,552	63,138
	4	A	22,072	54541	1	1,005	2,483
	5	A	373,367	922589	4	21,060	52,040
Arizona	6	A	29,928	73953	1	2,690	6,646
	7	A	10,344	25559	1	1,512	3,735
Arkansas	8	NG	25,706	63519	1	2,444	6,039
	9	NG	12,480	30837	1	507	1,252
California	10	A	237,761	587508	7	52,441	129,582
Colorado	11	A	55,631	137463	1	6,318	15,611
Florida	12	NG	27,786	68658	1	5,910	14,603
Georgia	13	A	68,308	168788	8	6,501	16,063
	14	A	19,973	49353	3	1,573	3,887
	15	A	110,942	274137	1	4,936	12,197
Hawaii	16	A	176	434	1	23	56
	17	A	1,711	4227	1	1,391	3,436
	18	A	44,496	109950	1	18,553	45,845
	19	A	4,630	11441	1	1,836	4,537
Idaho	20	A	55,962	138283	1	1,349	3,334
Indiana	21	NG	12,905	31889	2	1,434	3,543
	22	A	425	1050	2	425	1,050
Kansas	23	A	37,499	92660	2	6,144	15,183
Kentucky	24	A	38,182	94348	4	9,025	22,301
	25	A	41,126	101623	10	16,720	41,315
Louisiana	26	A	56,146	138737	10	4,588	11,338
	27	A	13,539	33456	3	2,332	5,763
Maryland	28	A	26,002	64250	3	20,505	50,667
Massachusetts	31	A	7,185	17755	2	6	15
	30	NG	5,376	13285	1	895	2,211
	29	AR	1,857	4588	1	272	671

State	Map num-ber	Installation type	Size (ha)	Size (acres)	Num-ber dud areas	Dud areas (ha)	Dud areas (acres)
Michigan	32	NG	58,642	144904	2	3,222	7,961
	33	A	3,030	7487	1	1,032	2,550
Minnesota	34	NG	20,611	50929	3	2,500	6,178
Mississippi	35	NG	54,145	133793	1	1,890	4,669
Missouri	36	A	21,652	53502	2	3,692	9,122
	37	NG	403	997	1	21	52
Montana	38	A	7,738	19120	2	221	546
Nevada	39	A	14,484	35789	2	2,021	4,995
New Jersey	40	AR	11,332	28001	1	835	2,064
	41	A	49	120	1	7	18
New Mexico	42	A	1,848,435	4567483	3	18,334	45,303
		A					
New York	43	A	39,872	98524	1	8,204	20,271
	44	NG	713	1763	2	93	230
	45						
North Carolina	46	A	58,112	143594	4	12,137	29,990
Ohio	47	NG	139	343	1	0	0.08
	48	A	174	430	1	8	21
Oklahoma	49	A	34,400	85002	3	14,113	34,872
Pennsylvania	50	NG	6,046	14939	1	537	1,328
South Carolina	51	A	11,951	29532	1	2,209	5,459
Texas	52	A	443,607	1096153	11	166,717	411,957
	53	A	11,112	27457	1	2,253	5,566
	54	A	80,841	199758	2	5,684	14,044
Utah	55	A	308,820	763093	3	67,584	167,001
	56	NG	10,117	25000	4	2,712	6,701
Vermont	57	NG	4,347	10742	2	233	576
Virginia	58	A	881	2178	1	6	16
	59	A	30,607	75629	16	894	2,209
	60	A	1,398	3454	1	442	1,092
	61	NG	15,742	38899	1	609	1,505
Washington	62	A	31,395	77577	1	693	1,713
	63	A	131,242	324298	2	7,220	17,841
Wisconsin	64	AR	54,877	135601	1	2,943	7,273
Wyoming	65	NG	14,189	35062	2	1,044	2,580
Puerto Rico	66	A	4,874	12044	1	582	1,438

The Army has no uniform policy for clearing ranges. Surface UXO on paths to targets are often blown-in-place but sub-surface UXO or the HE residues released from training activities are generally not removed. Contamination from training activities has been documented in at least two cases: a wetland impact area at Eagle River Flats, Alaska, contained white phosphorous (WP), and RDX was found in the sole aquifer on Cape Cod beneath the Massachusetts Military Reservation (MMR). These instances have heightened public concern about military activities that could impact human health and the environment. At Eagle River Flats, white phosphorus rounds are banned and only wintertime firing onto a solid ice sheet is allowed. Temporary draining and drying of WP-containing sediments of the wetland are underway as the process accelerates the oxidation of the white phosphorus to phosphates. By comparison, MMR has been closed to training.

Because the types of training conducted at MMR are similar to those conducted on other ranges (Clausen et al. 2004), the soil HE residues and groundwater contamination found there illustrate the types of problems that could develop, or be present, at other ranges. Since its closure in 1997, MMR has been extensively studied. The data gathered there form much of the useful information about UXO that is presented throughout this report. Many of these data have not yet been published (AMEX, in review). The work done at MMR also illustrates the difficulties in characterizing and cleaning up ranges.

Massachusetts Military Reservation is a 8500-ha (21,000-acre) installation. The training ranges and central impact area cover about 5700 ha (14,000 acres) and are located on part of the installation known as Camp Edwards. After small concentrations of RDX were found in groundwater, studies were begun to determine the source or sources of the RDX. Three areas were found to be the mostly likely sources for the groundwater RDX plume: the central impact area, demolition 1 (Demo 1) area, and the southeast ranges.

The central impact area, approximately 810-ha (2200 acres) encompasses artillery and mortar targets and is surrounded by artillery and mortar firing points. Demo 1 is a 64- × 64-m (1 acre) depression where munitions were burned or detonated. Clausen et al. (2004) reported seeing chunks of C4, used to detonate munitions, on the ground at Demo 1, indicating that not all detonations were high-order. The highest concentrations of RDX—14,000 mg/kg—were found near a large intact fragment of C4 explosive. The southeast ranges are four separate ranges, J1, J2, J3, and L, which total 132-ha (329 acres) and were used for a variety of purposes. The J1 range was used to test weapons and as an antitank range. The J2 range was used as a rifle and musket range as well as a contractor

test range. The J3 range was used for mortar and machine gun practice and for a variety of munition tests. Ordnance and explosives were tested on the L range.

To date the following samples have been collected at MMR: 7833 surface soil samples from 1989 locations, 1533 soil cores from 146 places, 69 sediment samples and 64 water samples from 19 water bodies, 1467 groundwater samples and 3959 groundwater profile samples from 256 locations (Clausen et al. 2004). On the impact area, soil samples indicate that the explosive concentrations decrease rapidly with distance from the targets and with depth in the soil, a finding seen at other ranges (Jenkins et al. 1996, 1997; Thiboutot et al. 1998). Figure 2 shows the explosive, pyrotechnic, and propellant compounds found in the impact range soil samples. The acidic nature and low organic content of the soils limit biodegradation and the low clay content and low cation exchange capacity decrease sorption of explosives onto soils. It is, therefore, not surprising that RDX, HMX, and 2A-DNT and 4A-DNT, the transformation products of TNT, make up the bulk of the explosives found in the groundwater (Fig. 3) (AMEX, in review).

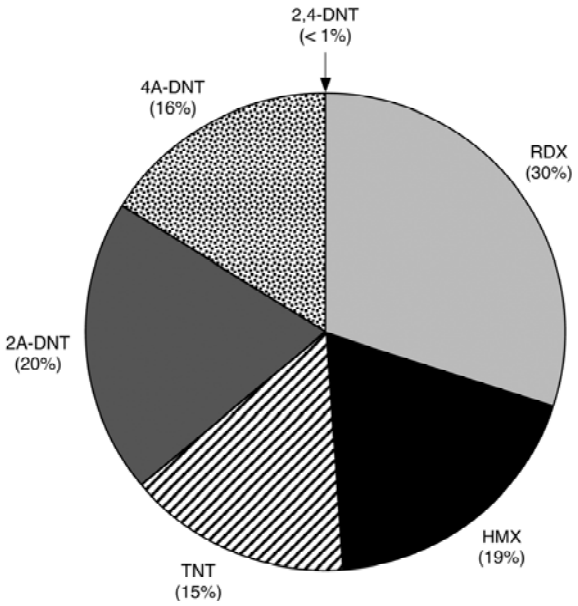

Figure 2. Concentration of explosives, pyrotechnics and propellants in the impact range soils at Massachusetts Military Range.

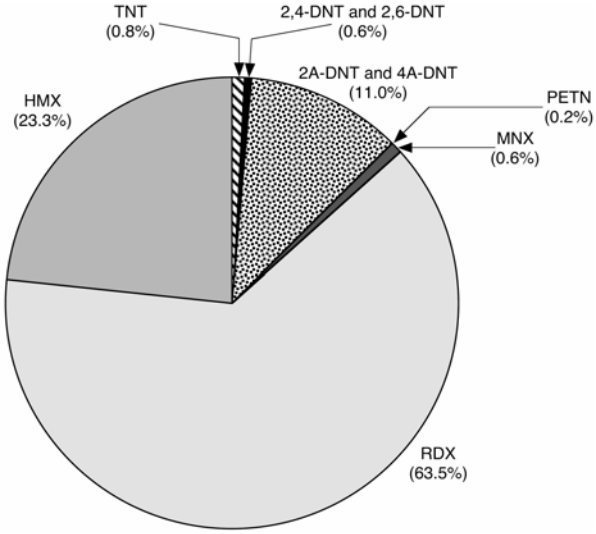

Figure 3. Concentration of explosives, pyrotechnics and propellants in the groundwater below the impact range at Massachusetts Military Range.

Six years of work have not found a specific source, such as an ammunition dump, for the aforementioned groundwater contamination. Based on the low levels of RDX in the groundwater, the contamination is thought to come from a nonspecific source. The flux of RDX to the aquifer also appears to be fairly constant. The size and movement of the RDX groundwater plume suggests that RDX has been migrating to the groundwater for the past 60 years and, because the rate appears constant, that the sources of RDX are still present (AMEX, in review). The plume emanating from the impact area is estimated at 3353 m (11,000 ft) long by 1524 m (5000 ft) wide suggesting that 3.3 ×109 to 4.9 × 1012 L (880 million to 1.3 billion gal.) of water are contaminated. The amount of RDX needed to contaminate this volume to the measured concentrations is 14 to 36 kg (30 to 80 lb) (AMEX, in review). Work by Tetra Tech (2002) concluded that intact UXO are not currently a major source of contamination at MMR.

The work at MMR shows the high expense and effort needed to characterize a range, let alone clean it up. The costs of removing UXO in formerly used defense sites (FUDS) and from base realignment and closure projects (BRAC) are unknown but estimated at between $14 and $60 billion (Delaney and Etter 2003). These estimates are for removing UXO from 1400 sites on 10 million acres.

3 MUNITIONS MOST COMMONLY USED BY THE ARMY

Records on the manufacture and production of the various HE rounds used by the Army are fairly complete since the 1960s and almost nonexistent prior to the 1940s. Each of the rounds that had total production runs greater than 3.9-million, as well as 120-mm mortars, are listed in Table 2. As technology and manufacturing methods evolved, variations on the rounds were developed, requiring different designations. These are listed under type in Table 2. Descriptions of each munition type can be found in the MIDAS database using the DODIC numbers given in Table 2. The specifications for these munitions were taken from Army Technical Manuals 43-0001-28 and 30 (U.S. Army 1981, 1994).

Table 2. Munitions produced and their characteristics.

Munition	Type	DODIC Number	Production ($\times 10^6$)	Wt. of round (kg)	HE load (kg)	Energetics type	Muzzle vel. (mps)	Projectile material	Mfg. process	Min. wall thk. (mm)	Mfg. Dates
40-mm HE											
Gun	HE-T, SD	B562	1.1	2.15	0.063	TNT or Tetryl	823	1335 Steel	Turned	6.2	1944
Grenade/ Gun	M383	B571	4.0	0.34	0.055	Comp A5 (RDX)	795	1009 Steel	Stamped	6.5	1973, 1990
Grenade/ Gun	M384	B470	17.0	0.34	0.055	Comp A5 (RDX)	795	1030 Steel	Stamped	2.7	1965, 1969
Grenade	M397	B569	1.4	0.23	0.032	Octal	76	6061 Al	Extruded	2.0	1964, 1965
Grenade	M406	B568	39.0	0.25	0.032	Comp B	76	1100 Al	Stamped?	1.2	1969, 1970
Gun	DP M430	B542	18.0	0.34	0.038	Comp A5 (RDX)	241	1009 Steel	Stamped	3.4	1983, 1994
Grenade	DP M433	B546	23.0	0.23	0.045	Comp A5 (RDX)	76	1009 Steel	Stamped	2.5	1998, 2001
Total			103.5	Avg.	0.046						
60-mm HE											
Mortar	M49A4	B632	1.9	1.40	0.190	TNT or Comp B	51 / 159	Pearlitic CI	Casting	5.9	1953, '71, '73
Mortar	M720	B642	1.2	1.70	0.191	Comp B	64 / 277	1340 Steel	Forged	5.1	1989, 1996
Mortar	M888	B643	3.0	1.77	0.358	Comp B		1340 Steel	Forged	5.1	1991, 1999
Total			6.1	Avg.	0.246						
81-mm HE											
Mortar	M43A1	C225	6.0	3.40	0.585	Comp B	72.5 / 254	1020 Steel	Forged	9.7	1966, 1971
Mortar	M362	C222	4.0	4.30	0.953	Comp B	55 / 236	1012 Steel	Forged	6.5	1955, 1964
Mortar	M362	C223	1.3	4.30	0.953	Comp B	55 / 236	1012 Steel	Forg/Cast	6.5	1958, 1970
Mortar	M374	C236	2.3	4.30	0.953	Comp B	64 / 261	1340 Steel	Forged	6.2	1966, 1976

Munition	Type	DODIC Number	Production ($\times 10^6$)	Wt. of round (kg)	HE load (kg)	Energetics type	Muzzle vel. (mps)	Projectile material	Mfg. process	Min. wall thk. (mm)	Mfg. Dates
Mortar	M374A3	C256	40.8	4.30	0.953	Comp B	66 / 268	1340 Steel	Forged	5.6	1971, 1990
Mortar	M821A1	C868	1.0	4.10	0.726	RDX / TNT	N/A	HF-1 Steel	Forged	N/A	1985, 2000
Mortar	M889	C869	1.4	4.10	0.726	RDX / TNT	N/A	HF-1 Steel	Forged	7.0	1986, 1999
Total			56.8	Avg.	0.836						
105-mm HE											
Howitzer	M1	C444	2.1	14.10	2.18 to 2.3	Comp B or TNT	198 / 494	HF-1/CStl	Forged	10.5	1953, 1970
Howitzer	M1	C445	20.0	14.10	2.18 to 2.3	Comp B or TNT	198 / 494	HF-1/CStl	Forged	10.5	1943, 1974
Howitzer	M1	C443	0.6	14.10	2.18 to 2.3	Comp B or TNT	198 / 494	HF-1/CStl	Forged	10.5	1953, 1966
Total			22.7	Avg.	2.239						
4.2-in. HE											
Mortar	M329A2	C697	1.3	9.98	2.610	Comp B	1,010	1340 Steel	Forged	7.5	1980–1992
Mortar		C699	1.0	9.98	2.610		1,010	1340 Steel	Forged	7.5	1981–1985
Mortar	M329A1	C704	0.4	12.30	3.377	TNT	981	Carbon Steel	Formed	7.5	1953, '69, '74
Mortar		C705	1.2	12.30	3.377	TNT	981	Carbon Steel	Formed	7.5	1980
Total			3.9	Avg.	2.994						
120-mm HE											
Mortar	M933	C623	0.4	14.20	2.990	Comp B		Carbon Steel	Formed	9.3	1993, 1999
Mortar	M934A1	C379	0.2	14.20	2.990	Comp B		Carbon Steel	Formed	9.3	1992, 2001
Total			0.6	Avg.	2.990						
155-mm HE											
Howitzer	M1918		0.7					Semi-Steel	Casting	16.3	1918
Howitzer	M107	D544	6.4	43.00	6.62 to 6.98	TNT / Comp B	207 / 684	Steel	Forged	13.5	1953–2001
Howitzer	RA M549	D579	1.1	43.50	6.94 to 7.26	TNT / Comp B	561 / 826	Steel	Forged	11.0	1976–1998
Howitzer	M795	D529	0.3	46.90	10.795	TNT	253 / 802	HF-1	Forged	10.9	1985, 2000
Total			7.8	Avg.	8.232						
8-in. HE											
Howitzer	M106	D680	11.5	93.00	16.47 to 17.60	TNT / Comp B	250 /594	1008 Steel	Forged	17.0	1956, 1980
Howitzer	RA M650	D624	0.3	91.00	11.300	TNT		HF-1 Steel	Forged	18.2	1980–1991
Total			11.8	Avg.	14.166						

The weights of the projectile and the HE filler were obtained from USAMC (1985) and U.S. Army (1994) and do not include the weight of the fuze or of the explosives used in the fuze. The weight of the round and its muzzle velocity,

which is its exit velocity from the gun barrel in meters per second (USAMC 1985), are important parameters for computer models that estimate impact speed and penetration depth of the round. If they do not detonate, larger munitions are more likely to penetrate the ground and become buried UXO than are smaller rounds. Also, larger munitions contain more explosives and can become a larger specific source of contamination than smaller rounds. For rounds with variable propellant loads, we have listed the weight ranges possible (USAMC 1985, U.S. Army 1994, Popadopoulas 2003).

Because we are interested in the corrosion of these rounds, we also obtained and tabulated information on the metals used to make the projectile body, the methods used to make the projectile, the projectiles minimum wall thickness, and dates when large quantities of each munition were manufactured. The manufactured date can be used as a proxy of when the round was used. This assumption must be viewed with some caution, however, as munitions are often used at later dates. For example, WWII-vintage ammunition was in use during the Vietnam War (1960–75) and old munitions are used preferentially during training.

The projectile body is usually made of steel or iron. Some rounds have copper alloy rotating bands. Fins and fuzes are typically made of aluminum. A mix of metals can set up galvanic currents and increase corrosion. The presence of a more noble metal in contact with the steel increases the corrosion rate. Primary among these is brass (copper and zinc alloy), which is used for the rotating bands on artillery rounds. A photograph of a 105-mm HE round fired into Eagle River Flats, an estuarine salt marsh, shows that after a few months, corrosion is occurring in the vicinity of the band (Fig. 4). However, in the same environment, the corrosion of steel can be slowed by the presence of aluminum. Mortars built after 1960, have aluminum alloy fins that act as anodes and rapidly corrode, thereby protecting the steel portion of the round (Fig. 5). Figure 5 shows a round that had been in the salt-marsh sediments at least 14 years with no visible corrosion of the steel. However, the fin assembly, which is made of aluminum, has totally corroded.

Given similar conditions, there is little difference between the stability of forged and cast steel of the same composition (Romanov 1957, Craig, 1989). The steel alloy composition, however, does play a major role in the corrosion resistance of the UXO. Chromium is a common additive to stainless steels, imparting appreciable corrosion resistance to the resulting alloy. The addition of copper or nickel to steels also greatly enhances their resistance to corrosion, but none of the rounds of concern contain effective amounts of these alloying elements (Papadopoulos 2003). In most cases, a rust-inhibiting paint is applied to the outside of the steel round. This will inhibit corrosion if the coating remains intact. However,

firing of the round often burns off some of the paint, exposing the iron shell to corrosion. As the round penetrates the soil, the coating will likely be abraded or the coating will, over time, be removed by corrosion. The result, a discontinuous coating of rust-inhibiting paint induces anodic metal corrosion at exposed areas, thereby enhancing pitting of the metal. Most important for calculating corrosion is the minimum wall thickness of the projectile body, as thickness determines the time it takes for corrosion to penetrate the round.

Figure 4. Corrosion of a copper rotating band on a 155-mm round found at Eagle River Flats, Alaska.

Figure 5. Corrosion of an aluminum fin on a 81-mm mortar found at Eagle River Flats, Alaska.

4 MUNITIONS AND THEIR FATE AFTER FIRING

A fired munition can experience one of many fates (Fig. 6). Generally, it will detonate as intended. However, it might also undergo a low-order (partial) detonation or be a dud (UXO). UXO may penetrate the ground to some depth or come to rest on the surface. Whether on the surface or underground, a UXO might suffer one of five outcomes leading to the release of HE. It can be blown-in-place (high or low order), it can be detonated sympathetically by a round exploding nearby to produce a low-order detonation, the casing might be split either by the initial impact or by a nearby explosion, or it can corrode over time. The following sections review the currently available information on each of these processes and provide estimates of their frequencies.

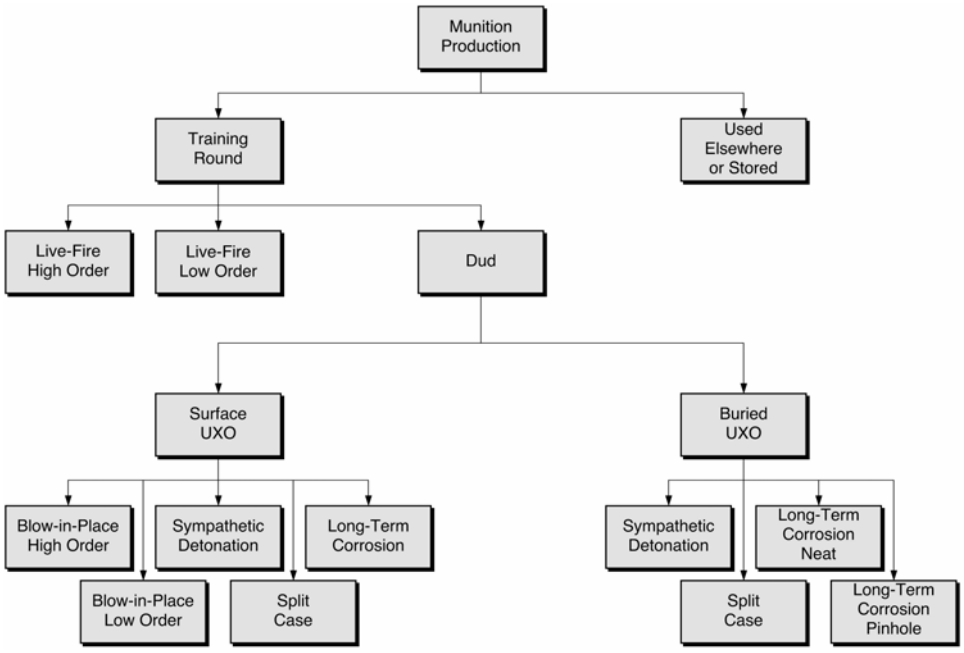

Figure 6. Possible fates of a fired munition.

4.1 Estimates of Dud and Low-Order Detonation rates

Accurate records of the number and types of munitions fired during training and whether or not the round functioned as intended are not available for Army training sites. Dauphin and Doyle (2000, 2001) estimated the dud, low-order, and high-order rates for a variety of munitions by compiling statistics from over

209,390 rounds that were fired as part of the Ammunition Stockpile Reliability Program (ASRP). They chose the data from this program because it best simulated the conditions encountered during training. For example, the rounds fired were taken from the same stockpile used by troops for training, so rounds from different production lots, ammunition manufacturers, and storage conditions were all tested. Dauphin and Doyle (2000, 2001) provide data on the dud and low-order rate for fuzes, grenades (hand, rifle and launcher), mines, pyrotechnics and artillery, mortar, gun and rocket ammunition for the following size and caliber rounds: 20-mm, 25-mm, 40-mm, 57-mm, 60-mm, 66-mm, 75-mm, 76-mm, 81-mm, 83-mm, 84-mm, 90-mm, 105-mm, 106-mm, 120-mm, 152-mm, 155-mm, 165-mm, 2.75-in., 3.5-in., 4.2-in., and 8-in. Table 3 shows the dud and low-order results for the most commonly manufactured munitions—40-mm grenades, 60-mm, 81-mm, 4.2-in., and 120-mm mortars, 105-mm and 155-mm and 8-in. howitzer rounds. The dud rate ranges from 1% for the 8-in. projectiles to 6% for the 4.2-in. rounds. The low-order rate ranges from 0.01% for the HE-filled 155-mm projectiles to 1% for all types of 155-mm and the 105-mm projectiles. With the exception of the 120-mm mortar and the 8-in. howitzer round, these munitions were some of the most frequently found as UXO at MMR (AMEX, in review).

Table 3. Measured Dud and LO rates for eitght types of munitions (Dauphin and Doyle 2000). We list the values for all fill types (target practice, illumination white phosphorus, etc.) and for HE-filled only.

Size	Family	Number fired	Number of duds	Number LO	Dud (%)	LO (%)
40-mm	Grenade/Gun	19,497	267	29	1.37	0.149
HE-only		15,735	208	24	1.32	0.153
60-mm	Mortar	27,614	646	6	2.34	0.0217
HE-only		13,742	341	0	2.48	0.00
81-mm	Mortar	28,759	671	33	2.33	0.115
HE-only		16,435	375	13	2.280	0.0791
4.2-in.	Mortar	14,491	743	20	5.13	0.138
HE-only		7,904	547	6	6.92	0.0759
120-mm HE	Gun	270	7	0	2.59	0.00
105-mm	Howitzer	27,100	1259	289	4.65	1.07
HE-only		13,017	644	12	4.95	0.0922
155-mm	Howitzer	15,108	341	150	2.26	0.993
HE-only		7,656	172	1	2.25	0.0131
8-in HE	Howitzer	1,010	10	0	0.9901	0.00

Experienced military personnel fired the rounds for the ASRP tests. This procedure is appropriate when assessing the reliability of the ammunition and the

fuzes, but may underestimate the dud and low-order rates obtained when inexperienced soldiers fire the rounds during training. For example, improperly installed fuzes may cause munitions to not detonate. One of the authors (Michael Walsh) found improperly fuzed 81-mm duds and was told that 80% of the rounds had not detonated at one of the training exercises. Live fire tests of eight 105-mm howitzers, six 81-mm, and five 60-mm mortars produced one dud each for the 105-mm and 60-mm rounds (Collins and Calkins 1995). It was noted that the point detonating fuzes (those used for these tests) performed well compared to the delay fuzes, which "operated very erratically in areas with frozen ground and an ice cover" (Collins and Calkins 1995). This suggests that the substrate being impacted may also affect the HO, LO and dud rate.

When estimating the mass of explosives remaining after a detonation, a limitation of the ASRP data is that each fired round is categorized as dud, a low-order, or a high-order detonation. The dud rate is easily determined by counting fired rounds that did not detonate. However, the distinction between a high- and low-order detonation is less clear. The term "order" is a subjective classification of explosive yield. In principle, the yield can be quantified based on air-blast parameters (Kingery and Bulmash 1984). These measurements require placing sensors around the detonation point to measure the blast wave and cannot be made during live fire. In practice, the classification of a detonation as high- or low-order is done on the basis of the sound of the detonation and the presence or absence of a shell carcass. A detonation may be measurably, but not audibly, less than 100% yield if the detonation wave does not propagate properly through the explosive fill. Defects in the shell casing or in the packing or pouring of the shell can cause low yields.

4.2 UXO Fate

4.2.1 Number of UXO Versus Depth

The UXO database* lists the number and type of UXO removed from 1.2 m (4 ft) depths at formerly used defense sites (FUDS), from base realignment and closure projects (BRAC), and installation restoration (IR) projects. The U.S. Army Engineering and Support Center in Huntsville, Alabama, compiled a database of UXO removed from Fort Ord, California; East Elliot, California; Camp Simms, Washington DC; Jefferson Proving Ground, Indiana; Fort Sill, Oklahoma; Camp Green, North Carolina; Fort Dix, New Jersey; Camp Croft, South Carolina; Motlow Range, Tennessee; Camp Maxey, Texas; and Dolly Sods Wil-

* Personal communication with Roger Young, USACE Huntsville, April 2004.

derness Area, West Virginia. The database includes information on the type of round (projectile, rocket, etc.), the item (81-mm mortar, etc.), the recovery depth (measured to the shallowest point on the round), and an assessment of whether the item was fired or buried (Adams 1999). Because the database will continue to be updated and the different versions are not published, we obtained the data for this report from the 2003 version that listed 7299 UXO as having been fired.

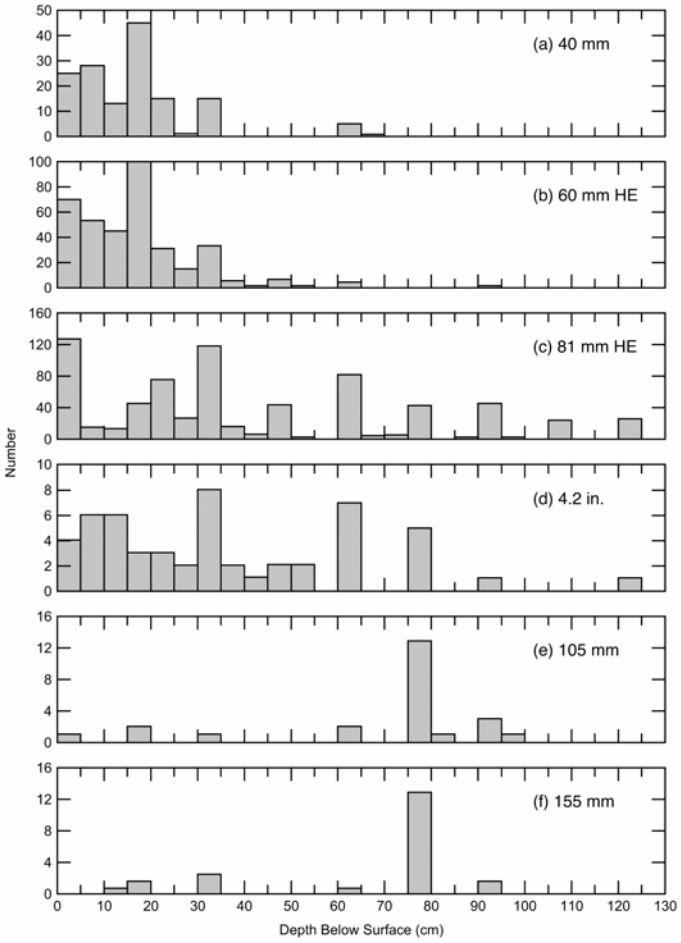

Figure 7. UXO as a function of depth.

There is a clear pattern relating the distribution of recovery depths to the munition type and size. Frequency histograms of the number of 40-mm grenades, 60-mm, 81-mm, and 4.2-in. mortars, and 105-mm and 155-mm howitzer rounds found as a function of depth below the surface shows a bimodal distribution of munition depths (Fig. 7a–f). The 40- and 60-mm rounds generally were found at shallow depths, between 0 and 20 cm, with the deepest 40-mm round at 65 cm

(Fig. 7a) and the deepest 60-mm mortar at 90 cm (Fig. 7b). The larger 81-mm and 4.2-in. rounds were distributed to 120-cm depths, with most at intermediate depths (Fig. 7c and d). Few 105-mm and 155-mm howitzer rounds were found but most of those were located at a depth of 75 cm (Fig. 7e and f).

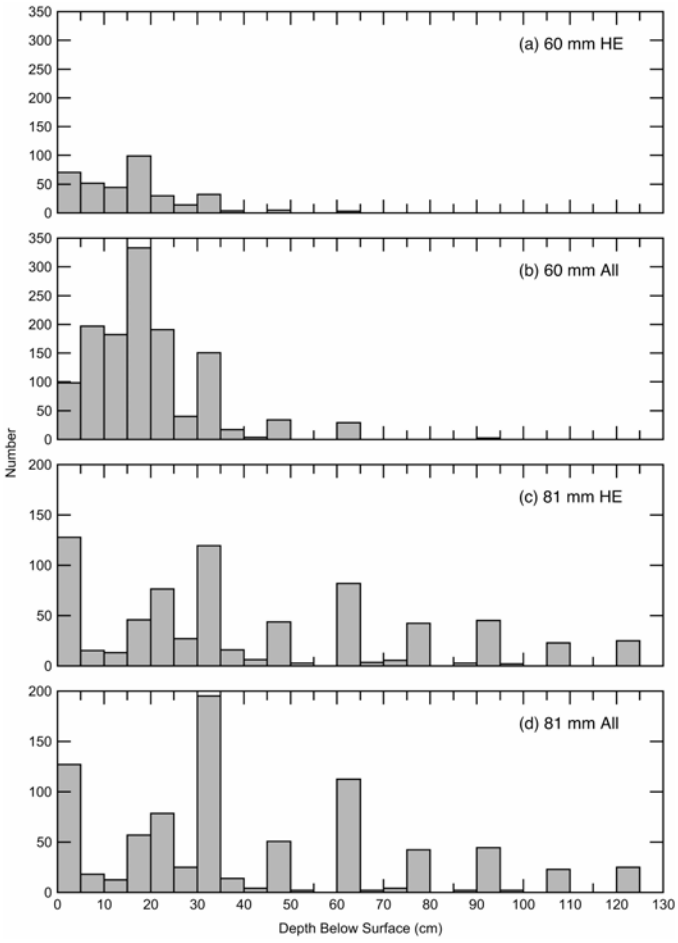

Figure 8. Comparison of HE-filled versus all UXO as a function of depth.

The depth distribution may also be influenced by the presence (or lack of) HE. A significant fraction the 60- and 81-mm rounds (72 and 17%, respectively) retrieved were inert practice rounds. We compared the distribution of the HE-filled rounds with the inert rounds to determine whether or not the inert rounds were preferentially found at certain depths (Fig. 8a–d). For the 60-mm mortars, the HE-filled rounds make up a higher proportion of the surface and shallow UXO than the inert rounds (Fig. 8a, b). For the 81-mm rounds, the two distribu-

tions are very similar but again HE-filled rounds make up most of the surface UXO (Fig. 8c and d). This difference in distribution suggests that HE explosives are encountered more often at the surface. Although the reason for the difference in distribution is not known, perhaps because they pose little risk, the inert rounds on the surface were previously picked up and therefore not accounted for in the database.

4.2.2 Modeled Ground Penetration

Predicting the depth to which a round can penetrate into the soil is important for many reasons. First, if these items are to be removed, they must be found, a practice that is straightforward with well-exposed munitions. Magnetometers, currently the most reliable tool for finding UXO, are accurate to a depth of about 60 cm (24 in.) with about 85% reliability. While this level of reliability is adequate for some efforts, often more complete cleanup is warranted for both environmental and safety reasons. If the area is to be completely cleared of ordnance to a very high degree of certainty, all the overlying soil to the maximum penetration depth of the ordnance must be removed and processed. Finally, the fate of buried munitions may vary substantially with burial depth. For example, corrosion rates for ferrous materials generally increase with depth of burial (Romanoff 1957).

Three methods are available to predict the depth to which a fired round will penetrate the ground. The simplest is an empirical equation that requires the weight of the ordnance, its impact velocity, and the soil type (U.S. Army 1998, TM 5-855-1,). Two mathematical models also exist. The PENCRV3D is a three-dimensional model that calculates the trajectory of the ordnance through soil using the projectiles' center of gravity, impact velocity, and angle of impact, together with the soil type as input parameters (Adley et al. 1997). The HULL hydrocode is a two- and three-dimensional dynamic continuum mechanics program (Fry et al. 1976). It requires the shape, weight, and impact velocity of the round as input parameters.

Crull et al. (1999) compared the empirical equation and the hydrocode for ease of use and accuracy of the results. As expected the one-dimensional equation required many fewer input parameters and was less difficult to use than the PENCRV3D or the more rigorous HULL hydrocode. Differences in penetration depths under the assumed conditions ($V_i = V_m$, $\Theta = 90°$, matrix = uniform sand) between the one-dimensional equation and the hydrocode ranged from 5 up to 22%, with the largest differences occurring for the largest rounds (155-mm, 105-mm, 75-mm) (Table 4). Grant and Crull (1999) examined the sensitivity of the PENCRV3D to input error. A small error (2%) in the center of gravity or the im-

pact angle will result in an error of 20% in the calculated penetration depth. A 6% error in the impact velocity will result in a similar error. These errors can accumulate to make ordnance depth predictions highly inaccurate. Thus, the empirical model is probably preferable to the more complex codes for most applications, as exact parameters for each shell trajectory are unknown.

Table 4. Predicted ordnance penetration depths into sand versus actual recovery depths for a variety of soils.

Ordnance	Wt. (lb)	Muzzle vel. (ft/s)	Predicted penetration depth (ft)			Depth of recovery** (ft)		Number of rounds
			Equation*	PENCRV3D†	HULL*		Median	
155-mm M107	96.75	2244	14	28.5	16.8	0.4 to 3.0	2.5	24
105-mm M1	33.95	1550	7.7	17.7	9.4	0 to 3.2	2.5	24
75-mm M48	14.6	1250	4.9	9.9	5.7	0 to 4	1	94
40-mm M822	5.5	1100	3.2	11.8	2.9	0 to 2.2	0.5	148
37-mm M63	1.61	2650	3.9	7.9	4.1	0 to 2.5	0.4	108
2.36-in. Rocket	3.4	265	0.4		0.5	0 to 4	0.4	2278

* From Crull et al. (1999).
† Adams (2001).
**UXO Recovery Depth Database.

The agreement between the predicted depth (for all models) and the measured depths of ordnance is poor (Table 4); however, validating model results using UXO depth data is problematic for several reasons. First, no data exist on how the UXO were fired, so their angle of impact and impact velocity are not known. For the PENCRV3D model, and probably the HULL model, estimates of these impact parameters will result in very large errors in penetration depth. Second, although the type of soil at the impact site can be determined, real soils are usually non-homogeneous. The error introduced by this effect is lacking from the models and may be large. Third, the UXO sample size is small for some rounds, invalidating any statistical comparisons. Because the impact velocity and the impact angle are unknown for UXO, these are often set equal the muzzle velocity and 90° respectively (Adams 2001). As the impact velocity is less than the muzzle velocity, and most projectiles impact at shallower angles than 90°, these parameter choices may cause the overestimation. Lastly, the measured depths only extend to 1.2 m.

4.2.3 Number of UXO Per Square Meter

Knowing the number of UXO per square meter and the impact rate per square meter helps to determine the likelihood of sympathetic detonations and is an input parameter for a model that predicts the potential for groundwater con-

tamination from buried UXO (Praxis 2004). Although the locations of UXO are documented during clearance, only a few reports give this information. Two areas on Fort Ord, cleared of UXO to a depth of 1.2 m (4 ft), yielded 13 and 23 UXO/acre. Two sites, Duck, North Carolina, and Camp Elliott, California, that were just surface cleared have much lower UXO values, 0.2 and 0.6 UXO/acre respectively (Nore 1994). Information on UXO spatial density is not tabulated in the UXO database* and is difficult to obtain for most sites.

About 20,000 UXO were removed from MMR. At this site, although we know the area of the impact range, the demolition area, and the separate rocket ranges, the different areas have not been entirely cleared of UXO and we do not know the proportion of each that has been cleared. The exception is a 3.6-acre, high-use training area (HUTA) that was cleared of UXO to a depth of 1.2 m (4 ft). Four HE-filled UXO were found on the surface and 112 HE-filled UXO were buried. This area was cleared in 120- by 30-m test plots whose areas overlapped (AMEX, in review, see Table 5). We have listed some other values for MMR, although we are not certain that the entire area was searched for UXO. Discounting the impact area, which has not been searched extensively, the values for the number of UXO per acre ranges from 4 to 89. Unfortunately, this value is not easily extrapolated to other ranges, as each range was used to a different extent and will have a corresponding variation in UXO density (Table 5).

Table 5. Estimates of the number of UXO per m^2.

Installation		HE-filled	Inert	# BIP	Area (acre)	Area (ha)	Area (m^2)	HE-live UXO/ acre	HE-live UXO/m^2	Comments	Reference
JPG, IN		73			120	49	486,000	0.6	1.5×10^{-4}		UXO database
		475			8			59.4		surface	
		1			100			0.0		cleared to 1.2 m (4 ft)	
Fort Ord, CA	OE-50	936		all	41	16	164,000	23.1	5.7×10^{-3}	cleared to 1.2 m (4 ft)	USA Environmental 2001
	OE-50	26		all	2	1	8,047	13.1	3.2×10^{-3}	cleared to 1.2 m (4 ft)	USA Environmental 2001
MMR, MA											AMEX, in review
Impact area		195	2768		2,200	890	8,900,000	0.1	2.2×10^{-5}	all area not searched	
High use training area		116			3.6	1.5	14,600	32.2	7.9×10^{-3}		
	Test Plot 1	7			0.9	0.36	3,600	7.9	1.9×10^{-3}	all area not searched	
	Test Plot 2	17			0.9	0.36	3,600	19.1	4.7×10^{-3}		

* Personal communication with Roger Young, USACE Huntsville, April 2004.

Installation		HE-filled	Inert	# BIP	Area (acre)	Area (ha)	Area (m^2)	HE-live UXO/ acre	HE-live UXO/m^2	Comments	Reference
	Test Plot 3	11			0.9	0.36	3,600	12.4	3.1×10^{-3}		
	Test Plot 4	17			0.9	0.36	3,600	19.1	4.7×10^{-3}		
	Test Plot 5	21			0.9	0.36	3,600	23.6	5.8×10^{-3}		
	Test Plot 6	21			0.9	0.36	3,600	23.6	5.8×10^{-3}		
J1 Range		558	1795	154	139	56	563,000	4.0	9.9×10^{-4}		
SE		17,454	13,396		329	132	1,320,000	53.1	1.3×10^{-2}		
Demo 1		89	28		1	0.4	4,000	89.0	2.2×10^{-2}		
Duck, NC											
Navy target facility		47		all	200	81	809,000	0.2	5.8×10^{-5}	surface UXO only	Nore (1994)
Camp Elliott, CA											
Tierrasanta		1065		51	1,904	771	7,705,000	0.6	1.4×10^{-4}	surface UXO only	Nore (1994)
Mission trails		205		5	322	130	1,303,000	0.6	1.6×10^{-4}	surface UXO only	Nore (1994)
Fort Sill, OK		9637		9,637	1,322	535	5,354,100	7.3	1.8×10^{-3}	surface UXO only	Nore (1994)
Assateague Island		212			2.4	1	9,720	88.3	2.2×10^{-2}	surface to 2 to 4 ft	NDCEE (2003)
Bergstrom AFB		4			3.5	1	14,175	1.1	2.8×10^{-4}	cleared to 2 ft	
Black Hills Army depot		1107			1,460	591	5,913,000	0.8	1.9×10^{-4}	surface only	
Blossom Point MD		720			76	31	307395	9.5	2.3×10^{-3}	surface to 2 to 4 ft	
Camp Croft		85			572	232	2316600	0.1	3.7×10^{-3}	cleared to 2 ft	
Fort McClellan		2			22	9	89,100	0.1	2.2×10^{-5}	cleared to 1.2 m (4 ft)	
Gaillard Cut Widening Pogram		841			204	83	826,200	4.1	1.0×10^{-3}	surface only	
Morgan Depot		1052			60	24	243,000	17.5	4.3×10^{-3}	cleared to 1.2 m (4 ft)	
Nebraska Ordnance Plant		13			6	2	24,300	2.2	5.3×10^{-4}	cleared to 1.2 m (4 ft)	
Southwestern Prooving Ground		2794			203	82	822,150	13.8	3.4×10^{-3}	variable 1 to 4 ft	
Tipton Army Airfield		1713			277	112	1,121,850	6.2	1.5×10^{-3}	cleared to 1.2 m (4 ft)	
USARSO Panama Canal		350			475	192	1,923,750	0.7	1.8×10^{-4}	surface	
		125			475	192	1,923,750	0.3	6.5×10^{-5}	cleared to 1.2 m (4 ft)	

4.2.4 UXO Clearance

To mitigate the explosive hazard, UXO are cleared in areas that are turned over to the public domain. The depth to which the UXO are cleared depends on the intended use of the land (Naval Explosive Ordnance Disposal Technology Division 1996). For limited public access, such as areas used for livestock graz-

ing or wildlife preserves, a depth of 30 cm (1 ft) is suggested. If the land is to be used for farming, recreation, or parking, ordnance is cleared to 1.2 m (4 ft). For unrestricted use, such as commercial and residential building, where construction is likely to take place, UXO are cleared to a depth of 3 m (10 ft).

Once unearthed, any ordnance deemed safe is moved to a selected open burn/open detonation site where it is destroyed. Ordnance deemed unsafe to move is detonated in place. This is the standard operating procedure set out in U.S. Army (1999) Technical Manual 60A-1-1-31. The clearance is done primarily to mitigate explosion hazard. The manual calls for pre- and post-clearance soil samples at the open burn/open detonation site to evaluate the contamination hazard. At MMR, to minimize explosives contamination, the vast majority of rounds were moved to, and blown up in, a blast chamber. Of approximately 20,000 UXO recovered, only 648 were blown-in-place because of safety reasons and the rest were destroyed in a blast chamber.

Much of the expense of clearing UXO is finding the buried rounds. In areas where the ground freezes, rounds above the frost line can be brought to the surface by the action of frost heave (Isaksen and Sollid 2002). If objects contained within the frozen ground heave upward, gaps are created beneath those objects. During the spring thaw, fine-grained materials fill in gaps under the objects. Over time this process will move the larger objects (stones, projectiles, etc.) toward the surface. The rate at which this occurs depends on a number of variables, including soil type, temperature, and moisture conditions in the soil. On Norway's Hjerkinn firing range, a frost heave transport rate has been estimated at 0.5 to 2 cm per year, corresponding to 10 to 40 years for the Earth's freeze–thaw action to bring rounds buried to a depth of 0.2 m to the surface.

5 UXO CORROSION

There is an unknown, but large, amount of unexploded ordnance (UXO) in ranges throughout the U.S., and on war fields and other ranges throughout the world. Some (Bucci and Buckley 1998; AMEX, in review) have suggested that corrosion of these munitions is minimal owing to the physicochemical properties of the casing, which is predominantly carbon steel. Support for this position comes from the lack of grossly contaminated soils, which would likely result from widespread failure of UXO.

5.1 Metal Corrosion

Corrosion may lead to either catastrophic failure of the casing or to the development of small holes (pinholes), processes that may release explosives into the environment. In Appendix A we discuss in detail the thermodynamic and kinetic effects occurring during corrosion of UXO in a variety of environments. Here, we describe corrosion as it relates to carbon steels and present our best estimates of generalized corrosion rates for carbon steels. Overall, we concur with the results of Fabian and Ostazeski (2002) concerning UXO failure in most soil environments.

Most corrosion processes are highly favored thermodynamically because the oxidation of metals is highly exergonic. For example, the corrosion of iron (the main constituent in steel) proceeds according to the following chemical reaction:

$$2\mathrm{Fe} + \frac{3}{2}\mathrm{O_2} \Leftrightarrow \mathrm{Fe_2O_3}\ \Delta G_{rxn}{}^{0} = -742\ \mathrm{kJ/mol} \qquad (1)$$

The release of free energy is typical of other corrosion processes and shows the drive for metals to dissolve to form other phases. In fact, iron is not stable under any typical soil water pH-E_h conditions (Fig. 9). Other metals and alloys, including steel, the most common casing for munitions, are similarly unstable under commonly encountered thermodynamic conditions (Fig. 10).

Although thermodynamic (energetic) considerations indicate that corrosion is favored under the most commonly encountered soil conditions, kinetic factors ultimately determine the *extent* to which this oxidation occurs, the ultimate reaction products of oxidation, and the distribution of these reaction products (e.g., whether they are attached to the surface). The most stable reaction products thermodynamically are often not formed during metal corrosion in soils because

of sluggish reaction kinetics, instead leading to the formation of other, metastable, reaction products.

Because the rate of corrosion depends on the rate of the anodic (oxidation) and cathodic (reduction) reactions, it is necessary to identify the dominant half reactions to estimate the rate of oxidation (Fig. 11). When alloys such as steel corrode, several anodic (oxidation) reactions may occur, each of which liberates a cation and electrons. In the case of carbon steel, the oxidation of elemental carbon to CO_2 (g) may occur at the anode. As CO_2 is soluble and diffuses away quickly relative to ions, carbon steels are more easily corroded than other steels.

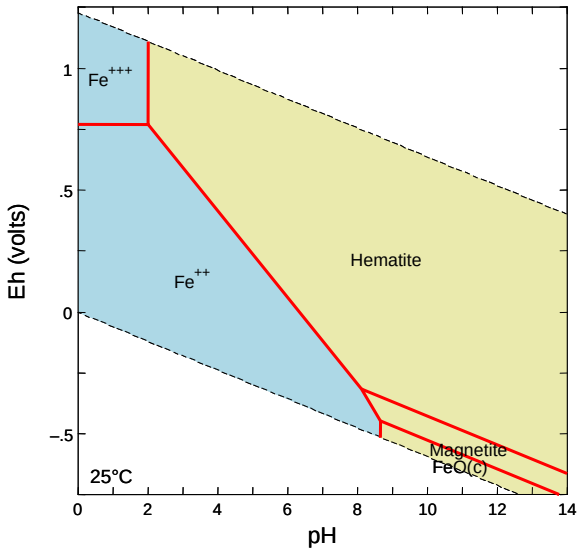

Figure 9. Fe phase diagram for Fe-O_2 system at 25ºC. The diagram is derived using a dissolved Fe concentration of 1 µM. Darker colored phases are aqueous, while lighter phases are solids. The diagonal dotted lines show boundaries for the stability of water; the vertical dotted line shows the change in carbonate speciation. Hematite is α-Fe_2O_3 (s).

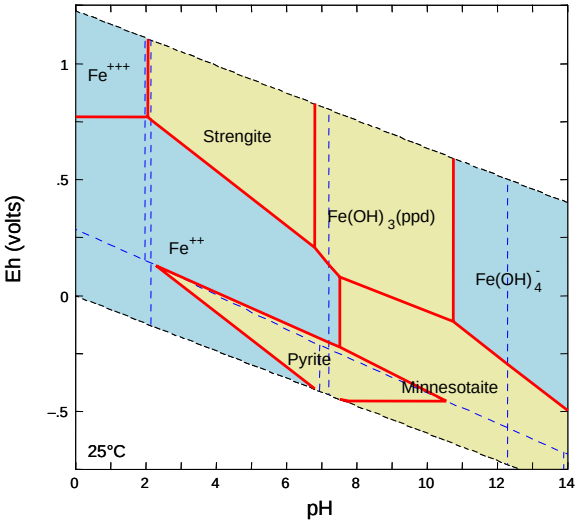

Figure 10. Fe phase diagram for $Fe\text{-}O_2\text{-}S\text{-}PO_4\text{-}CO_3\text{-}H_2O$ system at 25ºC. The diagram is derived using a dissolved Fe concentration of 1 µM, a total CO_3^{2-} of 0.1 mM, total PO_4^{3-} and SO_4^{2-} of 1 µM, SiO_2 of 50 µM; similar concentrations to those found in soils. Darker phases are aqueous, while lighter phases are solids. The diagonal dotted lines show boundaries for the stability of water; the vertical dotted lines show the change in carbonate, phosphate, and sulfur speciation. Minnesotaite is an iron-containing phyllosilicate, and strengite is hydrated $FePO_4$.

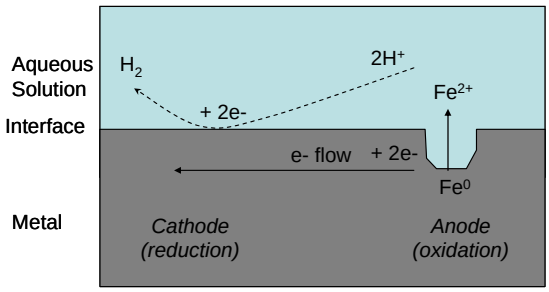

Figure 11. Corrosion of iron in an aqueous solution of HCl. The anodic reaction generates the dissolved metal and electrons, which are transferred to the cathode, where they are used to reduce protons in solution. The extent of proton transfer is equal to the electron flow, a condition required to maintain charge neutrality.

Generally, it is desirable from a remediation standpoint to produce solid phases during corrosion—they are more stable, they are less prone to transport, they react with potential contaminants (both inorganic and organic species adsorb strongly to iron oxides), and some oxidation products protect the metal surface from further oxidation (Kuznetsova et al. 1998, Ge et al. 2003, Virtanen and Buchler 2003). The protection of the surface is called passivation. This protection is a kinetic effect, in that the thermodynamic driving force for corrosion remains, but the surface oxidation is slowed by the presence of a passivating oxide. Such oxides can only protect surfaces if they form effective two-dimensional arrays there; thus, the microstructural compatibility of the interface between the surface and the overlying oxide film is important (Appendix A).

Most UXO are composed of carbon steel, though a limited number of aluminum grenades also have been used. Aluminum is effectively passivated by the formation of Al_2O_3 films, which are highly compatible with Al surfaces. This passivation leads to fairly corrosion resistant aluminum surfaces, except in chloride containing solutions (e.g., Fig. 5). In contrast, the steel UXO corrode to ferric (hydr)oxides, which do not bond strongly to the metal surface and consequently have only limited potential to passivate the metal surface (Fig. 12). This weak bonding is caused by unfavorable interactions between Fe at the surface and the oxide over layer. Nevertheless, under typical soil conditions (near neutral pH, moderately oxidizing conditions), iron, various alloys of steel, and aluminum are often stable in soil environments over long periods of time. Under such conditions, passivation films are formed that can slow the general corrosion rate by about three orders of magnitude.

Pitting corrosion is important for UXO. Pitting may result in pinhole failures in the UXO, which may release small amounts of explosives. Pinholes also provide an additional avenue for corrosion (corrosion can then occur from within), thereby increasing the rate of catastrophic failure. Many of the perforations in UXO are probably limited to relatively small holes formed as a result of pitting corrosion, but some small munitions, particularly in flooded soils and sediments with low hydrologic gradients, may also have failed through anaerobic corrosion induced by sulfate reducing bacteria.

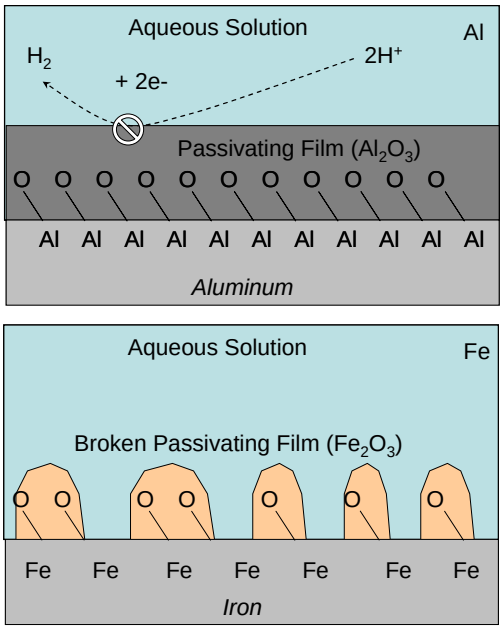

Figure 12. Formation of passivation layers during the corrosion of aluminum (Al) and iron (Fe). The passivation layer on Al is complete as the Al oxide forms a compatible passivating film. As drawn, the passivation occurs by blocking the cathodic reaction; however, anodic passivation is also possible. In contrast, the Fe oxide film is not compatible and forms oxides that are ineffective at blocking the surface.

5.2 Biologically Mediated Metal Corrosion

Biological reactions are ubiquitous in soil systems. Conditions conducive to biological activity, warm and wet, accelerate corrosion through a variety of processes (Prakash et al. 1988, Kloppel et al. 1997, Yfantis et al. 1998, xLi et al. 2001, Gu et al. 2002, Doyle et al. 2003). One of the most obvious and the most important means by which biological organisms accelerate corrosion is through the secretion of acid, directly as small organic acids, into the soil solution. Acid is released into soils by organisms as a result of nutrient uptake (cation uptake is balanced by excretion of H^+) and as a means of regulating their environment. Acidity is also generated by the excretion of respiratory carbon dioxide. Upon dissolution, this CO_2 forms carbonic acid.

Organic acids, such as oxalic acid ($H_2C_2O_4$), also influence corrosion by chelating metal ions. Such acids are important because they prevent passivation by oxide minerals, and may even dissolve oxidized layers formed prior to their introduction. Consequently, chelation by oxalate and other biologically produced chemical species (e.g., citrate, soil organic matter) also increases corrosion rates.

It should be noted that biologically facilitated reactions do not change the thermodynamics of corrosion; rather, they change the mechanism by which corrosion occurs and, thereby, potentially, the rate of corrosion and the phases that are formed through corrosion. Biological corrosion reactions often result in the production of unique, metastable solid phases with different stability than chemically produced solid phases. In some cases, corrosion can lead to the formation of metastable reaction products, such as magnetite, that have unusually stable structures and low reactivity (Veleva et al. 1998, Ishikawa et al. 2003). However, reactive phases, such as green rust, may also be formed through a combination of biological and chemical processes (Drissi et al. 1995, Simon et al. 1997, Genin et al. 1998, Refait et al. 1998). These solid phases are highly reactive, and may in fact react strongly with contaminants such as RDX and TNT that have been released from leaking UXO (Hundal et al. 1997, Scherer et al. 2001, Wildman and Alvarez 2001). These compounds also are formed primarily in anaerobic soils and wetlands, environments that likely contain a large number of corroded UXO.

5.3 UXO Corrosion Models

Empirical corrosion rates for steel and other metals in soils have been determined, but general expressions that relate soil chemical characteristics to corrosion rates do not yet exist. In an empirical study by Romanov (1957), pieces of metal were buried in a variety of soil types and corrosion measured over approximately 50 years. A different study examined the corrosion rates of galvanized steel, a project conducted to assess corrosion of culverts in California (California model). Other studies have measured soil, temperature, and climate parameters to determine which variables best correlate with measured corrosion (e.g., Lafayette model, DOE model, and Praxis model). The Lafayette model identified bicarbonate as an important soil variable (Fabian and Ostazeski 2002). The DOE model predicts corrosion based on temperature (Lee and Atkins 1995). The Praxis pitting model finds the amount of rainfall a significant variable for pit corrosion (Praxis 2004).

The Romanoff study of steel corrosion (Romanoff 1957) indicates that soil conditions influence corrosion rates considerably, and that saline, sulfidic, and anaerobic soils corrode steel more rapidly than other soils. These long-term studies are particularly useful for estimating corrosion rates, because corrosion

rates may not be strictly linear. A drawback is that the soil conditions are not well controlled. Additionally, soils that are found in proximity or with similar characteristics often have different corrosion rates, despite their similar characteristics. The California DOT model for the corrosion of galvanized steel (California Department of Transportation 1999) is not applicable, as UXO are neither galvanized (which slows the initial rate of corrosion) nor subjected to the same types of soil environments as deep culverts for which the model was developed.

The quantitative models (the Lafayette model, the DOE model) require a large quantity of environmental data as input parameters (DOE Performance Assessment 1995, Fabian and Ostazeski 2002). While variables such as soil conductivity, resistivity, salinity, relative humidity, soil temperature, and pH are admittedly important in determining corrosion rates, it often is not practical to measure each of these at a sufficient spatial resolution to estimate corrosion rates. The problem of measurement is especially acute given the large size of many of the training ranges in which UXO are located. Furthermore, the heterogeneity of soils is sufficient that a few measurements of these parameters often do not provide an accurate estimate of the average or extremes in corrosion at a given site. As a result, of nearly 30 measured parameters, only rainfall was found to correlate to measured pit corrosion rates (Praxis 2004). Often, soil heterogeneity occurs even on depth scales; Romanoff (1957) observed significant differences in corrosion rates between surface and subsurface horizons, but was unable to completely determine the reasons for these differences. Given the difficulty in relating these measured parameters, we think it justified to move from these conceptual models to more applied models of corrosion.

We favor a simple approach, which reports the range of corrosion rates for a specific soil environment. From the literature we compiled the range of corrosion rates for carbon steel in solutions and soils (Table 6). The variation in rates may result from uncertainties in the determination of corrosion rate, but, more likely, they reflect differences in steel properties or in soil chemical properties, each of which may impact the rate considerably. We use the rates reported in Table 6 to quantify the depth of uniform failure of steel, that is, the thinning rate of the entire UXO wall. Rates of pitting corrosion, which occurs more rapidly and is very important for UXO, are notoriously hard to predict, because the rate of pit corrosion strongly depends on diffusion, which depends on the shape and depth of pits. This geometric effect is difficult to quantify, but estimates of pit corrosion rates for carbon steels are usually about 5–15 times faster than the uniform corrosion rate.

Table 6. Corrosion rates (in mm/year) of commonly used steel alloys in a variety of different solutions. The solutions given are useful in that they are closely related to the conditions in soils, and thus indicate the rate of corrosion in other media. Pitting corrosion occurs at variable rates, but usually between 5 and 10 times more rapidly than the average rates of corrosion reported here. Data were assembled from *The Handbook of Corrosion Data* (Craig 1989) and literature values (cited in the text). Each of the steel types listed have been used in UXO.

Alloy	Composition	Dilute H_2SO_4[a]	Sea–water[a]	Nacl (1%)[a]	Water	Soil	Saline soil	Flooded soils; anaerobic; may be sulfidic
					Aerated			
					Aerobic	Typical soils		
1008 Steel	(0.1% C steel, ~0.5% Mn)	0.1	0.085	0.017	0.04	0.02–0.1 (0.025 ave)[c]	0.1[c]	1–1.5[c]
1009 Steel	(0.15% C steel, ~0.5% Mn)	0.1	0.105	0.021	0.04	0.02–0.1 (0.025 ave)[c]	0.1[c]	1–1.5[c]
1012 Steel	(0.12% C steel, ~0.5% Mn)	0.11	0.12	0.024	0.05	0.02–0.1 (0.025 ave)[c]	0.1[c]	1–1.5[c]
1020 Steel	(0.2% C steel, ~0.5% Mn)	0.15	0.15	0.03	0.045	0.02–0.1 (0.025 ave)[c]	0.1[c]	1–1.5[c]
1030 Steel	(0.3% C steel, ~0.5% Mn)	0.2	0.15	0.03	0.05	0.02–0.1 (0.025 ave)[c]	0.1[c]	1–1.5[c]
1335 Steel	(0.35% C steel, 2% Mn)	0.25	0.15	0.03	0.055	0.02–0.1 (0.025 ave)[c]	0.1[c]	1–1.5[c]
1340 Steel	(0.4% C steel, 2% Mn)	0.25	0.15	0.03	0.055	0.02–0.1 (0.025 ave)[c]	0.1[c]	1–1.5[c]
Carbon Steel	Unknown composition	0.1–1.5	0.2–270[b]	0.05–50	0.05–5	0.02–0.1 (0.025 ave)[c]	0.1[c]	1–1.5[c]
HF–1 C Steel	High frag. unknown alloy	—	—	—	0.01 (est.)	0.02–0.1 (0.025 ave)[c]	0.1[c]	1–1.5[c]
316ss	Stainless Steel	<0.001	0.05	<0.001	<0.001	0.001–0.005[d]	0.03[d]	0.005–0.01[d]
1100 Al	Al– rel. pure	0.01	0.015	0.2	<0.001	0.01–0.02[d]	0.01–0.03[d]	0.03–1[d]
6061 Al	Al–Mg–Si alloy	0.25	~0.3	0.2	—	0.1–0.2[d]	0.1–0.25[d]	0.04–2[d]

[a] Assuming no stirring.
[b] The low value is for low carbon steels, the high value is for high carbon steel.
[c] The rates of carbon steel corrosion in soil environments do not vary appreciably with steel alloy type—soil variables are more important. Consequently, the general values for carbon steel corrosion rates, determined with rates in the scientific literature, are adequate for most purposes.
[d] The corrosion rates of stainless steels and Al alloys, which are rarely present in UXO, are approximations assembled from literature values.

The corrosion rates reported in Table 6 compare well with those previously determined for a variety of steel alloys. For example, the corrosion rates in well oxygenated, upland soils are generally about 0.025 mm per year. This rate is somewhat more rapid than that reported by the Lafayette model, but nearly in line with the DOE model and the Romanoff estimate for these types of soils. The rates of corrosion in Table 6 for saline and anaerobic soils also are similar to the empirical rates of Romanoff (1957), but the other models are poorly equipped to deal with these "special cases."

The rates of corrosion in aerated soils shown in Table 6 are not particularly rapid, and would lead to the uniform failure of small munitions (grenades, etc., with minimum wall thicknesses of 2–5 mm) in about 80–200 years. Larger munitions with thicker walls (5–10 mm) would fail in 200–400 years. Pitting corrosion is more prevalent than uniform corrosion in soils (Frankel 1998, Doyle et al. 2003, Norin and Vinka 2003) and produces deep pits, potentially decreasing the time required to perforate the UXO to about 20 and 50 years for small and larger munitions, respectively. These are reasonable but conservative estimates of the relative rates of both pit and uniform corrosion; Romanoff (1957) suggests that corrosion may be somewhat slower than these estimates in the environment. In reducing soils, munitions could corrode much more rapidly, in as little as a few years; consequently, the casings of munitions in wetlands likely have corroded through to the HE fill (Fig. 13). Saline environments, such as those encountered in proving grounds in arid basins such as China Lake, California, also may have saline soil chemical conditions favorable for enhanced corrosion. While saline environments such as those at China Lake accelerate corrosion, they are also dry, which slows corrosion. Salt crusts often protect water beneath the surface of salt deposits, so the soils in these saline environments may remain sufficiently moist for corrosion to occur unabated. More research is needed to reconcile the various factors that could influence corrosion in these arid environments.

Corrosion of steels in soil varies significantly, depending on the alloy type and reaction conditions (Table 6). In each case, corrosion is fastest in acidic conditions, where passivation is less pronounced, or in saline environments, where the dissolved salts increase the conductivity of the solution and chloride complexes of Al and Fe increase their solubility. Most munitions have been produced from low to moderate carbon content steels, as carbon steels have the highest strengths. This carbon steel is highly reactive, corroding more rapidly than other steels and also undergoing extensive pit corrosion. In contrast, the most stable alloys of stainless steel (e.g., Alloy 316) are nearly 100 times less reactive. Unfortunately, few munitions are constructed of stainless, as it has less desirable mechanical properties.

Figure 13. Corroded 155-mm howitzer round found in wetland sediments at Eagle River Flats, Alaska.

In summary, corrosion in soils occurs more rapidly than in solutions of a single constituent composition (e.g., NaCl). For most corroding low-carbon steels, the corrosion rate occurs at about 0.02–0.1 (average of 0.025) mm/year (Penhale 1971, Levlin 1996, Norin and Vinka 2003) in oxidizing soil environments. Steel corrosion is accelerated in sulfidic anaerobic environments, often corroding up to 1 mm/year (Hamilton 1983, 1985, 2003; Little et al. 1991; Schutt and Rhodes 1996; Kajiyama and Okamura 1999; Videla 2000; Li et al. 2001). These rates are similar to those calculated using the UXO corrosion model of Garber and Adams (included in Fabian and Ostazeski 2002), although our estimates are somewhat more general and require much less input information. Fortunately, the corrosion rate of steel in a wide variety of soils apparently only varies by a factor of 2 to 5. Conservative estimates of failure rates can be calculated based on the most rapid corrosion rate for a given soil chemical environment.

5.4 Condition of Recovered UXO

Few studies have examined soils near buried UXO to determine if the rounds were leaking explosives into the environment and, if so, what were the concentrations in the surrounding soil. High explosive-filled rounds were fired into the impact area at MMR between 1911 and 1989 (Clausen et al. 2004). Work being done by AMEC to determine the contamination source or sources at MMR found that none of the 18,000 HE-filled UXO had visibly corroded through the casing to the HE fill. They found that 148 rounds were leaking explosives but that these were cracked (44), or had undergone a low-order detonation (AMEX, in review). Of the 116 UXO found in a high use, 3.6-acre target area, most were corroded to some degree, 19 were in good condition, 11 were ruptured, 7 were leaking their

HE filler, and explosives were detected in the soil around 6 of them. Information on the exact nature of the leaks is not given.

Praxis Environmental examined soil near the nose and end of 59 HE-filled UXO that were found at four sites (Praxis 2004). A control soil sample was also taken in the pit, dug to expose the UXO, but as far from the UXO as possible. Table 7 lists the site conditions and the type and burial age of the ordnance found. The soils were analyzed for 21 explosives, propellants, or their breakdown products.

Table 7. Site characteristics for four locations where UXO were studied (Praxis 2004).

Site	Rainfall (cm/yr)	Rainfall (In./yr)	Avg. temp. (°C)	Munition type	Burial age (years)
A	109	43	11.4	60-mm mortars (7) 37-mm mortar (1) 3-in. stoke mortars (4) 81-mm mortars (3)	57–60
B	81	32	28	105-mm projectiles (3) 4.2-in. mortars (2) M1 tank mines (2)	55–60
C	135	53	17	60-mm mortars (2) M8 landmine (1) Rifle grenade (1) Unspecified (3)	52–77
D	41	16	8.3	75-mm projectile (1)	34–42

Of these 59 items, explosives were unambiguously detected around 1 (2%) UXO. This round was a 60-mm mortar—the smallest of the rounds examined and it came from site A. Soil concentrations near this mortar contained TNT, its breakdown products 4A-DNT, 2A-DNT, and manufacturing impurities 2,6-DNT, 2,4-DNT that ranged from 1600 to 34,000µg/kg (ppb). The concentrations of all the explosives were higher in soil near the mortar and lower in the control sample, 30 cm away, suggesting that explosives were moving from the perforated round to the surrounding soil. Soil adjacent to three other 60-mm mortars from this site had below-detection values of RDX, 4A-DNT, and 2-NT, and similar, low concentrations of these analytes in the control samples. These rounds lack clear evidence of leaking fill.

Even fewer studies have examined UXO in the ocean. Detonation of a bunker filled with HE munitions in 1945 sent intact and ruptured ordnance into Halifax Harbor, Canada. Scuba divers collected sediment samples next to seven munitions, four that appeared ruptured and three that appeared intact. Samples were taken at distances of 15 to 30 cm (6 to 12 in.) at the four cardinal points around each UXO (Darrach et al. 1998). A background sediment sample was also collected. Interestingly, all three intact items had detectable levels of either TNT or DNT in their surrounding soils. Low ppb concentrations of TNT or DNT were found around two intact 5-in. shells and high ppt levels of DNT were found in the sediments adjacent to a 9-in. shell. Explosives were not found in sediments surrounding any of the ruptured rounds or in the background sediment sample (Darrach et al. 1998). Apparently, any HE present in the ruptured munitions has dissolved, and been biodegraded or transported away from the round, in the 60 years since the accident. The munitions that appear to be intact, however, are slowly leaking their explosive fill into the surrounding sediments, possibly through pinhole corrosion pits. Thus, visual inspection for obvious corrosion may be inadequate for determining if the round is leaking HE into the environment.

6 STUDIES OF EXPLOSIVE RESIDUES FROM ABOVE-GROUND SOURCES

Above-ground residues result from high-order and low-order detonations, from surface UXO that are blown in place, split open, detonate sympathetically, or corrode in place. Other sources include munition firing points and open burn/open detonate operations to destroy ordnance. Estimating the load of explosives requires good records of the types and numbers of rounds fired and information on the contamination generated by individual detonations of each type of munition. Accurate range records are generally not available, and quantifying contamination by detonation type is still in its infancy.

Two types of studies have been conducted to help assess the amount of HE contamination on training ranges. In site characterization studies, soils are sampled on training ranges to provide estimates of background HE concentrations at impact areas and firing points (Jenkins et al. 1998, 2001; Thiboutot et al. 1998, Ampleman et al. 2003). Detonations of individual munitions (Jenkins et al. 2000, Hewitt et al 2003), on the other hand, measure the HE residues deposited by a single round. The latter tests are conducted on clean snow or clean tarps to minimize the amount of soil involved in the detonation and make it feasible to find and examine the detonation residues. Both types of studies were funded by SERDP and conducted by Dr. Judy Pennington and Dr. Thomas Jenkins and their collaborators (Pennington et al. 2001, 2002, 2003).

6.1 Site Characterization Studies

The explosives found in soils at different types of ranges are listed in Table 8. These include hand grenade, antitank rocket, artillery, and bombing ranges and the firing points for artillery and antitank rounds. For specifics on the sampling plans used and the explosive concentrations found, see the individual studies.

For hand grenade ranges, which are just a few acres in size and are heavily cratered, concentrations of RDX and TNT in the soil range from the high parts per billion (µg/kg) to low parts per million (mg/kg). A variety of sampling protocols was used to characterize the soils at hand grenade ranges (an example of one study is shown in Fig. 14). Soil samples were taken 1) along transects 15, 20 and 25 m from where the grenades were thrown, 2) as a function of depth (surface, 10, 15, 23, and 30 cm), and 3) around one point to assess the short distance heterogeneity (Fig. 14).

Table 8. Ranges whose soils have been analyzed for explosives. The concentrations found vary significantly, depending on where the soil samples were taken relative to targets or low-order detonation debris.

Range Location	Range Type	Contaminants	Reference
US			
Eagle River Flats, Alaska	Ordnance disposal area	2,4-DNT, TNT, RDX	Racine et al. (1992)
Fort Richardson, Alaska	Hand grenade range	RDX, and TNT	Jenkins et al. (2001)
Fort Greely, Alaska	Impact area	RDX, TNT and HMX	Walsh et al. (2001)
	40-mm impact berm	RDX, HMX, low TNT	Walsh et al. (2003)
	TOW antitank range	RDX, PETN, HMX and TNT	
	Firing points	NG and 2,4-DNT	
Fort Ord, CA	LAW rocket range	HMX and TNT	Jenkins et al. (1998)
Pohakuloa Training Area, Hawaii	Firing points	NG and 2,4-DNT	Hewitt et al. (2004)
	Impact range	NG and 2,4-DNT	
	Hand grenade range	RDX, TNT and HMX	
	Demolition range	RDX,HMX,NG,2,4-DNT,TNT	
Scholfield Barracks, Hawaii	Firing points	NG and 2,4-DNT	Hewitt et al. (2004)
	Artillery impact range	low RDX, 2ADNT & 4ADNT	
	Demolition range	RDX and HMX	
	Anti-armor range	HMX,TNT,RDX,TNB & NG	
	Hand grenade range	TNT, RDX and HMX	
MMR, Massachusetts	Firing points	NG and 2,4-DNT	Ogden (2000)
	Central impact area	RDX, TNT, 2ADNT& 4ADNT	AMEX (in review)
	Gun & mortar firing points	2,4-DNT and 2,6-DNT	
	Southeast ranges	HMX, RDX	
	Demolition Area 1	RDX, TNT, HMX & DNTs	
	Rocket range	NG> HMX,RDX, & TNT	
Camp Shelby, Mississippi	Firing points	NG and 2,4-DNT	USACHPPM (2000)
Fort Bliss, New Mexico	Artillery targets	HMX,RDX, TNT & NG	Pennington et al. (2003)
	Firing points	NG	
Fort Lewis, Washington	Impact area	RDX, TNT & DNTs	Jenkins et al. (2001)
	Artillery firing points	2,4-DNT and other DNTs	
	Hand grenade range	RDX, TNT and HMX	
Yakima Training Center, Washington	Antitank range	HMX>RDX>>TNT	Pennington et al. (2002)
	Tank firing points	NG, 2,4-DNT,2,6-DNT	
	Howitzer firing Points	NG and 2,4-DNT	
	Mortar firing points	NG	
	Central impact area	RDX,	

Range Location	Range Type	Contaminants	Reference
Camp Guernsey, Wyoming	Artillery impact area	HMX, 2ADNT and 4ADNT	Pennington et al. (2002)
	Atrillery firing points	below detection	
Canada			
Cold Lake Air Weapons Range, Alberta	Bomb impact area	mainly TNT and RDX	Ampleman et al. (2003b)
	Ordnance disposal area	2,4-DNT and TNT	
Western Area Training, Alberta	Antitank range	HMX>> TNT	Thiboutout et al. (1998)
CFB Chilliwack, British Columbia	Hand grenade range	TNT, RDX and HMX	Ampleman et al. (2000)
	Antitank range		
CFB Shilo, Manitoba	Hand grenade range	TNT, RDX, tetryl, HMX and breakdown products	Ampleman et al. (2003)
	Battleruns	TNT,RDX,NG and 2,4-DNT	
CFTR Tracadie, New Brunswick	Artillery range	below detection	Ampleman et al. (2000)
CFB Gagetown, New Brunswick	Antitank Range	HMX and TNT	Dube et al. (1999)
	Grenade range	TNT and RDX	
	Anti-armor firing points	NG and 2,4-DNT	Thiboutout et al. (2003)
	Anti-armor impact area	RDX, TNT, HMX & NG	
	Rocket range firing point	NG	
	Rocket range impact area	HMX>TNT>RDX	
	Grenade range	RDX,TNT, HMX	
	Impact range	mainly RDX and TNT	
	Ordnance disposal area	mainly 2,4-DNT	
CFB Dundurn, Saskatchewan	Antitank range	HMX>> TNT	Thiboutout et al. (1998)
CFB Valcartier, Quebec	Antitank range	HMX>> TNT	Thiboutout et al. (1998)

Antitank rocket ranges are much larger than grenade ranges, often hundreds of acres in size. The most common antitank rocket, the M-72 LAW, is filled with Octol, a 70% HMX, 30% TNT mix. HMX is the major high explosive contaminant found in soil, followed by TNT concentrations that are two orders of magnitude lower than the HMX because TNT degrades much more readily than HMX. The HE residues are found mainly in the top 10 cm of the soil and the concentrations decrease with distance from the target. The LAW rocket is a line of sight rocket that burns a double base propellant all the way to the target. Chunks of propellant are often found at the firing points and NG from the propellant is generally detected along the track between the firing point and the target. Because the LAW is a thin-skinned rocket that is fired parallel to the ground, it is susceptible to rupture if it misses its target and intersects the ground at a shallow angle. Carcasses of these rounds are often observed at MMR (AMEX, in

review) and a 48% dud rate was reported for a test in which 220 were fired (Thiboutot et al. 1998).

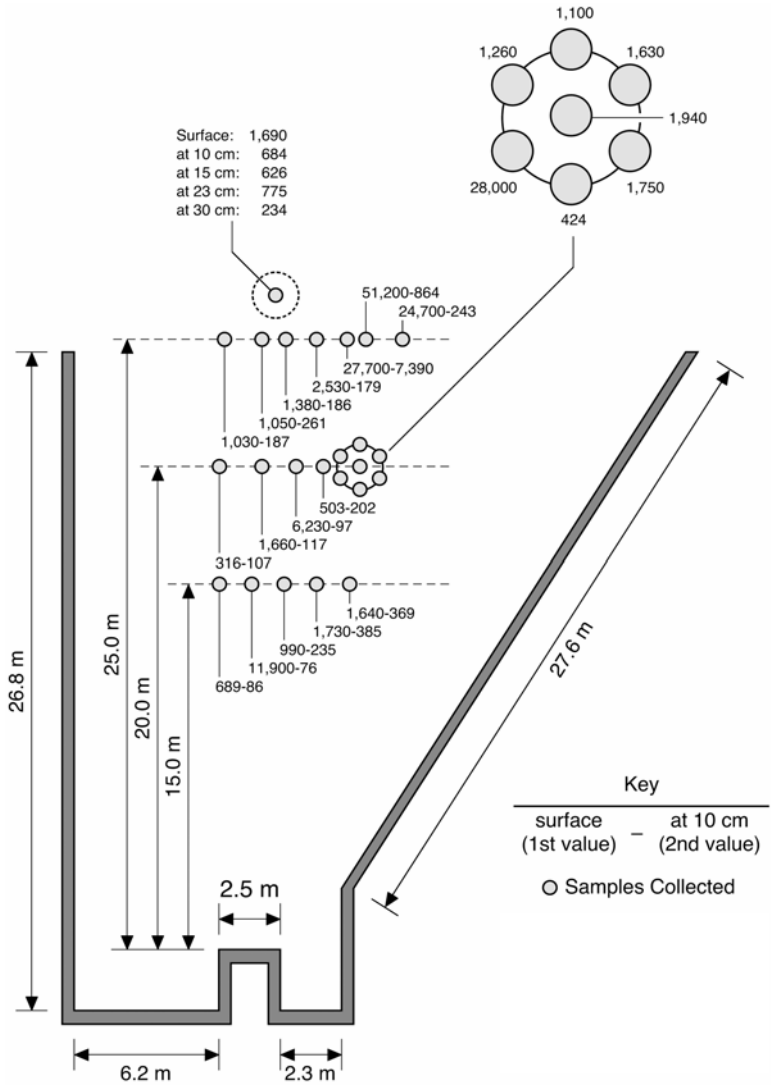

Figure 14. Sampling grids used for a hand grenade range on Fort Lewis, Washington.

Artillery ranges are very large and often many different types of ordnance have been fired into these areas. Surface and sub-surface UXO are present. Soil samples of the impact areas were found to have low ppb concentrations of TNT, RDX, HMX, and NG. Very high concentrations were found near low-order detonations where part of the round and its fill were lying on the ground (Fig. 15).

Because these ranges are so large, a random stratified sampling scheme, like that used for the small hand grenade ranges, would be unlikely to find those areas near targets or low-order detonations where explosive are found as chunks on the ground (Fig. 16). For large ranges, non-random, judgmental sampling at heavily contaminated sites is needed to characterize the widely scattered contaminated sites within a much larger uncontaminated range.

Figure 15. Low-order detonation of a 155-mm round.

Figure 16. Pieces of explosives collected from a 10- by 10-m area on Fort Bliss, New Mexico.

Considerable contamination also may result from firing a weapon, even if the munition detonates successfully. The firing points for 105- and 155-mm howitzers and 60- and 81-mm mortars were sampled to test this idea. The howitzer rounds use a single base propellant consisting of NC fibers impregnated with 2,4-

DNT, which were easily seen when firing occurred on a snow cover (Fig. 17). Walsh et al. (2001) found that firing points were often contaminated with 2,4-DNT from single based propellants and with NG from double and triple based propellants. Samples collected at 10-m intervals, 120 m down range from a howitzer muzzle and 90 m on either side of the gun contained 2,4-DNT at an average concentration of ~1 mg/kg (ppm) (Walsh et al. 2004).

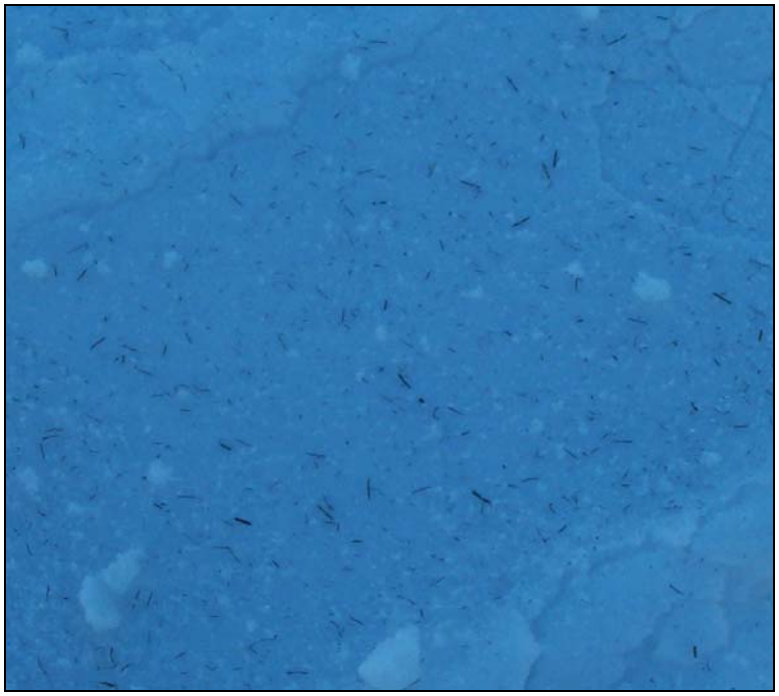

Figure 17. Propellant grains on snow at howitzer firing point, Fort Richardson, Alaska.

Bombing ranges are hundreds of acres in size. At the ranges studied, the surface soil had TNT concentrations as high as 400 mg/kg (ppm). Bomb payloads can be very large (230–910 kg, 500–20,000 lb) and one low-order detonation or a sympathetic detonation of a UXO from a nearby detonation can add kilograms of explosive to the soil (Fig. 18). Furthermore, these processes may emplace large masses of HE at a single site, both limiting dispersal, and, potentially, increasing the threat of extreme localized contamination. Both the U.S. and Canada perform regular maintenance to remove surface UXO from bombing ranges. The purpose of the maintenance is not to mitigate contamination, rather it is to decrease the explosion hazard. To minimize environmental hazards, large, intact explosive pieces should also be removed and disposed of in a way that does not scatter explosive particles into the environment.

Figure 18. Low-order detonation of a 500-lb bomb.

These studies indicate that explosive residues are not homogeneously distributed on training ranges, but are localized in hot spots. Areas with high explosive concentrations are often found around carcasses of munitions that were only partly detonated. Heavily cratered areas often have below detection or low HE concentrations, suggesting that high-order detonations leave only trace amounts of HE residues. The heterogeneity and non-random distributions of explosive residues need to be considered when evaluating the contamination risks associated with UXO and HE pieces.

6.2 Explosive Residue from Individual Detonations

Knowing the amount of HE residue deposited by an individual munition and how this varies among multiple detonations of the same munition is important to better estimate total HE loading at firing ranges. The explosive residue generated by individual munitions, coupled with firing records of the number and type of round fired, could be used to estimate the load of explosives on a range. The difficulties encountered in this approach include 1) the lack of accurate firing records over the lifetime of the range, 2) knowing the area over which the HE residue is deposited, and 3) obtaining representative samples that can accurately determine an average concentration. Nevertheless, investigations examining individual detonations provide considerable insight into the release of HE into the environment.

6.2.1 Rounds Fired into Snow-Covered Ranges

To estimate the mass of explosives remaining after high-order detonations, Jenkins et al. (2000) collected and analyzed residue-covered snow samples from wintertime detonations. The frozen ground minimized soil contamination, and the snow provided a clean sampling background that decreased the chances of cross-contamination from prior range activities. The snow also made the dark

detonation residue highly visible, allowing the residue plume to be mapped and measured. Jenkins et al. (2000) used multiple snow samples, taken within the residue plume, to estimate the deposited mass of explosive from high-order detonations. The sampling has yielded consistently low explosive concentrations, $\mu g/m^2$ quantities, for a variety of tactically detonated munitions (Table 9, Jenkins et al. 2000, Hewitt et al. 2003).

Table 9. Concentration of high explosives found after live fire into snow covered ranges. The rounds were all filled with Comp B. All data from Hewitt et al. (2003).

Item	Munition	Explosive fill (g)	Number samples /test	Sampled area (m^2)	Estimated total mass deposited (µg)			
					TNT	RDX	HMX	Other
Mortars	60-mm	360		2.8	bd	5.2	3.9	
				5	2.2	6.6	0.57	
				4.3	11	28	4.5	
				7.8	40	150	43	
				3.6	17	180	42	
	81-mm	930	14	15.1	2,200	5,300		3,100[c]
			43	75	1,000	8,500		4,600[c]
								Residue from thirteen 81 mm mortar rounds
	120-mm	2990	18	30	170	1,100	87	94[a]
			5	24	16	460	23	140[a]
			8	5.6	370	2,400	150	7,200[a]
			7	7.2	42	790	48	220[a]
			8	10.2	47	430	37	260[a]
			7	6.1	1,500	16,000	410	720[a]
			7	10.4	150	5,300	60	130[a]
Howitzer	105-mm	2090	7	7	130	84		
			15	15	290	170		
			8	8	210	170		
			31	31	250	82		Residue from four 105-mm rounds
			22	22	43	25		
			10		130	56		
			8	8	29	260		
			8	8	160	100		
			6	6	210	38		
Rifle grenades	40-mm	32		2	7.7	1,400	180	
				3.6	6.8	3,400	440	
				2.5	1.1	25	15	

Item	Munition	Explosive fill (g)	Number samples /test	Sampled area (m^2)	Estimated total mass deposited (µg)			
					TNT	RDX	HMX	Other
Hand Grenade	M67	186	6	7.6		22		13[b]
			4	5		17		13[b]
			5	5.5		10		11[b]
			5	5.4		9		6[b]
			4	9.1		13		5[b]
			5	7		28		5[b]
			14	22.7	ND	57		14[b]
Torpedo	Bangelore		7	12.5		90,000	20,000	
Shape Charge			10	12		4,200,000	340,000	

a NG
b 2,6-DNT
c 4AmDNT

6.2.2 Blow-in-Place Detonations on Snow

Many different blow-in-place studies have been conducted and the results of some of these tests are listed in Table 10. These are sometimes used as proxies for live-fire tests. Although live-fire tests more accurately represent the residues deposited by training, they are difficult to sample as rounds may not land in the desired area and trays cannot be put out to collect particles. The blow-in-place tests, however, provide information on contamination resulting from the blow-in-place operations used to dispose of ordnance on ranges.

Hewitt et al. (2003) found that high-order detonations produced by blow-in-place procedures leave more explosive residue than rounds that are fired. This suggests that the way in which the detonation was initiated, specifically whether the designed initiation train was used (fuze, booster), can affect the amount of HE remaining.

For blow-in-place detonations of 155-mm howitzer rounds Taylor et al. (2004a) found particles of TNT both in snow samples and in two of the four aluminum trays (north and east trays) placed 20 m around the point of detonation (Fig. 19). The variability in TNT concentration seen in the snow samples collected within the plume (Tables 11 and 12) suggests that the TNT particles, not the ubiquitous soot, carry the TNT. Particles of TNT were found on the north tray—outside the plume area (Fig. 19). This finding suggests that the TNT particles, because of their greater size and mass, are not as affected by wind conditions as the soot. It also suggests that estimates of HE deposition, based on the

plume area, may underestimate the HE deposited if particles are routinely found outside the plume area.

Table 10. Concentration of high explosives found after blow-in-place operations on snow. The data from Valcartier Quebec are from Lewis et al. (2002); all the rest are taken from Hewitt et al. (2003)

Munition		Fill	Wt. Fill (g)	Wt. C4 (g)	Number samples per test	Estimated total mass deposited (µg)			Installation
						TNT	RDX	HMX	
Mortar	60-mm	TNT	300	286.5	4	52,000	22,000		Valcartier, Quebec
					4	8,700	28,000		
					4	960	20,000		
					3	1,100	9,000		
			300	95.5	2	6,900	81,000	20	
					3	450	18,000		
					2	3,200	96,000	140	
					4	6,300	75,000		
	81-mm	Comp B	950	570	7	38	12,000	2,600	Camp Ethan Allen, VT
	81-mm	Comp B	816	286.5	4	6.20×10^6	13,000		Valcartier, Quebec
				286.5	4	160,000	6,900		
				115	1	18,000	5,200		
				76.4	3	27,000	15,000	34	
				76.4	2	150,000	8,800		
				76.4	3	33,000	39,000	6,000	
Howitzer	105-mm	Comp B	2000	191	3	2.50×10^6	24,000		Valcartier, Quebec
	155-mm	TNT	6800	570	15	110×10^6			Camp Ethan Allen, VT
					7	38×10^6			
					11	45,000			
					9	500			
					10	6.9×10^6			
					10	200,000			
					11	80,000			
Torpedos	Bangalor	Comp B	4860		11	150	110,000	18,000	Fort Drum, NY
Antitank mines	M19	Comp B	9530	280	11		2,700	8,300	
	M15	Comp B	10300	280	13	76	40,000	4,100	

Munition		Fill	Wt. Fill (g)	Wt. C4 (g)	Number samples per test	Estimated total mass deposited (µg)			Installation
						TNT	RDX	HMX	
Anti-personnel mines	Claymore	C4	680		7		13,000	3,000	Camp Ethan Allen, VT
					7		6,100	3,000	
					12		1,900	1,800	
					7		5,700	2,500	
					8		1,100	390	
					6		26,000	9,500	
					7		17,000	4,800	
					6		50,000	34,000	Fort Drum, NY
Anti-personnel mines	PMA-1A	TNT	200	b.c.	7	280,000			Camp Ethan Allen, VT
					8	1.1×10^{6}			
	PMA-2	TNT	100	b.c.	5	2300	640		
					8	550,000	1,500		
			100	9.5	1	1.7×10^{66}	120,000		Valcartier, Quebec
			100	38.2	1	40×10^{6}	990,000		
					2	3,700,000	33,000		
	PPM-2	TNT	130	280	7	980,000	47,000	7,900	Camp Ethan Allen, VT
					8	6.6×10^{6}	42,000		
	VS-50	RDX	43	280	8		140,000	5,300	
	VS-50				8		89,000	3,000	
C4 blocks		94% RDX	570	b.c.	9		38,000	16,000	Camp Ethan Allen, VT
					16		12,000	5,100	
					8		18,000	6,200	
					7		3,600	550	
					8		12,000	4,100	
					8		3,900	3,000	
					7		3,100	2,000	
					6		4,300	2,000	
Hand Grenades	M67	Comp B	176	0	5	2,800	350		Valcartier, Quebec
					2		200		
					2		1,400	110	
					4	3,500	540	78	
		Comp B	176	191	4	1,300	160,000	56	
					2	7,300	260,000	210	
					3	5,900	130,000	120	
					4		210,000	390	

Figure 19. Locations of snow samples and the trays (marked by triangles) at Camp Ethan Allen relative to the detonation point. Soot darkened areas of snow (the plume) are delineated, the visible plume by the outer line and the sootiest area by the inner line.

Table 11. HE mass recovered from blow-in-place of seven 155-mm rounds.

Test	Number of samples averaged	Avg. TNT conc.	Std. Dev	Plume area (m^2)	Plume mass	Crater mass	% Recovered
1	15	220 mg/m^2	337 mg/m^2	496	109 g	1.8 g	1.64
2	9	124 mg/m^2	203 mg/m^2	311	38.3g	0.11 g	0.568
3	11	118 µg/m^2	222 µg/m^2	345	40.4 mg	7.1 µg	5.98×10^{-4}
4	9	1.47 µg/m^2	2.34 µg/m^2	344	0.5 mg	3.64 µg	7.40×10^{-6}
5	11	16.9 mg/m^2	12.6 mg/m^2	406	6.8 g	19 mg	0.101
6	10	679 µg/m^2	1774 µg/m^2	301	204 mg	0.4 µg	3.02×10^{-3}
7	11	168 µg/m^2	243 µg/m^2	476	79.8 mg	0.2 µg	1.18×10^{-3}

Table 12. Individual sample concentrations for the first test.

Sample test 1	Distance to crater (m)	Sample area (m^2)	TNT conc. (mg/m^2)
S-1*	12.6	1.0	184
S-2	10.0	1.0	49.0
S-3	8.3	1.0	170
S-4	6.2	1.0	200
S-5	3.8	1.0	530
S-6	1.8	1.0	330
S-7	2.0	1.0	19.0
S-8	4.4	1.0	1.00
S-9	6.0	1.0	3.20
S-10	8.0	1.0	4.30
S-11	1.5	1.0	1300
S-12	4.0	1.0	340
S-13	6.6	1.0	140
S-14	4.6	1.0	15.0
S-15	6.8	1.0	21.0
Crater**	—	1.0	1800
Avg. *n*=15			220
Std. Dev			337
Area of soot plume		496 m^2	

*Estimated from particle counts in the filter and TNT concentration in the melt.
** Not included in average.

6.2.3 Explosive Residue from Individual Low-Order Detonations

To estimate the mass of explosives remaining after low-order detonations, Pennington et al. (2003) sampled the residues from detonations on a large tarp at Blossom Point (BP), Maryland. The tarp also helped minimize any cross-contamination from the underlying soil and made it easier to see and pick up the explosive pieces scattered by the detonation. Taylor et al. (2004a) measured the mass of scattered Comp B and TNT and the resulting particle size distributions for one 81-mm and one 155-mm low-order detonation (Fig. 20). The low-order detonations produced a wide range of particle types; they ranged from crystalline to partially or totally melted (Fig. 21). For the 155-mm low-order detonation, most of the HE mass deposited was in centimeter-sized pieces, whereas particles

less than 1 mm in size were responsible for most of the surface area of the deposited HE (Fig 22). For the 81-mm low-order detonation, 50% of the HE mass was in pieces smaller than 1 cm, whereas particles less than 1cm in size were responsible for 80% of the surface area of the deposited HE (Fig. 23). The number of HE particles and their sizes were measured as a function of distance from the detonation for the 81-mm round. The number of particles was found to decrease rapidly away from the detonation point, but the average size of the particles increased with distance (Taylor et al. 2004b).

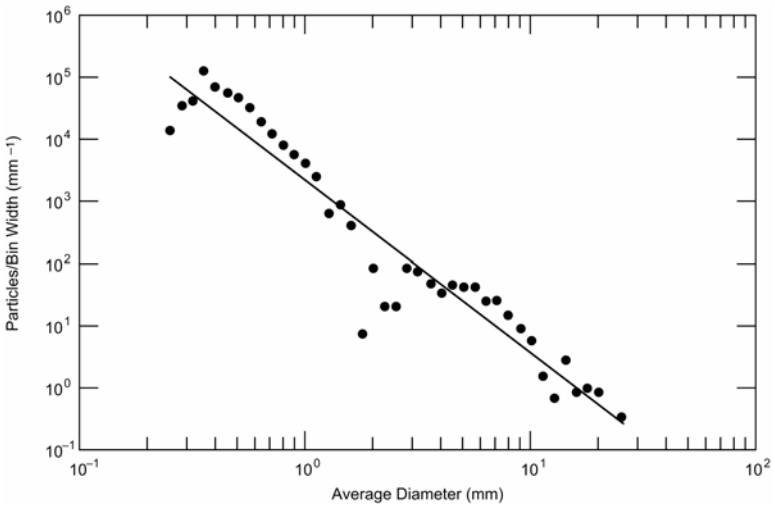

a. 81-mm mortar.

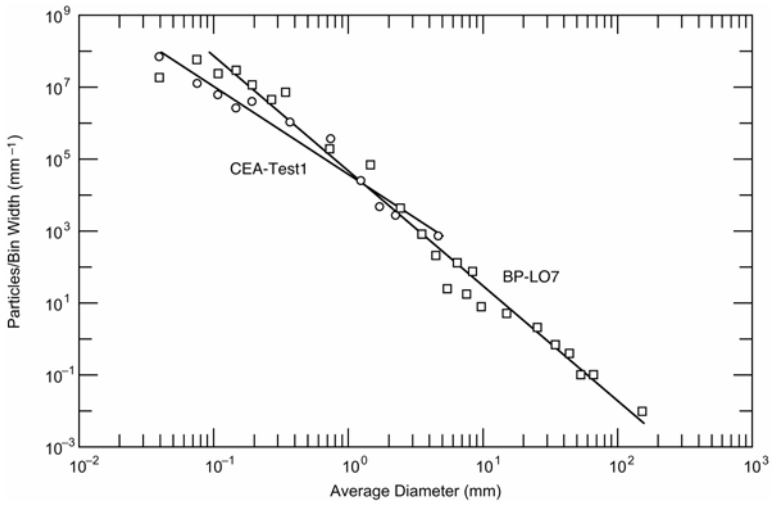

b. 155-mm shell.

Figure 20. Size distribution of HE particles collected from low-order detonations.

Figure 21. Variety of Comp B particles.

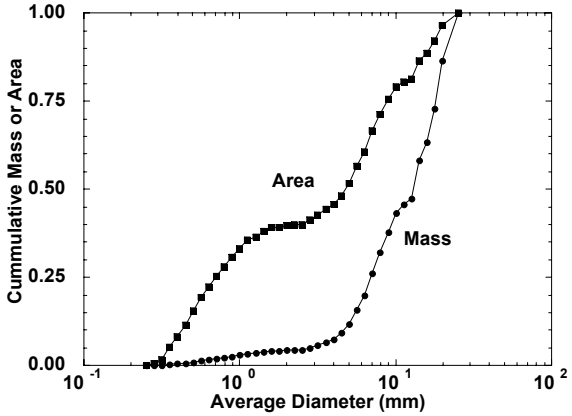

Figure 22. Cumulative mass and surface area of HE residue collected from a low-order detonation of an 81-mm mortar.

Underwater low-order detonations were conducted at Aberdeen Test Center to determine if these could reliably reduce blast effects from underwater detonations (Pedersen et al. 2002). Blast effects from high-order underwater detonations can harm marine mammals and destroy coral reefs (Pedersen et al. 2002 and references therein). Tests were conducted on 155-mm projectiles and Mk 82 bombs. Low-order detonations were achieved in all 21 of the 155-mm trials and in 8 of 11 Mk 82 Bomb trials. Debris from 16 tests of 155-mm shells and 13 tests of Mk 82 bombs was captured with a closed weave cargo net (of unknown mesh opening) positioned about 5 m beneath the detonation. For the 155-mm projectiles, between 9 and 47% of the initial 7-kg fill was recovered as explosive pieces (av-

erage 24 ± 13%). For the Mk 80 bomb, of the initial 87 kg of tritonal, 41 to 89% was recovered as chunk material (average 72 ± 13%). The values are minimum estimates as, in all likelihood, some small pieces were not captured by the net or were missed by the divers sent to retrieve them.

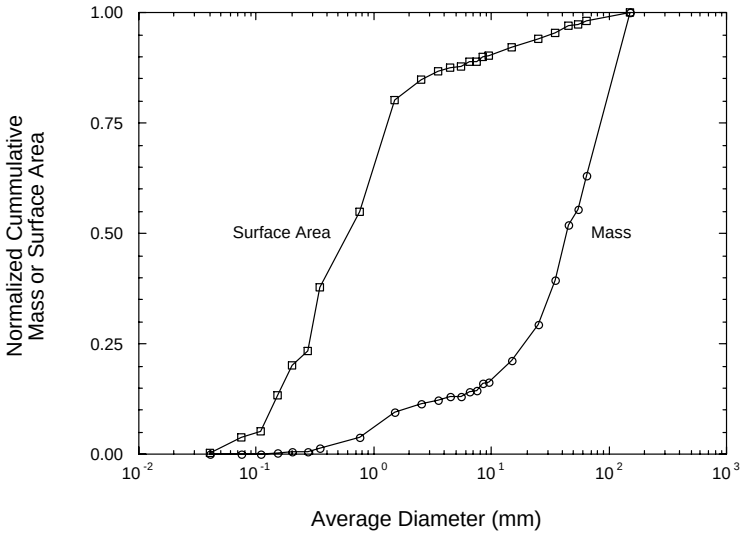

Figure 23. Cumulative mass and surface area of HE residue collected from a low-order detonation of a 155-mm artillery shell.

6.3 Sampling Problems and Sub-sampling Issues

An important issue for all of these studies is how to collect representative samples. Efforts to estimate a mean explosive concentration from the residues of an individual detonation often yield disparate results. The reason is that high explosives such as TNT and RDX are solids at environmental temperatures, and their residues exist as particles of various sizes (Radtke et al. 2002, Taylor et al. 2004a,b). Also, post-blast residues from detonations of HE ordnance are non-uniformly dispersed, resulting in extreme spatial heterogeneity of the explosives. Explosive concentrations in soil samples taken near a detonation therefore often range over orders of magnitude and are not normally distributed.

Given that the HE residues are particulates that are non-uniformly dispersed in a particulate media, and that residue samples are inherently heterogeneous, sampling error is unavoidable and one needs to understand the sources of error to minimize it (Walsh et al. 2002). Pierre Gy developed theories on the sources of

sampling error and based on these theories, Francis Pitard developed practical sampling methods (Pitard 1993). The heterogeneity attributable to the complex mixture of components that make up the HE-contaminated soil or snow is termed constitutional heterogeneity (Pitard 1993), and the error associated with constitutional heterogeneity is called fundamental error. Fundamental error is minimized if a sample includes all constituents in the same proportions as the HE-contaminated soil or snow (i.e., all constitutive elements have an equal probability of being selected for a sample). In other words, the sample must contain in the proper proportion all the different sizes and compositions of the HE particles.

Walsh et al. are developing multi-increment or composite sampling methods that reduce the fundamental error and improve estimates of average HE concentrations in soil. A sufficient number of increments must be taken to minimize the error associated with the distributional heterogeneity of the HE residues, and the sample mass must be large enough to minimize the error associated with compositional heterogeneity. Grinding and homogenizing the sample also helps obtain a reproducible average concentration. Replicate samples from a hand-grenade range indicated that 50-increment 4-kg samples were adequate to estimate residues from grenade detonations (Walsh et al. 2002).

Figure 24 illustrates how composite samples can decrease the variability and provide a better estimate for the mean concentration of a sample. A frequency diagram of the individual NG concentrations found in soil show an order-of-magnitude variation in the concentration (Fig. 24a). If individual concentration values are randomly chosen and combined mathematically to simulate multi-increment samples that contain 5, 30, and 50 samples, one can see that, as the number of increments increases, the variability is reduced and the data become normally distributed (Fig, 24b,c,d). This effect can also be observed with composite soil samples collected in the field. As the number of composites making up a sample increases, the data begin to plot as a straight line on a probability plot (Fig. 25), indicating a normal distribution.

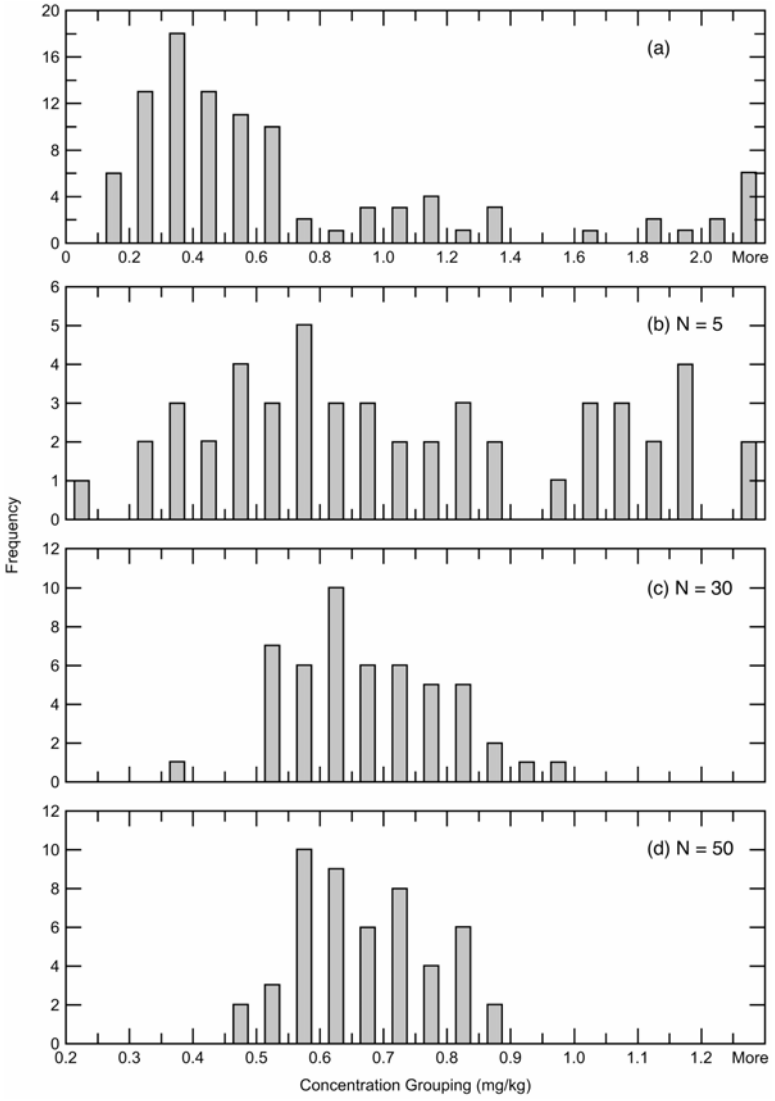

Figure 24. Concentration distribution of NG in soil samples (a) and the change in the distribution if 5 (b), 30 (c), and 50 (d) randomly selected samples are mathematically combined into composite samples.

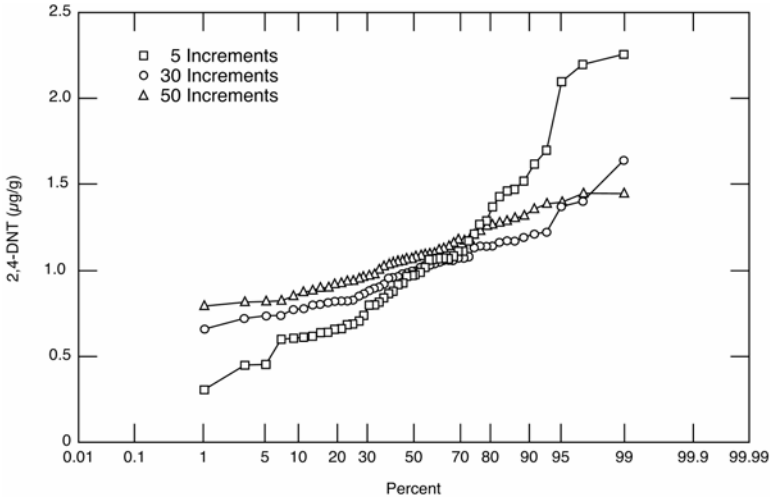

Figure 25. Probability plot showing how increasing the number of sub-samples in a composite sample gives rise to distributions that are normally distributed (straight line on the plot).

7 DISSOLUTION OF HE MASSES

Environmental contamination by HE residues from HO detonations, LO detonations, or duds occurs through dissolution by rainwater. The size of the HE residues varies from the full explosive filler (tens of centimeters) to small particles from HO detonations (micrometers in size). Here, we review efforts to quantify dissolution rates for HE masses as a function of particle size, HE type, flow rate and temperature. Table 13 compares estimates for dissolution times versus HE particle size using data and assumptions from these sources.

Table 13. Comparison of expected dissolution times (years) by particle size based on 75 cm/yr rainfall.

Source and method	Matyskiela (2003): –Dissolution theory for neat Comp B mass in porous soil. –Time based on theory that includes size effect.	Lynch et al. (2002): –Stirred volume, 0.04–4 mm RDX and TNT particles. –Time based on constant dissolution coefficient (eq 8).	Phelen et al. (2003): –Uniform porous flow, 0.1-mm and 1-mm Comp B particles. –Time based on scaled experiment duration.	Lever et al. (in prep) –Dripped flow, single 2-mm Comp B particle. –Time based on constant mass-loss rate
HE Particle Size (mm)	Comp B	RDX/TNT	Comp B	Comp B
0.1	0.8	0.005/0.001	0.8	0.004
1	20	0.05/0.01	20	4
10	800	0.5/0.1		4000
100	20,000			

Average annual rainfall in the U.S. varies from a low of about 13 cm/yr in Nevada to a high of about 250 cm/yr along the Pacific Northwest (Department of Commerce 1968, Wexler 1991). Most of the country falls in the range 50–150 cm/yr, and 75 cm/yr represents a reasonable average value. Instantaneous rainfall rates are much higher, broadly ranging 0.1–10 cm/hr, with typical values of the order 1 cm/hr. Stable-isotope measurements indicate that most rainfall percolates directly into the soil and, except in areas having highly impermeable surfaces (urban areas), very little runs overland into rivers (Buttle 1997). This is true even for storms. Consequently, instantaneous rainfall rates approximate instantaneous infiltration rates. Because HE dissolution rates can vary with flow rate, it is important to conduct laboratory measurements or theoretical analyses with realistic infiltration rates to estimate field dissolution rates. Provided this is done, total annual rainfall will scale total annual dissolved mass. We will use 75 cm/yr for this purpose.

Matyskiela (2003) modeled the mass transfer (dissolution) of a “neat” cylindrical block of Comp B in direct contact with porous soil. This model includes both diffusion and advection of dissolved RDX and TNT through a stagnant

boundary layer adjacent to the Comp B block. It treats these two constituents independently. For dissolution of Comp B through a shell casing newly perforated by corrosion, it assumes a stagnant boundary layer is created by capillary suction of water into the gap between the explosive fill and the casing. Dissolution is then by diffusion only, and the active open area is the small (1-mm-diameter) pinhole. The theory includes the dimensions of the cylindrical block, and the region of validity is defined by $VR/D_j > 4$, where V is pore water velocity, R is block radius and D_j is diffusion coefficient for component j. Assuming 1 cm/hr infiltration rate and 50% soil porosity, we can apply the theory to RDX particles larger than about 0.2 mm and TNT particles larger than about 0.5 mm. These sizes correspond roughly to ~ 0.6-mm-scale particle of Comp B. Matyskiela (2003) computed RDX and TNT dissolution rates for a 1-kg block of Comp B using parameters for 10 sites where UXO have been recovered. The largest infiltration rate at these sites was 26 cm/yr. He examined the influence of infiltration rate by using generic soil conditions with measured 5-minute rainfall rates. He also examined the effect of particle size on dissolution of RDX using a 25-cm/yr infiltration rate.

The analysis provides several results of interest. Firstly, diffusion is negligible relative to advection for all rainfall rates and sites examined. Secondly, advection mass-transfer varies as $V^{1/2}$, so mass-loss based on annual average flow, rather than "burst" rainstorm flow, probably overpredicts actual loss rates for a site. This is because the rate of dissolution increases proportionally less than the duration decreases for the same total annual rainfall. Thirdly, dissolution rates for 1-mm pinhole perforation of a shell casing are about 10^{-7} times those of a neat block. Considering that corrosion of the pinhole opening will require tens of years, buried UXO will probably have negligible contamination potential unless the initial impact or later nearby detonations split open the casing or until long-term corrosion effectively renders the casing permeable to water flow.

Matyskiela's results highlight the importance of using realistic infiltration rates to calculate dissolution rates. At the single site examined, the annual infiltration rate was 30 cm/yr. The calculated dissolution rate decreased by a factor of ~ 8 when based on 5-minute, rather than annual, infiltration rates. Thus, the $V^{1/2}$ dependence implies that the effective average infiltration rate was ~ 0.2 cm/hr, near the low end of typical rainfall rates.

The explicit dependence of advection dissolution rate on particle radius, $R^{-3/2}$, allows us to apply Matyskiela's model to predict dissolution time-scale across the particle sizes of interest. However, we must make two assumptions: 1) that dissolution of RDX establishes the time scale for dissolution of Comp B because it dissolves more slowly than TNT, and 2) that the ratio of effective aver-

age infiltration rate to annual rainfall rate is approximately the same for all sites. Note that this last assumption yields an effective average infiltration rate of ~ 0.5 cm/hr for an annual rainfall rate of 75 cm/yr.

Table 13 shows the resulting predictions for dissolution time-scale versus particle size. For example, a buried 1-kg (~ 10-cm-scale) neat block of Comp B will require about 20,000 years to dissolve. Of course, this time applies after the shell casing has effectively disappeared (complete corrosion or fracture by nearby detonations). The model's $R^{-3/2}$ dependence suggests that a 1-mm particle will dissolve after about 20 years. Because the particles become smaller as they dissolve, these times slightly overpredict dissolution time, but they are adequate estimates for the general time scales.

Lynch et al. (2002) dissolved small quantities of TNT, RDX, and HMX in a fixed water volume while stirring at a constant rate and temperature. The outcome was the initial dissolution rate, measured before the bulk concentration of HE exceeded 20% of the saturated concentration and particle area loss exceeded 5%. Particle sizes ranged from 0.04–4 mm and surface areas were based on military specifications (RDX and HMX) or microscopic measurements (TNT). Tests were conducted at 10 to 30°C and several mixing rates between 90 and 250 rpm.

The underlying mechanism of dissolution for this experiment is diffusion of HE through a stagnant layer surround the particle:

$$V\,dC/dt = \mathrm{D}/h\,S\,(Cs - C) \tag{2}$$

where

V = volume of water

t = time

C = HE concentration in the water

D = diffusion coefficient

h = stagnant layer thickness

S = particle surface area

Cs = saturation concentration of the HE in water.

The particle mass loss rate is

$$-dM/dt = kS \tag{3}$$

where M is particle mass and k is the dissolution coefficient. Comparing eq 2 and 3 for $C << Cs$ indicates that k varies inversely with stagnant layer thickness:

$$k = D/h\ Cs \tag{4}$$

The role of increased stirring (or turbulent energy in the flow) is to decrease h and consequently increase k. The authors argue that the range of mixing power input in the experiments broadly overlaps the power of rainfall for the U.S., and, thus, the measured dissolution rates should approximate field values for similar particles. At 20°C and 150 rpm, the measured dissolution rates were TNT = 1.4×10^{-2} (mg/min)/cm^2, RDX = 3.0×10^{-3} (mg/min)/cm^2, and HMX= 1.3×10^{-2} (mg/min)/cm^2. For roughly spherical particles of radius r and density ρ, we may approximate the mass loss as

$$dM = \rho\ S\ dr \tag{5}$$

Substituting eq 5 into 3 yields

$$dr/dt = -k/\rho = (D/h)(S/\rho) \tag{6}$$

If dissolution rate k (or stagnation layer thickness h) is independent of particle size, integration of eq 6 yields

$$r(t) = r_0 - k/\rho\ t \tag{7}$$

where r_0 is the initial particle radius. Setting $r(t) = 0$ provides an estimate of dissolution time τ for the particle:

$$\tau = r_0\ \rho/k \tag{8}$$

Note that if the stagnation layer thickness scales with particle size, the dissolution rate will increase with decreasing particle size and eq 8 will overestimate the time for complete particle loss. Nevertheless, based on eq 8 and the dissolution rates measured by Lynch et al. (2002), the time taken for 1-mm-diameter HE particles to dissolve would be about 4 days for TNT and 20 days for RDX. The corresponding times for 0.1-mm particles would be 0.4 days and 2 days, while for 1-cm particles the times would be 40 and 200 days for TNT and RDX, respectively. These times are much shorter than the predictions based on Matyskiela (2003) (Table 13).

Phelan et al. (2003) layered Comp B particles within a matrix of glass beads in a cylindrical column and subjected them to steady water flow through the porous medium. The particles were sieved to produce narrow size distributions centered on 0.1- and 1-mm diameters. The experiments were run at room temperature (~ 20°C). Infiltration rates ranged 0.16 to 0.70 cm/hr, within the range of rainfall infiltration rates. The corresponding pore velocities were 0.55 to 2.4 cm/hr. The concentration of TNT and RDX in the effluent was measured at regular intervals, and the TNT and RDX residues in the glass-bead matrix were measured at the end of each experiment to check for mass balance. Bed loading (i.e., Comp B concentration in the bed layer) was sufficiently high in some cases that interaction between Comp B particles in the bed layer probably occurred. Here, we consider only the results from the bed loads where the Comp B particles occupied less than 10% of the cross-sectional area of the column.

Measured mass balances for RDX ranged between 59 and 174% with most tests falling in the range 80–90%. For TNT, measured mass balances ranged between 35 and 89% with most tests falling in the 50–70% range. The authors could not account for these low values. The five tests that used 0.1-mm particles and constant infiltration rate of 0.35 cm/hr had an average duration of about 160 hours, and the effluent accounted for about 96% of the recovered mass. We may assume that all 0.1-mm Comp B particles would dissolve, based on a total infiltration of 160 hr/0.96 × 0.35 cm/hr = 57 cm.

The experiments showed a very minor effect of flow velocity on dissolution rate; scatter between nominally identical tests was more significant. Because the velocities used were within the range for typical rainfall infiltration rates, the dissolution rates should approximate field values. We may thus use total infiltration to scale dissolution time. The resulting estimate to dissolve 0.1-mm Comp B particles at the U.S. average annual rainfall is 57 cm/(75 cm/yr) = 0.8 yr.

The single low-concentration test with 1-mm Comp B particles ran for about 300 hours at a 0.35-cm/hr infiltration rate. The effluent accounted for only 3% of the recovered RDX and 11% of the recovered TNT. These results suggest that about 4300 hours or 1500 cm total infiltration would be needed to dissolve 1-mm Comp B particles. Thus, the expected dissolution time for 1-mm Comp B particles would be about 20 years for the U.S. average annual rainfall. These are remarkably similar to the predictions based on Matyskiela (2003) (Table 13).

Lever et al. (in prep) placed a single Comp B particle (about 2 mm across) on a filter within an 11-mm-diameter cylindrical tube. Water dripped on the center of the filter at a constant rate of 0.52 mL/hr, about 20 drops per hour. This corresponds to a rainfall rate of about 0.55 cm/hr, although the average drop size of 4 mm was larger than the 1.4-mm average raindrop size expected for that rainfall

rate (Pruppacher and Klett 1997). The Comp B particle was free to move around on the filter so it was not struck by every drop. The water passing by the particle was collected into vials every 2 hours and analyzed for RDX and TNT. Only a single experiment has been completed to date.

The experiment produced several interesting observations. The surface of the Comp B particle, retrieved from a blow-in-place low-order detonation, was initially fairly smooth. During the early stages of the experiment, the TNT matrix preferentially dissolved faster than the embedded RDX crystals, increasing the exposed surface area of RDX and giving the particle a lumpy surface texture. The ratio of RDX/TNT dissolved in each water sample varied over an order of magnitude around its long-term average of 1.73, apparently reflecting the relative ratios in exposed surfaces and dissolution rates of the these constituents. Some RDX crystals (typically about 0.1-mm in size) also broke free from the main particle. Clearly, particle dissolution did not proceed as if the RDX and TNT were homogeneously mixed and dissolving independently. The nominal composition of Comp B is 60% RDX and 40% TNT, with small percentages of HMX as a by-product of the RDX manufacturing. Negligible amounts of HMX were recovered from this particular particle.

The original particle lost about 2.72 mg of Comp B (about 97% of the total mass) over the 68-day experiment. The particle mass at the end was 0.092 mg, consisting of about 90% RDX. Interestingly, the cumulative mass-loss of both RDX and TNT was nearly linear with time, indicating approximately constant dissolution rate (mg/hr) although the TNT dissolution rate did decrease near the end of the experiment (Fig. 26). If the flow had been uniform rather than impinging drops, this result would imply that the product of exposed surface area and dissolution coefficient (kS in eq 3) remained nearly constant for both constituents as particle size decreased. Here, the result is consistent with saturation-limited dissolution into a nearly constant water volume surrounding the particle after each drop, and the sweeping away of that dissolved material upon arrival of the next drop 3 minutes later.

This experiment simulates an HE particle on the soil surface exposed to rainfall but without significant pooling of the water. Because the rainfall rate was realistic, the measured dissolution rate should approximate field values. Again, this permits scaling the measured mass-loss by total infiltration and suggests that a 1-mm Comp B particle would dissolve within 4 years at the U.S. annual rainfall rate of 75 cm/yr. This is comparable to the results based on Phelan et al. (2003) and Matyskiela (2003) where the particle is within a porous soil matrix rather than lying on the surface. Extrapolating the drip-experiment results suggest a 0.1-mm Comp B particle would dissolve in less than 2 days, whereas a 1-cm particle

would require about 4000 years to dissolve. The latter result is so long that mechanical breakup of the particles by weathering or nearby detonations is likely to occur before the particles dissolve under the action of rain-impingement alone.

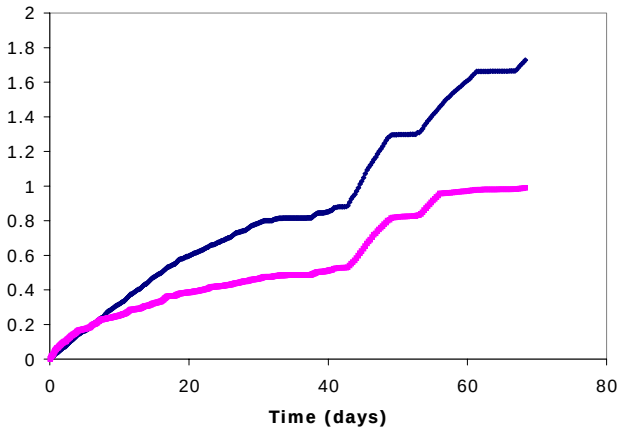

Figure 26. Mass loss of RDX and TNT with time from a single grain of Comp B.

Radtke et al. (2002) sampled surface soils at a site in southeastern Idaho where the explosive contamination (TNT) was at least 50 years old. By analyzing sieved soils, they found that particles larger than 3 mm accounted for more than 96% of the TNT contamination. The average particle mass was 0.087 g, indicating that the mass-average particle diameter was about 5 mm. The authors did not speculate on the original source of the particles, and there is no information on their original size distribution.

We may view 50 years as a conservative estimate of the time required for 3-mm surface TNT particles to dissolve under average U.S. conditions. Annual rainfall in southeastern Idaho averages only about 20 cm/yr, and particles initially larger than 3 mm could account for the less-than 3-mm contamination found in the study.

These studies suggest that much of the HE filler in UXO may persist even after the UXO casing is compromised. By comparison, smaller HE particles from detonations (high- and low-order) will dissolve much more rapidly. The relative importance of these contaminant sources is evaluated in the next section by accounting for the expected masses and dissolution rates of HE from each possible fate of a fired munition.

8 A MODEL TO ESTIMATE HE CONTAMINATION RATES

Figure 27 identifies the possible fates and their probabilities for HE rounds fired during training. By assigning probabilities and consequences to each fate for the most significant munitions, we may estimate the annual influx of dissolved HE and the relative contribution of each fate. We used a spreadsheet model to estimate the yearly dissolved HE input to the soil. Although many parameters are estimates, we can easily change them if better data, national or site-specific, become available.

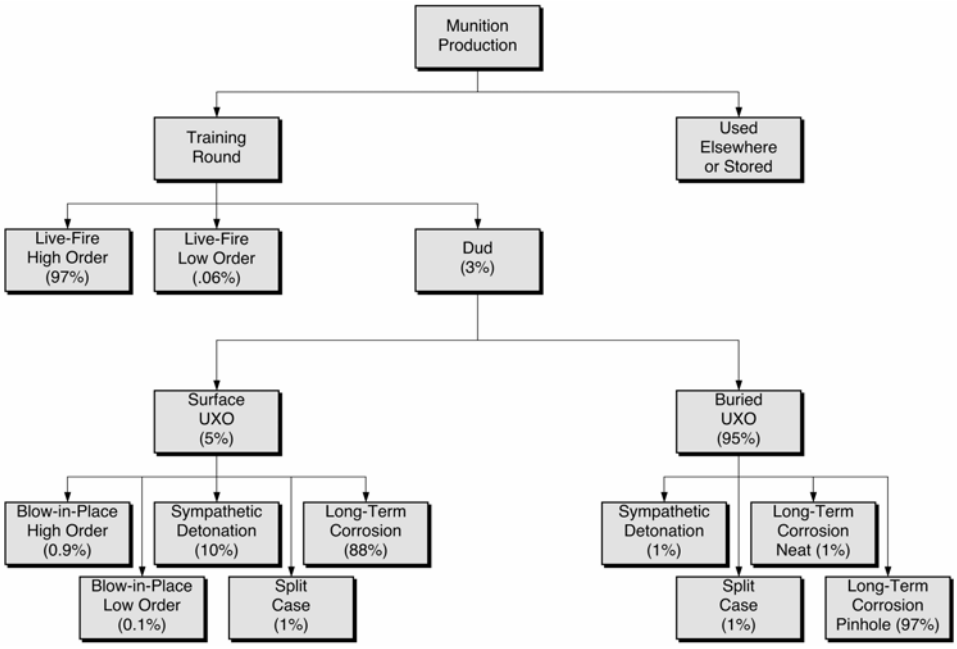

Figure 27. Possible fates of a fired munition and their estimated probabilities.

A fired round might detonate at high order or low order, or it might be a dud. The first two outcomes immediately release HE particles onto the soil surface. Duds can either penetrate the ground or remain on the surface. The most likely outcomes for surface UXO are blow-in-place detonation (HO or LO), sympathetic detonation initiated from a subsequent detonation nearby, splitting of the shell casing, and corrosive perforation of the shell casing. Similar fates exist for buried UXO, except that we neglect blow-in-place operations and identify two corrosion categories (neat and pinhole) that reflect how easily water can flow past the HE fill within the corroded round. The time scale for dissolution of a

round's HE depends strongly on its fate: detonations of all forms release relatively small particles of HE that can dissolve quickly; splitting or corrosion of the shell casing both leave the HE charge intact, and much slower dissolution rates result.

Table 14. Model input parameters and percent contribution of each fate to annual dissolved HE on training ranges. For the top five munitions (by HE mass produced): 81-mm, 4.2-in mortar; 105-mm, 155-mm, 8-in. howitzer. Total HE production of these munitions over 50 years was 3.4 x 10^8 kg, about 80% of which was used in live-fire training.

Fate	Probability (%)			HE mass release (%)	HE particle size (mm)	Dissolution mechanism	Dissolution time (yr)	Percent contribution	Notes
High Order (HO)	97			0.001	<<1	Particle	1	4	1
Low Order (LO)	0.06			50	<100	Particle	100	55	2
Dud (UXO)	3								3
Surface UXO		5							4
BIP- HO			0.9	0.3	<10	Particle	50	0.01	5
BIP- LO			0.1	50	<100	Particle	100	0.1	5
Sympathetic			10	50	<100	Particle	100	14	6
Split Casing			1	100	100	Neat	10,000	0.03	7
Corrosion-P			88	100	100	Pinhole	1×10^{10}	2×10^{-6}	8
Buried UXO		95							4
Sympathetic			1	50	<100	Particle	100	26	6
Split Casing			1	100	100	Neat	10,000	0.5	7
Corrosion-N			1	100	100	Neat	10,000	0.5	8
Corrosion-P			97	100	100	Pinhole	1×10^{10}	5×10^{-5}	8

1. Live-fire high-order probability is 100% minus sum of live-fire low-order and dud rates.
2. Live-fire low-order probability is weighted average (by HE mass) of LO rates determined by Dauphin and Doyle (2000). It could underestimate LO probability for untrained gun crews or impacts onto hard soils/rock where duds might detonate at low order.
3. Dud rate is weighted average (by HE mass) of dud rates determined by Dauphin and Doyle (2000). Anecdotal evidence suggests that it underestimates dud rates for untrained gun crews.
4. Probabilities for surface and buried UXO estimated from UXO database of 11 closed and cleared training ranges.
5. No uniform Army policy exists to clear UXO on active ranges. Surface UXO are blown along routes used to place or move targets; HO and LO probabilities reflect consensus that most BIP operations produce HO detonations. Few, if any, buried UXO are blown in place.
6. Probabilities for sympathetic detonations are highly uncertain. A 10% probability indicates that one surface UXO will detonate sympathetically for every ~300 live-fire detonations on the range. The estimated 1% probability for buried UXO reflects likely buffering effect of the soil.
7. Split casing UXO offer essentially no impediment to flow. Its probability is highly uncertain. We chose 1% based on anecdotal evidence that split casings occur but are rare.
8. Corrosion probabilities are 100% minus sum of other UXO fates. Dissolution of HE at the pinhole rate is extremely slow and the results here ignore the time delay for pinhole corrosion to occur. Eventually sufficient corrosion will occur that the much higher neat dissolution rate will prevail. The estimated 1% probability acknowledges that some buried UXO are already fully corroded. This probability will increase with time as UXO continue to corrode.

Here, we estimate the probability of each fate and the resulting consequences in terms of dissolved HE influx to the soil. Table 14 summarizes the data used and results obtained for the most significant munitions used on Army training ranges. Because of large uncertainties in many estimates, separating the results by munition type is not warranted at this time. The following sections include attempts to justify the model inputs and they show the overall results obtained.

8.1 Model Parameters

8.1.1 Most Significant Munitions

Table 2 lists the most commonly used munitions and their production numbers over time. By far, most of the munitions listed were manufactured after WWII, roughly a 50-year time span. We calculated the total potential HE available from UXO for each family of rounds based on dud rates estimated by Dauphin and Doyle (2000) and assuming that 80% of the rounds manufactured were used for training (Table 15). The 80% estimate is based on the percentage of artillery rounds used in training to those produced in 2003 (Delaney and Etter 2003). In peacetime similar numbers of munitions are used as are produced (although older munitions are used) to avoid stockpiling items. The average dud rate for all rounds studied by Dauphin and Doyle (2000) was 3.45%. For all HE rounds it was 3.37%. For all howitzer and mortar rounds it was 3.75 and 2.91%, respectively. For all gun-fired grenades, it was 1.78%.

Table 14. Dud rates for different munitions (from Dauphin and Doyle 2000, 2001).

Munition	Type	DODIC number	Production (millions)	HE Load (kg)	Energetics type	Dud rates (%)				
						Avg.	App. B	For size	HE type	Family
40-mm HE										
Gun	HE-T, SD	B562	1.1	0.063	TNT or Tetryl	3.45	0.0	1.37	3.37	1.78
Grenade/Gun	M383	B571	4.0	0.055	Comp A5 (RDX)	3.45	0.3	1.37	3.37	1.78
Grenade/Gun	M384	B470	17.0	0.055	Comp A5 (RDX)	3.45	5.3	1.37	3.37	1.78
Grenade	M397	B569	1.4	0.032	Octal	3.45	0.8	1.37	3.37	1.78
Grenade	M406	B568	39.0	0.032	Comp B	3.45	1.5	1.37	3.37	1.78
Gun	DP M430	B542	18.0	0.038	Comp A5 (RDX)	3.45	0.3	1.37	3.37	1.78
Grenade	DP M433	B546	23.0	0.045	Comp A5 (RDX)	3.45	1.1	1.37	3.37	1.78
			103.5	0.046						

Munition	Type	DODIC number	Production (millions)	HE Load (kg)	Energetics type	Dud rates (%)				
						Avg.	App. B	For size	HE type	Fam-ily
60-mm HE										
Mortar	M49A4	B632	1.9	0.190	TNT or Comp B	3.45	3.3	2.34	3.37	2.91
Mortar	M720	B642	1.2	0.191	Comp B	3.45	1.1	2.34	3.37	2.91
Mortar	M888	B643	3.0	0.358	Comp B	3.45	1.9	2.34	3.37	2.91
			6.1	0.246						
81-mm HE										
Mortar	M43A1	C225	6.0	0.585	Comp B	3.45	3.9	2.33	3.37	2.91
Mortar	M362	C222	4.0	0.953	Comp B	3.45	1.6	2.33	3.37	2.91
Mortar	M362	C223	1.3	0.953	Comp B	3.45	1.6	2.33	3.37	2.91
Mortar	M374	C236	2.3	0.953	Comp B	3.45	1.3	2.33	3.37	2.91
Mortar	M374A3	C256	40.8	0.953	Comp B	3.45	2.4	2.33	3.37	2.91
Mortar	M821A1	C868	1.0	0.726	RDX / TNT	3.45	1.7	2.33	3.37	2.91
Mortar	M889	C869	1.4	0.726	RDX / TNT	3.45	2.4	2.33	3.37	2.91
			56.8	0.836						
105-mm HE										
Howitzer	M1	C444	2.1	2.3 / 2.177	Comp B or TNT	3.45	9.6	4.65	3.37	3.75
Howitzer	M1	C445	20.0	2.3 / 2.177	Comp B or TNT	3.45	4.4	4.65	3.37	3.75
Howitzer	M1	C443	0.6	2.3 / 2.177	Comp B or TNT	3.45		4.65	3.37	3.75
			22.7	2.239						
4.2-in. HE										
Mortar	M329A2	C697	1.3	2.610	Comp B	3.45	2.2	5.13	3.37	2.91
Mortar		C699	1.0	2.610		3.45	2.2	5.13	3.37	2.91
Mortar	M329A1	C704	0.4	3.377	TNT	3.45	10.7	5.13	3.37	2.91
Mortar		C705	1.2	3.377	TNT	3.45	10.7	5.13	3.37	2.91
			3.9	2.994						
120-mm HE										
Mortar	M933	C623	0.4	2.990	Comp B	3.45			3.37	2.91
Mortar	M934A1	C379	0.2	2.990	Comp B	3.45			3.37	2.91
			0.6	2.990						
155-mm HE										
Howitzer	M1918		0.7					2.26	3.37	3.75
Howitzer	M107	D544	6.4	6.622/6.985	TNT / Comp B	3.45	2.8	2.26	3.37	3.75
Howitzer	RA M549	D579	1.1	6.940/7.257	TNT / Comp B	3.45	0.0	2.26	3.37	3.75
Howitzer	M795	D529	0.3	10.795	TNT	3.45		2.26	3.37	3.75
			7.8	8.232						

Munition	Type	DODIC number	Production (millions)	HE Load (kg)	Energetics type	Dud rates (%) Avg.	App. B	For size	HE type	Fam-ily
8-in. HE										
Howitzer	M106	D680	11.5	16.465/17.599	TNT / Comp B	3.45	2.2	0.99	3.37	3.75
Howitzer	RA M650	D624	0.3	11.300	TNT	3.45	0.2	0.99	3.37	3.75
			11.8	14.166						

*Potential residue calculation: Assumed that 80% of rounds manufactured were used for practice on ranges. Dud rates were not available for 120-mm mortars.

Table 14 (cont'd).

Munition	Potential residue (kg) Avg.	App. B	Size	HE type	Family	Number of rounds	Tested/ manf. ratio (%)
40-mm HE							
Gun	1,913		760	1,868	987	82	0.007
Grenade/Gun	6,017	488	2,389	5,877	3,104	360	0.009
Grenade/Gun	25,571	39,506	10,154	24,978	13,193	563	0.003
Grenade	1,244	303	494	1,215	642	474	0.034
Grenade	34,660	15,371	13,764	33,856	17,883	2,546	0.007
Gun	18,878	1,860	7,497	18,441	9,740	5,363	0.030
Grenade	28,566	9,108	11,344	27,904	14,738	4,084	0.018
	116,850	66,637	46,401	114,140	60,288	13,472	0.013
60-mm HE							
Mortar	9,964	9,588	6,758	9,733	8,404	7,792	0.410
Mortar	6,326	1,962	4,291	6,179	5,336	3,838	0.320
Mortar	29,642	16,668	20,105	28,955	25,003	2,112	0.070
	45,932	28,219	31,154	44,867	38,743	13,742	0.225
81-mm HE							
Mortar	96,876	109,512	65,426	94,630	81,713	1,998	0.033
Mortar	105,211	47,574	71,056	102,772	88,743	367	0.009
Mortar	34,194	15,461	23,093	33,401	28,842	-	-
Mortar	60,496	22,620	40,857	59,094	51,027	1,633	0.071
Mortar	1,073,154	730,989	724,768	1,048,270	905,182	7,489	0.018
Mortar	20,038	9,816	13,533	19,573	16,901	3,491	0.349
Mortar	28,053	19,515	18,946	27,402	23,662	1,457	0.104
	1,418,022	955,487	957,678	1,385,140	1,196,071	16,435	0.029

Munition	Potential residue (kg) Avg.	App. B	Size	HE type	Family	Number of rounds	Tested/ manf. ratio (%)
105-mm HE							
Howitzer	133,308	360,273	174,872	126,735	141,026	2,045	0.097
Howitzer	1,269,600	1,572,322	1,665,444	1,206,999	1,343,100	10,003	0.050
Howitzer	38,088		49,963	36,210	40,293		0.000
	1,440,996	1,932,596	1,890,279	1,369,944	1,524,419	12,048	0.053
4.2-in. HE							
Mortar	93,647	60,803	139,249	91,475	78,989	1,518	0.066
Mortar	72,036	46,771	107,114	70,366	60,761		0.000
Mortar	37,282	116,061	55,437	36,418	31,447	6,386	0.399
Mortar	111,846	348,182	166,310	109,253	94,340		0.000
		571,817	468,110	307,511	265,536	7,904	0.203
120-mm HE							
Mortar	33,010			32,244	27,843		0.000
Mortar	16,505			16,122	13,921		0.000
	49,514			48,366	41,764		
155-mm HE							
Howitzer							
Howitzer	1,201,770	968,383	787,247	1,173,903	1,306,272	6,216	0.097
Howitzer	206,554		141,205	210,558	73,219	1,152	0.105
Howitzer	56,333		58,552	87,310	30,361		0.000
	1,464,657	968,383	987,003	1,471,771	1,409,852	7,368	0.094
8-in. HE							
Howitzer	5,395,800	3,494,285	1,548,360	5,270,680	5,865,000	403	0.004
Howitzer	140,760	4,882	40,392	91,394	101,700	571	0.190
	5,536,560	3,499,167	1,588,752	5,362,074	5,966,700	974.00	0.008

These calculations suggest that five types of rounds, termed the most significant, will contribute most of the HE to the soil and groundwater: 81-mm and 4.2-in. mortars and 105-mm, 155-mm, and 8-in. howitzers. Other rounds that may be worth considering are 60-mm and 120-mm mortars, primarily because of the method of firing. They impact at a near vertical angle to the ground and if they do not detonate they would be likely to penetrate the soil. However, the combined release from these rounds would not add up to the potential contamination from any of the most significant rounds.

8.1.2 Training Use Rates

Detailed records on training use of munitions are almost nonexistent. For modeling, we will assume that 80% of the most significant munitions manufactured over the period since WWII were fired on training ranges and that they were fired at a uniform rate of $1/50^{th}$ per year. Annual use rates limit contamination by fates that quickly release HE (e.g., HO detonations) whereas processes that slowly release HE (e.g., corrosive perforation) can operate on the entire mass of HE used over the 50-year period.

8.1.3 Detonation Rates

Dauphin and Doyle (2000) estimated HO, LO, and dud rates for the most commonly used munitions from the ASRP data (Table 3). Dauphin and Doyle make a strong argument that these data are the best available for approximating training use, and we use their results here. However, they probably underestimate LO and dud rates for reasons mentioned earlier (training involves inexperienced gun crews; duds become LO detonations for impacts onto hard soils and rocks).

For the most significant munitions, ASRP-based LO rates range from 10^{-1} to 10^{-2}% and dud rates from 2 to 6% (Table 3). Note that the ASRP tests included too few firings of 8-in. howitzer rounds for reliable LO estimates. For the five munitions of interest, the average dud and LO rates, weighted by the total HE mass produced for each type, are 3 and 6×10^{-2}%, respectively.

8.1.4 HE Releases from High- and Low-Order Detonations, Live-Fire, and Blow-in-Place

Field experiments characterizing HE releases from individual detonations (see Section 6.2) allow us to estimate amounts and sizes of HE particles released for each type of detonation for use in our model.

Hewitt et al. (2003) summarize measurements of the residues recovered from live-fire (tactically detonated) and blow-in-place operations for a variety of munitions. For live-fired 60-, 81-, 120-mm mortar rounds and 105-mm howitzer rounds, the recovered residues range from about 10^{-5} to 10^{-3}% of the original HE mass in the round. The residues were recovered by sampling about 1% of the area of soot footprints on clean snow made by the detonations. Larger but more rare HE particles scattered beyond the plume or not falling within the sampled areas would not be included in these estimates. For these reasons, we use here the upper value of 10^{-3}% to approximate the proportion of HE residue released from a HO live-fire detonation.

Similarly sampled high-order blow-in-place detonations of 81-mm mortar and 155-mm howitzer rounds yielded average HE releases of 10^{-3} and 3×10^{-1}%, respectively. Interestingly, one of the seven 155-mm tests yielded percent-level concentrations of TNT, yet was classified by EOD personnel as a HO detonation. The BIP method uses C4 charges attached to the side of a round. Because this does not trigger the designed detonation sequence, it is reasonable that higher HE releases occur for BIP than for live-fire HO detonations. Thus, we use the higher value of 3×10^{-1}% to approximate the proportion of HE released from a high-order BIP detonation.

Taylor et al. (2004a,b) collected the HE residue from low-order BIP detonations of 81-mm mortar and 155-mm howitzer rounds. The results indicated that 20 to 80% of the HE charge was scattered. Air blast measurements produced a similar yield estimate (Pennington et al. 2003). These tests were specifically conducted to produce LO detonations and did not reflect EOD best practice for BIP operations. No measurements have yet been made on the HE releases from LO live-fire detonations, in part because these occur infrequently. Because the design detonation sequence does not occur for either live-fire or BIP low-order detonations, it seems likely that the releases would cover a similar range for both cases. Thus, we will crudely estimate that 50% of the HE charge is released from a low-order detonation (either live-fire or BIP).

Taylor et al. (2004a,b) also measured the size, mass, and area distributions of the HE particles recovered after BIP high-order and low-order detonations of 81-mm mortar and 155-mm howitzer rounds. For a BIP detonation with 2% HE released, most of the released mass consisted of particles smaller than a few millimeters. High-order detonations with lower release levels, such as those measured for live-fire detonations, would presumably produce much smaller particles. Conversely, for low-order detonations with 20 to 40% HE release, most of the released mass consisted of particles larger than a few millimeters, though chunks of HE measuring a few centimeters across were also recovered (see Fig. 22 and 23).

Of concern is whether a significant fraction of live-fire HO detonations yield percent-level HE releases. Measurements on snow have not revealed such high releases (Hewitt et al. 2003). However, a few widely scattered millimeter-sized particles could easily escape collection and significantly affect the measured releases. The estimated HE deposited from HO live-fire detonations would double if as few as one-in-1000 of these detonations produced percent-level releases. The few rounds sampled thus far would be unlikely to detect such an effect.

8.1.5 UXO Fates

The eventual release of HE from a dud depends strongly on its fate (Fig. 27). Unfortunately, statistics on the fates of duds are difficult to obtain. Consequently, many of the fate probabilities used here are order-of-magnitude estimates based on limited data or subjective reasoning; they necessarily include large uncertainties. For now, they serve to indicate the relative significance of the fates of UXO and which fates warrant more detailed investigation.

Dud rounds may either penetrate into the soil or remain on the surface, depending on the type of round, its impact velocity and angle, and the soil conditions. Data on the burial depths of 7299 UXO that had been fired into 11 different impact areas (UXO database) indicate that about 5% of duds remain on the surface weighted by the total masses of HE for the five most significant munitions (see Fig. 7). We will use this value as an approximation for all locations and munitions. This is roughly consistent with the value determined for the MMR HUTA (4/116 = 3%, see Section 4.23).

Whether on the surface or buried, one of five fates might befall a UXO: blow-in-place detonation (HO or LO), sympathetic detonation from a nearby explosion of a round, splitting of the shell casing, or corrosive perforation of the shell casing (Fig. 27). We list these roughly in order of increasing time scale for the release of the HE charge in the UXO. Because sympathetic detonations are triggered by uncontrolled processes, which bypass the rounds' detonation chain (a shock wave or frag. impact), we assume they would produce low-order detonations and scatter HE particles similar to BIP low-order detonations. For the split-casing and corrosive-perforation cases, we assume the HE charges remain intact. Note that the relative proportions for each fate vary depending on whether the UXO lies on the surface or is buried.

Surface UXO. The Army has no standard policy to blow UXO for range maintenance. The only routine BIP operations are those used to clear access roads to targets. We therefore estimate that only 1% of surface UXO are blown in place. We further assume that 90% of these operations produce HO detonations and 10% produce LO detonations (to allow for poor access to the round or a malfunctioning C4 charge). At MMR, two of the four surface UXO had split casings. This proportion is high compared with anecdotal evidence that suggests split-casing UXO are rare. We, therefore, use 1% as our order-of-magnitude estimate. Any estimate of the probability of sympathetic detonations is also highly uncertain because little direct evidence remains and LO live-fire detonations produce similar debris. At a 10% level, one sympathetic detonation would occur for every ~300 HO live-fire detonations. We use this as our order-of-magnitude estimate

for sympathetically detonated surface UXO. The remaining surface UXO (88%) undergo long-term corrosion.

Buried UXO. We know of no routine BIP operations to clear buried UXO, and we, therefore, assign zero probability to that fate. As with surface UXO, we assume 1% of the buried UXO have split casings. This is consistent with the data from the MMR HUTA, where 1 of the 112 buried UXO had split casings. It also appears that three of the buried rounds had detonated sympathetically because they looked like LO detonations but were at least 0.25 m below the surface. This high-use area should experience higher-than average sympathetic detonations rates. Therefore, we estimate that 1% of all buried UXO undergo sympathetic detonation on average. At a 1% level, one sympathetic detonation would occur for every ~3000 HO live-fire detonations. The remaining rounds eventually experience corrosive perforation. Some UXO have been corroding for decades, so that some proportion could already be quite permeable to water flow. For example, corrosion rates of 0.1 mm/yr are possible in aerated or saline soils and 1.5 mm/yr in flooded soils (see Table 6). In such locations, complete corrosion of UXO casings could occur within 10–100 years. We, therefore, use 1% as our order-of-magnitude estimate for currently buried UXO that are fully permeable to flow and consequently undergoing neat dissolution. The remaining 97% are developing pinhole perforations and at most are leaking HE at the pinhole rate. We use two fates for corroding buried UXO because the applicable dissolution rates are vastly different.

Clearly, the uncertainty in all of these estimates could be reduced with further study. EOD records could form the basis for improved estimates of BIP rates and the proportion of HO and LO outcomes. Likewise, estimates for sympathetic detonations could be based on observations or derived from UXO areal densities and crater diameters from HO live-fire rounds. Similarly, case-splitting rates could be obtained from data on recovered UXO or models similar to those used to estimate UXO penetration depths. Also, the condition of corroded UXO could be more thoroughly investigated to assess the proportion that is essentially impermeable to water flow. All such efforts, however, are beyond the scope of this work.

8.1.6 Dissolution Times for each Munition Fate

The time estimates for dissolution of HE particles, based on available information, vary significantly (Table 13). Nevertheless, we may make order-of-magnitude estimates that pertain to the fates of munitions fired on training ranges (Table 14). Note that if the dissolution time, τ, for a given fate is less than 50 years (the assumed period of training use), then the annual occurrence rate for

that fate governs its contribution to present-day dissolved HE flux. For example, if τ = 10 years, only 10 years of munitions experiencing that fate will be present, and each year's mass will dissolve by $1/10^{th}$. Conversely, if τ is greater than 50 years, present-day dissolution will operate on the total mass contributed by that fate, M_f. The present-day dissolved HE flux will thus be M_f/τ.

Particles scattered on the surface by live-fire high-order detonations (where most of the mass consists of particles << 1 mm) should dissolve within a year. Blow-in-place HO detonations produce larger particles (up to a few millimeters) but these should dissolve in less than 50 years. Thus, for both types of HO detonations, their annual occurrence rates govern their contribution to training-range dissolved HE flux.

The dissolution time for particles scattered on the surface by low-order detonations (live-fire or BIP) is more uncertain. Most of the scattered mass consists of particles smaller than a few centimeters. Simple dissolution could require hundreds of years, but the particles are friable and likely to break apart under the action of weathering and mechanical agitation from subsequent detonations. We will therefore use τ = 100 years as an estimate for particles from all LO detonations (live-fire, surface BIP, and buried BIP). We will also use this value for mass scattered by sympathetic detonations of UXO (surface or buried) because these detonations are probably low order.

We assume that a split-shell UXO has its entire HE charge exposed to dissolution. Clearly, the degree of damage to the casing will influence its role in impeding water flow. However, corrosion of the casing will probably accelerate, so the impediment to flow will likely be temporary. For simplicity, we assume that if the split-shell UXO is buried, the shell does not impede dissolution by advection, and, thus, the HE mass will undergo "neat" dissolution with τ = 10,000 years. On the surface, such a round might not be fully wetted. Nevertheless, we will assume that it also undergoes dissolution at the neat rate. These assumptions probably cause our results to over-estimate somewhat the contribution of HE contamination from split-shell UXO.

Intact UXO, either surface or buried, will not begin to release HE until corrosion perforates the shell casing. This process can take decades to centuries. Buried UXO would then undergo pinhole dissolution as modeled by Matyskiela (2003). The dissolution rate is about 10^{-7} times smaller than the neat rate based on annual average rainfall rate; that is $\tau \sim 10^{10}$ years for pinhole dissolution. For a surface UXO with a pinhole perforation, water might not completely saturate the HE-to-casing gap, and dissolution would be slower than the pinhole rate. To be conservative, we will neglect the time needed for pinhole corrosion and assume that present-day surface intact UXO and most buried intact UXO release

HE at the pinhole dissolution rate. For UXO buried, we have assumed that a small proportion (1%) of shell casings might already be fully permeable to water flow. For this fate we assume that the much shorter neat dissolution time applies (τ = 10,000 yr).

8.2 Estimated Dissolved HE Flux

Table 14 summarizes our model estimates for the relative contribution of each munition fate to annual dissolved HE on training ranges. These results must be treated cautiously owing to the high uncertainties in many input parameters.

Generally, detonations that release explosives at percent levels as particles will deliver significant fluxes of dissolved HE to the soil. This includes LO live-fire and sympathetic detonations of surface and buried UXO. Also, HO live-fire produces a fairly significant HE flux, despite the low mass released per round, because it's by far the most common fate. Neat dissolution of buried UXO, with split or fully corroded casings, collectively contribute about 1% of the annual dissolved HE.

The model predicts a total HE dissolved flux of ~ 10^3 kg/yr for all training use of munitions. About 60% of this flux is from live-fire, primarily LO, detonations (Fig. 28). UXO of all fates account for the other 40%, most of which derives from sympathetic detonations of surface and buried UXO. The importance of sympathetic detonations hinges on the highly uncertain assumptions that 10% of the surface and 1% of the buried UXO will detonate sympathetically from nearby live-fire detonations. These probabilities correspond to ratios of 1:300 and 1:3000 sympathetic detonations to HO live-fire detonations.

Not surprisingly, the model indicates that the flux of HE released through pinhole corrosion of UXO is insignificant compared with other fates, even neglecting the time needed for corrosion to produce a pinhole perforation. This is because dissolution at the pinhole rate is extremely slow. However, for soils where corrosion removes the casing as an impediment to water flow, the neat dissolution rate will prevail, and it is 10^6 times higher. Figure 28 illustrates the relative HE contamination if 1% of the buried UXO are dissolving at the neat rate. However, if 10% of buried UXO are sufficiently corroded to allow dissolution at the neat rate, their dissolved HE flux will exceed that produced by live fire HO detonations (Fig. 29). Furthermore, because the neat dissolution rate increases strongly with decreasing particle size, nearby detonations that cause HE blocks to fragment (but not detonate) will significantly increase the contribution of this fate.

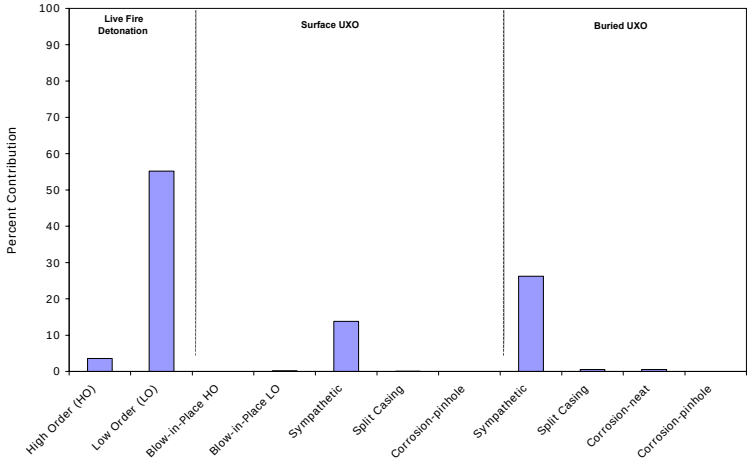

Figure 28. Estimated contamination rate by fate of the munition. Here 1% of the UXO are fully corroded and undergoing neat dissolution.

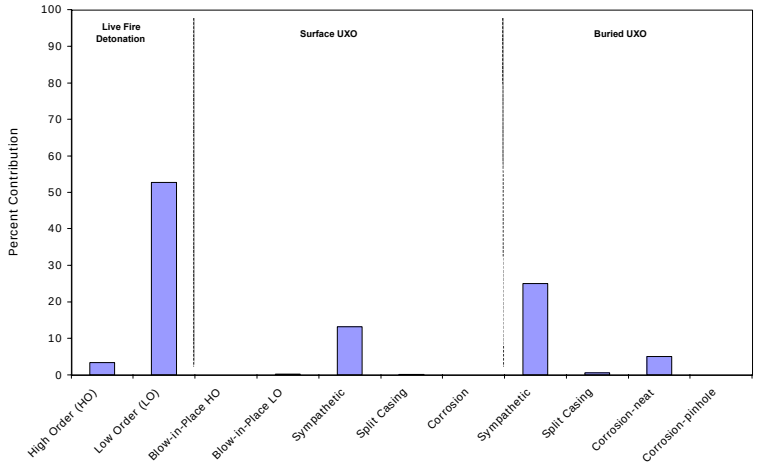

Figure 29. Estimated contamination rate by fate of the munition with 10% fully corroded and undergoing neat dissolution.

Clearly, corrosion will steadily increase the proportion of existing UXO with fully corroded casings and, thus, will increase the dissolved HE flux from this fate. Furthermore, whenever training ranges are no longer subject to live fire (e.g., BRAC, range abandonment), particulate HE will not be replenished as it dissolves, and dissolution of corroded UXO will grow in importance with time;

eventually, it will predominate the dissolved HE flux. That is, the low present-day ranking of corroding UXO as contaminant sources does not imply that UXO should remain in the ground indefinitely to corrode. It simply means that compared with on-going detonations, corroding UXO are only a small contribution to the overall dissolved HE flux.

The model necessarily approximates many processes, and the results will change depending on the parameters chosen. Insofar as possible, we have tried to justify our choices. Listed here are the most significant uncertainties associated with the model:

- The ASRP data (Dauphin and Doyle 2000) may underestimate the dud and low-order probabilities for munitions fired during training by inexperienced crews. Also, impacts into hard soils or rock on training ranges could trigger LO detonations from what would otherwise be dud rounds. Because HO detonations produce much lower dissolved HE flux, any increase in dud or LO probabilities is significant.
- High-order detonations would increase in significance if current measures of HE mass-release omit scarce millimeter-sized particles thrown outside the soot plume or area sampled. Also, the ASRP test firings are classified as high order by sound and the absence of LO debris. Detonations that produce yields greater than 90% would probably be classified as high order yet would scatter percent-level explosives as fine particles. The small number of high-order live-fire rounds sampled to date for HE residues would be unlikely to have captured this effect, if it occurs. Because live-fire HO detonation is the most likely fate, any increase in the mass released by these detonations would be significant.
- The proportion of UXO likely to detonate sympathetically is unknown at this time. We chose probabilities of 1% for buried UXO and 10% for surface UXO, and the model then ranks these fates as the second and third highest contributors to dissolved HE flux. These results highlight the potential importance of sympathetic detonations and the need to quantify their probabilities more reliably.
- Time scales for HE particle dissolution are uncertain and more work is needed to constrain them. In addition, the action of weather and mechanical agitation to break large particles into small ones needs investigation because the resulting small particles dissolve quickly. This includes the effect of nearby detonations that could fragment an HE block (even without causing sympathetic detonation).
- Buried UXO with split casings are potentially important sources of dissolved HE flux. We chose a 1% probability for both surface and buried

UXO. Whether this number is a good national average is uncertain. Also, our definition implies that the split casing offers no impediment to flow. We do not know whether this definition is consistent with that used to categorize inspected UXO. However, a damaged casing should corrode open rapidly and consequently become consistent with our definition within a short time. Because corrosion of an intact casing is so slow, some effort is warranted to quantify numbers and types of split casings and the rates at which they corrode.

- The proportion of buried UXO that is fully corroded is highly uncertain. In this context, fully corroded implies that the casing does not significantly impede water flow, and the HE fill dissolves at the neat rate. We used 1% as an order-of-magnitude estimate for this fate, but regardless of its current value, the importance of this fate will increase with time as older UXO more fully corrode.
- The model used here does not account separately for TNT and Comp B (i.e., RXD and TNT) rounds. However, only RDX is found in appreciable quantities in groundwater because it does not readily break down. Our HE flux estimates should not be used to estimate RDX input unless they are corrected for the relative proportion of TNT- and Comp B-filled rounds.
- The model input parameters are estimates based on average conditions across all Army training ranges. Local variations could be significant owing to soil types, rainfall rates, munitions fired, training practices, etc.

9 SUMMARY

A fired munition can suffer one of many fates. Using data on the relative rates of the different outcomes suggests that various types of LO detonations (live fire and sympathetic detonations), where a significant amount of the explosive filler is released, are the largest contributors to dissolved HE flux on training ranges. Also, HO live-fire produces a fairly significant HE flux, despite the low mass released per round, because it is by far the most common fate. The significance of neat dissolution from fully corroded rounds will increase with time and, when about 10% of the current UXO corrode to the point where they are permeable to water flow, UXO will rival HO detonations as a source of dissolved HE flux. At present, however, the available information on corrosion rates, measured leak rates of corroded ordnance, and the dissolution rates for bulk explosive masses suggest that UXO are not currently a source of widespread HE flux on our ranges.

We find that corrosion of low-carbon steel, the most commonly used steel in UXO, probably occurs at about 0.025 mm per year. Interestingly, variations in corrosion rate attributable to soil conditions and the casing alloy are within a factor of 5. This suggests that most UXO, which have a minimum wall thickness between 2 and 10 mm, will corrode within 80 to 400 years in aerated soils. Under reducing conditions similar to those encountered in wetlands and other anaerobic and flooded environments, sulfide production accelerates corrosion by about a factor of 10 (with considerable variability), resulting in perforation of the round after approximately 10–40 years. Pit corrosion is also common in soil environments and results in deep, small perforations that leak HE at a very slow, pinhole rate. An intriguing possibility is that the reactive intermediates formed during metal corrosion may facilitate the degradation of RDX, TNT, and other explosives as they leak from the UXO casing. More work is warranted in this area, although the first-order questions of the number, type, and distribution of UXO at ranges need to be addressed before these secondary effects can be quantified.

Future studies would benefit from accurate, long-term range firing records. Such records could be obtained if the Army developed and implemented an easy to use method for recording, transferring, and saving firing records. Possibly seismic arrays, acoustic sensors, or other methods could be developed to automatically keep track of the number of rounds fired and their fate. Currently, only order-of-magnitude estimates of HE release are possible owing to a lack of information on the number and actual fates experienced by different types of fired munitions.

Currently, LO detonations appear to be the main source of HE release on training ranges. Therefore, any action that decreases the rate of LO detonations, either live fire or sympathetic, is important, for example, improving the reliability of munitions and fuzes, incorporating tags into rounds so that duds and LO can be found, and removing low-order rounds while their positions are known and before their HE is scattered by subsequent detonations.

Because all UXO will eventually corrode if left in place and release their contents into the ground, it is advisable to 1) remove as many UXO as possible before they perforate, and 2) minimize the number of new UXO. This is especially important for ranges overlying important aquifers or where soil conditions are known to accelerate corrosion (wetlands). Priority items would be those that contain a lot of HE or those that contain explosives known to migrate to the groundwater (primarily RDX).

It is preferable to destroy all movable UXO in a blast chamber where the residues are contained. The residues from the blast chamber along with any chunk explosives found on the range could then be destroyed in a non- contaminating manner, such as dissolution followed by chemical or thermal destruction (e.g., Thorne 2003). If some rounds have to be blown-in-place, techniques that produce a high-order detonations are preferable. Also an alternative to C4, which is mostly RDX and does not always fully detonate, could be considered. Its replacement with a non-contaminating explosive that is highly efficient in producing high-order detonations would decrease the release of RDX.

Because each installation is unique, range management and practices could be tailored to sustain training activities and avoid offsite contamination given the ranges' geologic and climactic setting. For example inert rounds could be used for training on ranges that have high rainfall and shallow water tables and HE rounds reserved for ranges where the transport of HE to groundwater is slow (low rainfall, deep groundwater table). Good stewardship of the training lands improves the Army's relationship with residents living near the installations, extends the life of the ranges, and lowers costs if and when the installation is closed.

REFERENCES

Adams, J.B. (2001) Modeling the corrosion rate of unexploded ordnances. Session 48, *Geological Society of America Annual Meeting, 5–9 November 2001*.

Adams, J.B. (1999) Unexploded ordnance recovery depth database. Abstract in *UXO Forum*.

Adley, M.D, R.P. Berger, J.D. Cargile, H.G. White, and D.C. Creighton (1997) Three-dimensional projectile penetration into curvilinear geologic / structural target: User's guide for PENCRV3D. U.S. Army Waterways Experiment Station, Vicksburg, Mississippi.

AMEX (in review) Link between military training activities and grounwater contamination of propellant, explosive, and pyrotechnic (PEP) compounds. USACE Report MMR-6810, pp. 1–165.

Ampleman G., S. Thiboutot, S. Désilets, A. Gagnon, and A. Marois (2000) Evaluation of the soils contaminated by explosives at CFB Chilliwack and CFAD Rocky Point. DREV Report TR-2000-102.

Ampleman G., S. Thiboutot, J. Lewis, A. Marois, A. Gagnon, M. Bouchard, R. Martel, R. Lefebvre, C. Gauthier, J.M Ballard, T.A. Ranney , T.F. Jenkins, and J. Pennington (2003a) Evaluation of the impacts of live fire training at CFB Shilo. Final Report. Defense R&D Canada—Valcartier, TR 2003-066.

Ampleman G., S. Thiboutot, J. Lewis, A. Marois, A. Gagnon, M. Gagnon, S. Jean, T.F. Jenkins, A. Hewitt, J. Pennington, and T.A. Ranney (2003b) Evaluation of the contamination by explosives in soils, biomass and surface water at Cold Lake Air Weapons Range (CLAWR), Alberta. Phase I Report, Defense Research Establishment, Department of National Defense, Canada.

Arshed, M., M. Anwarulislam, M. Siddique, and N.M. Butt (1993) Study of the corrosion of mild-steel due to prolonged immersion in deionized water. *Journal of Radioanalytical and Nuclear Chemistry-Letters*, **175**(6): 467–472.

Arshed, M., N.M. Butt, M. Siddique, and M. Anwarulislam (1992) Study of corrosion of ss-304 exposed to sea-water. *Journal of Radioanalytical and Nuclear Chemistry-Letters*, **165**(2): 107–113.

Booth, G.H., and A.K. Tiller (1968) Cathodic characteristics of mild steel in suspensions of sulphate-reducing bacteria. *Corrosion Science*, **8**(8): 583.

Bucci, J.E., and P. F. Buckley (1998) Modeling the degradation of unexploded ordnance (UXO) and its use as a tool in the development of risk assessments. (https://www.denix.osd.mil/denix/Public/News/OSD/UXO/Conferences/Forum/Bucci.pdf)

Buttle, J.M. (1994) Isotope hydrograph separations and rapid delivery of pre-event water from drainage basins. *Progress in Physical Geography*, **18**: 16–41.

California Department of Transportation (1999) Method for estimating the service life of steel culverts. California Test Method 643. Engineering Service Center, California Department of Transportation, Sacramento.

Clausen J, J. Robb, D. Curry and N. Korte (2004) A case study of contaminants in military ranges: Camp Edwards, Massachusetts, USA. *Environmental Pollution*, **129**: 13–21.

Collins, C.M., and D.J. Calkins (1995) Winter tests of artillery firing into Eagle River Flats, Fort Richardson, Alaska. U.S. Army Cold Regions Research and Engineering Laboratory, Special Report 95-2.

Craig, B.D. (ed.) (1989) *Handbook of Corrosion Data*. Metals Park, Ohio: ASM International.

Crull, M., L. Taylor, and J. Tipton (1999) Estimating ordnance penetration into earth. *UXO/Countermine Forum*. Atlanta, Georgia.

Darrach, M.R., A. Chutjian, and G.A. Plett (1998) Trace explosive signatures from World War II unexploded undersea ordnance. *Environmental Science and Technology*, **32**: 1354–1358.

Dauphin, L., and C. Doyle (2000) Study of ammunition dud and low order detonation rates. U.S. Army Defense Ammunition Center—Technical Center for Explosives Safety. Technical Report written for U.S. Army Environmental Center, Aberdeen Proving Ground, Maryland.

Dauphin, L., and C. Doyle (2001) Phase II study of ammunition dud and low order rates. U.S. Army Defense Ammunition Center—Technical Center for Explosives Safety. Technical Report written for U.S. Army Environmental Center, Aberdeen Proving Ground, Maryland.

Davalos, J., J.F. Marco, M. Gracia, and J.R. Gancedo (1991) The corrosion products of weathering steel and pure iron in simulated wet-dry cycles. *Hyperfine Interactions*, **66**(1–4): 63–70.

Delaney W.P., and D. Etter (2003) *Unexploded Ordnance (UXO).* Report of the Defense Science Board Task Force, Office of the Under Secretary of Defense for Acquisition, Technology and Logistics, Washington DC. http://www.acq.osd.mil/dsb/uxo.pdf

Department of Commerce (1968) *Climatic Atlas of the United States*.

Doyle, G., M.V. Seica, and M.W.F. Grabinsky (2003) The role of soil in the external corrosion of cast iron water mains in Toronto, Canada. *Canadian Geotechnical Journal*, **40**(2): 225–236.

Drissi S.H., P. Refait, M. Abdelmoula, and J.M.R. Genin (1995) The preparation and thermodynamic properties of Fe(II)-Fe(III) hydroxide-carbonate (green-rust-1) - pourbaix diagram of iron in carbonate-containing aqueous-media. *Corrosion Science*, **37**(12): 2025–2041.

Dube P., G. Ampleman, S. Thiboutot, A. Gagnon, and A. Marois (1999) Characterization of potentially explosives-contaminated sites at CFB Gagetown, 14 Wing Greenwood and CFAD Bedford. Defense Research Establishment, Valcartier, Quebec, DREV-TR-1999-137.

Edyvean, R.G.J., and H.A. Videla (1991) Biological corrosion. *Interdisciplinary Science Reviews*, **16**(3): 267–282.

Fabian, G.L., and S. Ostazeski (2002) Corrosion of unexploded ordnance (final report). U.S. Army Environmental Center Report SFIM-AEC-PC-CR-2002041.

Foster, J. (1998) Report of the Defense Science Board Task Force on Unexploded Ordnance (UXO) Clearance, Active Range UXO Clearance, and Explosive Ordnance Disposal (EOD) Programs.

Frankel, G.S. (1998) Pitting corrosion of metals—A review of the critical factors. *Journal of the Electrochemical Society*, **145**(6): 2186–2198.

Fry, M.A., R.E. Durrett, G.P. Ganong, D.A. Matuska, and M.D. Stucker (1976) The HULL Hydrodynamics computer code. Air Force Weapons Laboratory, Kirtland Air Force Base, New Mexico, AFWL-TR-76-183.

Ge, H.H., D.D. Zhou, and W.Q. Wu (2003) Passivation model of 316 stainless steel in simulated cooling water and the effect of sulfide on the passive film. *Applied Surface Science*, 211(1-4): 321–334.

Genin, J.M.R., G. Bourrie, F. Trolard, M. Abdelmoula, A. Jaffrezic, P. Refait, V. Maitre, B. Humbert, and A. Herbillon (1998) Thermodynamic equilibria in aqueous suspensions of synthetic and natural Fe(II)-Fe(III) green rusts: Occurrences of the mineral in hydromorphic soils. *Environmental Science and Technology*, **32**(8): 1058–1068.

Grant, D.E., and M. Crull (1999) Evaluation of PENCRV3D for determination of ordnance ground penetration. *UXO/Countermine Forum*. Atlanta, Georgia.

Gu, B.H., D.B. Watson, L.Y. Wu, D.H. Phillips, D.C. White, and J.Z. Zhou (2002) Microbiological characteristics in a zero-valent iron reactive barrier. *Environmental Monitoring and Assessment*, **77**(3): 293–309.

Hamilton, W.A. (1983) The role of sulfate-reducing bacteria in anaerobic corrosion. *Journal of Applied Bacteriology*, **55**(3): R3–R3.

Hamilton, W.A. (1985) Sulfate-reducing bacteria and anaerobic corrosion. *Annual Review of Microbiology*, **39**: 195–217.

Hamilton, W.A. (1998) Bioenergetics of sulphate-reducing bacteria in relation to their environmental impact. *Biodegradation*, **9**(3–4): 201–212.

Hamilton, W.A. (2003) Microbially influenced corrosion as a model system for the study of metal microbe interactions: A unifying electron transfer hypothesis. *Biofouling*, **19**(1): 65–76.

Hewitt, A.D., T.F. Jenkins, T. Ranney, D. Lambert, and N. Perron (2004) Characterization of energetic residues at military firing ranges: Scholfield Barracks and Pohakuloa Training Area. Chapter 3, Distribution and fate of energetics on DoD test and training ranges: Interin report 4. U.S. Army Research and Development Center, ERDC TR-04-4.

Hewitt, A.D., T.F. Jenkins, T. Ranney, J. Stark, M.E. Walsh, S. Taylor, M. Walsh, D. Lambert, N. Perron, N. Collins, and R. Karn (2003) Estimates for explosive residue deposition from the detonation of army munitions. U.S. Army Engineer Research and Development Center, Cold Regions Research and Engineering Laboratory, Technical Report ERDC/CRREL TR-03-16.

Hundal, L.S., J. Singh, E.L. Bier, P.J. Shea, S.D. Comfort, and W.L. Powers (1997) Removal of TNT and RDX from water and soil using iron metal. *Environmental Pollution*, **97**(1–2): 55–64.

Isaksen, K., and J.L. Sollid (2002) *Losavleiringer og permafrost i Hjerkinn skytefelt, Dovrefjell.*

Ishikawa, T., T. Ueno, A. Yasukawa, K. Kandori, T. Nakayama, and T. Tsubota (2003) Influence of metal ions on the structure of poorly crystallized iron oxide rusts. *Corrosion Science*, **45**(5): 1037–1049.

Jenkins, T.J., C.L. Grant, G.S. Brar, P.G. Thorne, T.A. Ranney, and P.W. Schumacher (1996) Assessment of sampling error associated with collection and analysis of soil samples at explosive-contaminated sites. U.S. Army Cold Regions Research and Engineering Laboratory, Special Report 96-15.

Jenkins T.J., M.E Walsh, P.G. Thorne, S. Thiboutot, G. Ampleman, T.A. Ranney, and C.L. Grant (1997) Assessment of sampling error associated with collection and analysis of soil samples at a firing range contaminated with HMX. U.S. Army Cold Regions Research and Engineering Laboratory, Special Report 97-22.

Jenkins T.J., M.E Walsh, P.G. Thorne, P.H Miyares, T.A. Ranney, C.L. Grant, and J.R. Esparza (1998) Site characterization for explosives contamination at a military firing range impact area, U.S. Army Cold Regions Research and Engineering Laboratory, Special Report 98-9.

Jenkins, T.J., T.A. Ranney, M.E. Walsh, P.H. Miyares, A.D. Hewitt, and N.H. Collins (2000) Evaluating the use of snow-covered ranges to estimate the explosives residues that result from detonation of Army munitions. U.S. Army Engineer Research and Development Center, Cold Regions Research and Engineering Laboratory, Technical Report ERDC/CRREL TR-00-15.

Jenkins, T.J., J.C. Pennington, T.A. Ranney, T.E. Berry Jr., P.H. Miyares, M.E. Walsh, A.D. Hewitt, N.M. Perron, L.V. Parker, C.A. Hayes, and E.G. Wahlgren (2001) Characterization of explosives contamination at military firing ranges. U.S. Army Engineer Research and Development Center, Cold Regions Research and Engineering Laboratory, Technical Report ERDC/CRREL TR-01-5.

Jones D.A. (1996) *Principles and Prevention of Corrosion*. Prentice Hall.

Kajiyama, F., and K. Okamura (1999) Evaluating cathodic protection reliability on steel pipe in microbially active soils. *Corrosion*, **55**(1): 74–80.

Kholodenko, V.P., S.K. Jigletsova, V.A. Chugunov, V.B. Rodin, V.S. Kobelev, and S.V. Karpov (2000) Chemicomicrobiological diagnostics of stress corrosion cracking of trunk pipelines. *Applied Biochemistry and Microbiology*, **36**(6): 594–601.

Kingery, C.N, and G. Bulmash (1984) Airblast parameters from TNT spherical air burst and hemispherical surface burst. U.S. Armament Research and Development Center, Ballistics Research Laboratory, Aberdeen Proving Ground, Maryland. Technical report ARBRL-TR-02555.

Kloppel, H., A. Fliedner, and W. Kordel (1997) Behavior and ecotoxicology of aluminum in soil and water—Review of the scientific literature. *Chemosphere*, **35**(1–2): 353–363.

Kuznetsova, A., T.D. Burleigh, V. Zhukov, J. Blachere, and J.T. Yates (1998) Electrochemical evaluation of a new type of corrosion passivation layer: Artificially produced Al_2O_3 films on aluminum. *Langmuir*, **14**(9): 2502–2507.

Lee, A.K., and D.K. Newman (2003) Microbial iron respiration: impacts on corrosion processes. *Applied Microbiology and Biotechnology*, **62**(2–3): 134–139.

Lee, J.H., and J.E. Atkins (1995) Performance Assessment 1995. Chapter 5, Waste Package Degradation. Office of Civilian Radioactive Waste Management, Department of Energy, pp. 5-1 to 5-17.

Lever J., S. Taylor, L. Perovich, K. Bjella, and B. Packer (in prep) Dissolution of Composition B. U.S. Army Engineer Research and Development Center, Cold Regions Research and Engineering Laboratory

Levlin, E. (1996) Aeration cell corrosion of carbon steel in soil: In situ monitoring cell current and potential. *Corrosion Science*, **38**(12): 2083–2090.

Lewis J. S. Thiboutot, G. Ampleman, S. Brochu, T. Ranney, and S. Taylor (2002) Open detonation of military munitions on snow: An investigation of the quantities of energetic material residues produced. RDDC-DRDC—Valcartier.

Li, S.Y., Y.G. Kim, K.S. Jeon, Y.T. Kho, and T. Kang (2001) Microbiologically influenced corrosion of carbon steel exposed to anaerobic soil. *Corrosion*, **57**(9): 815–828.

Linhardt, P. (1997) Corrosion of metals in natural waters influenced by manganese oxidizing microorganisms. *Biodegradation*, **8**: 201–210.

Little B., P. Wagner, and F. Mansfeld (1991) Microbiologically influenced corrosion of metals and alloys. *International Materials Review*, **36**(6): 253–272.

Little, B., P. Wagner, K. Hart, R. Ray, D. Lavoie, K. Nealson, and C. Aguilar (1998) The role of biomineralization in microbiologically influenced corrosion. *Biodegradation*, **9**(1): 1–10.

Little, B., R. Ray, and R. Pope (2000) Relationship between corrosion and the biological sulfur cycle: A review. *Corrosion*, **56**: 433–443.

Lyman, T. (1961) *Metals Handbook*.Volume 1. *Properties and Selection of Metals*. Metals Park, Ohio: ASM International.

Lynch, J.C, J.M. Brannon, and J.J. Delfino (2002) Dissolution rates of three high explosive compounds: TNT, RDX and HMX. *Chemosphere*, **47**: 725–734.

Matyskiela (2003) Modeling of chemical transport from UXO to surrounding soil. Final Report submitted to Praxis Environmental Technologies, Burlingame, California.

Murad, E., and U. Schwertmann (1980) The Mossbauer spectrum of ferrihydrite and its relations to those of other iron-oxides. *American Mineralogist*, **65**(9–10): 1044–1049.

Music, S., D. Dragcevic, I. CzakoNagy, and S. Popovic (1997) FT-IR and Mossbauer study of corrosion of steel in tap and mineral water. *Croatica Chemica Acta,* **70**(2): 689–702.

Music, S., M. Gotic, and S. Popovic (1993) X-Ray-diffraction and Fourier-transform infrared-analysis of the rust formed by corrosion of steel in aqueous-solutions. *Journal of Materials Science,* **28**(21): 5744–5752.

Naval Explosive Ordnance Disposal Technology Division (1996) Unexploded Ordnance (UXO): An overview. (https://www.denix.osd.mil/Pubilc/Library/Explosives/uxo/uxo.html#for)

NDCEE (2003) Unexploded Ordnance (UXO) Task 307; Subtask 4: UXO Recovery Database [Computer Software]. Limited-access Online database. 10 January 2004. http://uxords.ctcgsc.org.

Nordstrom, D.K., and C.N. Alpers (1999) Negative pH, efflorescent mineralogy, and consequences for environmental restoration at the Iron Mountain Superfund site, California. *Proceedings of the National Academy of Sciences of the United States of America*, **96**(7): 3455–3462.

Nordstrom, D.K., C.N. Alpers, C.J. Ptacek, and D.W. Blowes (2000) Negative pH and extremely acidic mine waters from Iron Mountain, California. *Environmental Science and Technology*, **34**(2): 254–258.

Nore, R. (1994) Report on selected ordnance removal projects. *Proceedings, Twenty-Sixth, DoD Explosives Safety Seminar. Alexandria, Virginia*. Department of Defense, Explosives Safety Board, 1997, CD-ROM.

Norin, M., and T.G. Vinka (2003) Corrosion of carbon steel in filling material in an urban environment. *Materials and Corrosion—Werkstoffe Und Korrosion*, **54**(9): 641–651.

Ogden Environmental and Energy Services (2000) Client draft IAGS Technical Team Memorandum 00-3: Evaluation of gun and mortar firing positions for the Camp Edwards impact groundwater quality study, MMR, Cape Code, Massachusetts. Nashville, Tennessee.

Papadopoulos, J.A. (2003) Munition metal parts manufacturing changes, 1920 to present, for unexploded ordnance database. U.S. Army Armament Research, Development, and Engineering Center, Picatinny Arsenal, New Jersey, Special Publication ARWEC-SP-02001.

Pedersen M.A., J. Nokes and D. Wardlaw (2002) Low-order, underwater detonation. Environmental Security Technology Certification Program, ESTCP Report UX-0104.

Penhale, H.R. (1971) Corrosion of mild steel plates in some New-Zealand soils, *New Zealand Journal of Science*, **14**(2): 336–337.

Pennington, J.C., T. F. Jenkins, J.M. Brannon, J. Lynch, T.A. Ranney, T.E. Berry, Jr., C.A. Hayes, P.H. Miyares, M.E. Walsh, A.D. Hewitt, N. Perron, and J.J. Delfino (2001) Distribution and fate of energetics on DoD test and training ranges: Interim Report 1. U. S. Army Engineer Research and Development Center, ERDC TR-01-13.

Pennington, J.C., T.F. Jenkins, G. Ampleman, S. Thiboutot, J.M. Brannon, J. Lynch, T.A. Ranney, J.A. Stark, M.E Walsh, J. Lewis, C.A. Hayes, J.E. Mirecki, A.D. Hewitt, N.M. Perron, D. Lambert, J. Clausen, and J.J. Delfino (2002) Distribution and fate of energetics on DoD test and training ranges: Report 2. U.S. Army Engineer Research and Development Center, Environmental Laboratory Technical Report, ERDC/EL TR-01-13.

Pennington, J.C., T.F. Jenkins, G. Ampleman, S. Thiboutot, J.M. Brannon, J. Lewis, J.E. Delaney, J. Clausen, A.D. Hewitt, M.A. Hollander, C.A. Hayes, J.A. Stark, A. Marois, S. Brochu, H.Q. Dinh, D. Lambert, R. Martel, P. Brousseau, N.M. Perron, R. Lefebvre, W. Davis, T.A. Ranney, C. Gauthier, S. Taylor, and J.M. Ballard (2003) Distribution and fate of energetics on DoD test and training ranges: Report 3. U. S. Army Engineer Research and Development Center, Environmental Laboratory Technical Report, ERDC/EL TR-02-EL-191.

Phambu, N. (2003) Characterization of aluminum hydroxide thin film on metallic aluminum powder. *Materials Letters*, **57**(19): 2907–2913.

Phelan J.M., S.W. Webb, J.V. Romero, J.L. Barnett, F. Griffin and M. Eliassi (2003) Measurement and modeling of energetic material mass transfer to soil pore water—Project CP-1227. Sandia Report 2003-0153.

Pitard, F.F. (1993) *Pierre Gy's Sampling Theory and Sampling Practice: Heterogeneity, Sampling Correctness, and Statistical Process Control*. Boca Raton, Florida: CRC Press.

Prakash, N., K. Srivastava, and S.B. Gupta (1988) Corrosion of mild-steel by soil containing sulfate reducing bacteria. *Journal of Microbial Biotechnology*, **3**(2): 79–84.

Praxis (2004) UXO Corrosion in soil, SERDP final technical report prepared for U.S. Army Environmental Center. Burlingame, California.

Pruppacher, H.R., and J.D. Klett (1997) *Microphysics of Clouds and Precipitation*. Boston: D. Reidel.

Racine, C.H, M.E. Walsh, C.M. Collins, D.J. Calkins, B.D. Roebuck and L. Reitsma (1992) Waterfowl mortality in Eagle River Flats, Alaska: The Role of munition residues. U.S. Army Cold Regions Research and Engineering Laboratory, CRREL Report 92-5.

Radtke, C.W., D. Gianotto, and F.F. Roberto (2002) Effects of particulate explosives on estimating contamination at a historical explosives testing area. *Chemosphere*, **46**: 3–9.

Refait, P.H., M. Abdelmoula, and J.M.R. Genin (1998) Mechanisms of formation and structure of green rust one in aqueous corrosion of iron in the presence of chloride ions. *Corrosion Science*, **40**(9), 1547–1560.

Romanov, M. (1957) *Underground Corrosion*. National Bureau of Standards Circular 579, US Government Printing Office, Washington, DC.

Scherer, M.M., S. Richter, R.L. Valentine, and P.J.J. Alvarez (2000) Chemistry and microbiology of permeable reactive barriers for in situ groundwater clean up. *Critical Reviews in Microbiology*, **26**(4): 221–264.

Scherer, M.M., K.M. Johnson, J.C. Westall, and P.G. Tratnyek (2001) Mass transport effects on the kinetics of nitrobenzene reduction by iron metal. *Environmental Science and Technology*, **35**(13): 2804–2811.

Schutt, H.U., and P.R. Rhodes (1996) Corrosion in an aqueous hydrogen sulfide, ammonia, and oxygen system. *Corrosion*, **52**(12): 947–952.

Simon, L., J.M.R. Genin, and P.H. Refait (1997) Standard free enthalpy of formation of Fe(II)-Fe(III) hydroxysulphite green rust one and its oxidation into hydroxysulphate green rust two. *Corrosion Science*, **39**(9): 1673–1685.

Stumm, W. (Ed.) (1987) *Aquatic Surface Chemistry: Chemical Processes at the Particle-Water Interface*. Wiley.

Talbot D.D., and E.J. Talbot (1998) *Corrosion Science and Technology*. Boca Raton, Florida: CRC Press.

Taylor S., J. Lever, L. Perovich, E. Campbell, and J. Pennington (2004b) A study of Composition B particle from 81-mm mortar detonations. *Sustainable Range Management Conference.*

Taylor, S., A. Hewitt, J. Lever, C. Hayes, L. Perovich, P. Thorne, and C. Daghlian (2004a) TNT particle size distributions from detonated 155-mm howitzer rounds. *Chemosphere*, **55**: 357–367.

TetraTech (2002) Draft, final high use target area investigation report. Phase II (HUTA II). Massachusetts Military Reservation Camp Edwards. (MMR-6900), November, Tetra Tech Inc. Brookfield, Wisconsin.

Thiboutot, S., G. Ampleman, A. Gagnon, A. Marois, T.F. Jenkins, M.E. Walsh, P.G. Thorne, and T.A. Ranney (1998) Characterization of antitank firing ranges at CDB Valcartier, WATC Wainwright, and CFAD Dundrum. Defense Research Establishment, Department of National Defense, Canada.

Thiboutot, S., G. Ampleman, J. Lewis, D. Faucher, A. Marois, R. Martel, J.M. Ballard, S. Downe, T.F. Jenkins, and A. Hewitt (2003) Environmental conditions of surface soils and biomass prevailing in the training area at CFB Gagetown, New Brunswick. Defense Research Establishment, Department of National Defense, Canada, TR 2003-152.

Thorne, P. (2003) On-range treatment of ordnance debris and bulk energetics resulting from low-order detonations. SERDP project CP-1330.

USA Environmental, Inc. (2001) 100% grid sampling and 4-ft OE removal after action report. Inland Range contract report, former Fort Ord, California, site OE-50. Prepared for U.S. Army Engineer District, Sacramento.

U.S. Army (1981) Army ammunition data sheets—Rockets. Technical Manual 43-0001-30.

U.S. Army (1994) Army munitions data sheets for artillery ammunition: Guns, howitzers, mortars, recoilless rifles, grenade launchers, and artillery fuzes. Department of the Army Technical Manual TM 43-0001-28.

U.S. Army (1998) Design and analysis of hardened structures to conventional weapons effects. Technical Manual 5-855-1.

U.S. Army (1999) Establishing a temporary open burn and open detonation site for conventional ordnance and explosives projects. Technical Manual 60A-1-1-31.

U.S. Army (undated) Army active/inactive range inventory (managed by AEC—Lisa Greenfeld).

U.S. Army Center for Health Promotion and Preventive Medicine (2000) Training range site characterization and risk screening, Camp Shelby Mississippi, 7–23 September 1999. USACHPPM, Aberdeen Proving Ground, Geohydrologic study No. 38-EH-8879-99.

U.S. Government Printing Office (1989) *Department of Defense Dictionary of Military and Associated Terms*. Joint Pub 1-02.

USAMC (1985) Complete round charts—Artillery ammunition, U.S. Army Materiel Command Pamphlet AMC-P 700-3-3

UXO Corrosion, Annual report to SERDP—CP1226

UXO Recovery Depth Database (unpublished) provided by R.Young, USACE, Huntsville.

Veleva, L., P. Castro, G. Hernandez-Duque, and M. Schorr (1998) The corrosion performance of steel and reinforced concrete in a tropical humid climate. A review. *Corrosion Reviews*, **16**(3): 235—–284.

Videla, H.A. (2000) An overview of mechanisms by which sulphate-reducing bacteria influence corrosion of steel in marine environments. *Biofouling*, **15**(1–3): 37–47.

Videla, H.A. (2002) Prevention and control of biocorrosion. *International Biodeterioration and Biodegradation*, **49**(4): 259–270.

Virtanen, S., and M. Buchler (2003) Electrochemical behavior of surface films formed on Fe in chromate solutions. *Corrosion Science*, **45**(7): 1405–1419.

Walsh M.E., C.M. Collins, C.H. Racine, T.F. Jenkins, A.B. Gelvin, and T.A. Ranney (2001) Sampling for Explosive Residues at Fort Greely, Alaska. U.S. Army Engineer Research and Development Center, Cold Regions Research and Engineering Laboratory, Technical Report ERDC/CRREL TR-01-15.

Walsh, M.E., C.A. Ramsey, and T.F. Jenkins (2002) The effect of particle size reduction by grinding on sub-sampling variance of explosives residues in soil. *Chemosphere*, **49**: 1267–1273.

Walsh, M.E., C.M. Collins, T.F. Jenkins, A.D. Hewitt, J. Stark,, and K. Myers (2003) Sampling for explosives at Fort Greely, Alaska. *Soil and Sediment Contamination*, **12**: 631–645.

Walsh, M.E., C.M. Collins, A.D. Hewitt, M.R. Walsh, T.F. Jenkins, J. Stark, A. B. Gelvin, T. Douglas, N. Perron, D. Lambert, R. Bailey, and K. Myers (2004) Range characterization studies at Donnelly training area, Alaska 2001 and 2002. U.S. Army Engineer Research and Development Center, Cold Regions Research and Engineering Laboratory, Technical Report ERDC/CRREL TR-04-5.

Wexler, R.L. (1991) Hourly and daily precipitation frequencies for the United States. Engineering and Topographic Laboratory.

Wildman, M.J., and P.J.J. Alvarez (2001) RDX degradation using an integrated Fe(0)-microbial treatment approach. *Water Science and Technology*, **43**(2): 25–33.

Yfantis, D.K., A.D. Yfantis, and I. Anastassopoulou (1998) Biological corrosion of metallic parts in underground irrigation system: study of alternative materials. *British Corrosion Journal*, **33**(3): 237–240.

Zhang, X.G.(1999) Corrosion ratios of steel to zinc in natural corrosion environments. *Corrosion*, **55**(8): 787–794.

APPENDIX A: CORROSION OF UXO

Thermodynamics of Corrosion

Unexploded ordnance contain explosives, a metal casing and other components. Initially, neither the explosives nor the metals are soluble; thus, they pose only moderate environmental risk. However, following corrosion of the metal casing, toxic explosives and metals may be leached from UXO, potentially contaminating soils and groundwater. Additionally, corrosion may lead to either catastrophic failure of the casing or to the development of small holes (pinholes), processes that may release explosives into the environment. Consequently, an understanding of the mechanism of UXO corrosion in soils is needed to ascertain the risks associated with their presence in the environment.

Most corrosion processes are highly favored thermodynamically as the oxidation of metals is highly exergonic. For example, the corrosion of iron (the main constituent in steel) proceeds according to the following chemical reaction:

$$2\mathrm{Fe} + \frac{3}{2}\mathrm{O_2} \Leftrightarrow \mathrm{Fe_2O_3}\ \Delta G_{rxn}{}^{0} = -742\ \mathrm{kJ/mol} \qquad \text{(A1)}$$

The release of free energy is typical of other corrosion processes and shows the drive for metals to dissolve to form other phases. In fact, iron is not stable under any typical soil water pH-E_h conditions (Fig. A1). Other metals and alloys, including steel, the most common casing for munitions, are similarly unstable under commonly encountered thermodynamic conditions.

Reaction A1 shows the production of a solid phase, Fe_2O_3. When conditions of pH and E_h change, solution phases such as dissolved Fe(II) and Fe(III) also may form (Fig. A1). Generally, it is desirable from a remediation standpoint to produce solid phases during corrosion—they are more stable, less prone to transport, they react with potential contaminants (both inorganic and organic species adsorb strongly to iron oxides), and some oxidation products protect the metal surface from further oxidation (Kuznetsova et al. 1998, Ge et al. 2003, Virtanen and Buchler 2003). The protection of the surface is called passivation. Passivation is seen graphically in the case of aluminum corrosion. Aluminum is a highly reactive metal that is susceptible to corrosion. However, Al corrosion is actually quite slow under normal soil conditions (near neutral pH, low ionic strength). Aluminum corrodes through the formation of Al_2O_3 on the metal surface, which protects it from further oxidation or deterioration (Kloppel et al. 1997, Kuznetsova et al. 1998, Phambu 2003). This protection is a kinetic effect, in that

the thermodynamic driving force for corrosion remains, but the surface oxidation is slowed by the presence of a passivating oxide. Passivation is discussed in detail below.

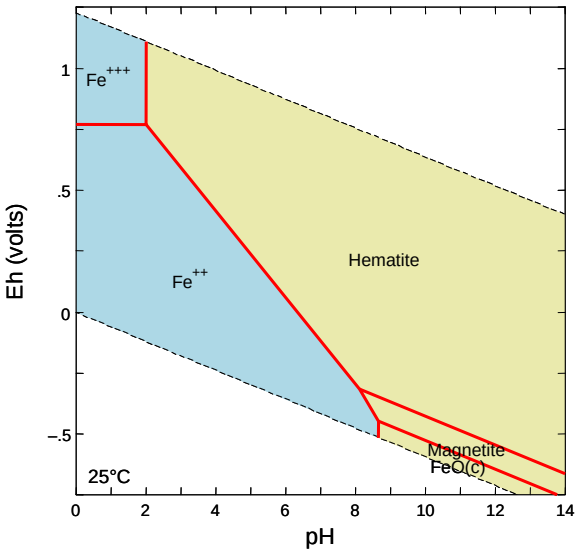

Figure A1. Fe phase diagram for Fe-O_2 system at 25ºC. The diagram is derived using a dissolved Fe concentration of 1 µM. Dark shaded phases are aqueous, while lighter phases are solids. The diagonal dotted lines show boundaries for the stability of water; the vertical dotted line shows the change in carbonate speciation. Hematite is α-Fe_2O_3 (s).

The presence of other species, as occurs in soils and sediments, strongly impacts corrosion and may also affect the formation of corrosion products (Kajiyama and Okamura 1999, Kholodenko et al. 2000, Li et al. 2001). In the case of iron, many soil species, including sulfate, phosphate, and dissolved silica, affect mineral formation (Fig. A2). Iron may form stable solid phases with Si, P, and other phases in this system; thus, knowing the solution composition is critical to understanding the products of steel and iron within soil. These precipitated solids may also form on the metal surface, thereby influencing corrosion. Conversely, some species (e.g., chloride) in solution may help to dissolve passivating oxides, thereby accelerating corrosion.

The thermodynamic effects described above focus on the corrosion of Fe. Steel corrosion has been studied in detail (Zhang 1999), and is analogous to Fe corrosion. One important difference between iron and steel is the chemical addi-

tives (e.g., Cr, C, and Mn) present in steel. These additives are minor, and do not typically influence the phase diagrams for steel relative to iron corrosion; however, additives strongly alter the kinetics of chemical corrosion. Limited attention has been devoted to the specific mechanism of UXO corrosion (Bucci and Buckley 1998, Fabian and Ostazeski 2002, Praxis 2004, AMEX, in review); we focus on mechanistic studies that examine steel and iron corrosion, and apply these mechanistic studies to our understanding of the processes by which UXO corrode and perforate.

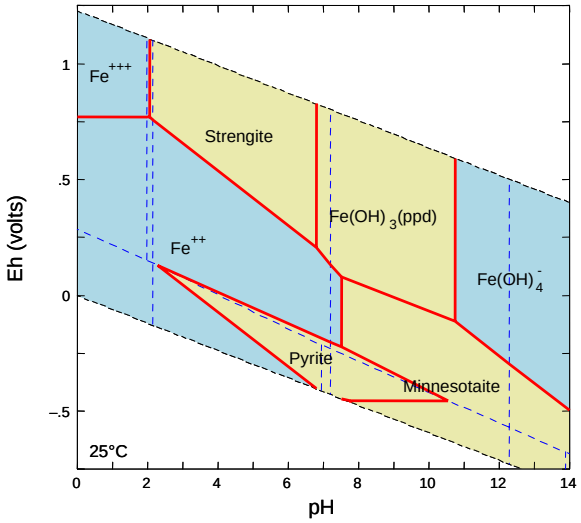

Figure A2. Fe phase diagram for Fe-O_2-S-PO_4-CO_3-H_2O system at 25ºC. The diagram is derived using a dissolved Fe concentration of 1 µM, a total CO_3^{2-} of 0.1 mM, total PO_4^{3-} and SO_4^{2-} of 1 µM, and SiO_2 of 50 µM, similar concentrations to those found in soils. Darker shaded phases are aqueous, while lighter phases are solids. The diagonal dotted lines show boundaries for the stability of water; the vertical dotted lines show the change in carbonate, phosphate, and sulfur speciation. Minnesotaite is an iron-containing phyllosilicate, and strengite is hydrated $FePO_4$.

Kinetics of Corrosion

Although thermodynamic (energetic) considerations indicate that corrosion is favored under the most commonly encountered soil conditions, kinetic factors ultimately determine the *extent* to which this oxidation occurs, the ultimate reac-

tion products of oxidation, and the distribution of these reaction products (e.g., whether they are attached to the surface). The most stable reaction products thermodynamically are often not formed during metal corrosion in soils because of sluggish reaction kinetics, instead leading to the formation of other, metastable, reaction products. For example, magnetite (Fe_3O_4) and maghemite (γ-FeOOH) production usually is favored over minnesotaite or other ferrous silicates under slightly reducing, sulfide deficient pH-E_h conditions. Similarly, ferrihydrite [$Fe(OH)_3$], lepidocrosite (γ-FeOOH), or green rusts [mixed Fe(II)/Fe(III) hydroxides] usually are produced instead of hematite (Fe_2O_3), the most stable ferric mineral, during iron oxidation (Murad and Schwertmann 1980; Davalos et al. 1991; Arshed et al. 1992, 1993; Music et al. 1993, 1997). These metastable products may be somewhat resistant to further chemical reaction; however, others, such as green rust, are highly reactive and may be important in other chemical processes. Below we discuss two important aspects of corrosion kinetics: passivation of metal surfaces and biologically mediated metal corrosion.

Fundamentals of Corrosion Kinetics

The most important means of quantifying the rate of chemical corrosion is using the corrosion potential and current. As corrosion involves disequilibrium, the corrosion potential reflects the E_h at which corrosion occurs, while the corrosion current indicates the rate of electron transfer. The extent of electrochemical reactions is determined by the rate of electron transfer; understanding this corrosion current is vital to estimate the rate of chemical corrosion. For a more complete discussion of these principles, consult one of many excellent reviews of the subject (Jones 1996, Talbot and Talbot 1998).

For understanding corrosion kinetics, it is useful to describe the electrochemical reactions that occur during corrosion in terms of their half reactions. For example, the corrosion of iron in hydrochloric acid solution can be described using the following set of half reactions, which sum to a complete expression of the total reaction:

Oxidation (at anode)	$Fe^0 \rightarrow Fe^{2+}(aq) + 2e^-$	(A2)
Reduction (at cathode)	$2HCl + 2e^- \rightarrow 2Cl^-(aq) + H_2(g)$	(A3)
Net Reaction	$Fe^0 + 2HCl \rightarrow Fe^{2+}(aq) + 2Cl^-(aq) + H_2(g)$	(A4)

Both the oxidation and reduction reactions occur at the surface of the corroding metal; however, the anode (where oxidation occurs) and cathode (where

reduction occurs) are separated on the metal surface (Fig. A3). Consequently, both chemical species and electrons flow from the anode to the cathode during oxidation. The rate of both half reactions must be equal so as to maintain electrical and charge neutrality. Thus, if either the anodic or cathodic reaction proceeds very slowly, the net rate of corrosion also will be slow.

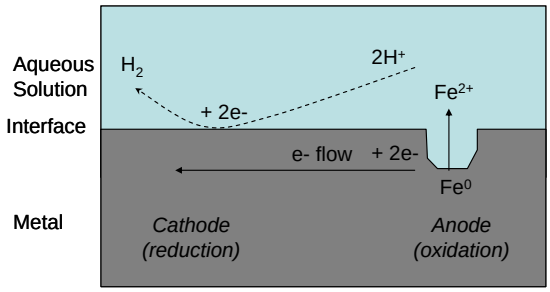

Figure A3. Corrosion of iron in an aqueous solution of HCl. The anodic reaction generates the dissolved metal and electrons, which are transferred to the cathode, where they are used to reduce protons in solution. The extent of proton transfer is equal to the electron flow, a condition required to maintain charge neutrality.

Because the rate of corrosion depends on the rate of the anodic (oxidation) and cathodic (reduction) reactions, it is necessary to identify the dominant half reactions to estimate the rate of oxidation. When alloys such as steel corrode, several anodic (oxidation) reactions may occur, each of which liberates a cation and electrons. For example, a Cr and Mn-containing steel could undergo the following anodic reactions:

$$Fe^0 \rightarrow Fe^{2+}(aq) + 2e^- \quad \text{(A5)}$$

$$Cr^0 \rightarrow Cr^{3+}(aq) + 3e^- \quad \text{(A6)}$$

$$Mn^0 \rightarrow Mn^{2+}(aq) + 2e^- \quad \text{(A7)}$$

In the case of carbon steel, the oxidation of elemental carbon to $CO_2(g)$ also may occur at the anode. As CO_2 is soluble and diffuses away quickly relative to

ions, carbon steels are more easily corroded than other steels. Anodic reactions are usually straightforward to predict; however, iron and some other metals may form multiple oxidation states, and therefore be oxidized through multiple anodic reactions. For example, iron may also be oxidized to the trivalent state:

$$Fe^0 \rightarrow Fe^{3+}(aq) + 3e^- \quad \text{(A8)}$$

Each of the thermodynamically viable reactions contributes to the overall rate of corrosion; however, the relative contribution of each depends on the rate of each process. Slow reactions contribute little to the total reaction rate; thus, the fastest reactions will predominate when multiple oxidation reactions occur.

Cathodic reactions are somewhat more complex in that many possible reactions may occur, depending on the solution conditions. For example, hydrogen may be evolved from an acidic solution as in the above example:

$$2H^+ + 2e^- \rightarrow H_2(g) \quad \text{(A9)}$$

Alternatively, oxygen may, when present, be reduced in acidic solutions:

$$O_2 + 4e^- + 4H^+ \rightarrow 2H_2O \quad \text{(A10)}$$

Oxygen reduction may also occur in neutral or alkaline solutions through a different pathway:

$$O_2 + 4e^- + 2H_2O \rightarrow 4OH^- \quad \text{(A11)}$$

Other reactions, including the reduction of a solution species (such as Fe^{3+} or NO_3^-), may occur simultaneously. Complications also may arise if solid phases (e.g., ferrihydrite during iron or steel corrosion) are produced directly during corrosion. As these products are quite stable, their formation influences the thermodynamics of corrosion, but their presence also can influence the rate of corrosion because solid phases may block surface sites reactive towards oxidation.

Mixed potential theory provides a basis for determining electrochemical reaction rates. This theory is based on two principal assumptions. First, the theory assumes that the anodic current and the cathodic current are equal and opposite. In fact, the number of electrons transferred in each must be equal to maintain charge neutrality. The second assumption is more tenuous and depends on the assumption that electrochemical oxidation and reduction processes occur inde-

pendently and that they can be separated into distinct processes. This is precisely what we have done in the above example of iron corrosion in HCl, and it is a generally good approximation for many systems; however, care must be taken to avoid applying this theory to systems that have dependent cathodic and anodic processes.

Mixed potential theory is grounded in transition state theory, which assumes that the rate of a chemical reaction depends on the activation energy, and the thermodynamic driving force for the chemical reaction is described by change in free energy of the system (Fig. A4). The net change in free energy can also be related to a net change in potential, called an overpotential (η_{anodic}) by the expression $\Delta G = -nF\eta$. The current (which is proportional to rate) of the resulting chemical reaction can then be expressed using conventional theory as:

$$\text{Current} = \text{A}\exp\left[\frac{-\Delta G}{\text{R}T}\right] = A\exp\left[\frac{-n\text{F}\eta}{\text{R}T}\right] \tag{A12}$$

Where A is a proportionality constant, ΔG is the change in free energy, R is the Ideal Gas Constant, T is the temperature in K, n is the number of electrons in the half reaction, and F is Faraday's constant. Note that this expression implies that the voltage of the over-potential is proportional to the log of the current ($\eta \propto \log i$). Thus, as the thermodynamic driving force increases, so does the rate of corrosion. This can be expressed for both the anode and cathode using the following expressions:

$$\eta_a = \alpha_a + \beta_a \log i_a \tag{A13}$$

$$\eta_c = \alpha_c + \beta_c \log i_c \tag{A14}$$

Where α and β are Tafel constants for the anodic (a) and cathodic (c) reactions. Note that the current i is the same for both anodic and cathodic processes.

The aforementioned kinetic control is called *activation polarization*, and occurs when chemical processes control reaction rate. Activation potential can easily be identified in Tafel plots (Fig. A5). In such cases, the rate of the anodic reaction current (rate) increases with increasing potential (oxidation is favored under increasingly high potential), and the cathodic reaction current increases as the potential drops, as reduction is favored under negative relative potentials.

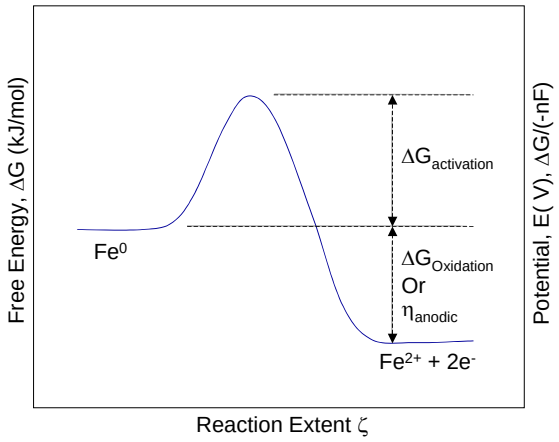

Figure A4. Coordinate diagram for an activation controlled (chemically controlled) reaction. The reaction extent describes the conversion of reactants at the left, to products at the right. The reaction rate is proportional to current, and depends on the fraction of the population that has energy in excess of the free energy of activation (which is determined by Boltzmann's distribution).

Under extremely rapid reaction rates, concentrations of either reactants or products may build up (or be depleted) at the surface of the corroding metal. In such cases, the reaction rate depends on the concentration of these species and the electrochemical reaction is controlled by *concentration polarization* (Fig. A6). Under conditions of concentration polarization, the current drops sharply at a limiting current (i_L), which is determined by the diffusion constant (D) and concentration (C) of the diffusing species and thickness d of the diffusion layer:

$$i_L = \left(\frac{DnF}{\delta} \right) C \qquad \text{(A15)}$$

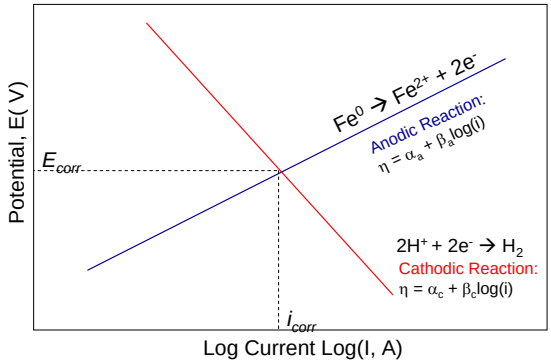

Figure A5. Activation polarization curves for both anodic and cathodic reactions of Fe corrosion in dilute acid. The point at which the currents are equal defines the corrosion potential and current for the system. The curve with the steepest slope ultimately controls the corrosion potential as small changes in its slope or position significantly change the corrosion current.

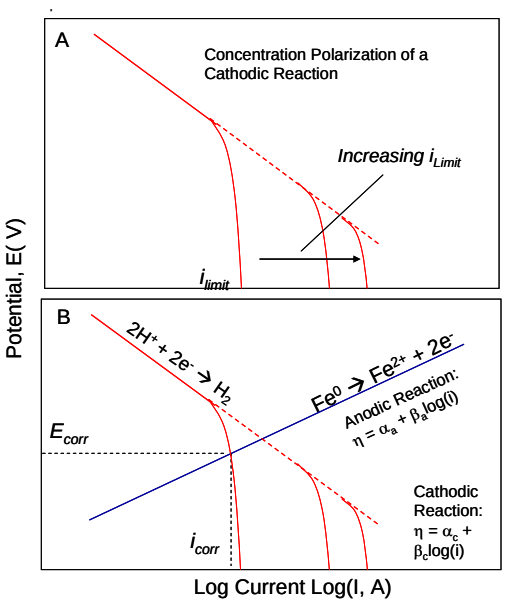

Figure A6. Effect of concentration polarization on the current of corrosion. The limiting current (i_{limit}) depends on diffusion through a surface layer (A); increasing the velocity of agitation, temperature, or concentration will increase i_{limit}. As the corrosion of the anodic reaction is equal to that of the cathode, the corrosion potential and voltage are decreased by concentration polarization relative to activation polarization. At currents below that of the limiting current, corrosion occurs through conventional, activation polarization conditions.

For example, in the case of steel corrosion, the cathodic reaction may be limited by the diffusion of H^+ to the surface to be reduced to H_2.

The overall rate of an electrochemical reaction is determined by the potential at which the anodic and cathodic currents are equal (Fig. A5 and A6). Conceptually, this crossover results in a set potential (E_{corr}) and current (i_{corr}) at which corrosion proceeds. This current is essentially constant; thus, neither corrosion rates nor corrosion potentials change during electrochemical corrosion unless reaction products form that induce concentration polarization. This leads to an effective electrochemical buffer in which the redox status of the system is maintained over extended periods. This electrochemical buffer is referred to as *apoise*. For systems in which the anodic and cathodic reactions are known, the Tafel constants can be used to determine the corrosion potential and rate. Under diffusion-limited conditions, i_L will determine the overall corrosion rate.

In many laboratory systems, stirring limits the diffusion layer thickness, thereby increasing i_L so that concentration polarization may not be observed; however, concentration polarization occurs more often in soil systems. Water is frequently immobile and poorly mixed in soil systems, leading to diffusional limitations and concentration polarization. Slow diffusion also can lead to the build-up of oxidation products locally at the metal surface, which may lead to the precipitation of an insoluble surface layer that will decrease the overall reaction rate. Thus, corrosion rates estimated from Tafel constants alone represent high estimates of corrosion rates in soil systems. Similarly, care must be exercised when extrapolating corrosion rates determined for steel in aqueous solutions to complex soil matrices.

For poorly conducting solids, ohmic polarization, which limits the flow of electrons from the anode to the cathode, may limit corrosion rates. Ohmic polarization is caused by the formation of a potential difference between the anode and cathode (under non-ohmic conditions, the potential of the anode and cathode are equal and set by the corrosion potential). Although ohmic polarization results in unequal potentials at the anode and cathode, the current is the same at both the anode and cathode. Ohmic polarization is observed in systems where charge is transferred via ion transport because solutions are not conductive; however, it seldom is limiting for metal corrosion.

Changing the composition of the solution changes the driving force for corrosion by changing the value of the Tafel constants α or β. This can be seen graphically in Figure A7, which shows the effect of changing pH on the cathodic reaction. As the acidity increases (as the pH drops), so does the hydrogen ion concentration. The resulting increase in hydrogen ion activity enhances the reduction of hydrogen ions to hydrogen gas, increasing the cathodic current at all

potentials. This shift in the cathodic polarization curve leads to a different cross-over point with the anodic reaction (which is not affected by pH in this simplistic system); thus, the corrosion current and potentials increase. Often both the cathodic and anodic polarization curves are affected by a change in solution composition. For example, in the case of the corrosion of a passivating metal, both the cathodic and anodic polarization curves will shift, also causing the corrosion potential and current to change.

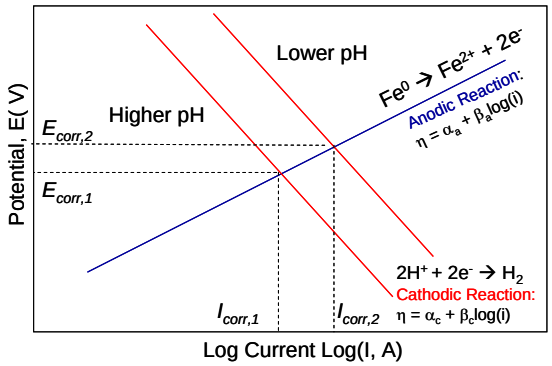

Figure A7. Influence of pH on the corrosion rate of an active metal. The example would apply for the acidic corrosion of Fe metal. The corrosion current and potential at the lower pH ($i_{corr,2}$, $E_{corr,2}$) is higher than at higher pH. It is fairly straightforward to predict which reactions will be impacted by changes in solution composition. As only the cathodic reaction involves H^+, it is the only reaction affected by changes in pH (unless the pH is high enough to induce Fe^{2+}hydrolysis). Similarly, complexation of Fe(II) by citric acid would change the pH and Fe(II) activity, changing both the anodic and cathodic polarization curves.

Passivation of Metal Surfaces

Corrosion processes are ultimately dependent on surface mediated processes. In metal corrosion, the metal surface corrodes through the chemical reaction of a dissolved solute (e.g., oxygen) with a reactive metal surface. Consequently, the rate of the reaction depends in some manner on the reactive surface area of the metal. Frequently, passivation occurs through the formation of an insoluble metal oxide film that blocks the metal surface from oxidants in solution (Fig. A8).

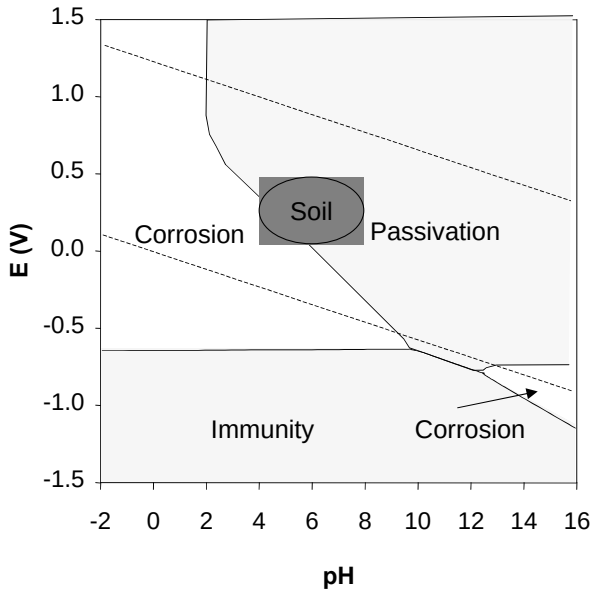

Figure A8. Domains in which passivation of iron can occur. Note that these domains are very similar to those in which solid phases are formed. Immunity occurs in E-pH domains where there is no thermodynamic driving force for corrosion. The dotted lines indicate the stability zone of water and the shaded oval is the domain in E-pH space that is most prevalent in soils.

Such films are only effective in passivating surfaces if they form effective two-dimensional arrays on the surface; thus, the microstructural compatibility of the interface between the surface and the overlying oxide film is important. This compatibility can be expressed using the following expression (Stumm 1987):

$$\Delta G_{\text{interface}} = \overline{\delta}_{\text{NW}} S_{\text{NW}} + (\overline{\delta}_{\text{NS}} + \overline{\delta}_{\text{SW}}) S_{\text{NS}} \quad \text{(A16)}$$

Where the $\overline{\delta}$ refers to the surface free energy of the given surface, and *S* is the surface area, and *NW*, *NS* and *SW* refer to the nuclei (of the metal oxide)–water, nuclei–substrate, and substrate (the metal)–water interactions. Passivation occurs under the specific case that the lattice of the metal oxide has attractive and comparable surface energy and similar lattice dimensions (implying that $\overline{\delta}_{\text{NW}} \approx \overline{\delta}_{\text{SW}}, \overline{\delta}_{\text{NS}} < \overline{\delta}_{\text{NW}}$):

$$\Delta G_{\text{interface}} = \overline{\delta}_{\text{NW}} (S_{\text{NW}} - S_{\text{NS}}) \quad \text{(A17)}$$

Under these conditions, the surface oxide can effectively cover the surface with a passivating layer, thereby preventing further oxidation (Fig. A9). However, if the corroding metal substrate and the oxide have dissimilar energies, then the surface coating will not develop into a crystalline solid, nor will it effectively protect the surface from further oxidation.

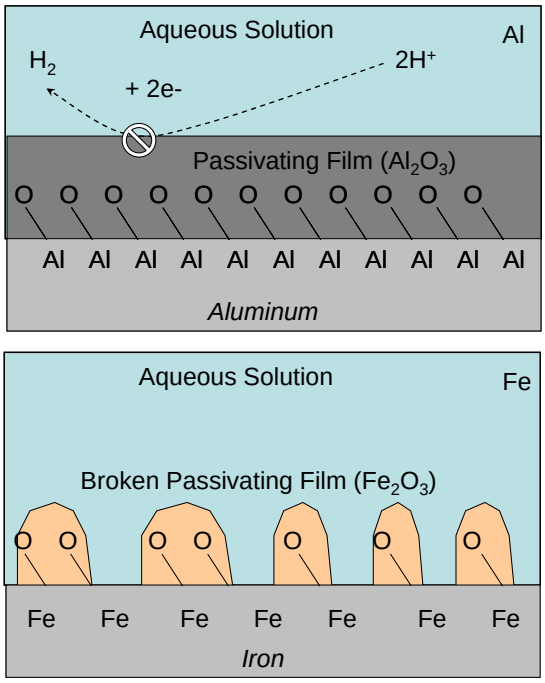

Figure A9. Formation of passivation layers during the corrosion of iron (Fe) and aluminum (Al). The passivation layer on Al is complete because the Al oxide forms a compatible passivating film. As drawn, the passivation occurs by blocking the cathodic reaction; however, anodic passivation is also possible. In contrast, the Fe oxide film is not compatible and forms oxides that are ineffective at blocking the surface.

Most UXO are composed of carbon steel, though a limited number of aluminum grenades also have been used. Aluminum is effectively passivated by the formation of Al_2O_3 films, which are highly compatible with Al surfaces (Fig. A9). This passivation leads to fairly corrosion resistant aluminum surfaces except

in chloride containing solutions. This protection occurs despite aluminum metal being sufficiently reactive that fine Al powders oxidize sufficiently rapidly to induce explosions. In contrast, steel UXO corrode to ferric (hydr)oxides, which do not bond strongly to the metal surface and consequently have only limited potential to passivate the metal surface (Fig. A9). This weak bonding is caused by unfavorable interactions between Fe at the surface and the oxide over layer. Stainless steels, however, are frequently passivated though the addition of chemical modifiers that can form compatible oxide films. For example, Cr in stainless steel forms passivating Cr_2O_3 films on steel. Thus, knowing the type of material composing the UXO shell is important for understanding its overall corrosion rate.

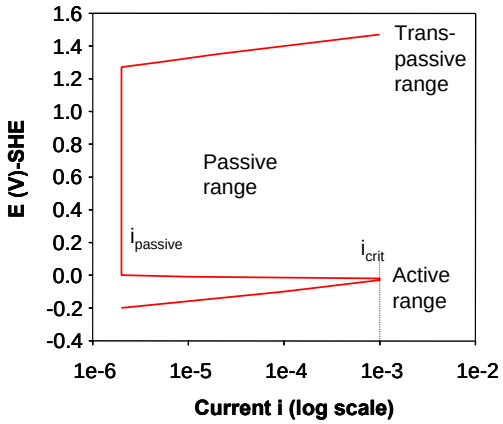

Figure A10. Passivation influences on corrosion current for stainless steel corrosion. Anodic polarization for AISI304 Stainless Steel in 0.05 M H2SO4 (pH 1.2). In the active range, corrosion increases with overpotential, in the passive region, the production of an oxide overgrowth at i_{crit} limits corrosion currents to a constant value ($i_{passive}$), and in the transpassive region, this overlayer breakdown permits increased reaction rates. Based on data from Talbot and Talbot (1998).

Passivation influences both the corrosion potential and current. For stainless steel, the current of the anodic reaction changes rapidly as the potential increases (Fig. A10). This response is caused by sufficiently rapid corrosion to develop large surface concentrations of the dissolved ion, thereby inducing precipitation

of an insoluble metal hydroxide or oxide. In this passivated range of potentials, the current is limited by diffusion and is nearly independent of potential. At extremely high over potentials, however, the current again increases as there is sufficient driving force to overcome the passivation layer. In this high potential region, the passivation layer is breached, typically at the anode, resulting in rapid oxidation at a specific and small location. In this case, the resulting pitting may severely undermine the strength and integrity of the steel. In contrast, oxidation proceeds *uniformly* (equal rates across the surface) when the reaction is controlled by activation or concentration polarization. This pitting mechanism has been discussed at some length by Fabian and Ostazeski (2002), who also identify pitting corrosion as a potentially important mechanism of UXO failure. Unfortunately, the shape and depth of corrosion pits, and the rate of pitting corrosion, are very difficult to estimate as they vary with steel type, impact, and construction stresses, the extent of overpotential in the soil, and a variety of other factors.

Often, steels are treated with *inhibitors* to decrease the rate of corrosion by increasing passivation. One such inhibitor is dissolved chromate, which oxidizes any evolved ferrous iron to insoluble oxides, and also forms a passivating insoluble oxide:

Chromate reduction:	$2CrO_4^{2-} + 10H^+ + 6e^- \rightarrow Cr_2O_3(s) + 5H_2O$	(A18)
Fe oxidation:	$6Fe^{2+} + 9H_2O \rightarrow 3Fe_2O_3(s) + 18H^+ + 6e^-$	(A19)
Net Reaction:	$2CrO_4^{2-} + 6Fe^{2+} + 4H_2O \rightarrow Cr_2O_3(s) + 3Fe_2O_3(s) + 8H^+$	(A20)

This reaction is sufficiently favorable that even low concentrations of chromate can help to form insoluble oxides on the metal surface that are sufficiently thick and uniform to slow corrosion. There are also many elements found in soil that may passivate the metal surface. One possible soil oxidant is manganese (III, IV) oxides, which are ubiquitous in soils (average concentrations in soil of about 0.1–0.2%).

$$MnO_2 + 4H^+ + 2e^- \rightarrow Mn^{2+} + 2H_2O \quad \text{(A21)}$$

Manganese(IV) reduction itself does not passivate the metal; rather, manganese oxides react with reduced ferrous iron produced at the anode to form iron oxide films.

Biologically Mediated Metal Corrosion

Biological reactions are ubiquitous in soil systems. Frequently, biological processes accelerate corrosion through a variety of processes (Prakash et al. 1988, Kloppel et al. 1997, Yfantis et al. 1998, Kajiyama and Okamura 1999, Li et al. 2001, Gu et al. 2002, Doyle et al. 2003). One of the most obvious and most important means by which biological organisms accelerate corrosion is through the secretion of acid, directly as small organic acids, into the soil solution. Acid is released into soils by organisms as a result of nutrient uptake (cation uptake is balanced by excretion of H^+) and as a means of regulating their environment. Acidity is also generated by the excretion of respiratory carbon dioxide. Upon dissolution, this CO_2 forms carbonic acid, which is a weak acid:

$$CH_2O+O_2 \xrightarrow{respiration} H_2O + CO_2(g) \rightarrow H_2CO_3(aq) \Leftrightarrow H^+ + HCO_3^- \quad \text{(A22)}$$

Some metabolic processes involve the direct production of acid; sulfur oxidizers such as *Thiobacillus spp*. oxidize inorganic sulfide and elemental sulfur to sulfate, producing considerable acidity.

$$HS^- + 4H_2O \rightarrow SO_4^{2-} + 9H^+ + 8e^- \quad \text{(A23)}$$

Such acid generation can be severe—the pH of soil pore waters at Iron Mountain, California, have decreased to negative values as a result of such oxidative processes (Nordstrom and Alpers 1999, Nordstrom et al. 2000). As metal passivation does not occur under acidic conditions, chemical oxidation is typically enhanced in acidic soils and other environments.

Organic acids such as oxalic acid ($H_2C_2O_4$) also influence corrosion by complexing metal ions. For example, aluminum is complexed by oxalate through the following reaction:

$$AlOOH + 3C_2O_4^{2-} + 3H^+ \rightarrow Al(C_2O_4)_3^{3-} + 2H_2O \quad \text{(A24)}$$

Such reactions are important because they prevent passivation by oxide minerals such as AlOOH, and may even dissolve oxidized layers formed prior to their introduction. Consequently, complexation by oxalate and other biologically produced chemical species (e.g., citrate, soil organic matter) also increases corrosion rates.

In a given environment, specific metabolites may exert considerable influence on corrosion rates. In particular, the excretion of hydrogen sulfide by sulfate

reducing bacteria (SRB) can contribute to corrosion in anaerobic environments (Booth and Tiller 1968; Edyvean and Videla 1991; Hamilton 1985, 1998; Videla 2002). SRBs reduce sulfate to hydrogen sulfide, usually using a carbon source as the electron donor (the reverse reaction to eq A9). Hydrogen sulfide then can be re-oxidized through chemical or biological processes, producing sulfuric acid. Alternatively, it can precipitate out with iron or other cations to make sulfide minerals such as mackinawite (FeS_{1-x}). These solids reduce the polarization resistance for cathodic (reductive) corrosion, thereby increasing the corrosion rate by as much as an order of magnitude (Kajiyama and Okamura 1999, Li et al. 2001). Ammonia and other nitrogen oxoanions also are produced through biological processes and influence corrosion.

Bacteria also may accelerate steel and iron corrosion by changing the concentration of dissolved iron (Hamilton 1985, 2003; Little et al. 1991, 1998; Lee and Newman 2003). This effect is limited to anaerobic soils and sediments where dissimilatory (metabolic) iron reduction is favored, as assimilatory pathways (those used for cellular incorporation) typically require little Fe and do not change the dissolved concentration appreciably. Dissimilatory iron reduction involves the reduction of insoluble iron oxides to Fe(II) either through direct contact or via a solution-phase electron shuttle or extracellular protein. Under static conditions in which iron reducing bacteria are actively reducing suspended Fe(III), the corrosion rate may actually be slowed as their metabolic processes consume oxygen in the system that would otherwise attack the metal. However, bacteria in a flowing, slightly aerated environment would reduce passivating Fe(III) oxide films, while flow would facilitate reactant transport, increasing corrosion rates. More research is needed to determine the interplay between these two possibilities.

It should be noted that biologically facilitated reactions do not change the energetics (thermodynamics) of corrosion, rather they change the mechanism by which corrosion occurs and, thereby, potentially, the rate of corrosion and the phases that are formed through corrosion. Biological corrosion reactions often result in the production of unique, metastable solid phases with different stability than chemically produced solid phases. In some cases, corrosion can lead to the formation of metastable reaction products, such as magnetite, that have unusually stable structures and low reactivity (Veleva et al. 1998, Ishikawa et al. 2003). However, reactive phases, such as green rust, may also be formed through a combination of biological and chemical processes (Drissi et al. 1995, Simon et al. 1997, Genin et al. 1998, Refait et al. 1998). These solid phases are highly reactive, and may in fact react strongly with contaminants such as RDX and TNT that have been released from leaking UXO (Hundal et al. 1997, Scherer et al. 2001, Wildman and Alvarez 2001). These compounds also are formed primarily in an-

aerobic soils and wetlands, environments that likely contain a large number of corroded UXO.

UXO Corrosion Rates in Soils

Under typical soil conditions (near neutral pH, moderately oxidizing conditions), iron, various alloys of steel, and aluminum are chemically unstable. Despite this instability, UXO and other metallic objects are often stable in soil environments over long periods. This is easily explained using the equations given here. Aerated soils are typically close to neutral with redox potentials of about 0.5 V. Under such conditions, passivation films are formed (Fig. A8) that can slow the corrosion rate by about three orders of magnitude (Fig. A10). Slow diffusion and near neutral pH in soils enhance the production of passivating oxides in soils, further slowing the corrosion rate.

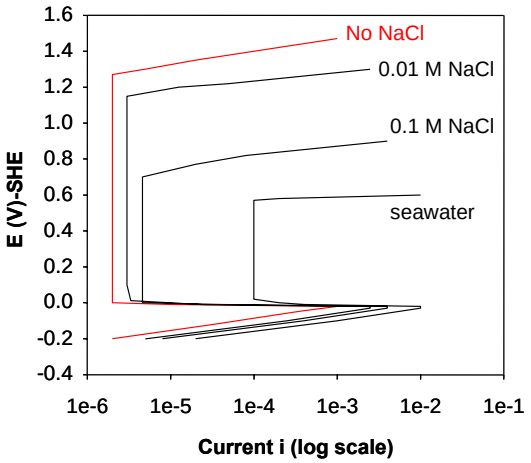

Figure A11. Effect of added chloride on steel corrosion. Anodic polarization for AISI304 Stainless Steel in 0.05 M H_2SO_4 and varying concentrations of NaCl. Salt changes the corrosion current in the active region to some extent, but it appreciably alters the passive corrosion current, and lowers the potential of the transpassive region, where pitting occurs. Thus, pitting is the dominant form of corrosion in oxygenated waters (E ~ 0.55 V) under these conditions. Based on data from Talbot and Talbot (1998).

Often, corrosion in soils occurs at a different rate than is predicted on the basis of laboratory studies. Many of these differences are ascribable to differences

in chemical composition in soils from experimental conditions. For example, changes in pH or dissolved ions result in significant changes in the anodic or cathodic polarization curves and in secondary mineral precipitation, thereby influencing the corrosion rate (Fig. A11). As a result, the corrosion rate of steel in soil systems is often determined empirically by measuring a loss in weight over time, or by measuring the thickness change over time (Romanov 1957). This approach works well for active materials (those that do not form surface coatings) that corrode uniformly with little pitting, and rapidly enough to ensure accurate measurements. It is problematic for stainless steels and other resistant alloys, which react slowly enough that there is appreciable error in the measurements. The principal model for UXO corrosion estimates corrosion rates based on an empirical study of galvanized steel (Bucci and Buckley 1998, AMEX, in review). Although useful, estimates based on galvanized metals may be grossly in error, as galvanization is designed to protect the steel by coating the metal with zinc that corrodes preferentially. However, once this coating corrodes, the steel corrodes in much the same way as ungalvanized steel. Despite these limitations, empirical corrosion rates of many steels have been estimated in a wide range of media (see the *Handbook of Corrosion Data* [Craig 1989]). For the steel alloys commonly used in UXO production, the corrosion rates in a variety of media are shown in Table 6.

It is clear from Table 6 that corrosion of steels in soil varies significantly, depending on the alloy type and reaction conditions. In each case, corrosion is fastest in acidic conditions, where passivation is less pronounced, or in saline environments, where the dissolved salts increase the conductivity of the solution and chloride complexes of Al and Fe increase their solubility. Most munitions have been produced from low to moderate carbon content steels, as carbon steels have the highest strengths. This carbon steel is highly reactive, corroding more rapidly than other steels and also undergoing extensive pit corrosion. In contrast, the most stable alloys of stainless steel (e.g., Alloy 316) are nearly 100 times less reactive. Thus, munitions made with recalcitrant alloys are much less likely to fail through corrosion. Unfortunately, few munitions are constructed of such alloys; only a few types of grenades are constructed of resistant Al alloys, and none of the steel alloys used in munitions are stainless, as it has less desirable mechanical properties.

Empirical corrosion rates for steel and other metals in soils have also been determined, but relatively little work has been done to create general expressions that relate soil chemical characteristics to corrosion rates. In general, corrosion in soils occurs more rapidly than in solutions of a single constituent composition (e.g., NaCl). For most corroding low-carbon steels, the corrosion of carbon steels occurs at about 0.02–0.1 (average of 0.025) mm/year (Penhale 1971, Levlin

1996, Norin and Vinka 2003) in oxidizing soil environments. This rate is at least 10× slower for stainless steels, which corrode at less than 0.01 mm/year (Kajiyama and Okamura 1999). Steel corrosion is accelerated in sulfidic anaerobic environments, often corroding up to 1 mm/year (Hamilton 1983, 1985, 2003; Little et al. 1991; Schutt and Rhodes 1996; Kajiyama and Okamura 1999; Li et al. 2001; Videla 2000). These rates are similar to those calculated using the UXO corrosion model of Garber and Adams (included in Fabian and Ostazeski 2002), although our estimates are somewhat more general and require much less input information.

The rates of corrosion in aerated soils shown in Table 6 are not particularly rapid, and would lead to the uniform failure of small munitions (grenades, etc., with minimum wall thicknesses of 2–5 mm) in about 80–200 years. Larger munitions with thicker walls (5–10 mm walls) would fail in 200–400 years. Pitting corrosion is more prevalent than uniform corrosion in soils (Frankel 1998, Doyle et al. 2003, Norin and Vinka 2003) and also results in much deeper corrosion, potentially decreasing the time required to perforate the UXO to about 20 and 50 years for small and larger munitions, respectively. In reducing soils, munitions could corrode much more rapidly, in as little as a few years; consequently, the casings of munitions in wetlands likely have corroded through to the HE fill. Saline environments, such as those encountered in proving grounds in arid basins such as China Lake, California, also may have saline soil chemical conditions favorable for enhanced corrosion.

The above estimated corrosion rates should be viewed with some caution, as it is difficult to determine precisely the rate of corrosion in soils, in part because of variation in soil pH, salinity (conductivity), moisture, and age. In general, more acidic soils will corrode steel more readily than alkaline soils because of increasing passivation, and soils with high concentrations of dissolved salts cause rapid corrosion because of complexation of oxidation products with dissolved ions, improved diffusion (which increases limiting currents), and other factors. Soil organic matter (and other organic molecules) also may influence corrosion through adsorption and blocking of active sites. Fortunately, the corrosion rate of steel in a broad variety of soils apparently only varies by a factor of 2 to 5.

The effect of increasing soil water content on corrosion is more complex. In aerated soils, increasing the water content leads to increased corrosion rates as the oxidation products are more easily removed from the surface under conditions of flow; however, under anaerobic conditions, which occur in many flooded soils, microbial processes may lead to the reduction of iron(III) hydroxides and sulfate, preventing passivation and also activating the cathode for further oxidation. These biological effects can be quite significant, increasing the corrosion

rate by an order of magnitude or more, but more work is needed to better understand and quantify the processes by which biological corrosion occurs in soils.

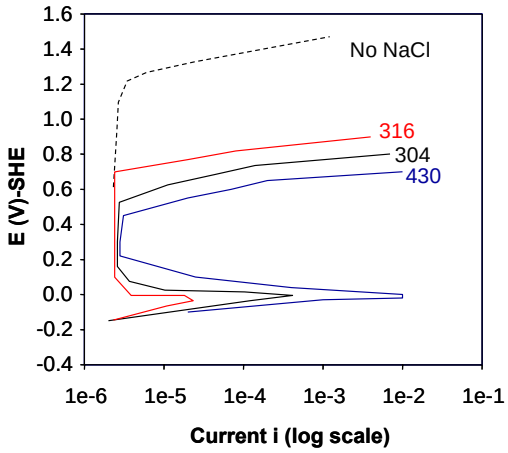

Figure A12. Effect of alloy composition on steel corrosion. Anodic polarization for Stainless Steels of various composition (316, 304, and 430) in 0.05 M H_2SO_4 and 0.01 M NaCl. The steel allow changes the corrosion in the active region, and influences the potential of the transpassive region, where pitting occurs. The dotted line shows the anodic polarization curve for all steels in the absence of NaCl. Based on data from Talbot and Talbot (1998).

Some dissolved soil constituents (e.g., phosphate) may react with corrosion products (e.g., Fe^{3+}) to form precipitates that are effective in slowing corrosion. Such approaches are commonly used to regulate the oxidation of buried metals and other oxidation sensitive materials (e.g., sulfide minerals). Additionally, the alloy of steel also influences the overpotential required for pitting (Fig. A12). In the case of carbon steels (the form of steel in most UXO), the overpotential required for transpassive corrosion is low, and thus they are commonly corroded through rapid pitting. Although the chemical conditions present in the soil may accelerate corrosion relative to the rate predicted for simple passivated metals, the extent and depth of pitting are difficult to quantify.

Pitting corrosion is especially pertinent for UXO and the soil solutions in which they are found. Stainless steels (although not all steels) are normally passivated under typical redox potentials. However, soil solutions contain apprecia-

ble solutes, which can influence the overpotential required for transpassive corrosion and induce pitting corrosion (Fig. A11). Such pitting may result in pinhole failures in the UXO, which may release small volumes of explosives contained within them. Pinholes also provide an additional avenue for corrosion (corrosion can then occur from within), thereby increasing the rate of catastrophic failure. Pitting also influences UXO integrity and strength, potentially destabilizing the UXO to mechanical breakdown.

Summary of UXO Corrosion Data

The mechanism of metal corrosion can have a profound impact on explosives ultimate release; however, little specific work has been done on the corrosion of UXOs in the environment. Here, we report theoretical and empirical (experimentally determined) corrosion rates for steel in soil. In general, we find that steel corrosion will eventually lead to the failure of UXOs and other munitions, with failure taking between 10 years for some thin-walled munitions in wetlands and other flooded environments, and up to a few hundred years for larger munitions in aerated environments. Pitting corrosion is much more rapid, potentially leading to failure 5 to 15 times more rapidly than the uniform corrosion rates stated above. There are many approximations in this work. The most significant approximation involves the use of a single corrosion rate for all soils and alloys. This is clearly not the case; UXOs are found in soils with a wide variety of water contents, salinities, compositions, and pH. While more research is needed to refine our understanding of UXO corrosion in environments such as firing ranges that are contaminated with UXOs, the rate estimation is justified in that most empirical corrosion rates are within a factor of 2 to 5 from this rate, and most of the alloys used in the production of UXOs are low carbon steel with similar corrosion characteristics. It should be noted that these corrosion rates are sufficiently slow that corrosion of UXOs in most soil environments is limited, primarily because of passivation. Exceptions arise when evaluating corrosion rates in marine environments and poorly aerated (flooded) soils, where corrosion may occur much more rapidly and lead to pitting. Previous studies on UXO corrosion have implied that corrosion in soils is slowed by passivation, and thus not a major concern (Bucci and Buckley 1998, AMEC, in review). While our results are not inconsistent with these findings, the presence of dissolved solutes and lower pH in some soils may prevent passivation and lead to considerably increased corrosion rates. Thus, site-specific evaluations of corrosion rates (or potential corrosion rates) should be performed prior to extrapolating to UXOs in all soil environments.

The observed reaction rates are sufficiently rapid that some fraction of the UXO are corroded sufficiently to release explosives and other contaminants into

soils and sediments. There are limited reports in the literature of the detection of organics associated with UXO failure, although the concentrations are typically small and it is difficult to know whether corrosion or physical damage to the munitions caused their release. A quantitative assessment of the number of failing UXO also is not possible given the uncertainty in UXO distribution, coverage, age, and dud rates (estimated at 1 to10%), each of which affects their number and corrosion characteristics. The physical condition of UXO in the field is also not well known; stresses applied to UXO during fabrication, launch, and impact are important as stresses can facilitate corrosion through metal activation. Furthermore, a quantitative estimate of the number of UXO buried in unusually corrosive (anaerobic and saline) environments is also poorly constrained. Thus, it is difficult to determine both the number of UXO, and their corrosion rate, particularly for corrosion in sensitive areas.

Many of the perforations in UXO are probably limited to relatively small holes formed as a result of pitting corrosion, but some small munitions, particularly in flooded soils and sediments with low hydrologic gradients, may also have failed through anaerobic corrosion induced by sulfate reducing bacteria. However, there are major questions about the extent to which these pinholes will release these toxins, and the interactions of these toxins with the corroding metals and soil microbial populations. One intriguing possibility is that the reactive intermediates formed during metal corrosion may facilitate the degradation of RDX, TNT, and other explosives during discharge from the UXO hull (Hundal et al. 1997, Scherer et al. 2000). More work also is warranted in this area, although the first-order questions of the characterization and distribution of UXO at a variety of different locations needs to be addressed before the effects of such secondary reactions can be quantified.

REPORT DOCUMENTATION PAGE

Form Approved
OMB No. 0704-0188

1. REPORT DATE *(DD-MM-YYYY)*	2. REPORT TYPE	3. DATES COVERED *(From - To)*
December 2004	Final Technical	2003-2004

4. TITLE AND SUBTITLE

Underground UXO: Are They a Significant Source of Explosives in Soil Compared to Low- and High-Order Detonations?

5a. CONTRACT NUMBER

5b. GRANT NUMBER

5c. PROGRAM ELEMENT NUMBER

6. AUTHOR(S)

Susan Taylor, James Lever, Michael Walsh, Marianne E. Walsh, Benjamin Bostick, and Bonnie Packer

5d. PROJECT NUMBER
T03-006

5e. TASK NUMBER

5f. WORK UNIT NUMBER

7. PERFORMING ORGANIZATION NAME(S) AND ADDRESS(ES)

Cold Regions Research and Engineering Laboratory
U.S. Army Engineer Research and Development Center
72 Lyme Road
Hanover, NH 03755

8. PERFORMING ORGANIZATION REPORT NUMBER

ERDC/CRREL TR-04-23

9. SPONSORING / MONITORING AGENCY NAME(S) AND ADDRESS(ES)

USAEC
ATTN: SFIM-AEC-PCT
Aberdeen Proving Ground, MD 20101-540

10. SPONSOR/MONITOR'S ACRONYM(S)

USAEC

11. SPONSOR/MONITOR'S REPORT NUMBER(S)

SFIM-AEC-AT-CR-2004022

12. DISTRIBUTION / AVAILABILITY STATEMENT

Approved for public release; distribution is unlimited

13. SUPPLEMENTARY NOTES

Project participants/contributors included: Dartmouth College and AEC

14. ABSTRACT

Are the amounts of explosives leaking from UXO significant compared to other sources? To answer this question we compiled data on the contamination released by above ground detonations of different order and by the rupture or corrosion of UXO. The results indicate that low-order detonations, be they from malfunctioning munitions or sympathetic detonations, are currently the largest contributors to range contamination. Also, dissolution of the explosive charge from heavily corroded UXO is significant and will increase in importance with time. Unfortunately, only order-of-magnitude estimates are possible due to shortage of data on the actual fates experienced by different types of munitions. However, the framework used here for compiling and ranking the explosive sources canhelp guide policy-making and future research activity to reduce range contamination.

15. SUBJECT TERMS

Corrosion
Explosives transport
Low-order detonations
Munition fate
UXO (Unexploded Ordnance)

16. SECURITY CLASSIFICATION OF:			17. LIMITATION OF ABSTRACT	18. NUMBER OF PAGES	19a. NAME OF RESPONSIBLE PERSON
a. REPORT	b. ABSTRACT	c. THIS PAGE			19b. TELEPHONE NUMBER *(include area code)*
U	U	U	U	129	

ERDC/CRREL TR-04-23

Cold Regions Research and Engineering Laboratory

US Army Corps of Engineers®
Engineer Research and Development Center

Underground UXO: Are They a Significant Source of Explosives in Soil Compared to Low- and High-Order Detonations?

Susan Taylor, James Lever, Michael Walsh, Marianne E. Walsh, Benjamin Bostick, and Bonnie Packer

December 2004

ERDC/CRREL TR-04-23
December 2004

Underground UXO: Are They a Significant Source of Explosives in Soil Compared to Low- and High-Order Detonations?

Susan Taylor, James Lever, Michael Walsh, Marianne E. Walsh

Cold Regions Research and Engineering Laboratory
U.S. Army Engineer Research and Development Center
72 Lyme Road
Hanover, NH 03755

Benjamin Bostick

Earth Science Department
Dartmouth College
Hanover, New Hampshire 03755

Bonnie Packer

U.S. Army Environmental Center
Aberdeen Proving Ground, Maryland 20101-5401

Final report

Prepared for U.S. Army Environmental Center

ABSTRACT

Are the amounts of explosives leaking from UXO significant compared to other sources? To answer this question, data were compiled on the contamination released by above ground detonations of different order and by the rupture or corrosion of UXO. The results indicate that low-order detonations, be they from malfunctioning munitions or sympathetic detonations, are currently the largest contributors to range contamination. Also, dissolution of the explosive charge from heavily corroded UXO is significant and will increase in importance with time. Unfortunately, only order-of-magnitude estimates are possible due to shortage of data on the actual fates experienced by different types of munitions. However, the framework used here for compiling and ranking the explosive sources can help guide policy-making and future research activity to reduce range contamination.

CONTENTS

ILLUSTRATIONS

TABLES

CONVERSION FACTORS, NON-SI TO SI UNITS OF MEASUREMENT

Non-SI units of measurement used in this report can be converted to SI units as follows:

Multiply	By	To obtain
acres	4,046.873	square meters
acres	0.4046873	hectare (10,000 m^2)
feet	0.3048	meters
feet per second	0.3048	meters per second
inches	0.0254	meters
pounds (mass)	0.4535924	kilograms

PREFACE

This report was prepared by Dr. Susan Taylor, Research Physical Scientist, Environmental Sciences Branch, Dr. James Lever, Mechanical Engineer, Applied Military Engineering Branch, Michael Walsh, Mechanical Engineer, Engineering Resources Branch, Marianne E. Walsh, Chemical Engineer, Environmental Sciences Branch, Cold Regions Research and Engineering Laboratory, Benjamin Bostick, Assistant Professor, Earth Science Department, Dartmouth College, and Bonnie Packer, Research Scientist, U.S. Army Environmental Center.

The authors thank the U.S. Army Environmental Center for funding this work. To help us determine the relative importance of UXO as a contaminant source, we obtained important information from Jay Clausen (AMEC), Roger Young (USACE, Huntsville), Travis Boyer (CTC), Lisa Greenfeld (AEC), Philip Thorne (ARA) and Peter Keene, Dr. Thomas Jenkins and Alan Hewitt (CRREL). We thank them for their contribution to this report. We thank Dr. David Ringelberg and Laura Perovich, from CRREL for helpful comments on the manuscript and Dr. Clarence Grant, Philip Thorne and Martin Stutz for reviewing and suggesting improvements to this document. We also thank Jane Mason and Mark Hardenberg for their help illustrating and editing the report.

This report was prepared under the general supervision of Dr. J-C. Tatinclaux, Chief, Environmental Sciences Branch; Dr. Lance Hansen, Deputy Director, and James Wuebben, Acting Director, CRREL.

The Commander and Executive Director of the Engineer Research and Development Center is COL James R. Rowen, EN. The Director is Dr. James R. Houston.

EXECUTIVE SUMMARY

A fired munition will experience one of many possible fates. Generally, it will detonate as intended. However, it is also possible that it will go low-order or be a dud. A dud might penetrate the ground or come to rest on the surface. Whether on the surface or underground, unexploded ordnance (UXO) will suffer one of the following fates: it can be intentionally blown-in-place, a round exploding nearby could detonate it sympathetically, the casing might be split during the initial impact or by nearby detonations, or the shell can remain intact and corrode over time. UXO pose two types of risk: the risk of detonation if the round is moved or stepped on, and the risk of leaking explosives into the environment if the round is not removed and disposed of properly. This report focuses on the environmental hazard.

The physical and chemical breakdown of UXO is a potentially important source of explosives to the environment. The rate, extent, and hazard potential of UXO breakdown depend in part on how the casings corrode in soil. It is, therefore, important to understand the mechanism by which corrosion occurs in soil systems. Here, we present an overview of metal corrosion with special focus on the corrosion of UXO related materials. Overall, we find that corrosion of low-carbon steel, the most commonly used steel in UXO, probably occurs at about 0.025 mm per year. Interestingly, variations in corrosion rate attributable to soil chemical conditions and the casing alloy are within a factor of 5. This suggests that most UXO, which have a minimum wall thickness between 2 and 10 mm, will corrode within 80 to 400 years under normal aerated soil conditions. Under reducing conditions similar to those encountered in wetlands and other anaerobic and flooded environments, sulfide production accelerates corrosion by about a factor of 10 (with considerable variability), resulting in perforation of the round after approximately 10–40 years. Pit corrosion is also common in soil environments and often results in much deeper, though much smaller, surface corrosion. Further refinement of the rate of UXO corrosion is not possible given the variability in soil chemical parameters, including pH, dissolved solute concentration, and biological activity. Nevertheless, these data suggest that corrosion has already caused some leakage of explosives from munitions and that leakage will increase significantly over the next 100 years.

Are the amounts of explosives leaking from UXO significant compared to other sources? To answer this question, we compiled data on the contamination released by above-ground detonations of different order and by the rupture or corrosion of UXO. The results indicate that low-order detonations, be they from malfunctioning munitions or sympathetic detonations, are currently the largest contributors to range contamination. Also, dissolution of the explosive charge

from heavily corroded UXO is significant and will increase in importance with time. Unfortunately, only order-of-magnitude estimates are possible owing to a shortage of data on the actual fates experienced by different types of munitions. However, the framework used here for compiling and ranking the explosive sources can help guide policy-making and future research activity to reduce range contamination.

LIST OF ABBREVIATIONS AND DEFINITIONS

AEC	U.S. Army Environmental Center.
ASRP	Ammunition Stockpile Reliability Program.
BIP	Blow-in-Place, an operation where EOD personnel destroyed one or more munitions. Munitions are blown-in-place when they have been damaged, are out of date, or are UXO that are dangerous to move. Generally, a block of C4 is strapped to the round and initiated electronically.
BRAC	Base Realignment and Closure Act.
C4	Mixture of 90% RDX (cyclonite, cyclotrimethylene trinitramine) and a binder (often polyisobutylene or dioctyl adipate), a plasticizer [di(2-ethylhexyl) or dioctyl sebacate], and petroleum oil.
Composition A5	Wax-coated, granular explosive consisting of RDX and plasticizing wax, mixed with 1.5% stearic acid.
Composition B	60–39 mixture of RDX and TNT that contains ~1% wax.
CRREL	Cold Regions Research and Engineering Laboratory.
DoD	Department of Defense.
DODIC Number	Department of Defense identification code designation for the munition type.
Dud (UXO)	Round that is fired but which completely fails to detonate at the target. Upon impact a dud can penetrate the ground or come to rest on the soil surface. During this process it either remains intact or breaks open.
EOD	Explosive ordnance disposal.
ERF	Eagle River Flats, a salt water marsh that is the impact area for Fort Richardson, Alaska.
ESTCP	Environmental Security Technology Certification Program.
HE	High explosive.
High-order	(HO) detonation: a term that refers to a munition that has high yield—the explosive filler generated a shock wave that travels at supersonic velocities.
HUTA	High use training area at MMR.
Frag.	Contraction for ordnance fragment.
FUDS	Formerly Used Defense Sites.
HMX	High explosive, octahydro-1,3,5,7-tetranitro-1,3,5,7-tetrazocine, used in octol (a 70–30,TNT–HMX mixture) often found as a bi-product of RDX production.

Live Fire	Tactically detonated munition, one that was detonated via the designed detonation chain: fuze, booster, main HE round.
Low-order	(LO) detonation (partial detonation): one where only a part of the explosive detonates. Generally, large fragments of shell casing and particles of explosives are scattered close to where the shell detonated. Some of the original explosive charge might remain in the shell.
MIDAS	Munitions Items Disposition Action System database.
MMR	Massachusetts Military Reservation.
NG	Nitroglycerine.
Octol	High explosive made of 70% HMX and 30% TNT, used mainly in rockets.
Passivation	Blocking of the metal surface by a non-reactive species, often through the formation of an insoluble metal oxide film that protects the metal surface from oxidants in solution.
ppm	Parts per million, mg/L, mg/kg.
ppb	Parts per billion, µg/L, µg/kg.
Propellants	Explosive charge used for propelling a projectile:
Single base	Nitrocellulose.
Double base	Nitrocellulose with nitroglycerine.
Triple base	Nitrocellulose, nitroglycerine and nitroguanidine.
RDX	High energy explosive, Hexahydro-1,3,5- trinitro-1,3,5-triazine.
SERDP	Strategic Environmental Research and Development Program.
TNT	2,4,6-trinitrotoluene, a high energy explosive.
UXO	Unexploded Explosive Ordnance, defined as an “explosive ordnance which has been primed, fuzed, armed, or otherwise prepared for action, and which has been fired, dropped, launched, projected, or placed in such a manner as to constitute a hazard to operations, installations, personnel, or materiel, and remains unexploded either by malfunction or design or for any other cause” (GPO 1989).
2,4-DNT/2,6-DNT	2,4- and 2,6-dinitrotoluene; two of six possible dinitrotoluenes, impurities in the making of TNT. The DNTs are used as propellants.
2A-DNT/4A -DNT	two different amino dinitrotoluenes that are breakdown products of TNT.

Underground UXO: Are They a Significant Source of Explosives in Soil Compared to Low- and High-Order Detonations?

SUSAN TAYLOR, JAMES LEVER, MICHAEL WALSH, MARIANNE E. WALSH, BENJAMIN BOSTICK, AND BONNIE PACKER

1 INTRODUCTION

The 1998 Defense Science Board report estimated that 1500 different sites, encompassing 15 million acres of land, contain Department of Defense (DoD) Unexploded Ordinance (UXO) (Foster 1998). Unexploded Ordnance (UXO) pose two types of risk: the risk of detonation if the round is moved or stepped on, and the risk of leaking explosives into the environment if the round is not removed and disposed of properly. Here, we address the second risk, environmental contamination.

UXO are composed of high explosives (e.g., RDX, TNT, HMX, Tetryl), a metallic casing, and lesser quantities of fuze materials. While the metallic casing is not hazardous to human health, the fill components each have their own characteristic toxicity, temperature-dependant solubility, and propensity for sorption, and, thus, differing potentials to impact surface water and groundwater quality.

Corrosion of the casing exposes the high explosive (HE) in UXO to dissolution by water moving through the soil. Previous studies have found that UXO buried in soil corrode at rates that depend on site- and munition-specific factors, including soil type and composition of the casing. Estimates for corrosion breakthrough vary from 10 years to several thousand years. The rates of corrosion are needed to predict the time scales over which HE will be released into the environment.

In this report we evaluate the rate of high explosive released from corroded UXO in comparison to that released by detonations or ruptured rounds. We begin by briefly summarizing UXO and explosive-contamination issues on training ranges and describe the properties of the most commonly manufactured munitions. Because UXO in the U.S. results primarily from live-fire testing and train-

ing, we focused on Army impact ranges. The plethora of different munitions and changes in munitions through time also necessitated that we focus our attention on types with production rates exceeding half a million rounds a year: 40-mm grenades, 60-mm, 81-mm, 4.2-in. and 120-mm mortars, 105-mm, 155-mm and 8-in. howitzer rounds.

The report then describes what is known about the fate of a round after it is fired. Generally, a round will detonate as intended. However, it might also undergo a low-order (incomplete) detonation or be a dud. These duds can penetrate the ground to some depth or come to rest on the surface. Whether on the surface or underground, the resulting UXO might be blown-in-place, detonated sympathetically, split open or left to corrode. The rate of HE released into the environment depends on the fate. Because the majority of UXO corrode in place, we have summarized what is known about corrosion in soil and its dependence on soil properties and climate. As dissolution of explosives precedes transport, we then summarize what is known about the dissolution of different HE particle masses. Using estimates of the HE contamination released from a munition experiencing a particular fate, the probability that it will experience that fate, and its dissolution rate, we have made order-of-magnitude estimates of which fates release the most HE into the environment. Although only order-of-magnitude estimates are possible, the framework used here for compiling and ranking the explosive sources can help guide policy-making and future research activity to reduce range contamination.

Lack of data necessitated that we focus on estimating average HE release rates across all U.S. Army training sites. Consequently, this report does not address site-specific range-management issues or the release rates of specific HE, such as TNT and Comp B. We also did not address HE transport processes or releases from heavy metals in UXO.

2 TRAINING RANGES

Training ranges provide soldiers the opportunity to practice using a variety of weapons and munitions. However, as a result of training, explosive residues from high-order detonations (HO), low-order detonations (LO—where a significant fraction of the explosive remains undetonated), and UXO may contaminate the soil and the groundwater, and consequently pose environmental and human health risks. The amount of explosive remaining after a detonation depends on the type of munition, its HE fill, its casing, and how the detonation was initiated and proceeded.

According to the data compiled by the Army Environmental Center (AEC) in their Active/Inactive Range Inventory, there are 66 active Army installations, which together cover 16.7 million acres of land (Fig. 1 and Table 1). The impact areas at these installations cover 1.36 million acres (Table 1). These data do not include impact areas on closed Army installations or those belonging to the other service branches. The impact areas vary in terms of their size, the intensity and types of training conducted on them, their climate, soil type, and underlying geology. UXO are generally found in the impact areas but have also been found outside these areas.

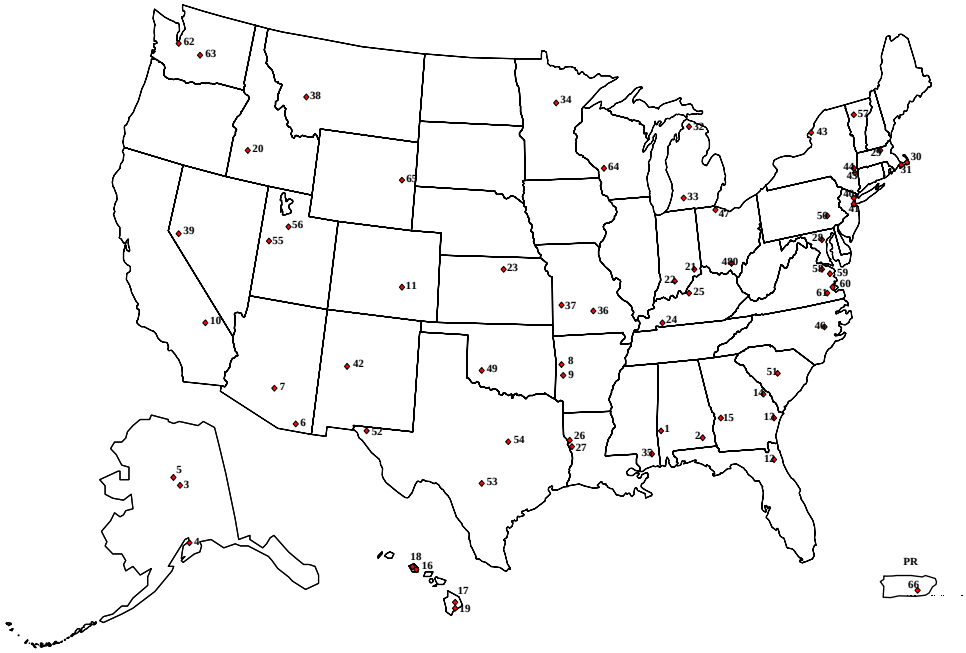

Figure 1. Locations of Army installations in the U.S.

Table 1. Army Installations (Army, National Guard, Army Reserve) that have impact areas. The states of Connecticut, Delaware, Illinois, Iowa, Maine, Nebraska, New Hampshire, Oregon, Rhode Island, South Dakota, Tennessee, West Virginia, and the District of Columbia have no listed impact areas.

State	Map number	Installation type	Size (ha)	Size (acres)	Number dud areas	Dud areas (ha)	Dud areas (acres)
Alabama	1	A	8,961	22142	2	1,514	3,741
	2	A	23,571	58244	1	1,219	3,013
Alaska	3	A	255,622	631642	4	25,552	63,138
	4	A	22,072	54541	1	1,005	2,483
	5	A	373,367	922589	4	21,060	52,040
Arizona	6	A	29,928	73953	1	2,690	6,646
	7	A	10,344	25559	1	1,512	3,735
Arkansas	8	NG	25,706	63519	1	2,444	6,039
	9	NG	12,480	30837	1	507	1,252
California	10	A	237,761	587508	7	52,441	129,582
Colorado	11	A	55,631	137463	1	6,318	15,611
Florida	12	NG	27,786	68658	1	5,910	14,603
Georgia	13	A	68,308	168788	8	6,501	16,063
	14	A	19,973	49353	3	1,573	3,887
	15	A	110,942	274137	1	4,936	12,197
Hawaii	16	A	176	434	1	23	56
	17	A	1,711	4227	1	1,391	3,436
	18	A	44,496	109950	1	18,553	45,845
	19	A	4,630	11441	1	1,836	4,537
Idaho	20	A	55,962	138283	1	1,349	3,334
Indiana	21	NG	12,905	31889	2	1,434	3,543
	22	A	425	1050	2	425	1,050
Kansas	23	A	37,499	92660	2	6,144	15,183
Kentucky	24	A	38,182	94348	4	9,025	22,301
	25	A	41,126	101623	10	16,720	41,315
Louisiana	26	A	56,146	138737	10	4,588	11,338
	27	A	13,539	33456	3	2,332	5,763
Maryland	28	A	26,002	64250	3	20,505	50,667
Massachusetts	31	A	7,185	17755	2	6	15
	30	NG	5,376	13285	1	895	2,211
	29	AR	1,857	4588	1	272	671

State	Map num-ber	Installation type	Size (ha)	Size (acres)	Num-ber dud areas	Dud areas (ha)	Dud areas (acres)
Michigan	32	NG	58,642	144904	2	3,222	7,961
	33	A	3,030	7487	1	1,032	2,550
Minnesota	34	NG	20,611	50929	3	2,500	6,178
Mississippi	35	NG	54,145	133793	1	1,890	4,669
Missouri	36	A	21,652	53502	2	3,692	9,122
	37	NG	403	997	1	21	52
Montana	38	A	7,738	19120	2	221	546
Nevada	39	A	14,484	35789	2	2,021	4,995
New Jersey	40	AR	11,332	28001	1	835	2,064
	41	A	49	120	1	7	18
New Mexico	42	A	1,848,435	4567483	3	18,334	45,303
		A					
New York	43	A	39,872	98524	1	8,204	20,271
	44	NG	713	1763	2	93	230
	45						
North Carolina	46	A	58,112	143594	4	12,137	29,990
Ohio	47	NG	139	343	1	0	0.08
	48	A	174	430	1	8	21
Oklahoma	49	A	34,400	85002	3	14,113	34,872
Pennsylvania	50	NG	6,046	14939	1	537	1,328
South Carolina	51	A	11,951	29532	1	2,209	5,459
Texas	52	A	443,607	1096153	11	166,717	411,957
	53	A	11,112	27457	1	2,253	5,566
	54	A	80,841	199758	2	5,684	14,044
Utah	55	A	308,820	763093	3	67,584	167,001
	56	NG	10,117	25000	4	2,712	6,701
Vermont	57	NG	4,347	10742	2	233	576
Virginia	58	A	881	2178	1	6	16
	59	A	30,607	75629	16	894	2,209
	60	A	1,398	3454	1	442	1,092
	61	NG	15,742	38899	1	609	1,505
Washington	62	A	31,395	77577	1	693	1,713
	63	A	131,242	324298	2	7,220	17,841
Wisconsin	64	AR	54,877	135601	1	2,943	7,273
Wyoming	65	NG	14,189	35062	2	1,044	2,580
Puerto Rico	66	A	4,874	12044	1	582	1,438

The Army has no uniform policy for clearing ranges. Surface UXO on paths to targets are often blown-in-place but sub-surface UXO or the HE residues released from training activities are generally not removed. Contamination from training activities has been documented in at least two cases: a wetland impact area at Eagle River Flats, Alaska, contained white phosphorous (WP), and RDX was found in the sole aquifer on Cape Cod beneath the Massachusetts Military Reservation (MMR). These instances have heightened public concern about military activities that could impact human health and the environment. At Eagle River Flats, white phosphorus rounds are banned and only wintertime firing onto a solid ice sheet is allowed. Temporary draining and drying of WP-containing sediments of the wetland are underway as the process accelerates the oxidation of the white phosphorus to phosphates. By comparison, MMR has been closed to training.

Because the types of training conducted at MMR are similar to those conducted on other ranges (Clausen et al. 2004), the soil HE residues and groundwater contamination found there illustrate the types of problems that could develop, or be present, at other ranges. Since its closure in 1997, MMR has been extensively studied. The data gathered there form much of the useful information about UXO that is presented throughout this report. Many of these data have not yet been published (AMEX, in review). The work done at MMR also illustrates the difficulties in characterizing and cleaning up ranges.

Massachusetts Military Reservation is a 8500-ha (21,000-acre) installation. The training ranges and central impact area cover about 5700 ha (14,000 acres) and are located on part of the installation known as Camp Edwards. After small concentrations of RDX were found in groundwater, studies were begun to determine the source or sources of the RDX. Three areas were found to be the mostly likely sources for the groundwater RDX plume: the central impact area, demolition 1 (Demo 1) area, and the southeast ranges.

The central impact area, approximately 810-ha (2200 acres) encompasses artillery and mortar targets and is surrounded by artillery and mortar firing points. Demo 1 is a 64- × 64-m (1 acre) depression where munitions were burned or detonated. Clausen et al. (2004) reported seeing chunks of C4, used to detonate munitions, on the ground at Demo 1, indicating that not all detonations were high-order. The highest concentrations of RDX—14,000 mg/kg—were found near a large intact fragment of C4 explosive. The southeast ranges are four separate ranges, J1, J2, J3, and L, which total 132-ha (329 acres) and were used for a variety of purposes. The J1 range was used to test weapons and as an antitank range. The J2 range was used as a rifle and musket range as well as a contractor

test range. The J3 range was used for mortar and machine gun practice and for a variety of munition tests. Ordnance and explosives were tested on the L range.

To date the following samples have been collected at MMR: 7833 surface soil samples from 1989 locations, 1533 soil cores from 146 places, 69 sediment samples and 64 water samples from 19 water bodies, 1467 groundwater samples and 3959 groundwater profile samples from 256 locations (Clausen et al. 2004). On the impact area, soil samples indicate that the explosive concentrations decrease rapidly with distance from the targets and with depth in the soil, a finding seen at other ranges (Jenkins et al. 1996, 1997; Thiboutot et al. 1998). Figure 2 shows the explosive, pyrotechnic, and propellant compounds found in the impact range soil samples. The acidic nature and low organic content of the soils limit biodegradation and the low clay content and low cation exchange capacity decrease sorption of explosives onto soils. It is, therefore, not surprising that RDX, HMX, and 2A-DNT and 4A-DNT, the transformation products of TNT, make up the bulk of the explosives found in the groundwater (Fig. 3) (AMEX, in review).

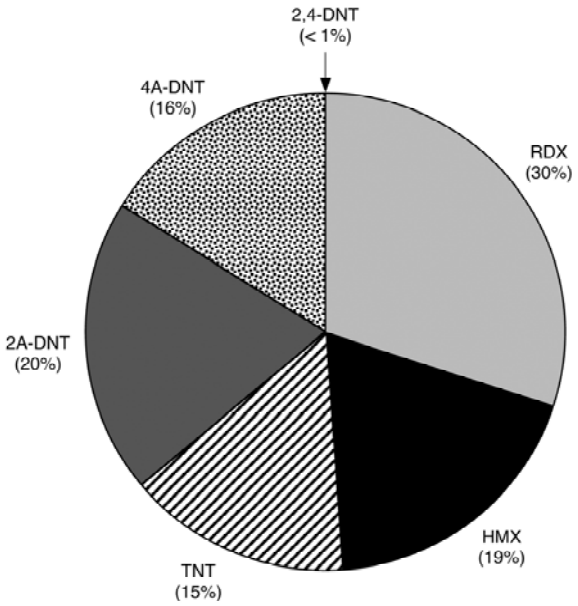

Figure 2. Concentration of explosives, pyrotechnics and propellants in the impact range soils at Massachusetts Military Range.

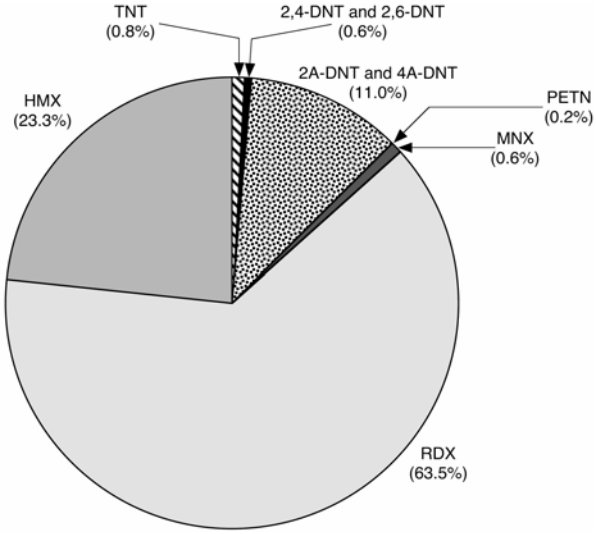

Figure 3. Concentration of explosives, pyrotechnics and propellants in the groundwater below the impact range at Massachusetts Military Range.

Six years of work have not found a specific source, such as an ammunition dump, for the aforementioned groundwater contamination. Based on the low levels of RDX in the groundwater, the contamination is thought to come from a nonspecific source. The flux of RDX to the aquifer also appears to be fairly constant. The size and movement of the RDX groundwater plume suggests that RDX has been migrating to the groundwater for the past 60 years and, because the rate appears constant, that the sources of RDX are still present (AMEX, in review). The plume emanating from the impact area is estimated at 3353 m (11,000 ft) long by 1524 m (5000 ft) wide suggesting that 3.3 ×109 to 4.9 × 1012 L (880 million to 1.3 billion gal.) of water are contaminated. The amount of RDX needed to contaminate this volume to the measured concentrations is 14 to 36 kg (30 to 80 lb) (AMEX, in review). Work by Tetra Tech (2002) concluded that intact UXO are not currently a major source of contamination at MMR.

The work at MMR shows the high expense and effort needed to characterize a range, let alone clean it up. The costs of removing UXO in formerly used defense sites (FUDS) and from base realignment and closure projects (BRAC) are unknown but estimated at between $14 and $60 billion (Delaney and Etter 2003). These estimates are for removing UXO from 1400 sites on 10 million acres.

3 MUNITIONS MOST COMMONLY USED BY THE ARMY

Records on the manufacture and production of the various HE rounds used by the Army are fairly complete since the 1960s and almost nonexistent prior to the 1940s. Each of the rounds that had total production runs greater than 3.9-million, as well as 120-mm mortars, are listed in Table 2. As technology and manufacturing methods evolved, variations on the rounds were developed, requiring different designations. These are listed under type in Table 2. Descriptions of each munition type can be found in the MIDAS database using the DODIC numbers given in Table 2. The specifications for these munitions were taken from Army Technical Manuals 43-0001-28 and 30 (U.S. Army 1981, 1994).

Table 2. Munitions produced and their characteristics.

Munition	Type	DODIC Number	Production ($\times 10^6$)	Wt. of round (kg)	HE load (kg)	Energetics type	Muzzle vel. (mps)	Projectile material	Mfg. process	Min. wall thk. (mm)	Mfg. Dates
40-mm HE											
Gun	HE-T, SD	B562	1.1	2.15	0.063	TNT or Tetryl	823	1335 Steel	Turned	6.2	1944
Grenade/ Gun	M383	B571	4.0	0.34	0.055	Comp A5 (RDX)	795	1009 Steel	Stamped	6.5	1973, 1990
Grenade/ Gun	M384	B470	17.0	0.34	0.055	Comp A5 (RDX)	795	1030 Steel	Stamped	2.7	1965, 1969
Grenade	M397	B569	1.4	0.23	0.032	Octal	76	6061 Al	Extruded	2.0	1964, 1965
Grenade	M406	B568	39.0	0.25	0.032	Comp B	76	1100 Al	Stamped?	1.2	1969, 1970
Gun	DP M430	B542	18.0	0.34	0.038	Comp A5 (RDX)	241	1009 Steel	Stamped	3.4	1983, 1994
Grenade	DP M433	B546	23.0	0.23	0.045	Comp A5 (RDX)	76	1009 Steel	Stamped	2.5	1998, 2001
Total			103.5	Avg.	0.046						
60-mm HE											
Mortar	M49A4	B632	1.9	1.40	0.190	TNT or Comp B	51 / 159	Pearlitic CI	Casting	5.9	1953, '71, '73
Mortar	M720	B642	1.2	1.70	0.191	Comp B	64 / 277	1340 Steel	Forged	5.1	1989, 1996
Mortar	M888	B643	3.0	1.77	0.358	Comp B		1340 Steel	Forged	5.1	1991, 1999
Total			6.1	Avg.	0.246						
81-mm HE											
Mortar	M43A1	C225	6.0	3.40	0.585	Comp B	72.5 / 254	1020 Steel	Forged	9.7	1966, 1971
Mortar	M362	C222	4.0	4.30	0.953	Comp B	55 / 236	1012 Steel	Forged	6.5	1955, 1964
Mortar	M362	C223	1.3	4.30	0.953	Comp B	55 / 236	1012 Steel	Forg/Cast	6.5	1958, 1970
Mortar	M374	C236	2.3	4.30	0.953	Comp B	64 / 261	1340 Steel	Forged	6.2	1966, 1976

Munition	Type	DODIC Number	Production ($\times 10^6$)	Wt. of round (kg)	HE load (kg)	Energetics type	Muzzle vel. (mps)	Projectile material	Mfg. process	Min. wall thk. (mm)	Mfg. Dates
Mortar	M374A3	C256	40.8	4.30	0.953	Comp B	66 / 268	1340 Steel	Forged	5.6	1971, 1990
Mortar	M821A1	C868	1.0	4.10	0.726	RDX / TNT	N/A	HF-1 Steel	Forged	N/A	1985, 2000
Mortar	M889	C869	1.4	4.10	0.726	RDX / TNT	N/A	HF-1 Steel	Forged	7.0	1986, 1999
Total			56.8	Avg.	0.836						
105-mm HE											
Howitzer	M1	C444	2.1	14.10	2.18 to 2.3	Comp B or TNT	198 / 494	HF-1/CStl	Forged	10.5	1953, 1970
Howitzer	M1	C445	20.0	14.10	2.18 to 2.3	Comp B or TNT	198 / 494	HF-1/CStl	Forged	10.5	1943, 1974
Howitzer	M1	C443	0.6	14.10	2.18 to 2.3	Comp B or TNT	198 / 494	HF-1/CStl	Forged	10.5	1953, 1966
Total			22.7	Avg.	2.239						
4.2-in. HE											
Mortar	M329A2	C697	1.3	9.98	2.610	Comp B	1,010	1340 Steel	Forged	7.5	1980–1992
Mortar		C699	1.0	9.98	2.610		1,010	1340 Steel	Forged	7.5	1981–1985
Mortar	M329A1	C704	0.4	12.30	3.377	TNT	981	Carbon Steel	Formed	7.5	1953, '69, '74
Mortar		C705	1.2	12.30	3.377	TNT	981	Carbon Steel	Formed	7.5	1980
Total			3.9	Avg.	2.994						
120-mm HE											
Mortar	M933	C623	0.4	14.20	2.990	Comp B		Carbon Steel	Formed	9.3	1993, 1999
Mortar	M934A1	C379	0.2	14.20	2.990	Comp B		Carbon Steel	Formed	9.3	1992, 2001
Total			0.6	Avg.	2.990						
155-mm HE											
Howitzer	M1918		0.7					Semi-Steel	Casting	16.3	1918
Howitzer	M107	D544	6.4	43.00	6.62 to 6.98	TNT / Comp B	207 / 684	Steel	Forged	13.5	1953–2001
Howitzer	RA M549	D579	1.1	43.50	6.94 to 7.26	TNT / Comp B	561 / 826	Steel	Forged	11.0	1976–1998
Howitzer	M795	D529	0.3	46.90	10.795	TNT	253 / 802	HF-1	Forged	10.9	1985, 2000
Total			7.8	Avg.	8.232						
8-in. HE											
Howitzer	M106	D680	11.5	93.00	16.47 to 17.60	TNT / Comp B	250 /594	1008 Steel	Forged	17.0	1956, 1980
Howitzer	RA M650	D624	0.3	91.00	11.300	TNT		HF-1 Steel	Forged	18.2	1980–1991
Total			11.8	Avg.	14.166						

The weights of the projectile and the HE filler were obtained from USAMC (1985) and U.S. Army (1994) and do not include the weight of the fuze or of the explosives used in the fuze. The weight of the round and its muzzle velocity,

which is its exit velocity from the gun barrel in meters per second (USAMC 1985), are important parameters for computer models that estimate impact speed and penetration depth of the round. If they do not detonate, larger munitions are more likely to penetrate the ground and become buried UXO than are smaller rounds. Also, larger munitions contain more explosives and can become a larger specific source of contamination than smaller rounds. For rounds with variable propellant loads, we have listed the weight ranges possible (USAMC 1985, U.S. Army 1994, Popadopoulas 2003).

Because we are interested in the corrosion of these rounds, we also obtained and tabulated information on the metals used to make the projectile body, the methods used to make the projectile, the projectiles minimum wall thickness, and dates when large quantities of each munition were manufactured. The manufactured date can be used as a proxy of when the round was used. This assumption must be viewed with some caution, however, as munitions are often used at later dates. For example, WWII-vintage ammunition was in use during the Vietnam War (1960–75) and old munitions are used preferentially during training.

The projectile body is usually made of steel or iron. Some rounds have copper alloy rotating bands. Fins and fuzes are typically made of aluminum. A mix of metals can set up galvanic currents and increase corrosion. The presence of a more noble metal in contact with the steel increases the corrosion rate. Primary among these is brass (copper and zinc alloy), which is used for the rotating bands on artillery rounds. A photograph of a 105-mm HE round fired into Eagle River Flats, an estuarine salt marsh, shows that after a few months, corrosion is occurring in the vicinity of the band (Fig. 4). However, in the same environment, the corrosion of steel can be slowed by the presence of aluminum. Mortars built after 1960, have aluminum alloy fins that act as anodes and rapidly corrode, thereby protecting the steel portion of the round (Fig. 5). Figure 5 shows a round that had been in the salt-marsh sediments at least 14 years with no visible corrosion of the steel. However, the fin assembly, which is made of aluminum, has totally corroded.

Given similar conditions, there is little difference between the stability of forged and cast steel of the same composition (Romanov 1957, Craig, 1989). The steel alloy composition, however, does play a major role in the corrosion resistance of the UXO. Chromium is a common additive to stainless steels, imparting appreciable corrosion resistance to the resulting alloy. The addition of copper or nickel to steels also greatly enhances their resistance to corrosion, but none of the rounds of concern contain effective amounts of these alloying elements (Papadopoulos 2003). In most cases, a rust-inhibiting paint is applied to the outside of the steel round. This will inhibit corrosion if the coating remains intact. However,

firing of the round often burns off some of the paint, exposing the iron shell to corrosion. As the round penetrates the soil, the coating will likely be abraded or the coating will, over time, be removed by corrosion. The result, a discontinuous coating of rust-inhibiting paint induces anodic metal corrosion at exposed areas, thereby enhancing pitting of the metal. Most important for calculating corrosion is the minimum wall thickness of the projectile body, as thickness determines the time it takes for corrosion to penetrate the round.

Figure 4. Corrosion of a copper rotating band on a 155-mm round found at Eagle River Flats, Alaska.

Figure 5. Corrosion of an aluminum fin on a 81-mm mortar found at Eagle River Flats, Alaska.

4 MUNITIONS AND THEIR FATE AFTER FIRING

A fired munition can experience one of many fates (Fig. 6). Generally, it will detonate as intended. However, it might also undergo a low-order (partial) detonation or be a dud (UXO). UXO may penetrate the ground to some depth or come to rest on the surface. Whether on the surface or underground, a UXO might suffer one of five outcomes leading to the release of HE. It can be blown-in-place (high or low order), it can be detonated sympathetically by a round exploding nearby to produce a low-order detonation, the casing might be split either by the initial impact or by a nearby explosion, or it can corrode over time. The following sections review the currently available information on each of these processes and provide estimates of their frequencies.

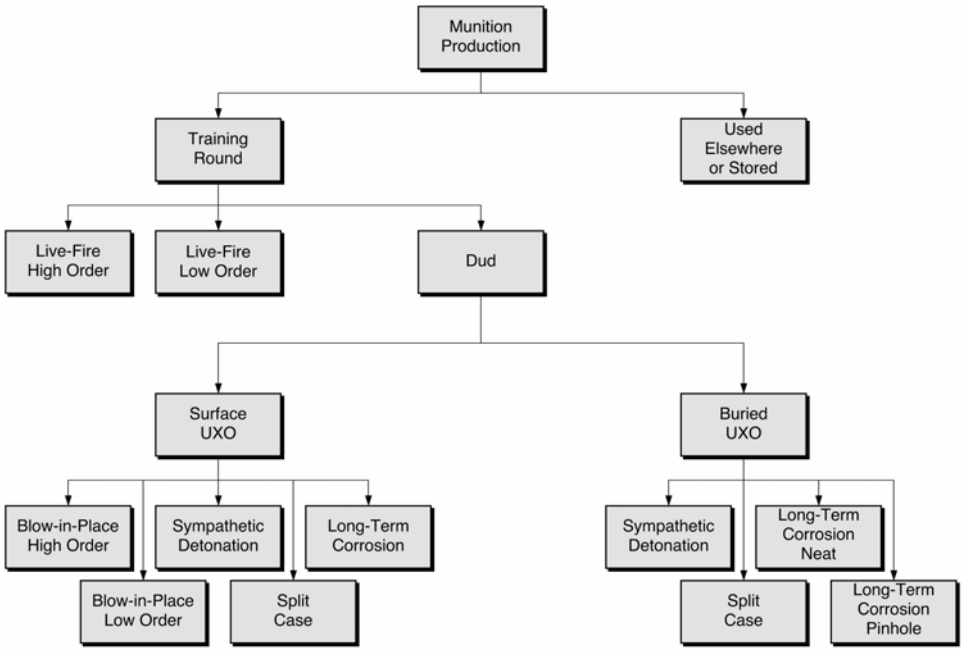

Figure 6. Possible fates of a fired munition.

4.1 Estimates of Dud and Low-Order Detonation rates

Accurate records of the number and types of munitions fired during training and whether or not the round functioned as intended are not available for Army training sites. Dauphin and Doyle (2000, 2001) estimated the dud, low-order, and high-order rates for a variety of munitions by compiling statistics from over

209,390 rounds that were fired as part of the Ammunition Stockpile Reliability Program (ASRP). They chose the data from this program because it best simulated the conditions encountered during training. For example, the rounds fired were taken from the same stockpile used by troops for training, so rounds from different production lots, ammunition manufacturers, and storage conditions were all tested. Dauphin and Doyle (2000, 2001) provide data on the dud and low-order rate for fuzes, grenades (hand, rifle and launcher), mines, pyrotechnics and artillery, mortar, gun and rocket ammunition for the following size and caliber rounds: 20-mm, 25-mm, 40-mm, 57-mm, 60-mm, 66-mm, 75-mm, 76-mm, 81-mm, 83-mm, 84-mm, 90-mm, 105-mm, 106-mm, 120-mm, 152-mm, 155-mm, 165-mm, 2.75-in., 3.5-in., 4.2-in., and 8-in. Table 3 shows the dud and low-order results for the most commonly manufactured munitions—40-mm grenades, 60-mm, 81-mm, 4.2-in., and 120-mm mortars, 105-mm and 155-mm and 8-in. howitzer rounds. The dud rate ranges from 1% for the 8-in. projectiles to 6% for the 4.2-in. rounds. The low-order rate ranges from 0.01% for the HE-filled 155-mm projectiles to 1% for all types of 155-mm and the 105-mm projectiles. With the exception of the 120-mm mortar and the 8-in. howitzer round, these munitions were some of the most frequently found as UXO at MMR (AMEX, in review).

Table 3. Measured Dud and LO rates for eitght types of munitions (Dauphin and Doyle 2000). We list the values for all fill types (target practice, illumination white phosphorus, etc.) and for HE-filled only.

Size	Family	Number fired	Number of duds	Number LO	Dud (%)	LO (%)
40-mm	Grenade/Gun	19,497	267	29	1.37	0.149
HE-only		15,735	208	24	1.32	0.153
60-mm	Mortar	27,614	646	6	2.34	0.0217
HE-only		13,742	341	0	2.48	0.00
81-mm	Mortar	28,759	671	33	2.33	0.115
HE-only		16,435	375	13	2.280	0.0791
4.2-in.	Mortar	14,491	743	20	5.13	0.138
HE-only		7,904	547	6	6.92	0.0759
120-mm HE	Gun	270	7	0	2.59	0.00
105-mm	Howitzer	27,100	1259	289	4.65	1.07
HE-only		13,017	644	12	4.95	0.0922
155-mm	Howitzer	15,108	341	150	2.26	0.993
HE-only		7,656	172	1	2.25	0.0131
8-in HE	Howitzer	1,010	10	0	0.9901	0.00

Experienced military personnel fired the rounds for the ASRP tests. This procedure is appropriate when assessing the reliability of the ammunition and the

fuzes, but may underestimate the dud and low-order rates obtained when inexperienced soldiers fire the rounds during training. For example, improperly installed fuzes may cause munitions to not detonate. One of the authors (Michael Walsh) found improperly fuzed 81-mm duds and was told that 80% of the rounds had not detonated at one of the training exercises. Live fire tests of eight 105-mm howitzers, six 81-mm, and five 60-mm mortars produced one dud each for the 105-mm and 60-mm rounds (Collins and Calkins 1995). It was noted that the point detonating fuzes (those used for these tests) performed well compared to the delay fuzes, which "operated very erratically in areas with frozen ground and an ice cover" (Collins and Calkins 1995). This suggests that the substrate being impacted may also affect the HO, LO and dud rate.

When estimating the mass of explosives remaining after a detonation, a limitation of the ASRP data is that each fired round is categorized as dud, a low-order, or a high-order detonation. The dud rate is easily determined by counting fired rounds that did not detonate. However, the distinction between a high- and low-order detonation is less clear. The term "order" is a subjective classification of explosive yield. In principle, the yield can be quantified based on air-blast parameters (Kingery and Bulmash 1984). These measurements require placing sensors around the detonation point to measure the blast wave and cannot be made during live fire. In practice, the classification of a detonation as high- or low-order is done on the basis of the sound of the detonation and the presence or absence of a shell carcass. A detonation may be measurably, but not audibly, less than 100% yield if the detonation wave does not propagate properly through the explosive fill. Defects in the shell casing or in the packing or pouring of the shell can cause low yields.

4.2 UXO Fate

4.2.1 Number of UXO Versus Depth

The UXO database* lists the number and type of UXO removed from 1.2 m (4 ft) depths at formerly used defense sites (FUDS), from base realignment and closure projects (BRAC), and installation restoration (IR) projects. The U.S. Army Engineering and Support Center in Huntsville, Alabama, compiled a database of UXO removed from Fort Ord, California; East Elliot, California; Camp Simms, Washington DC; Jefferson Proving Ground, Indiana; Fort Sill, Oklahoma; Camp Green, North Carolina; Fort Dix, New Jersey; Camp Croft, South Carolina; Motlow Range, Tennessee; Camp Maxey, Texas; and Dolly Sods Wil-

* Personal communication with Roger Young, USACE Huntsville, April 2004.

derness Area, West Virginia. The database includes information on the type of round (projectile, rocket, etc.), the item (81-mm mortar, etc.), the recovery depth (measured to the shallowest point on the round), and an assessment of whether the item was fired or buried (Adams 1999). Because the database will continue to be updated and the different versions are not published, we obtained the data for this report from the 2003 version that listed 7299 UXO as having been fired.

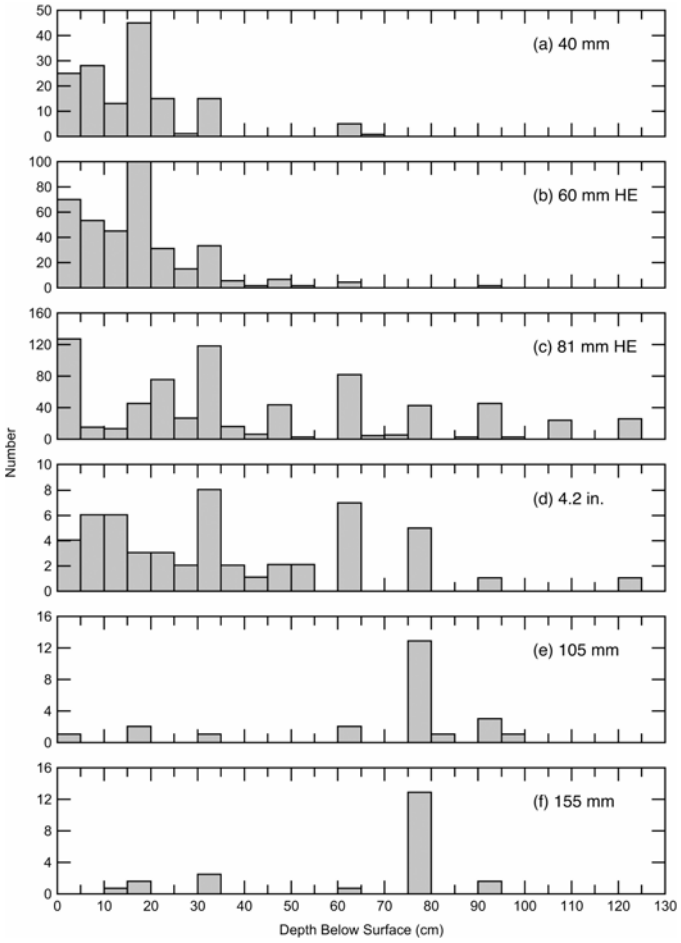

Figure 7. UXO as a function of depth.

There is a clear pattern relating the distribution of recovery depths to the munition type and size. Frequency histograms of the number of 40-mm grenades, 60-mm, 81-mm, and 4.2-in. mortars, and 105-mm and 155-mm howitzer rounds found as a function of depth below the surface shows a bimodal distribution of munition depths (Fig. 7a–f). The 40- and 60-mm rounds generally were found at shallow depths, between 0 and 20 cm, with the deepest 40-mm round at 65 cm

(Fig. 7a) and the deepest 60-mm mortar at 90 cm (Fig. 7b). The larger 81-mm and 4.2-in. rounds were distributed to 120-cm depths, with most at intermediate depths (Fig. 7c and d). Few 105-mm and 155-mm howitzer rounds were found but most of those were located at a depth of 75 cm (Fig. 7e and f).

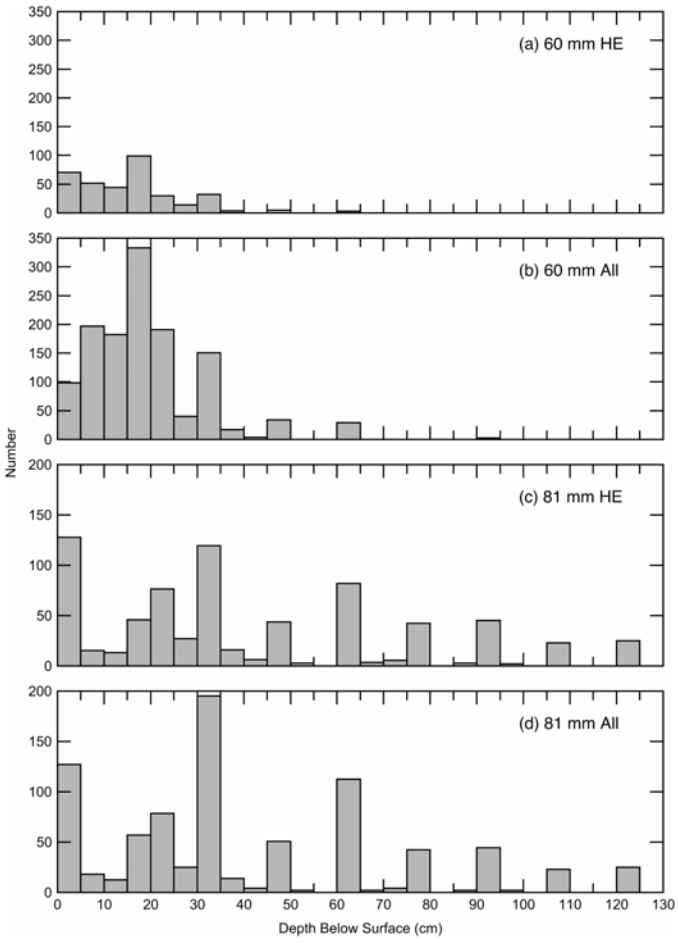

Figure 8. Comparison of HE-filled versus all UXO as a function of depth.

The depth distribution may also be influenced by the presence (or lack of) HE. A significant fraction the 60- and 81-mm rounds (72 and 17%, respectively) retrieved were inert practice rounds. We compared the distribution of the HE-filled rounds with the inert rounds to determine whether or not the inert rounds were preferentially found at certain depths (Fig. 8a–d). For the 60-mm mortars, the HE-filled rounds make up a higher proportion of the surface and shallow UXO than the inert rounds (Fig. 8a, b). For the 81-mm rounds, the two distribu-

tions are very similar but again HE-filled rounds make up most of the surface UXO (Fig. 8c and d). This difference in distribution suggests that HE explosives are encountered more often at the surface. Although the reason for the difference in distribution is not known, perhaps because they pose little risk, the inert rounds on the surface were previously picked up and therefore not accounted for in the database.

4.2.2 Modeled Ground Penetration

Predicting the depth to which a round can penetrate into the soil is important for many reasons. First, if these items are to be removed, they must be found, a practice that is straightforward with well-exposed munitions. Magnetometers, currently the most reliable tool for finding UXO, are accurate to a depth of about 60 cm (24 in.) with about 85% reliability. While this level of reliability is adequate for some efforts, often more complete cleanup is warranted for both environmental and safety reasons. If the area is to be completely cleared of ordnance to a very high degree of certainty, all the overlying soil to the maximum penetration depth of the ordnance must be removed and processed. Finally, the fate of buried munitions may vary substantially with burial depth. For example, corrosion rates for ferrous materials generally increase with depth of burial (Romanoff 1957).

Three methods are available to predict the depth to which a fired round will penetrate the ground. The simplest is an empirical equation that requires the weight of the ordnance, its impact velocity, and the soil type (U.S. Army 1998, TM 5-855-1,). Two mathematical models also exist. The PENCRV3D is a three-dimensional model that calculates the trajectory of the ordnance through soil using the projectiles' center of gravity, impact velocity, and angle of impact, together with the soil type as input parameters (Adley et al. 1997). The HULL hydrocode is a two- and three-dimensional dynamic continuum mechanics program (Fry et al. 1976). It requires the shape, weight, and impact velocity of the round as input parameters.

Crull et al. (1999) compared the empirical equation and the hydrocode for ease of use and accuracy of the results. As expected the one-dimensional equation required many fewer input parameters and was less difficult to use than the PENCRV3D or the more rigorous HULL hydrocode. Differences in penetration depths under the assumed conditions ($V_i = V_m$, $\Theta = 90°$, matrix = uniform sand) between the one-dimensional equation and the hydrocode ranged from 5 up to 22%, with the largest differences occurring for the largest rounds (155-mm, 105-mm, 75-mm) (Table 4). Grant and Crull (1999) examined the sensitivity of the PENCRV3D to input error. A small error (2%) in the center of gravity or the im-

pact angle will result in an error of 20% in the calculated penetration depth. A 6% error in the impact velocity will result in a similar error. These errors can accumulate to make ordnance depth predictions highly inaccurate. Thus, the empirical model is probably preferable to the more complex codes for most applications, as exact parameters for each shell trajectory are unknown.

Table 4. Predicted ordnance penetration depths into sand versus actual recovery depths for a variety of soils.

Ordnance	Wt. (lb)	Muzzle vel. (ft/s)	Predicted penetration depth (ft)			Depth of recovery** (ft)		Number of rounds
			Equation*	PENCRV3D†	HULL*		Median	
155-mm M107	96.75	2244	14	28.5	16.8	0.4 to 3.0	2.5	24
105-mm M1	33.95	1550	7.7	17.7	9.4	0 to 3.2	2.5	24
75-mm M48	14.6	1250	4.9	9.9	5.7	0 to 4	1	94
40-mm M822	5.5	1100	3.2	11.8	2.9	0 to 2.2	0.5	148
37-mm M63	1.61	2650	3.9	7.9	4.1	0 to 2.5	0.4	108
2.36-in. Rocket	3.4	265	0.4		0.5	0 to 4	0.4	2278

* From Crull et al. (1999).
† Adams (2001).
**UXO Recovery Depth Database.

The agreement between the predicted depth (for all models) and the measured depths of ordnance is poor (Table 4); however, validating model results using UXO depth data is problematic for several reasons. First, no data exist on how the UXO were fired, so their angle of impact and impact velocity are not known. For the PENCRV3D model, and probably the HULL model, estimates of these impact parameters will result in very large errors in penetration depth. Second, although the type of soil at the impact site can be determined, real soils are usually non-homogeneous. The error introduced by this effect is lacking from the models and may be large. Third, the UXO sample size is small for some rounds, invalidating any statistical comparisons. Because the impact velocity and the impact angle are unknown for UXO, these are often set equal the muzzle velocity and 90° respectively (Adams 2001). As the impact velocity is less than the muzzle velocity, and most projectiles impact at shallower angles than 90°, these parameter choices may cause the overestimation. Lastly, the measured depths only extend to 1.2 m.

4.2.3 Number of UXO Per Square Meter

Knowing the number of UXO per square meter and the impact rate per square meter helps to determine the likelihood of sympathetic detonations and is an input parameter for a model that predicts the potential for groundwater con-

tamination from buried UXO (Praxis 2004). Although the locations of UXO are documented during clearance, only a few reports give this information. Two areas on Fort Ord, cleared of UXO to a depth of 1.2 m (4 ft), yielded 13 and 23 UXO/acre. Two sites, Duck, North Carolina, and Camp Elliott, California, that were just surface cleared have much lower UXO values, 0.2 and 0.6 UXO/acre respectively (Nore 1994). Information on UXO spatial density is not tabulated in the UXO database* and is difficult to obtain for most sites.

About 20,000 UXO were removed from MMR. At this site, although we know the area of the impact range, the demolition area, and the separate rocket ranges, the different areas have not been entirely cleared of UXO and we do not know the proportion of each that has been cleared. The exception is a 3.6-acre, high-use training area (HUTA) that was cleared of UXO to a depth of 1.2 m (4 ft). Four HE-filled UXO were found on the surface and 112 HE-filled UXO were buried. This area was cleared in 120- by 30-m test plots whose areas overlapped (AMEX, in review, see Table 5). We have listed some other values for MMR, although we are not certain that the entire area was searched for UXO. Discounting the impact area, which has not been searched extensively, the values for the number of UXO per acre ranges from 4 to 89. Unfortunately, this value is not easily extrapolated to other ranges, as each range was used to a different extent and will have a corresponding variation in UXO density (Table 5).

Table 5. Estimates of the number of UXO per m^2.

Installation		HE-filled	Inert	# BIP	Area (acre)	Area (ha)	Area (m^2)	HE-live UXO/ acre	HE-live UXO/m^2	Comments	Reference
JPG, IN		73			120	49	486,000	0.6	1.5×10^{-4}		UXO database
		475			8			59.4		surface	
		1			100			0.0		cleared to 1.2 m (4 ft)	
Fort Ord, CA	OE-50	936		all	41	16	164,000	23.1	5.7×10^{-3}	cleared to 1.2 m (4 ft)	USA Environmental 2001
	OE-50	26		all	2	1	8,047	13.1	3.2×10^{-3}	cleared to 1.2 m (4 ft)	USA Environmental 2001
MMR, MA											AMEX, in review
Impact area		195	2768		2,200	890	8,900,000	0.1	2.2×10^{-5}	all area not searched	
High use training area		116			3.6	1.5	14,600	32.2	7.9×10^{-3}		
	Test Plot 1	7			0.9	0.36	3,600	7.9	1.9×10^{-3}	all area not searched	
	Test Plot 2	17			0.9	0.36	3,600	19.1	4.7×10^{-3}		

* Personal communication with Roger Young, USACE Huntsville, April 2004.

Installation		HE-filled	Inert	# BIP	Area (acre)	Area (ha)	Area (m^2)	HE-live UXO/ acre	HE-live UXO/m^2	Comments	Reference
	Test Plot 3	11			0.9	0.36	3,600	12.4	3.1×10^{-3}		
	Test Plot 4	17			0.9	0.36	3,600	19.1	4.7×10^{-3}		
	Test Plot 5	21			0.9	0.36	3,600	23.6	5.8×10^{-3}		
	Test Plot 6	21			0.9	0.36	3,600	23.6	5.8×10^{-3}		
J1 Range		558	1795	154	139	56	563,000	4.0	9.9×10^{-4}		
SE		17,454	13,396		329	132	1,320,000	53.1	1.3×10^{-2}		
Demo 1		89	28		1	0.4	4,000	89.0	2.2×10^{-2}		
Duck, NC											
Navy target facility		47		all	200	81	809,000	0.2	5.8×10^{-5}	surface UXO only	Nore (1994)
Camp Elliott, CA											
Tierrasanta		1065		51	1,904	771	7,705,000	0.6	1.4×10^{-4}	surface UXO only	Nore (1994)
Mission trails		205		5	322	130	1,303,000	0.6	1.6×10^{-4}	surface UXO only	Nore (1994)
Fort Sill, OK		9637		9,637	1,322	535	5,354,100	7.3	1.8×10^{-3}	surface UXO only	Nore (1994)
Assateague Island		212			2.4	1	9,720	88.3	2.2×10^{-2}	surface to 2 to 4 ft	NDCEE (2003)
Bergstrom AFB		4			3.5	1	14,175	1.1	2.8×10^{-4}	cleared to 2 ft	
Black Hills Army depot		1107			1,460	591	5,913,000	0.8	1.9×10^{-4}	surface only	
Blossom Point MD		720			76	31	307395	9.5	2.3×10^{-3}	surface to 2 to 4 ft	
Camp Croft		85			572	232	2316600	0.1	3.7×10^{-3}	cleared to 2 ft	
Fort McClellan		2			22	9	89,100	0.1	2.2×10^{-5}	cleared to 1.2 m (4 ft)	
Gaillard Cut Widening Pogram		841			204	83	826,200	4.1	1.0×10^{-3}	surface only	
Morgan Depot		1052			60	24	243,000	17.5	4.3×10^{-3}	cleared to 1.2 m (4 ft)	
Nebraska Ordnance Plant		13			6	2	24,300	2.2	5.3×10^{-4}	cleared to 1.2 m (4 ft)	
Southwestern Prooving Ground		2794			203	82	822,150	13.8	3.4×10^{-3}	variable 1 to 4 ft	
Tipton Army Airfield		1713			277	112	1,121,850	6.2	1.5×10^{-3}	cleared to 1.2 m (4 ft)	
USARSO Panama Canal		350			475	192	1,923,750	0.7	1.8×10^{-4}	surface	
		125			475	192	1,923,750	0.3	6.5×10^{-5}	cleared to 1.2 m (4 ft)	

4.2.4 UXO Clearance

To mitigate the explosive hazard, UXO are cleared in areas that are turned over to the public domain. The depth to which the UXO are cleared depends on the intended use of the land (Naval Explosive Ordnance Disposal Technology Division 1996). For limited public access, such as areas used for livestock graz-

ing or wildlife preserves, a depth of 30 cm (1 ft) is suggested. If the land is to be used for farming, recreation, or parking, ordnance is cleared to 1.2 m (4 ft). For unrestricted use, such as commercial and residential building, where construction is likely to take place, UXO are cleared to a depth of 3 m (10 ft).

Once unearthed, any ordnance deemed safe is moved to a selected open burn/open detonation site where it is destroyed. Ordnance deemed unsafe to move is detonated in place. This is the standard operating procedure set out in U.S. Army (1999) Technical Manual 60A-1-1-31. The clearance is done primarily to mitigate explosion hazard. The manual calls for pre- and post-clearance soil samples at the open burn/open detonation site to evaluate the contamination hazard. At MMR, to minimize explosives contamination, the vast majority of rounds were moved to, and blown up in, a blast chamber. Of approximately 20,000 UXO recovered, only 648 were blown-in-place because of safety reasons and the rest were destroyed in a blast chamber.

Much of the expense of clearing UXO is finding the buried rounds. In areas where the ground freezes, rounds above the frost line can be brought to the surface by the action of frost heave (Isaksen and Sollid 2002). If objects contained within the frozen ground heave upward, gaps are created beneath those objects. During the spring thaw, fine-grained materials fill in gaps under the objects. Over time this process will move the larger objects (stones, projectiles, etc.) toward the surface. The rate at which this occurs depends on a number of variables, including soil type, temperature, and moisture conditions in the soil. On Norway's Hjerkinn firing range, a frost heave transport rate has been estimated at 0.5 to 2 cm per year, corresponding to 10 to 40 years for the Earth's freeze–thaw action to bring rounds buried to a depth of 0.2 m to the surface.

5 UXO CORROSION

There is an unknown, but large, amount of unexploded ordnance (UXO) in ranges throughout the U.S., and on war fields and other ranges throughout the world. Some (Bucci and Buckley 1998; AMEX, in review) have suggested that corrosion of these munitions is minimal owing to the physicochemical properties of the casing, which is predominantly carbon steel. Support for this position comes from the lack of grossly contaminated soils, which would likely result from widespread failure of UXO.

5.1 Metal Corrosion

Corrosion may lead to either catastrophic failure of the casing or to the development of small holes (pinholes), processes that may release explosives into the environment. In Appendix A we discuss in detail the thermodynamic and kinetic effects occurring during corrosion of UXO in a variety of environments. Here, we describe corrosion as it relates to carbon steels and present our best estimates of generalized corrosion rates for carbon steels. Overall, we concur with the results of Fabian and Ostazeski (2002) concerning UXO failure in most soil environments.

Most corrosion processes are highly favored thermodynamically because the oxidation of metals is highly exergonic. For example, the corrosion of iron (the main constituent in steel) proceeds according to the following chemical reaction:

$$2\mathrm{Fe} + \frac{3}{2}\mathrm{O_2} \Leftrightarrow \mathrm{Fe_2O_3}\ \Delta G_{rxn}{}^{0} = -742\ \mathrm{kJ/mol} \qquad (1)$$

The release of free energy is typical of other corrosion processes and shows the drive for metals to dissolve to form other phases. In fact, iron is not stable under any typical soil water pH-E_h conditions (Fig. 9). Other metals and alloys, including steel, the most common casing for munitions, are similarly unstable under commonly encountered thermodynamic conditions (Fig. 10).

Although thermodynamic (energetic) considerations indicate that corrosion is favored under the most commonly encountered soil conditions, kinetic factors ultimately determine the *extent* to which this oxidation occurs, the ultimate reaction products of oxidation, and the distribution of these reaction products (e.g., whether they are attached to the surface). The most stable reaction products thermodynamically are often not formed during metal corrosion in soils because

of sluggish reaction kinetics, instead leading to the formation of other, metastable, reaction products.

Because the rate of corrosion depends on the rate of the anodic (oxidation) and cathodic (reduction) reactions, it is necessary to identify the dominant half reactions to estimate the rate of oxidation (Fig. 11). When alloys such as steel corrode, several anodic (oxidation) reactions may occur, each of which liberates a cation and electrons. In the case of carbon steel, the oxidation of elemental carbon to CO_2 (g) may occur at the anode. As CO_2 is soluble and diffuses away quickly relative to ions, carbon steels are more easily corroded than other steels.

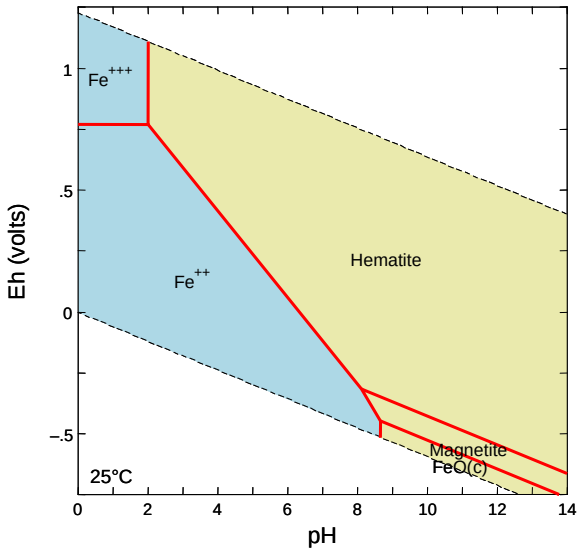

Figure 9. Fe phase diagram for Fe-O_2 system at 25ºC. The diagram is derived using a dissolved Fe concentration of 1 µM. Darker colored phases are aqueous, while lighter phases are solids. The diagonal dotted lines show boundaries for the stability of water; the vertical dotted line shows the change in carbonate speciation. Hematite is α-Fe_2O_3 (s).

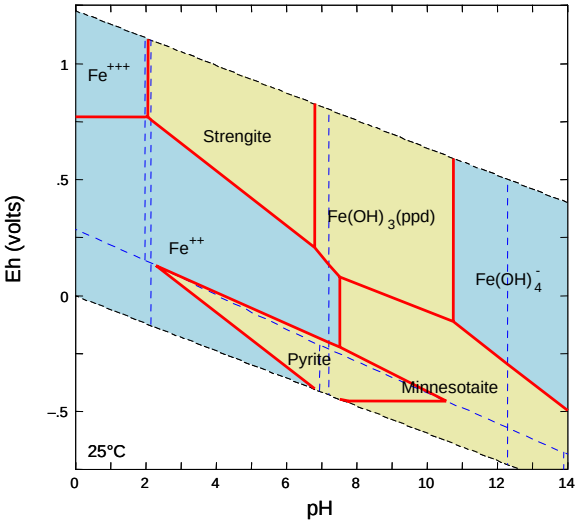

Figure 10. Fe phase diagram for $Fe\text{-}O_2\text{-}S\text{-}PO_4\text{-}CO_3\text{-}H_2O$ system at 25ºC. The diagram is derived using a dissolved Fe concentration of 1 µM, a total CO_3^{2-} of 0.1 mM, total PO_4^{3-} and SO_4^{2-} of 1 µM, SiO_2 of 50 µM; similar concentrations to those found in soils. Darker phases are aqueous, while lighter phases are solids. The diagonal dotted lines show boundaries for the stability of water; the vertical dotted lines show the change in carbonate, phosphate, and sulfur speciation. Minnesotaite is an iron-containing phyllosilicate, and strengite is hydrated $FePO_4$.

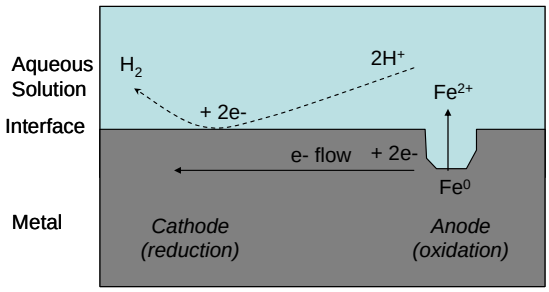

Figure 11. Corrosion of iron in an aqueous solution of HCl. The anodic reaction generates the dissolved metal and electrons, which are transferred to the cathode, where they are used to reduce protons in solution. The extent of proton transfer is equal to the electron flow, a condition required to maintain charge neutrality.

Generally, it is desirable from a remediation standpoint to produce solid phases during corrosion—they are more stable, they are less prone to transport, they react with potential contaminants (both inorganic and organic species adsorb strongly to iron oxides), and some oxidation products protect the metal surface from further oxidation (Kuznetsova et al. 1998, Ge et al. 2003, Virtanen and Buchler 2003). The protection of the surface is called passivation. This protection is a kinetic effect, in that the thermodynamic driving force for corrosion remains, but the surface oxidation is slowed by the presence of a passivating oxide. Such oxides can only protect surfaces if they form effective two-dimensional arrays there; thus, the microstructural compatibility of the interface between the surface and the overlying oxide film is important (Appendix A).

Most UXO are composed of carbon steel, though a limited number of aluminum grenades also have been used. Aluminum is effectively passivated by the formation of Al_2O_3 films, which are highly compatible with Al surfaces. This passivation leads to fairly corrosion resistant aluminum surfaces, except in chloride containing solutions (e.g., Fig. 5). In contrast, the steel UXO corrode to ferric (hydr)oxides, which do not bond strongly to the metal surface and consequently have only limited potential to passivate the metal surface (Fig. 12). This weak bonding is caused by unfavorable interactions between Fe at the surface and the oxide over layer. Nevertheless, under typical soil conditions (near neutral pH, moderately oxidizing conditions), iron, various alloys of steel, and aluminum are often stable in soil environments over long periods of time. Under such conditions, passivation films are formed that can slow the general corrosion rate by about three orders of magnitude.

Pitting corrosion is important for UXO. Pitting may result in pinhole failures in the UXO, which may release small amounts of explosives. Pinholes also provide an additional avenue for corrosion (corrosion can then occur from within), thereby increasing the rate of catastrophic failure. Many of the perforations in UXO are probably limited to relatively small holes formed as a result of pitting corrosion, but some small munitions, particularly in flooded soils and sediments with low hydrologic gradients, may also have failed through anaerobic corrosion induced by sulfate reducing bacteria.

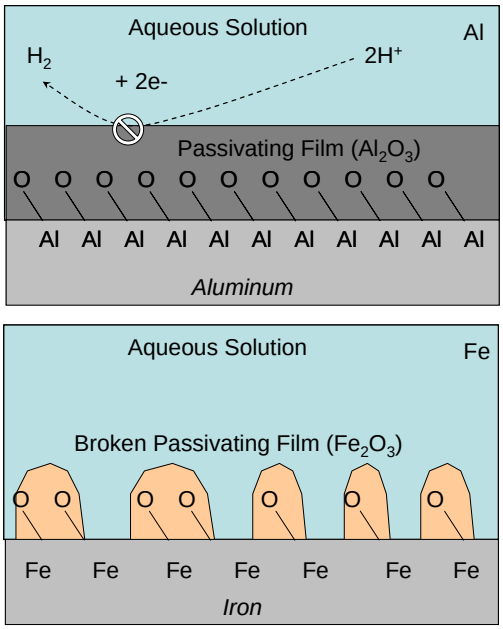

Figure 12. Formation of passivation layers during the corrosion of aluminum (Al) and iron (Fe). The passivation layer on Al is complete as the Al oxide forms a compatible passivating film. As drawn, the passivation occurs by blocking the cathodic reaction; however, anodic passivation is also possible. In contrast, the Fe oxide film is not compatible and forms oxides that are ineffective at blocking the surface.

5.2 Biologically Mediated Metal Corrosion

Biological reactions are ubiquitous in soil systems. Conditions conducive to biological activity, warm and wet, accelerate corrosion through a variety of processes (Prakash et al. 1988, Kloppel et al. 1997, Yfantis et al. 1998, xLi et al. 2001, Gu et al. 2002, Doyle et al. 2003). One of the most obvious and the most important means by which biological organisms accelerate corrosion is through the secretion of acid, directly as small organic acids, into the soil solution. Acid is released into soils by organisms as a result of nutrient uptake (cation uptake is balanced by excretion of H^+) and as a means of regulating their environment. Acidity is also generated by the excretion of respiratory carbon dioxide. Upon dissolution, this CO_2 forms carbonic acid.

Organic acids, such as oxalic acid ($H_2C_2O_4$), also influence corrosion by chelating metal ions. Such acids are important because they prevent passivation by oxide minerals, and may even dissolve oxidized layers formed prior to their introduction. Consequently, chelation by oxalate and other biologically produced chemical species (e.g., citrate, soil organic matter) also increases corrosion rates.

It should be noted that biologically facilitated reactions do not change the thermodynamics of corrosion; rather, they change the mechanism by which corrosion occurs and, thereby, potentially, the rate of corrosion and the phases that are formed through corrosion. Biological corrosion reactions often result in the production of unique, metastable solid phases with different stability than chemically produced solid phases. In some cases, corrosion can lead to the formation of metastable reaction products, such as magnetite, that have unusually stable structures and low reactivity (Veleva et al. 1998, Ishikawa et al. 2003). However, reactive phases, such as green rust, may also be formed through a combination of biological and chemical processes (Drissi et al. 1995, Simon et al. 1997, Genin et al. 1998, Refait et al. 1998). These solid phases are highly reactive, and may in fact react strongly with contaminants such as RDX and TNT that have been released from leaking UXO (Hundal et al. 1997, Scherer et al. 2001, Wildman and Alvarez 2001). These compounds also are formed primarily in anaerobic soils and wetlands, environments that likely contain a large number of corroded UXO.

5.3 UXO Corrosion Models

Empirical corrosion rates for steel and other metals in soils have been determined, but general expressions that relate soil chemical characteristics to corrosion rates do not yet exist. In an empirical study by Romanov (1957), pieces of metal were buried in a variety of soil types and corrosion measured over approximately 50 years. A different study examined the corrosion rates of galvanized steel, a project conducted to assess corrosion of culverts in California (California model). Other studies have measured soil, temperature, and climate parameters to determine which variables best correlate with measured corrosion (e.g., Lafayette model, DOE model, and Praxis model). The Lafayette model identified bicarbonate as an important soil variable (Fabian and Ostazeski 2002). The DOE model predicts corrosion based on temperature (Lee and Atkins 1995). The Praxis pitting model finds the amount of rainfall a significant variable for pit corrosion (Praxis 2004).

The Romanoff study of steel corrosion (Romanoff 1957) indicates that soil conditions influence corrosion rates considerably, and that saline, sulfidic, and anaerobic soils corrode steel more rapidly than other soils. These long-term studies are particularly useful for estimating corrosion rates, because corrosion

rates may not be strictly linear. A drawback is that the soil conditions are not well controlled. Additionally, soils that are found in proximity or with similar characteristics often have different corrosion rates, despite their similar characteristics. The California DOT model for the corrosion of galvanized steel (California Department of Transportation 1999) is not applicable, as UXO are neither galvanized (which slows the initial rate of corrosion) nor subjected to the same types of soil environments as deep culverts for which the model was developed.

The quantitative models (the Lafayette model, the DOE model) require a large quantity of environmental data as input parameters (DOE Performance Assessment 1995, Fabian and Ostazeski 2002). While variables such as soil conductivity, resistivity, salinity, relative humidity, soil temperature, and pH are admittedly important in determining corrosion rates, it often is not practical to measure each of these at a sufficient spatial resolution to estimate corrosion rates. The problem of measurement is especially acute given the large size of many of the training ranges in which UXO are located. Furthermore, the heterogeneity of soils is sufficient that a few measurements of these parameters often do not provide an accurate estimate of the average or extremes in corrosion at a given site. As a result, of nearly 30 measured parameters, only rainfall was found to correlate to measured pit corrosion rates (Praxis 2004). Often, soil heterogeneity occurs even on depth scales; Romanoff (1957) observed significant differences in corrosion rates between surface and subsurface horizons, but was unable to completely determine the reasons for these differences. Given the difficulty in relating these measured parameters, we think it justified to move from these conceptual models to more applied models of corrosion.

We favor a simple approach, which reports the range of corrosion rates for a specific soil environment. From the literature we compiled the range of corrosion rates for carbon steel in solutions and soils (Table 6). The variation in rates may result from uncertainties in the determination of corrosion rate, but, more likely, they reflect differences in steel properties or in soil chemical properties, each of which may impact the rate considerably. We use the rates reported in Table 6 to quantify the depth of uniform failure of steel, that is, the thinning rate of the entire UXO wall. Rates of pitting corrosion, which occurs more rapidly and is very important for UXO, are notoriously hard to predict, because the rate of pit corrosion strongly depends on diffusion, which depends on the shape and depth of pits. This geometric effect is difficult to quantify, but estimates of pit corrosion rates for carbon steels are usually about 5–15 times faster than the uniform corrosion rate.

Table 6. Corrosion rates (in mm/year) of commonly used steel alloys in a variety of different solutions. The solutions given are useful in that they are closely related to the conditions in soils, and thus indicate the rate of corrosion in other media. Pitting corrosion occurs at variable rates, but usually between 5 and 10 times more rapidly than the average rates of corrosion reported here. Data were assembled from *The Handbook of Corrosion Data* (Craig 1989) and literature values (cited in the text). Each of the steel types listed have been used in UXO.

Alloy	Composition	Dilute H_2SO_4[a]	Sea–water[a]	Nacl (1%)[a]	Water	Soil	Saline soil	Flooded soils; anaerobic; may be sulfidic
					Aerated			
					Aerobic	Typical soils		
1008 Steel	(0.1% C steel, ~0.5% Mn)	0.1	0.085	0.017	0.04	0.02–0.1 (0.025 ave)[c]	0.1[c]	1–1.5[c]
1009 Steel	(0.15% C steel, ~0.5% Mn)	0.1	0.105	0.021	0.04	0.02–0.1 (0.025 ave)[c]	0.1[c]	1–1.5[c]
1012 Steel	(0.12% C steel, ~0.5% Mn)	0.11	0.12	0.024	0.05	0.02–0.1 (0.025 ave)[c]	0.1[c]	1–1.5[c]
1020 Steel	(0.2% C steel, ~0.5% Mn)	0.15	0.15	0.03	0.045	0.02–0.1 (0.025 ave)[c]	0.1[c]	1–1.5[c]
1030 Steel	(0.3% C steel, ~0.5% Mn)	0.2	0.15	0.03	0.05	0.02–0.1 (0.025 ave)[c]	0.1[c]	1–1.5[c]
1335 Steel	(0.35% C steel, 2% Mn)	0.25	0.15	0.03	0.055	0.02–0.1 (0.025 ave)[c]	0.1[c]	1–1.5[c]
1340 Steel	(0.4% C steel, 2% Mn)	0.25	0.15	0.03	0.055	0.02–0.1 (0.025 ave)[c]	0.1[c]	1–1.5[c]
Carbon Steel	Unknown composition	0.1–1.5	0.2–270[b]	0.05–50	0.05–5	0.02–0.1 (0.025 ave)[c]	0.1[c]	1–1.5[c]
HF–1 C Steel	High frag. unknown alloy	—	—	—	0.01 (est.)	0.02–0.1 (0.025 ave)[c]	0.1[c]	1–1.5[c]
316ss	Stainless Steel	<0.001	0.05	<0.001	<0.001	0.001–0.005[d]	0.03[d]	0.005–0.01[d]
1100 Al	Al– rel. pure	0.01	0.015	0.2	<0.001	0.01–0.02[d]	0.01–0.03[d]	0.03–1[d]
6061 Al	Al–Mg–Si alloy	0.25	~0.3	0.2	—	0.1–0.2[d]	0.1–0.25[d]	0.04–2[d]

[a] Assuming no stirring.
[b] The low value is for low carbon steels, the high value is for high carbon steel.
[c] The rates of carbon steel corrosion in soil environments do not vary appreciably with steel alloy type—soil variables are more important. Consequently, the general values for carbon steel corrosion rates, determined with rates in the scientific literature, are adequate for most purposes.
[d] The corrosion rates of stainless steels and Al alloys, which are rarely present in UXO, are approximations assembled from literature values.

The corrosion rates reported in Table 6 compare well with those previously determined for a variety of steel alloys. For example, the corrosion rates in well oxygenated, upland soils are generally about 0.025 mm per year. This rate is somewhat more rapid than that reported by the Lafayette model, but nearly in line with the DOE model and the Romanoff estimate for these types of soils. The rates of corrosion in Table 6 for saline and anaerobic soils also are similar to the empirical rates of Romanoff (1957), but the other models are poorly equipped to deal with these "special cases."

The rates of corrosion in aerated soils shown in Table 6 are not particularly rapid, and would lead to the uniform failure of small munitions (grenades, etc., with minimum wall thicknesses of 2–5 mm) in about 80–200 years. Larger munitions with thicker walls (5–10 mm) would fail in 200–400 years. Pitting corrosion is more prevalent than uniform corrosion in soils (Frankel 1998, Doyle et al. 2003, Norin and Vinka 2003) and produces deep pits, potentially decreasing the time required to perforate the UXO to about 20 and 50 years for small and larger munitions, respectively. These are reasonable but conservative estimates of the relative rates of both pit and uniform corrosion; Romanoff (1957) suggests that corrosion may be somewhat slower than these estimates in the environment. In reducing soils, munitions could corrode much more rapidly, in as little as a few years; consequently, the casings of munitions in wetlands likely have corroded through to the HE fill (Fig. 13). Saline environments, such as those encountered in proving grounds in arid basins such as China Lake, California, also may have saline soil chemical conditions favorable for enhanced corrosion. While saline environments such as those at China Lake accelerate corrosion, they are also dry, which slows corrosion. Salt crusts often protect water beneath the surface of salt deposits, so the soils in these saline environments may remain sufficiently moist for corrosion to occur unabated. More research is needed to reconcile the various factors that could influence corrosion in these arid environments.

Corrosion of steels in soil varies significantly, depending on the alloy type and reaction conditions (Table 6). In each case, corrosion is fastest in acidic conditions, where passivation is less pronounced, or in saline environments, where the dissolved salts increase the conductivity of the solution and chloride complexes of Al and Fe increase their solubility. Most munitions have been produced from low to moderate carbon content steels, as carbon steels have the highest strengths. This carbon steel is highly reactive, corroding more rapidly than other steels and also undergoing extensive pit corrosion. In contrast, the most stable alloys of stainless steel (e.g., Alloy 316) are nearly 100 times less reactive. Unfortunately, few munitions are constructed of stainless, as it has less desirable mechanical properties.

Figure 13. Corroded 155-mm howitzer round found in wetland sediments at Eagle River Flats, Alaska.

In summary, corrosion in soils occurs more rapidly than in solutions of a single constituent composition (e.g., NaCl). For most corroding low-carbon steels, the corrosion rate occurs at about 0.02–0.1 (average of 0.025) mm/year (Penhale 1971, Levlin 1996, Norin and Vinka 2003) in oxidizing soil environments. Steel corrosion is accelerated in sulfidic anaerobic environments, often corroding up to 1 mm/year (Hamilton 1983, 1985, 2003; Little et al. 1991; Schutt and Rhodes 1996; Kajiyama and Okamura 1999; Videla 2000; Li et al. 2001). These rates are similar to those calculated using the UXO corrosion model of Garber and Adams (included in Fabian and Ostazeski 2002), although our estimates are somewhat more general and require much less input information. Fortunately, the corrosion rate of steel in a wide variety of soils apparently only varies by a factor of 2 to 5. Conservative estimates of failure rates can be calculated based on the most rapid corrosion rate for a given soil chemical environment.

5.4 Condition of Recovered UXO

Few studies have examined soils near buried UXO to determine if the rounds were leaking explosives into the environment and, if so, what were the concentrations in the surrounding soil. High explosive-filled rounds were fired into the impact area at MMR between 1911 and 1989 (Clausen et al. 2004). Work being done by AMEC to determine the contamination source or sources at MMR found that none of the 18,000 HE-filled UXO had visibly corroded through the casing to the HE fill. They found that 148 rounds were leaking explosives but that these were cracked (44), or had undergone a low-order detonation (AMEX, in review). Of the 116 UXO found in a high use, 3.6-acre target area, most were corroded to some degree, 19 were in good condition, 11 were ruptured, 7 were leaking their

HE filler, and explosives were detected in the soil around 6 of them. Information on the exact nature of the leaks is not given.

Praxis Environmental examined soil near the nose and end of 59 HE-filled UXO that were found at four sites (Praxis 2004). A control soil sample was also taken in the pit, dug to expose the UXO, but as far from the UXO as possible. Table 7 lists the site conditions and the type and burial age of the ordnance found. The soils were analyzed for 21 explosives, propellants, or their breakdown products.

Table 7. Site characteristics for four locations where UXO were studied (Praxis 2004).

Site	Rainfall (cm/yr)	Rainfall (In./yr)	Avg. temp. (°C)	Munition type	Burial age (years)
A	109	43	11.4	60-mm mortars (7) 37-mm mortar (1) 3-in. stoke mortars (4) 81-mm mortars (3)	57–60
B	81	32	28	105-mm projectiles (3) 4.2-in. mortars (2) M1 tank mines (2)	55–60
C	135	53	17	60-mm mortars (2) M8 landmine (1) Rifle grenade (1) Unspecified (3)	52–77
D	41	16	8.3	75-mm projectile (1)	34–42

Of these 59 items, explosives were unambiguously detected around 1 (2%) UXO. This round was a 60-mm mortar—the smallest of the rounds examined and it came from site A. Soil concentrations near this mortar contained TNT, its breakdown products 4A-DNT, 2A-DNT, and manufacturing impurities 2,6-DNT, 2,4-DNT that ranged from 1600 to 34,000µg/kg (ppb). The concentrations of all the explosives were higher in soil near the mortar and lower in the control sample, 30 cm away, suggesting that explosives were moving from the perforated round to the surrounding soil. Soil adjacent to three other 60-mm mortars from this site had below-detection values of RDX, 4A-DNT, and 2-NT, and similar, low concentrations of these analytes in the control samples. These rounds lack clear evidence of leaking fill.

Even fewer studies have examined UXO in the ocean. Detonation of a bunker filled with HE munitions in 1945 sent intact and ruptured ordnance into Halifax Harbor, Canada. Scuba divers collected sediment samples next to seven munitions, four that appeared ruptured and three that appeared intact. Samples were taken at distances of 15 to 30 cm (6 to 12 in.) at the four cardinal points around each UXO (Darrach et al. 1998). A background sediment sample was also collected. Interestingly, all three intact items had detectable levels of either TNT or DNT in their surrounding soils. Low ppb concentrations of TNT or DNT were found around two intact 5-in. shells and high ppt levels of DNT were found in the sediments adjacent to a 9-in. shell. Explosives were not found in sediments surrounding any of the ruptured rounds or in the background sediment sample (Darrach et al. 1998). Apparently, any HE present in the ruptured munitions has dissolved, and been biodegraded or transported away from the round, in the 60 years since the accident. The munitions that appear to be intact, however, are slowly leaking their explosive fill into the surrounding sediments, possibly through pinhole corrosion pits. Thus, visual inspection for obvious corrosion may be inadequate for determining if the round is leaking HE into the environment.

6 STUDIES OF EXPLOSIVE RESIDUES FROM ABOVE-GROUND SOURCES

Above-ground residues result from high-order and low-order detonations, from surface UXO that are blown in place, split open, detonate sympathetically, or corrode in place. Other sources include munition firing points and open burn/open detonate operations to destroy ordnance. Estimating the load of explosives requires good records of the types and numbers of rounds fired and information on the contamination generated by individual detonations of each type of munition. Accurate range records are generally not available, and quantifying contamination by detonation type is still in its infancy.

Two types of studies have been conducted to help assess the amount of HE contamination on training ranges. In site characterization studies, soils are sampled on training ranges to provide estimates of background HE concentrations at impact areas and firing points (Jenkins et al. 1998, 2001; Thiboutot et al. 1998, Ampleman et al. 2003). Detonations of individual munitions (Jenkins et al. 2000, Hewitt et al 2003), on the other hand, measure the HE residues deposited by a single round. The latter tests are conducted on clean snow or clean tarps to minimize the amount of soil involved in the detonation and make it feasible to find and examine the detonation residues. Both types of studies were funded by SERDP and conducted by Dr. Judy Pennington and Dr. Thomas Jenkins and their collaborators (Pennington et al. 2001, 2002, 2003).

6.1 Site Characterization Studies

The explosives found in soils at different types of ranges are listed in Table 8. These include hand grenade, antitank rocket, artillery, and bombing ranges and the firing points for artillery and antitank rounds. For specifics on the sampling plans used and the explosive concentrations found, see the individual studies.

For hand grenade ranges, which are just a few acres in size and are heavily cratered, concentrations of RDX and TNT in the soil range from the high parts per billion (µg/kg) to low parts per million (mg/kg). A variety of sampling protocols was used to characterize the soils at hand grenade ranges (an example of one study is shown in Fig. 14). Soil samples were taken 1) along transects 15, 20 and 25 m from where the grenades were thrown, 2) as a function of depth (surface, 10, 15, 23, and 30 cm), and 3) around one point to assess the short distance heterogeneity (Fig. 14).

Table 8. Ranges whose soils have been analyzed for explosives. The concentrations found vary significantly, depending on where the soil samples were taken relative to targets or low-order detonation debris.

Range Location	Range Type	Contaminants	Reference
US			
Eagle River Flats, Alaska	Ordnance disposal area	2,4-DNT, TNT, RDX	Racine et al. (1992)
Fort Richardson, Alaska	Hand grenade range	RDX, and TNT	Jenkins et al. (2001)
Fort Greely, Alaska	Impact area	RDX, TNT and HMX	Walsh et al. (2001)
	40-mm impact berm	RDX, HMX, low TNT	Walsh et al. (2003)
	TOW antitank range	RDX, PETN, HMX and TNT	
	Firing points	NG and 2,4-DNT	
Fort Ord, CA	LAW rocket range	HMX and TNT	Jenkins et al. (1998)
Pohakuloa Training Area, Hawaii	Firing points	NG and 2,4-DNT	Hewitt et al. (2004)
	Impact range	NG and 2,4-DNT	
	Hand grenade range	RDX, TNT and HMX	
	Demolition range	RDX,HMX,NG,2,4-DNT,TNT	
Scholfield Barracks, Hawaii	Firing points	NG and 2,4-DNT	Hewitt et al. (2004)
	Artillery impact range	low RDX, 2ADNT & 4ADNT	
	Demolition range	RDX and HMX	
	Anti-armor range	HMX,TNT,RDX,TNB & NG	
	Hand grenade range	TNT, RDX and HMX	
MMR, Massachusetts	Firing points	NG and 2,4-DNT	Ogden (2000)
	Central impact area	RDX, TNT, 2ADNT& 4ADNT	AMEX (in review)
	Gun & mortar firing points	2,4-DNT and 2,6-DNT	
	Southeast ranges	HMX, RDX	
	Demolition Area 1	RDX, TNT, HMX & DNTs	
	Rocket range	NG> HMX,RDX, & TNT	
Camp Shelby, Mississippi	Firing points	NG and 2,4-DNT	USACHPPM (2000)
Fort Bliss, New Mexico	Artillery targets	HMX,RDX, TNT & NG	Pennington et al. (2003)
	Firing points	NG	
Fort Lewis, Washington	Impact area	RDX, TNT & DNTs	Jenkins et al. (2001)
	Artillery firing points	2,4-DNT and other DNTs	
	Hand grenade range	RDX, TNT and HMX	
Yakima Training Center, Washington	Antitank range	HMX>RDX>>TNT	Pennington et al. (2002)
	Tank firing points	NG, 2,4-DNT,2,6-DNT	
	Howitzer firing Points	NG and 2,4-DNT	
	Mortar firing points	NG	
	Central impact area	RDX,	

Range Location	Range Type	Contaminants	Reference
Camp Guernsey, Wyoming	Artillery impact area	HMX, 2ADNT and 4ADNT	Pennington et al. (2002)
	Atrillery firing points	below detection	
Canada			
Cold Lake Air Weapons Range, Alberta	Bomb impact area	mainly TNT and RDX	Ampleman et al. (2003b)
	Ordnance disposal area	2,4-DNT and TNT	
Western Area Training, Alberta	Antitank range	HMX>> TNT	Thiboutout et al. (1998)
CFB Chilliwack, British Columbia	Hand grenade range	TNT, RDX and HMX	Ampleman et al. (2000)
	Antitank range		
CFB Shilo, Manitoba	Hand grenade range	TNT, RDX, tetryl, HMX and breakdown products	Ampleman et al. (2003)
	Battleruns	TNT,RDX,NG and 2,4-DNT	
CFTR Tracadie, New Brunswick	Artillery range	below detection	Ampleman et al. (2000)
CFB Gagetown, New Brunswick	Antitank Range	HMX and TNT	Dube et al. (1999)
	Grenade range	TNT and RDX	
	Anti-armor firing points	NG and 2,4-DNT	Thiboutout et al. (2003)
	Anti-armor impact area	RDX, TNT, HMX & NG	
	Rocket range firing point	NG	
	Rocket range impact area	HMX>TNT>RDX	
	Grenade range	RDX,TNT, HMX	
	Impact range	mainly RDX and TNT	
	Ordnance disposal area	mainly 2,4-DNT	
CFB Dundurn, Saskatchewan	Antitank range	HMX>> TNT	Thiboutout et al. (1998)
CFB Valcartier, Quebec	Antitank range	HMX>> TNT	Thiboutout et al. (1998)

Antitank rocket ranges are much larger than grenade ranges, often hundreds of acres in size. The most common antitank rocket, the M-72 LAW, is filled with Octol, a 70% HMX, 30% TNT mix. HMX is the major high explosive contaminant found in soil, followed by TNT concentrations that are two orders of magnitude lower than the HMX because TNT degrades much more readily than HMX. The HE residues are found mainly in the top 10 cm of the soil and the concentrations decrease with distance from the target. The LAW rocket is a line of sight rocket that burns a double base propellant all the way to the target. Chunks of propellant are often found at the firing points and NG from the propellant is generally detected along the track between the firing point and the target. Because the LAW is a thin-skinned rocket that is fired parallel to the ground, it is susceptible to rupture if it misses its target and intersects the ground at a shallow angle. Carcasses of these rounds are often observed at MMR (AMEX, in

review) and a 48% dud rate was reported for a test in which 220 were fired (Thiboutot et al. 1998).

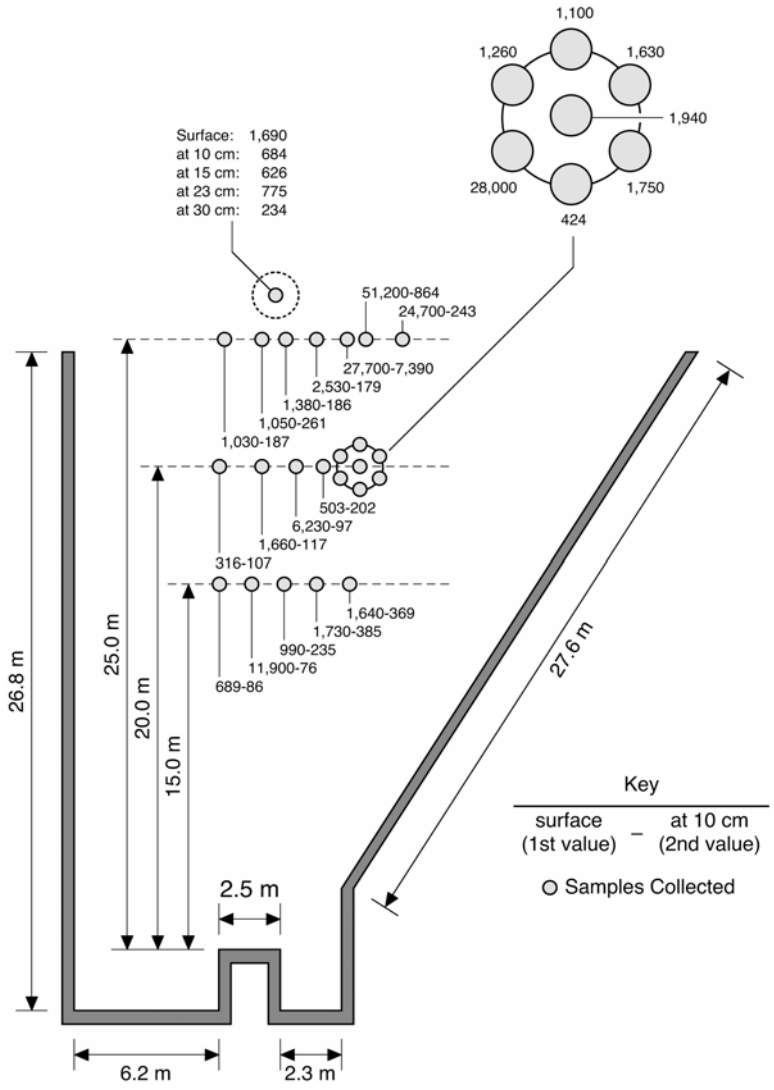

Figure 14. Sampling grids used for a hand grenade range on Fort Lewis, Washington.

Artillery ranges are very large and often many different types of ordnance have been fired into these areas. Surface and sub-surface UXO are present. Soil samples of the impact areas were found to have low ppb concentrations of TNT, RDX, HMX, and NG. Very high concentrations were found near low-order detonations where part of the round and its fill were lying on the ground (Fig. 15).

Because these ranges are so large, a random stratified sampling scheme, like that used for the small hand grenade ranges, would be unlikely to find those areas near targets or low-order detonations where explosive are found as chunks on the ground (Fig. 16). For large ranges, non-random, judgmental sampling at heavily contaminated sites is needed to characterize the widely scattered contaminated sites within a much larger uncontaminated range.

Figure 15. Low-order detonation of a 155-mm round.

Figure 16. Pieces of explosives collected from a 10- by 10-m area on Fort Bliss, New Mexico.

Considerable contamination also may result from firing a weapon, even if the munition detonates successfully. The firing points for 105- and 155-mm howitzers and 60- and 81-mm mortars were sampled to test this idea. The howitzer rounds use a single base propellant consisting of NC fibers impregnated with 2,4-

DNT, which were easily seen when firing occurred on a snow cover (Fig. 17). Walsh et al. (2001) found that firing points were often contaminated with 2,4-DNT from single based propellants and with NG from double and triple based propellants. Samples collected at 10-m intervals, 120 m down range from a howitzer muzzle and 90 m on either side of the gun contained 2,4-DNT at an average concentration of ~1 mg/kg (ppm) (Walsh et al. 2004).

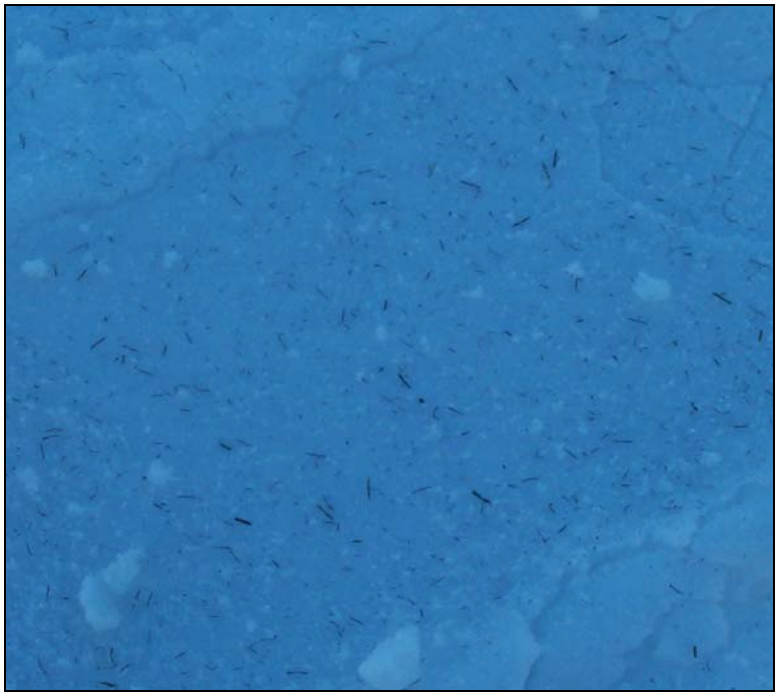

Figure 17. Propellant grains on snow at howitzer firing point, Fort Richardson, Alaska.

Bombing ranges are hundreds of acres in size. At the ranges studied, the surface soil had TNT concentrations as high as 400 mg/kg (ppm). Bomb payloads can be very large (230–910 kg, 500–20,000 lb) and one low-order detonation or a sympathetic detonation of a UXO from a nearby detonation can add kilograms of explosive to the soil (Fig. 18). Furthermore, these processes may emplace large masses of HE at a single site, both limiting dispersal, and, potentially, increasing the threat of extreme localized contamination. Both the U.S. and Canada perform regular maintenance to remove surface UXO from bombing ranges. The purpose of the maintenance is not to mitigate contamination, rather it is to decrease the explosion hazard. To minimize environmental hazards, large, intact explosive pieces should also be removed and disposed of in a way that does not scatter explosive particles into the environment.

Figure 18. Low-order detonation of a 500-lb bomb.

These studies indicate that explosive residues are not homogeneously distributed on training ranges, but are localized in hot spots. Areas with high explosive concentrations are often found around carcasses of munitions that were only partly detonated. Heavily cratered areas often have below detection or low HE concentrations, suggesting that high-order detonations leave only trace amounts of HE residues. The heterogeneity and non-random distributions of explosive residues need to be considered when evaluating the contamination risks associated with UXO and HE pieces.

6.2 Explosive Residue from Individual Detonations

Knowing the amount of HE residue deposited by an individual munition and how this varies among multiple detonations of the same munition is important to better estimate total HE loading at firing ranges. The explosive residue generated by individual munitions, coupled with firing records of the number and type of round fired, could be used to estimate the load of explosives on a range. The difficulties encountered in this approach include 1) the lack of accurate firing records over the lifetime of the range, 2) knowing the area over which the HE residue is deposited, and 3) obtaining representative samples that can accurately determine an average concentration. Nevertheless, investigations examining individual detonations provide considerable insight into the release of HE into the environment.

6.2.1 Rounds Fired into Snow-Covered Ranges

To estimate the mass of explosives remaining after high-order detonations, Jenkins et al. (2000) collected and analyzed residue-covered snow samples from wintertime detonations. The frozen ground minimized soil contamination, and the snow provided a clean sampling background that decreased the chances of cross-contamination from prior range activities. The snow also made the dark

detonation residue highly visible, allowing the residue plume to be mapped and measured. Jenkins et al. (2000) used multiple snow samples, taken within the residue plume, to estimate the deposited mass of explosive from high-order detonations. The sampling has yielded consistently low explosive concentrations, $\mu g/m^2$ quantities, for a variety of tactically detonated munitions (Table 9, Jenkins et al. 2000, Hewitt et al. 2003).

Table 9. Concentration of high explosives found after live fire into snow covered ranges. The rounds were all filled with Comp B. All data from Hewitt et al. (2003).

Item	Munition	Explosive fill (g)	Number samples /test	Sampled area (m^2)	Estimated total mass deposited (µg)			
					TNT	RDX	HMX	Other
Mortars	60-mm	360		2.8	bd	5.2	3.9	
				5	2.2	6.6	0.57	
				4.3	11	28	4.5	
				7.8	40	150	43	
				3.6	17	180	42	
	81-mm	930	14	15.1	2,200	5,300		3,100[c]
			43	75	1,000	8,500		4,600[c]
								Residue from thirteen 81 mm mortar rounds
	120-mm	2990	18	30	170	1,100	87	94[a]
			5	24	16	460	23	140[a]
			8	5.6	370	2,400	150	7,200[a]
			7	7.2	42	790	48	220[a]
			8	10.2	47	430	37	260[a]
			7	6.1	1,500	16,000	410	720[a]
			7	10.4	150	5,300	60	130[a]
Howitzer	105-mm	2090	7	7	130	84		
			15	15	290	170		
			8	8	210	170		
			31	31	250	82		Residue from four 105-mm rounds
			22	22	43	25		
			10		130	56		
			8	8	29	260		
			8	8	160	100		
			6	6	210	38		
Rifle grenades	40-mm	32		2	7.7	1,400	180	
				3.6	6.8	3,400	440	
				2.5	1.1	25	15	

Item	Munition	Explosive fill (g)	Number samples /test	Sampled area (m^2)	Estimated total mass deposited (µg)			
					TNT	RDX	HMX	Other
Hand Grenade	M67	186	6	7.6		22		13[b]
			4	5		17		13[b]
			5	5.5		10		11[b]
			5	5.4		9		6[b]
			4	9.1		13		5[b]
			5	7		28		5[b]
			14	22.7	ND	57		14[b]
Torpedo	Bangelore		7	12.5		90,000	20,000	
Shape Charge			10	12		4,200,000	340,000	

a NG
b 2,6-DNT
c 4AmDNT

6.2.2 Blow-in-Place Detonations on Snow

Many different blow-in-place studies have been conducted and the results of some of these tests are listed in Table 10. These are sometimes used as proxies for live-fire tests. Although live-fire tests more accurately represent the residues deposited by training, they are difficult to sample as rounds may not land in the desired area and trays cannot be put out to collect particles. The blow-in-place tests, however, provide information on contamination resulting from the blow-in-place operations used to dispose of ordnance on ranges.

Hewitt et al. (2003) found that high-order detonations produced by blow-in-place procedures leave more explosive residue than rounds that are fired. This suggests that the way in which the detonation was initiated, specifically whether the designed initiation train was used (fuze, booster), can affect the amount of HE remaining.

For blow-in-place detonations of 155-mm howitzer rounds Taylor et al. (2004a) found particles of TNT both in snow samples and in two of the four aluminum trays (north and east trays) placed 20 m around the point of detonation (Fig. 19). The variability in TNT concentration seen in the snow samples collected within the plume (Tables 11 and 12) suggests that the TNT particles, not the ubiquitous soot, carry the TNT. Particles of TNT were found on the north tray—outside the plume area (Fig. 19). This finding suggests that the TNT particles, because of their greater size and mass, are not as affected by wind conditions as the soot. It also suggests that estimates of HE deposition, based on the

plume area, may underestimate the HE deposited if particles are routinely found outside the plume area.

Table 10. Concentration of high explosives found after blow-in-place operations on snow. The data from Valcartier Quebec are from Lewis et al. (2002); all the rest are taken from Hewitt et al. (2003)

Munition		Fill	Wt. Fill (g)	Wt. C4 (g)	Number samples per test	Estimated total mass deposited (µg)			Installation
						TNT	RDX	HMX	
Mortar	60-mm	TNT	300	286.5	4	52,000	22,000		Valcartier, Quebec
					4	8,700	28,000		
					4	960	20,000		
					3	1,100	9,000		
			300	95.5	2	6,900	81,000	20	
					3	450	18,000		
					2	3,200	96,000	140	
					4	6,300	75,000		
	81-mm	Comp B	950	570	7	38	12,000	2,600	Camp Ethan Allen, VT
	81-mm	Comp B	816	286.5	4	6.20×10^6	13,000		Valcartier, Quebec
				286.5	4	160,000	6,900		
				115	1	18,000	5,200		
				76.4	3	27,000	15,000	34	
				76.4	2	150,000	8,800		
				76.4	3	33,000	39,000	6,000	
Howitzer	105-mm	Comp B	2000	191	3	2.50×10^6	24,000		Valcartier, Quebec
	155-mm	TNT	6800	570	15	110×10^6			Camp Ethan Allen, VT
					7	38×10^6			
					11	45,000			
					9	500			
					10	6.9×10^6			
					10	200,000			
					11	80,000			
Torpedos	Bangalor	Comp B	4860		11	150	110,000	18,000	Fort Drum, NY
Antitank mines	M19	Comp B	9530	280	11		2,700	8,300	
	M15	Comp B	10300	280	13	76	40,000	4,100	

Munition		Fill	Wt. Fill (g)	Wt. C4 (g)	Number samples per test	Estimated total mass deposited (µg)			Installation
						TNT	RDX	HMX	
Anti-personnel mines	Claymore	C4	680		7		13,000	3,000	Camp Ethan Allen, VT
					7		6,100	3,000	
					12		1,900	1,800	
					7		5,700	2,500	
					8		1,100	390	
					6		26,000	9,500	
					7		17,000	4,800	
					6		50,000	34,000	Fort Drum, NY
Anti-personnel mines	PMA-1A	TNT	200	b.c.	7	280,000			Camp Ethan Allen, VT
					8	1.1×10^{6}			
	PMA-2	TNT	100	b.c.	5	2300	640		
					8	550,000	1,500		
			100	9.5	1	1.7×10^{66}	120,000		Valcartier, Quebec
			100	38.2	1	40×10^{6}	990,000		
					2	3,700,000	33,000		
	PPM-2	TNT	130	280	7	980,000	47,000	7,900	Camp Ethan Allen, VT
					8	6.6×10^{6}	42,000		
	VS-50	RDX	43	280	8		140,000	5,300	
	VS-50				8		89,000	3,000	
C4 blocks		94% RDX	570	b.c.	9		38,000	16,000	Camp Ethan Allen, VT
					16		12,000	5,100	
					8		18,000	6,200	
					7		3,600	550	
					8		12,000	4,100	
					8		3,900	3,000	
					7		3,100	2,000	
					6		4,300	2,000	
Hand Grenades	M67	Comp B	176	0	5	2,800	350		Valcartier, Quebec
					2		200		
					2		1,400	110	
					4	3,500	540	78	
		Comp B	176	191	4	1,300	160,000	56	
					2	7,300	260,000	210	
					3	5,900	130,000	120	
					4		210,000	390	

Figure 19. Locations of snow samples and the trays (marked by triangles) at Camp Ethan Allen relative to the detonation point. Soot darkened areas of snow (the plume) are delineated, the visible plume by the outer line and the sootiest area by the inner line.

Table 11. HE mass recovered from blow-in-place of seven 155-mm rounds.

Test	Number of samples averaged	Avg. TNT conc.	Std. Dev	Plume area (m^2)	Plume mass	Crater mass	% Recovered
1	15	220 mg/m^2	337 mg/m^2	496	109 g	1.8 g	1.64
2	9	124 mg/m^2	203 mg/m^2	311	38.3g	0.11 g	0.568
3	11	118 µg/m^2	222 µg/m^2	345	40.4 mg	7.1 µg	5.98×10^{-4}
4	9	1.47 µg/m^2	2.34 µg/m^2	344	0.5 mg	3.64 µg	7.40×10^{-6}
5	11	16.9 mg/m^2	12.6 mg/m^2	406	6.8 g	19 mg	0.101
6	10	679 µg/m^2	1774 µg/m^2	301	204 mg	0.4 µg	3.02×10^{-3}
7	11	168 µg/m^2	243 µg/m^2	476	79.8 mg	0.2 µg	1.18×10^{-3}

Table 12. Individual sample concentrations for the first test.

Sample test 1	Distance to crater (m)	Sample area (m^2)	TNT conc. (mg/m^2)
S-1*	12.6	1.0	184
S-2	10.0	1.0	49.0
S-3	8.3	1.0	170
S-4	6.2	1.0	200
S-5	3.8	1.0	530
S-6	1.8	1.0	330
S-7	2.0	1.0	19.0
S-8	4.4	1.0	1.00
S-9	6.0	1.0	3.20
S-10	8.0	1.0	4.30
S-11	1.5	1.0	1300
S-12	4.0	1.0	340
S-13	6.6	1.0	140
S-14	4.6	1.0	15.0
S-15	6.8	1.0	21.0
Crater**	—	1.0	1800
Avg. *n*=15			220
Std. Dev			337
Area of soot plume		496 m^2	

*Estimated from particle counts in the filter and TNT concentration in the melt.
** Not included in average.

6.2.3 Explosive Residue from Individual Low-Order Detonations

To estimate the mass of explosives remaining after low-order detonations, Pennington et al. (2003) sampled the residues from detonations on a large tarp at Blossom Point (BP), Maryland. The tarp also helped minimize any cross-contamination from the underlying soil and made it easier to see and pick up the explosive pieces scattered by the detonation. Taylor et al. (2004a) measured the mass of scattered Comp B and TNT and the resulting particle size distributions for one 81-mm and one 155-mm low-order detonation (Fig. 20). The low-order detonations produced a wide range of particle types; they ranged from crystalline to partially or totally melted (Fig. 21). For the 155-mm low-order detonation, most of the HE mass deposited was in centimeter-sized pieces, whereas particles

less than 1 mm in size were responsible for most of the surface area of the deposited HE (Fig 22). For the 81-mm low-order detonation, 50% of the HE mass was in pieces smaller than 1 cm, whereas particles less than 1cm in size were responsible for 80% of the surface area of the deposited HE (Fig. 23). The number of HE particles and their sizes were measured as a function of distance from the detonation for the 81-mm round. The number of particles was found to decrease rapidly away from the detonation point, but the average size of the particles increased with distance (Taylor et al. 2004b).

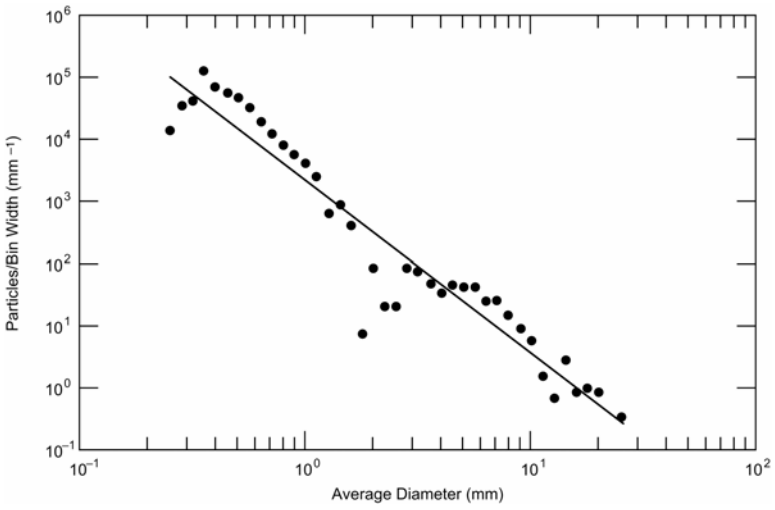

a. 81-mm mortar.

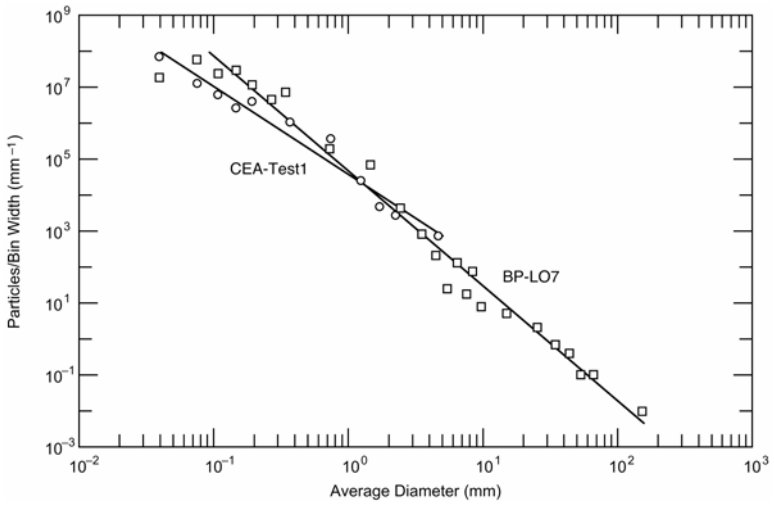

b. 155-mm shell.

Figure 20. Size distribution of HE particles collected from low-order detonations.

Figure 21. Variety of Comp B particles.

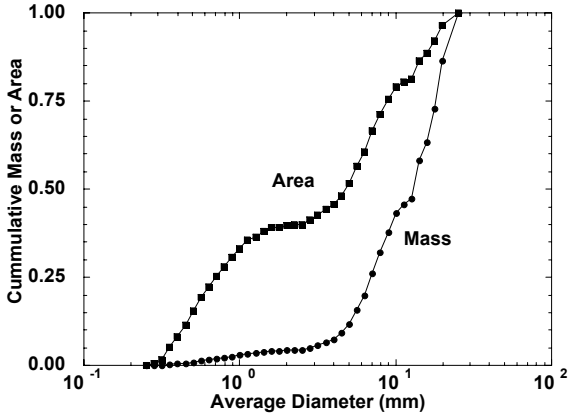

Figure 22. Cumulative mass and surface area of HE residue collected from a low-order detonation of an 81-mm mortar.

Underwater low-order detonations were conducted at Aberdeen Test Center to determine if these could reliably reduce blast effects from underwater detonations (Pedersen et al. 2002). Blast effects from high-order underwater detonations can harm marine mammals and destroy coral reefs (Pedersen et al. 2002 and references therein). Tests were conducted on 155-mm projectiles and Mk 82 bombs. Low-order detonations were achieved in all 21 of the 155-mm trials and in 8 of 11 Mk 82 Bomb trials. Debris from 16 tests of 155-mm shells and 13 tests of Mk 82 bombs was captured with a closed weave cargo net (of unknown mesh opening) positioned about 5 m beneath the detonation. For the 155-mm projectiles, between 9 and 47% of the initial 7-kg fill was recovered as explosive pieces (av-

erage 24 ± 13%). For the Mk 80 bomb, of the initial 87 kg of tritonal, 41 to 89% was recovered as chunk material (average 72 ± 13%). The values are minimum estimates as, in all likelihood, some small pieces were not captured by the net or were missed by the divers sent to retrieve them.

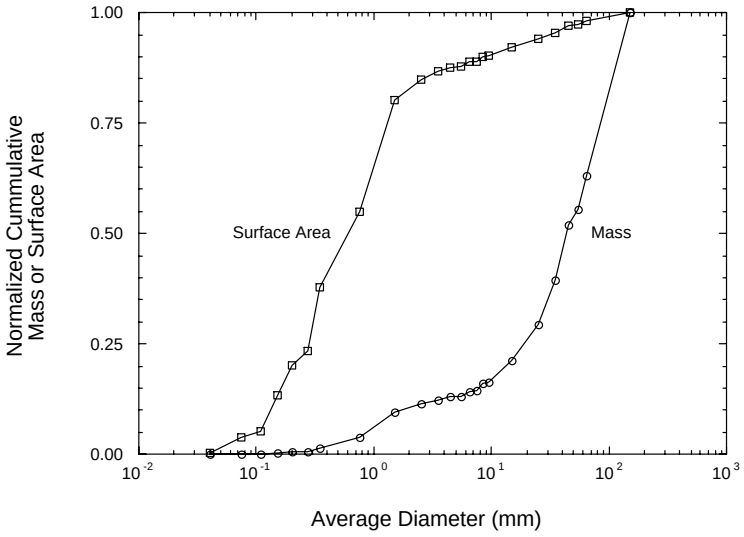

Figure 23. Cumulative mass and surface area of HE residue collected from a low-order detonation of a 155-mm artillery shell.

6.3 Sampling Problems and Sub-sampling Issues

An important issue for all of these studies is how to collect representative samples. Efforts to estimate a mean explosive concentration from the residues of an individual detonation often yield disparate results. The reason is that high explosives such as TNT and RDX are solids at environmental temperatures, and their residues exist as particles of various sizes (Radtke et al. 2002, Taylor et al. 2004a,b). Also, post-blast residues from detonations of HE ordnance are non-uniformly dispersed, resulting in extreme spatial heterogeneity of the explosives. Explosive concentrations in soil samples taken near a detonation therefore often range over orders of magnitude and are not normally distributed.

Given that the HE residues are particulates that are non-uniformly dispersed in a particulate media, and that residue samples are inherently heterogeneous, sampling error is unavoidable and one needs to understand the sources of error to minimize it (Walsh et al. 2002). Pierre Gy developed theories on the sources of

sampling error and based on these theories, Francis Pitard developed practical sampling methods (Pitard 1993). The heterogeneity attributable to the complex mixture of components that make up the HE-contaminated soil or snow is termed constitutional heterogeneity (Pitard 1993), and the error associated with constitutional heterogeneity is called fundamental error. Fundamental error is minimized if a sample includes all constituents in the same proportions as the HE-contaminated soil or snow (i.e., all constitutive elements have an equal probability of being selected for a sample). In other words, the sample must contain in the proper proportion all the different sizes and compositions of the HE particles.

Walsh et al. are developing multi-increment or composite sampling methods that reduce the fundamental error and improve estimates of average HE concentrations in soil. A sufficient number of increments must be taken to minimize the error associated with the distributional heterogeneity of the HE residues, and the sample mass must be large enough to minimize the error associated with compositional heterogeneity. Grinding and homogenizing the sample also helps obtain a reproducible average concentration. Replicate samples from a hand-grenade range indicated that 50-increment 4-kg samples were adequate to estimate residues from grenade detonations (Walsh et al. 2002).

Figure 24 illustrates how composite samples can decrease the variability and provide a better estimate for the mean concentration of a sample. A frequency diagram of the individual NG concentrations found in soil show an order-of-magnitude variation in the concentration (Fig. 24a). If individual concentration values are randomly chosen and combined mathematically to simulate multi-increment samples that contain 5, 30, and 50 samples, one can see that, as the number of increments increases, the variability is reduced and the data become normally distributed (Fig, 24b,c,d). This effect can also be observed with composite soil samples collected in the field. As the number of composites making up a sample increases, the data begin to plot as a straight line on a probability plot (Fig. 25), indicating a normal distribution.

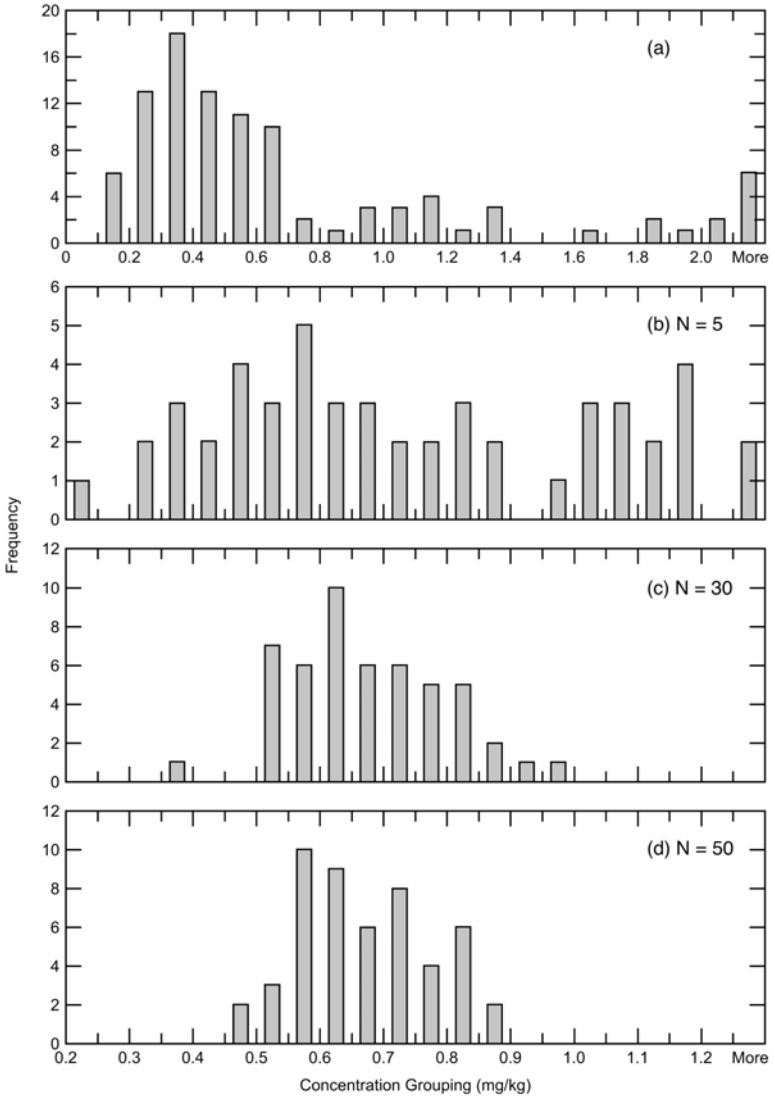

Figure 24. Concentration distribution of NG in soil samples (a) and the change in the distribution if 5 (b), 30 (c), and 50 (d) randomly selected samples are mathematically combined into composite samples.

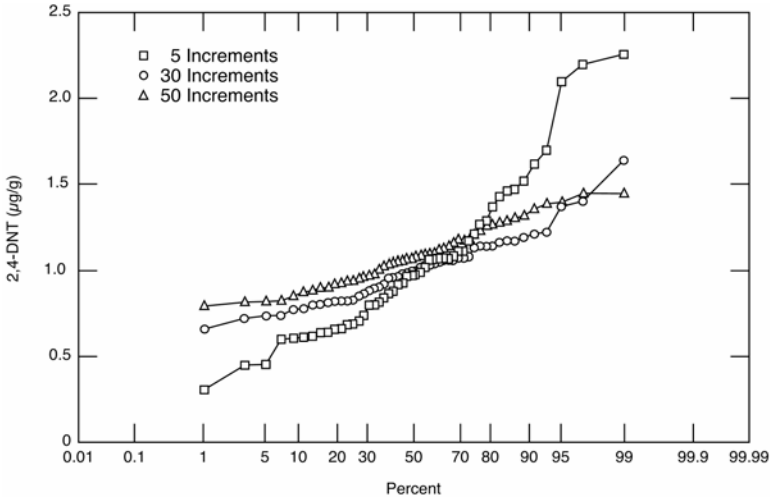

Figure 25. Probability plot showing how increasing the number of sub-samples in a composite sample gives rise to distributions that are normally distributed (straight line on the plot).

7 DISSOLUTION OF HE MASSES

Environmental contamination by HE residues from HO detonations, LO detonations, or duds occurs through dissolution by rainwater. The size of the HE residues varies from the full explosive filler (tens of centimeters) to small particles from HO detonations (micrometers in size). Here, we review efforts to quantify dissolution rates for HE masses as a function of particle size, HE type, flow rate and temperature. Table 13 compares estimates for dissolution times versus HE particle size using data and assumptions from these sources.

Table 13. Comparison of expected dissolution times (years) by particle size based on 75 cm/yr rainfall.

Source and method	Matyskiela (2003): –Dissolution theory for neat Comp B mass in porous soil. –Time based on theory that includes size effect.	Lynch et al. (2002): –Stirred volume, 0.04–4 mm RDX and TNT particles. –Time based on constant dissolution coefficient (eq 8).	Phelen et al. (2003): –Uniform porous flow, 0.1-mm and 1-mm Comp B particles. –Time based on scaled experiment duration.	Lever et al. (in prep) –Dripped flow, single 2-mm Comp B particle. –Time based on constant mass-loss rate
HE Particle Size (mm)	Comp B	RDX/TNT	Comp B	Comp B
0.1	0.8	0.005/0.001	0.8	0.004
1	20	0.05/0.01	20	4
10	800	0.5/0.1		4000
100	20,000			

Average annual rainfall in the U.S. varies from a low of about 13 cm/yr in Nevada to a high of about 250 cm/yr along the Pacific Northwest (Department of Commerce 1968, Wexler 1991). Most of the country falls in the range 50–150 cm/yr, and 75 cm/yr represents a reasonable average value. Instantaneous rainfall rates are much higher, broadly ranging 0.1–10 cm/hr, with typical values of the order 1 cm/hr. Stable-isotope measurements indicate that most rainfall percolates directly into the soil and, except in areas having highly impermeable surfaces (urban areas), very little runs overland into rivers (Buttle 1997). This is true even for storms. Consequently, instantaneous rainfall rates approximate instantaneous infiltration rates. Because HE dissolution rates can vary with flow rate, it is important to conduct laboratory measurements or theoretical analyses with realistic infiltration rates to estimate field dissolution rates. Provided this is done, total annual rainfall will scale total annual dissolved mass. We will use 75 cm/yr for this purpose.

Matyskiela (2003) modeled the mass transfer (dissolution) of a “neat” cylindrical block of Comp B in direct contact with porous soil. This model includes both diffusion and advection of dissolved RDX and TNT through a stagnant

boundary layer adjacent to the Comp B block. It treats these two constituents independently. For dissolution of Comp B through a shell casing newly perforated by corrosion, it assumes a stagnant boundary layer is created by capillary suction of water into the gap between the explosive fill and the casing. Dissolution is then by diffusion only, and the active open area is the small (1-mm-diameter) pinhole. The theory includes the dimensions of the cylindrical block, and the region of validity is defined by $VR/D_j > 4$, where V is pore water velocity, R is block radius and D_j is diffusion coefficient for component j. Assuming 1 cm/hr infiltration rate and 50% soil porosity, we can apply the theory to RDX particles larger than about 0.2 mm and TNT particles larger than about 0.5 mm. These sizes correspond roughly to ~ 0.6-mm-scale particle of Comp B. Matyskiela (2003) computed RDX and TNT dissolution rates for a 1-kg block of Comp B using parameters for 10 sites where UXO have been recovered. The largest infiltration rate at these sites was 26 cm/yr. He examined the influence of infiltration rate by using generic soil conditions with measured 5-minute rainfall rates. He also examined the effect of particle size on dissolution of RDX using a 25-cm/yr infiltration rate.

The analysis provides several results of interest. Firstly, diffusion is negligible relative to advection for all rainfall rates and sites examined. Secondly, advection mass-transfer varies as $V^{1/2}$, so mass-loss based on annual average flow, rather than "burst" rainstorm flow, probably overpredicts actual loss rates for a site. This is because the rate of dissolution increases proportionally less than the duration decreases for the same total annual rainfall. Thirdly, dissolution rates for 1-mm pinhole perforation of a shell casing are about 10^{-7} times those of a neat block. Considering that corrosion of the pinhole opening will require tens of years, buried UXO will probably have negligible contamination potential unless the initial impact or later nearby detonations split open the casing or until long-term corrosion effectively renders the casing permeable to water flow.

Matyskiela's results highlight the importance of using realistic infiltration rates to calculate dissolution rates. At the single site examined, the annual infiltration rate was 30 cm/yr. The calculated dissolution rate decreased by a factor of ~ 8 when based on 5-minute, rather than annual, infiltration rates. Thus, the $V^{1/2}$ dependence implies that the effective average infiltration rate was ~ 0.2 cm/hr, near the low end of typical rainfall rates.

The explicit dependence of advection dissolution rate on particle radius, $R^{-3/2}$, allows us to apply Matyskiela's model to predict dissolution time-scale across the particle sizes of interest. However, we must make two assumptions: 1) that dissolution of RDX establishes the time scale for dissolution of Comp B because it dissolves more slowly than TNT, and 2) that the ratio of effective aver-

age infiltration rate to annual rainfall rate is approximately the same for all sites. Note that this last assumption yields an effective average infiltration rate of ~ 0.5 cm/hr for an annual rainfall rate of 75 cm/yr.

Table 13 shows the resulting predictions for dissolution time-scale versus particle size. For example, a buried 1-kg (~ 10-cm-scale) neat block of Comp B will require about 20,000 years to dissolve. Of course, this time applies after the shell casing has effectively disappeared (complete corrosion or fracture by nearby detonations). The model's $R^{-3/2}$ dependence suggests that a 1-mm particle will dissolve after about 20 years. Because the particles become smaller as they dissolve, these times slightly overpredict dissolution time, but they are adequate estimates for the general time scales.

Lynch et al. (2002) dissolved small quantities of TNT, RDX, and HMX in a fixed water volume while stirring at a constant rate and temperature. The outcome was the initial dissolution rate, measured before the bulk concentration of HE exceeded 20% of the saturated concentration and particle area loss exceeded 5%. Particle sizes ranged from 0.04–4 mm and surface areas were based on military specifications (RDX and HMX) or microscopic measurements (TNT). Tests were conducted at 10 to 30°C and several mixing rates between 90 and 250 rpm.

The underlying mechanism of dissolution for this experiment is diffusion of HE through a stagnant layer surround the particle:

$$V\,dC/dt = \mathrm{D}/h\,S\,(Cs - C) \tag{2}$$

where

V = volume of water

t = time

C = HE concentration in the water

D = diffusion coefficient

h = stagnant layer thickness

S = particle surface area

Cs = saturation concentration of the HE in water.

The particle mass loss rate is

$$-dM/dt = kS \tag{3}$$

where M is particle mass and k is the dissolution coefficient. Comparing eq 2 and 3 for $C << Cs$ indicates that k varies inversely with stagnant layer thickness:

$$k = D/h\ Cs \tag{4}$$

The role of increased stirring (or turbulent energy in the flow) is to decrease h and consequently increase k. The authors argue that the range of mixing power input in the experiments broadly overlaps the power of rainfall for the U.S., and, thus, the measured dissolution rates should approximate field values for similar particles. At 20°C and 150 rpm, the measured dissolution rates were TNT = 1.4×10^{-2} (mg/min)/cm^2, RDX = 3.0×10^{-3} (mg/min)/cm^2, and HMX= 1.3×10^{-2} (mg/min)/cm^2. For roughly spherical particles of radius r and density ρ, we may approximate the mass loss as

$$dM = \rho\ S\ dr \tag{5}$$

Substituting eq 5 into 3 yields

$$dr/dt = -k/\rho = (D/h)(S/\rho) \tag{6}$$

If dissolution rate k (or stagnation layer thickness h) is independent of particle size, integration of eq 6 yields

$$r(t) = r_0 - k/\rho\ t \tag{7}$$

where r_0 is the initial particle radius. Setting $r(t) = 0$ provides an estimate of dissolution time τ for the particle:

$$\tau = r_0\ \rho/k \tag{8}$$

Note that if the stagnation layer thickness scales with particle size, the dissolution rate will increase with decreasing particle size and eq 8 will overestimate the time for complete particle loss. Nevertheless, based on eq 8 and the dissolution rates measured by Lynch et al. (2002), the time taken for 1-mm-diameter HE particles to dissolve would be about 4 days for TNT and 20 days for RDX. The corresponding times for 0.1-mm particles would be 0.4 days and 2 days, while for 1-cm particles the times would be 40 and 200 days for TNT and RDX, respectively. These times are much shorter than the predictions based on Matyskiela (2003) (Table 13).

Phelan et al. (2003) layered Comp B particles within a matrix of glass beads in a cylindrical column and subjected them to steady water flow through the porous medium. The particles were sieved to produce narrow size distributions centered on 0.1- and 1-mm diameters. The experiments were run at room temperature (~ 20°C). Infiltration rates ranged 0.16 to 0.70 cm/hr, within the range of rainfall infiltration rates. The corresponding pore velocities were 0.55 to 2.4 cm/hr. The concentration of TNT and RDX in the effluent was measured at regular intervals, and the TNT and RDX residues in the glass-bead matrix were measured at the end of each experiment to check for mass balance. Bed loading (i.e., Comp B concentration in the bed layer) was sufficiently high in some cases that interaction between Comp B particles in the bed layer probably occurred. Here, we consider only the results from the bed loads where the Comp B particles occupied less than 10% of the cross-sectional area of the column.

Measured mass balances for RDX ranged between 59 and 174% with most tests falling in the range 80–90%. For TNT, measured mass balances ranged between 35 and 89% with most tests falling in the 50–70% range. The authors could not account for these low values. The five tests that used 0.1-mm particles and constant infiltration rate of 0.35 cm/hr had an average duration of about 160 hours, and the effluent accounted for about 96% of the recovered mass. We may assume that all 0.1-mm Comp B particles would dissolve, based on a total infiltration of 160 hr/0.96 × 0.35 cm/hr = 57 cm.

The experiments showed a very minor effect of flow velocity on dissolution rate; scatter between nominally identical tests was more significant. Because the velocities used were within the range for typical rainfall infiltration rates, the dissolution rates should approximate field values. We may thus use total infiltration to scale dissolution time. The resulting estimate to dissolve 0.1-mm Comp B particles at the U.S. average annual rainfall is 57 cm/(75 cm/yr) = 0.8 yr.

The single low-concentration test with 1-mm Comp B particles ran for about 300 hours at a 0.35-cm/hr infiltration rate. The effluent accounted for only 3% of the recovered RDX and 11% of the recovered TNT. These results suggest that about 4300 hours or 1500 cm total infiltration would be needed to dissolve 1-mm Comp B particles. Thus, the expected dissolution time for 1-mm Comp B particles would be about 20 years for the U.S. average annual rainfall. These are remarkably similar to the predictions based on Matyskiela (2003) (Table 13).

Lever et al. (in prep) placed a single Comp B particle (about 2 mm across) on a filter within an 11-mm-diameter cylindrical tube. Water dripped on the center of the filter at a constant rate of 0.52 mL/hr, about 20 drops per hour. This corresponds to a rainfall rate of about 0.55 cm/hr, although the average drop size of 4 mm was larger than the 1.4-mm average raindrop size expected for that rainfall

rate (Pruppacher and Klett 1997). The Comp B particle was free to move around on the filter so it was not struck by every drop. The water passing by the particle was collected into vials every 2 hours and analyzed for RDX and TNT. Only a single experiment has been completed to date.

The experiment produced several interesting observations. The surface of the Comp B particle, retrieved from a blow-in-place low-order detonation, was initially fairly smooth. During the early stages of the experiment, the TNT matrix preferentially dissolved faster than the embedded RDX crystals, increasing the exposed surface area of RDX and giving the particle a lumpy surface texture. The ratio of RDX/TNT dissolved in each water sample varied over an order of magnitude around its long-term average of 1.73, apparently reflecting the relative ratios in exposed surfaces and dissolution rates of the these constituents. Some RDX crystals (typically about 0.1-mm in size) also broke free from the main particle. Clearly, particle dissolution did not proceed as if the RDX and TNT were homogeneously mixed and dissolving independently. The nominal composition of Comp B is 60% RDX and 40% TNT, with small percentages of HMX as a by-product of the RDX manufacturing. Negligible amounts of HMX were recovered from this particular particle.

The original particle lost about 2.72 mg of Comp B (about 97% of the total mass) over the 68-day experiment. The particle mass at the end was 0.092 mg, consisting of about 90% RDX. Interestingly, the cumulative mass-loss of both RDX and TNT was nearly linear with time, indicating approximately constant dissolution rate (mg/hr) although the TNT dissolution rate did decrease near the end of the experiment (Fig. 26). If the flow had been uniform rather than impinging drops, this result would imply that the product of exposed surface area and dissolution coefficient (kS in eq 3) remained nearly constant for both constituents as particle size decreased. Here, the result is consistent with saturation-limited dissolution into a nearly constant water volume surrounding the particle after each drop, and the sweeping away of that dissolved material upon arrival of the next drop 3 minutes later.

This experiment simulates an HE particle on the soil surface exposed to rainfall but without significant pooling of the water. Because the rainfall rate was realistic, the measured dissolution rate should approximate field values. Again, this permits scaling the measured mass-loss by total infiltration and suggests that a 1-mm Comp B particle would dissolve within 4 years at the U.S. annual rainfall rate of 75 cm/yr. This is comparable to the results based on Phelan et al. (2003) and Matyskiela (2003) where the particle is within a porous soil matrix rather than lying on the surface. Extrapolating the drip-experiment results suggest a 0.1-mm Comp B particle would dissolve in less than 2 days, whereas a 1-cm particle

would require about 4000 years to dissolve. The latter result is so long that mechanical breakup of the particles by weathering or nearby detonations is likely to occur before the particles dissolve under the action of rain-impingement alone.

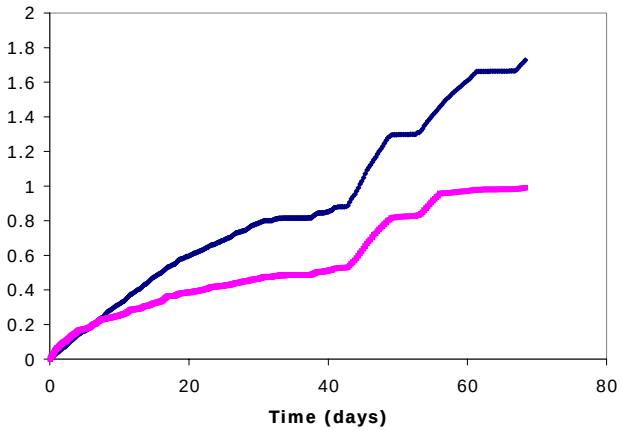

Figure 26. Mass loss of RDX and TNT with time from a single grain of Comp B.

Radtke et al. (2002) sampled surface soils at a site in southeastern Idaho where the explosive contamination (TNT) was at least 50 years old. By analyzing sieved soils, they found that particles larger than 3 mm accounted for more than 96% of the TNT contamination. The average particle mass was 0.087 g, indicating that the mass-average particle diameter was about 5 mm. The authors did not speculate on the original source of the particles, and there is no information on their original size distribution.

We may view 50 years as a conservative estimate of the time required for 3-mm surface TNT particles to dissolve under average U.S. conditions. Annual rainfall in southeastern Idaho averages only about 20 cm/yr, and particles initially larger than 3 mm could account for the less-than 3-mm contamination found in the study.

These studies suggest that much of the HE filler in UXO may persist even after the UXO casing is compromised. By comparison, smaller HE particles from detonations (high- and low-order) will dissolve much more rapidly. The relative importance of these contaminant sources is evaluated in the next section by accounting for the expected masses and dissolution rates of HE from each possible fate of a fired munition.

8 A MODEL TO ESTIMATE HE CONTAMINATION RATES

Figure 27 identifies the possible fates and their probabilities for HE rounds fired during training. By assigning probabilities and consequences to each fate for the most significant munitions, we may estimate the annual influx of dissolved HE and the relative contribution of each fate. We used a spreadsheet model to estimate the yearly dissolved HE input to the soil. Although many parameters are estimates, we can easily change them if better data, national or site-specific, become available.

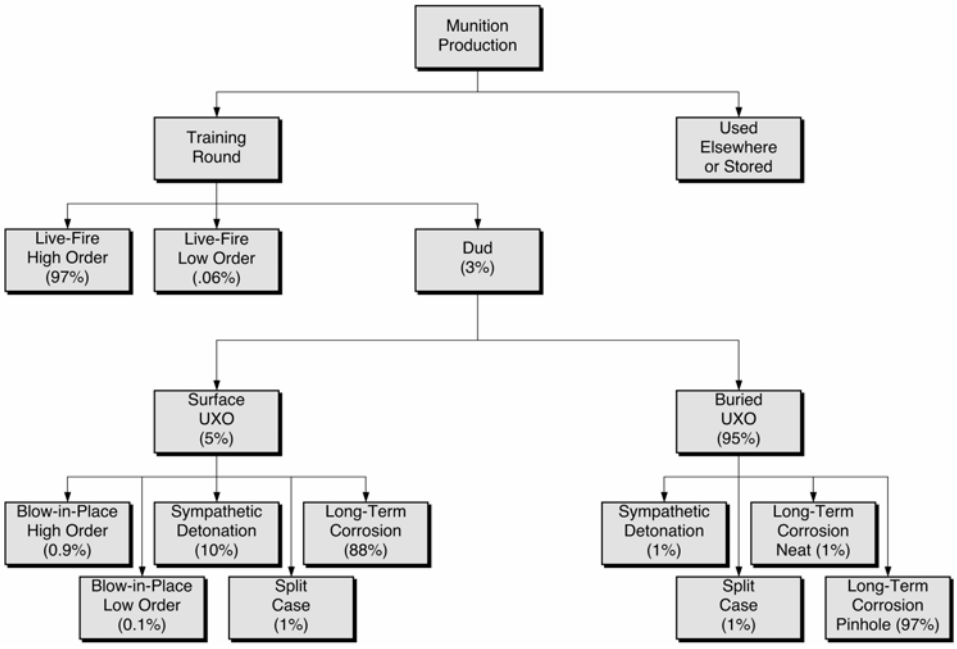

Figure 27. Possible fates of a fired munition and their estimated probabilities.

A fired round might detonate at high order or low order, or it might be a dud. The first two outcomes immediately release HE particles onto the soil surface. Duds can either penetrate the ground or remain on the surface. The most likely outcomes for surface UXO are blow-in-place detonation (HO or LO), sympathetic detonation initiated from a subsequent detonation nearby, splitting of the shell casing, and corrosive perforation of the shell casing. Similar fates exist for buried UXO, except that we neglect blow-in-place operations and identify two corrosion categories (neat and pinhole) that reflect how easily water can flow past the HE fill within the corroded round. The time scale for dissolution of a

round's HE depends strongly on its fate: detonations of all forms release relatively small particles of HE that can dissolve quickly; splitting or corrosion of the shell casing both leave the HE charge intact, and much slower dissolution rates result.

Table 14. Model input parameters and percent contribution of each fate to annual dissolved HE on training ranges. For the top five munitions (by HE mass produced): 81-mm, 4.2-in mortar; 105-mm, 155-mm, 8-in. howitzer. Total HE production of these munitions over 50 years was 3.4 x 10^8 kg, about 80% of which was used in live-fire training.

Fate	Probability (%)			HE mass release (%)	HE particle size (mm)	Dissolution mechanism	Dissolution time (yr)	Percent contribution	Notes
High Order (HO)	97			0.001	<<1	Particle	1	4	1
Low Order (LO)	0.06			50	<100	Particle	100	55	2
Dud (UXO)	3								3
Surface UXO		5							4
BIP- HO			0.9	0.3	<10	Particle	50	0.01	5
BIP- LO			0.1	50	<100	Particle	100	0.1	5
Sympathetic			10	50	<100	Particle	100	14	6
Split Casing			1	100	100	Neat	10,000	0.03	7
Corrosion-P			88	100	100	Pinhole	1×10^{10}	2×10^{-6}	8
Buried UXO		95							4
Sympathetic			1	50	<100	Particle	100	26	6
Split Casing			1	100	100	Neat	10,000	0.5	7
Corrosion-N			1	100	100	Neat	10,000	0.5	8
Corrosion-P			97	100	100	Pinhole	1×10^{10}	5×10^{-5}	8

1. Live-fire high-order probability is 100% minus sum of live-fire low-order and dud rates.
2. Live-fire low-order probability is weighted average (by HE mass) of LO rates determined by Dauphin and Doyle (2000). It could underestimate LO probability for untrained gun crews or impacts onto hard soils/rock where duds might detonate at low order.
3. Dud rate is weighted average (by HE mass) of dud rates determined by Dauphin and Doyle (2000). Anecdotal evidence suggests that it underestimates dud rates for untrained gun crews.
4. Probabilities for surface and buried UXO estimated from UXO database of 11 closed and cleared training ranges.
5. No uniform Army policy exists to clear UXO on active ranges. Surface UXO are blown along routes used to place or move targets; HO and LO probabilities reflect consensus that most BIP operations produce HO detonations. Few, if any, buried UXO are blown in place.
6. Probabilities for sympathetic detonations are highly uncertain. A 10% probability indicates that one surface UXO will detonate sympathetically for every ~300 live-fire detonations on the range. The estimated 1% probability for buried UXO reflects likely buffering effect of the soil.
7. Split casing UXO offer essentially no impediment to flow. Its probability is highly uncertain. We chose 1% based on anecdotal evidence that split casings occur but are rare.
8. Corrosion probabilities are 100% minus sum of other UXO fates. Dissolution of HE at the pinhole rate is extremely slow and the results here ignore the time delay for pinhole corrosion to occur. Eventually sufficient corrosion will occur that the much higher neat dissolution rate will prevail. The estimated 1% probability acknowledges that some buried UXO are already fully corroded. This probability will increase with time as UXO continue to corrode.

Here, we estimate the probability of each fate and the resulting consequences in terms of dissolved HE influx to the soil. Table 14 summarizes the data used and results obtained for the most significant munitions used on Army training ranges. Because of large uncertainties in many estimates, separating the results by munition type is not warranted at this time. The following sections include attempts to justify the model inputs and they show the overall results obtained.

8.1 Model Parameters

8.1.1 Most Significant Munitions

Table 2 lists the most commonly used munitions and their production numbers over time. By far, most of the munitions listed were manufactured after WWII, roughly a 50-year time span. We calculated the total potential HE available from UXO for each family of rounds based on dud rates estimated by Dauphin and Doyle (2000) and assuming that 80% of the rounds manufactured were used for training (Table 15). The 80% estimate is based on the percentage of artillery rounds used in training to those produced in 2003 (Delaney and Etter 2003). In peacetime similar numbers of munitions are used as are produced (although older munitions are used) to avoid stockpiling items. The average dud rate for all rounds studied by Dauphin and Doyle (2000) was 3.45%. For all HE rounds it was 3.37%. For all howitzer and mortar rounds it was 3.75 and 2.91%, respectively. For all gun-fired grenades, it was 1.78%.

Table 14. Dud rates for different munitions (from Dauphin and Doyle 2000, 2001).

Munition	Type	DODIC number	Production (millions)	HE Load (kg)	Energetics type	Dud rates (%)				
						Avg.	App. B	For size	HE type	Family
40-mm HE										
Gun	HE-T, SD	B562	1.1	0.063	TNT or Tetryl	3.45	0.0	1.37	3.37	1.78
Grenade/Gun	M383	B571	4.0	0.055	Comp A5 (RDX)	3.45	0.3	1.37	3.37	1.78
Grenade/Gun	M384	B470	17.0	0.055	Comp A5 (RDX)	3.45	5.3	1.37	3.37	1.78
Grenade	M397	B569	1.4	0.032	Octal	3.45	0.8	1.37	3.37	1.78
Grenade	M406	B568	39.0	0.032	Comp B	3.45	1.5	1.37	3.37	1.78
Gun	DP M430	B542	18.0	0.038	Comp A5 (RDX)	3.45	0.3	1.37	3.37	1.78
Grenade	DP M433	B546	23.0	0.045	Comp A5 (RDX)	3.45	1.1	1.37	3.37	1.78
			103.5	0.046						

Munition	Type	DODIC number	Production (millions)	HE Load (kg)	Energetics type	Dud rates (%)				
						Avg.	App. B	For size	HE type	Fam-ily
60-mm HE										
Mortar	M49A4	B632	1.9	0.190	TNT or Comp B	3.45	3.3	2.34	3.37	2.91
Mortar	M720	B642	1.2	0.191	Comp B	3.45	1.1	2.34	3.37	2.91
Mortar	M888	B643	3.0	0.358	Comp B	3.45	1.9	2.34	3.37	2.91
			6.1	0.246						
81-mm HE										
Mortar	M43A1	C225	6.0	0.585	Comp B	3.45	3.9	2.33	3.37	2.91
Mortar	M362	C222	4.0	0.953	Comp B	3.45	1.6	2.33	3.37	2.91
Mortar	M362	C223	1.3	0.953	Comp B	3.45	1.6	2.33	3.37	2.91
Mortar	M374	C236	2.3	0.953	Comp B	3.45	1.3	2.33	3.37	2.91
Mortar	M374A3	C256	40.8	0.953	Comp B	3.45	2.4	2.33	3.37	2.91
Mortar	M821A1	C868	1.0	0.726	RDX / TNT	3.45	1.7	2.33	3.37	2.91
Mortar	M889	C869	1.4	0.726	RDX / TNT	3.45	2.4	2.33	3.37	2.91
			56.8	0.836						
105-mm HE										
Howitzer	M1	C444	2.1	2.3 / 2.177	Comp B or TNT	3.45	9.6	4.65	3.37	3.75
Howitzer	M1	C445	20.0	2.3 / 2.177	Comp B or TNT	3.45	4.4	4.65	3.37	3.75
Howitzer	M1	C443	0.6	2.3 / 2.177	Comp B or TNT	3.45		4.65	3.37	3.75
			22.7	2.239						
4.2-in. HE										
Mortar	M329A2	C697	1.3	2.610	Comp B	3.45	2.2	5.13	3.37	2.91
Mortar		C699	1.0	2.610		3.45	2.2	5.13	3.37	2.91
Mortar	M329A1	C704	0.4	3.377	TNT	3.45	10.7	5.13	3.37	2.91
Mortar		C705	1.2	3.377	TNT	3.45	10.7	5.13	3.37	2.91
			3.9	2.994						
120-mm HE										
Mortar	M933	C623	0.4	2.990	Comp B	3.45			3.37	2.91
Mortar	M934A1	C379	0.2	2.990	Comp B	3.45			3.37	2.91
			0.6	2.990						
155-mm HE										
Howitzer	M1918		0.7					2.26	3.37	3.75
Howitzer	M107	D544	6.4	6.622/6.985	TNT / Comp B	3.45	2.8	2.26	3.37	3.75
Howitzer	RA M549	D579	1.1	6.940/7.257	TNT / Comp B	3.45	0.0	2.26	3.37	3.75
Howitzer	M795	D529	0.3	10.795	TNT	3.45		2.26	3.37	3.75
			7.8	8.232						

Munition	Type	DODIC number	Production (millions)	HE Load (kg)	Energetics type	Dud rates (%) Avg.	App. B	For size	HE type	Fam-ily
8-in. HE										
Howitzer	M106	D680	11.5	16.465/17.599	TNT / Comp B	3.45	2.2	0.99	3.37	3.75
Howitzer	RA M650	D624	0.3	11.300	TNT	3.45	0.2	0.99	3.37	3.75
			11.8	14.166						

*Potential residue calculation: Assumed that 80% of rounds manufactured were used for practice on ranges. Dud rates were not available for 120-mm mortars.

Table 14 (cont'd).

Munition	Potential residue (kg) Avg.	App. B	Size	HE type	Family	Number of rounds	Tested/ manf. ratio (%)
40-mm HE							
Gun	1,913		760	1,868	987	82	0.007
Grenade/Gun	6,017	488	2,389	5,877	3,104	360	0.009
Grenade/Gun	25,571	39,506	10,154	24,978	13,193	563	0.003
Grenade	1,244	303	494	1,215	642	474	0.034
Grenade	34,660	15,371	13,764	33,856	17,883	2,546	0.007
Gun	18,878	1,860	7,497	18,441	9,740	5,363	0.030
Grenade	28,566	9,108	11,344	27,904	14,738	4,084	0.018
	116,850	66,637	46,401	114,140	60,288	13,472	0.013
60-mm HE							
Mortar	9,964	9,588	6,758	9,733	8,404	7,792	0.410
Mortar	6,326	1,962	4,291	6,179	5,336	3,838	0.320
Mortar	29,642	16,668	20,105	28,955	25,003	2,112	0.070
	45,932	28,219	31,154	44,867	38,743	13,742	0.225
81-mm HE							
Mortar	96,876	109,512	65,426	94,630	81,713	1,998	0.033
Mortar	105,211	47,574	71,056	102,772	88,743	367	0.009
Mortar	34,194	15,461	23,093	33,401	28,842	-	-
Mortar	60,496	22,620	40,857	59,094	51,027	1,633	0.071
Mortar	1,073,154	730,989	724,768	1,048,270	905,182	7,489	0.018
Mortar	20,038	9,816	13,533	19,573	16,901	3,491	0.349
Mortar	28,053	19,515	18,946	27,402	23,662	1,457	0.104
	1,418,022	955,487	957,678	1,385,140	1,196,071	16,435	0.029

Munition	Potential residue (kg) Avg.	App. B	Size	HE type	Family	Number of rounds	Tested/ manf. ratio (%)
105-mm HE							
Howitzer	133,308	360,273	174,872	126,735	141,026	2,045	0.097
Howitzer	1,269,600	1,572,322	1,665,444	1,206,999	1,343,100	10,003	0.050
Howitzer	38,088		49,963	36,210	40,293		0.000
	1,440,996	1,932,596	1,890,279	1,369,944	1,524,419	12,048	0.053
4.2-in. HE							
Mortar	93,647	60,803	139,249	91,475	78,989	1,518	0.066
Mortar	72,036	46,771	107,114	70,366	60,761		0.000
Mortar	37,282	116,061	55,437	36,418	31,447	6,386	0.399
Mortar	111,846	348,182	166,310	109,253	94,340		0.000
		571,817	468,110	307,511	265,536	7,904	0.203
120-mm HE							
Mortar	33,010			32,244	27,843		0.000
Mortar	16,505			16,122	13,921		0.000
	49,514			48,366	41,764		
155-mm HE							
Howitzer							
Howitzer	1,201,770	968,383	787,247	1,173,903	1,306,272	6,216	0.097
Howitzer	206,554		141,205	210,558	73,219	1,152	0.105
Howitzer	56,333		58,552	87,310	30,361		0.000
	1,464,657	968,383	987,003	1,471,771	1,409,852	7,368	0.094
8-in. HE							
Howitzer	5,395,800	3,494,285	1,548,360	5,270,680	5,865,000	403	0.004
Howitzer	140,760	4,882	40,392	91,394	101,700	571	0.190
	5,536,560	3,499,167	1,588,752	5,362,074	5,966,700	974.00	0.008

These calculations suggest that five types of rounds, termed the most significant, will contribute most of the HE to the soil and groundwater: 81-mm and 4.2-in. mortars and 105-mm, 155-mm, and 8-in. howitzers. Other rounds that may be worth considering are 60-mm and 120-mm mortars, primarily because of the method of firing. They impact at a near vertical angle to the ground and if they do not detonate they would be likely to penetrate the soil. However, the combined release from these rounds would not add up to the potential contamination from any of the most significant rounds.

8.1.2 Training Use Rates

Detailed records on training use of munitions are almost nonexistent. For modeling, we will assume that 80% of the most significant munitions manufactured over the period since WWII were fired on training ranges and that they were fired at a uniform rate of $1/50^{th}$ per year. Annual use rates limit contamination by fates that quickly release HE (e.g., HO detonations) whereas processes that slowly release HE (e.g., corrosive perforation) can operate on the entire mass of HE used over the 50-year period.

8.1.3 Detonation Rates

Dauphin and Doyle (2000) estimated HO, LO, and dud rates for the most commonly used munitions from the ASRP data (Table 3). Dauphin and Doyle make a strong argument that these data are the best available for approximating training use, and we use their results here. However, they probably underestimate LO and dud rates for reasons mentioned earlier (training involves inexperienced gun crews; duds become LO detonations for impacts onto hard soils and rocks).

For the most significant munitions, ASRP-based LO rates range from 10^{-1} to 10^{-2}% and dud rates from 2 to 6% (Table 3). Note that the ASRP tests included too few firings of 8-in. howitzer rounds for reliable LO estimates. For the five munitions of interest, the average dud and LO rates, weighted by the total HE mass produced for each type, are 3 and 6×10^{-2}%, respectively.

8.1.4 HE Releases from High- and Low-Order Detonations, Live-Fire, and Blow-in-Place

Field experiments characterizing HE releases from individual detonations (see Section 6.2) allow us to estimate amounts and sizes of HE particles released for each type of detonation for use in our model.

Hewitt et al. (2003) summarize measurements of the residues recovered from live-fire (tactically detonated) and blow-in-place operations for a variety of munitions. For live-fired 60-, 81-, 120-mm mortar rounds and 105-mm howitzer rounds, the recovered residues range from about 10^{-5} to 10^{-3}% of the original HE mass in the round. The residues were recovered by sampling about 1% of the area of soot footprints on clean snow made by the detonations. Larger but more rare HE particles scattered beyond the plume or not falling within the sampled areas would not be included in these estimates. For these reasons, we use here the upper value of 10^{-3}% to approximate the proportion of HE residue released from a HO live-fire detonation.

Similarly sampled high-order blow-in-place detonations of 81-mm mortar and 155-mm howitzer rounds yielded average HE releases of 10^{-3} and 3×10^{-1}%, respectively. Interestingly, one of the seven 155-mm tests yielded percent-level concentrations of TNT, yet was classified by EOD personnel as a HO detonation. The BIP method uses C4 charges attached to the side of a round. Because this does not trigger the designed detonation sequence, it is reasonable that higher HE releases occur for BIP than for live-fire HO detonations. Thus, we use the higher value of 3×10^{-1}% to approximate the proportion of HE released from a high-order BIP detonation.

Taylor et al. (2004a,b) collected the HE residue from low-order BIP detonations of 81-mm mortar and 155-mm howitzer rounds. The results indicated that 20 to 80% of the HE charge was scattered. Air blast measurements produced a similar yield estimate (Pennington et al. 2003). These tests were specifically conducted to produce LO detonations and did not reflect EOD best practice for BIP operations. No measurements have yet been made on the HE releases from LO live-fire detonations, in part because these occur infrequently. Because the design detonation sequence does not occur for either live-fire or BIP low-order detonations, it seems likely that the releases would cover a similar range for both cases. Thus, we will crudely estimate that 50% of the HE charge is released from a low-order detonation (either live-fire or BIP).

Taylor et al. (2004a,b) also measured the size, mass, and area distributions of the HE particles recovered after BIP high-order and low-order detonations of 81-mm mortar and 155-mm howitzer rounds. For a BIP detonation with 2% HE released, most of the released mass consisted of particles smaller than a few millimeters. High-order detonations with lower release levels, such as those measured for live-fire detonations, would presumably produce much smaller particles. Conversely, for low-order detonations with 20 to 40% HE release, most of the released mass consisted of particles larger than a few millimeters, though chunks of HE measuring a few centimeters across were also recovered (see Fig. 22 and 23).

Of concern is whether a significant fraction of live-fire HO detonations yield percent-level HE releases. Measurements on snow have not revealed such high releases (Hewitt et al. 2003). However, a few widely scattered millimeter-sized particles could easily escape collection and significantly affect the measured releases. The estimated HE deposited from HO live-fire detonations would double if as few as one-in-1000 of these detonations produced percent-level releases. The few rounds sampled thus far would be unlikely to detect such an effect.

8.1.5 UXO Fates

The eventual release of HE from a dud depends strongly on its fate (Fig. 27). Unfortunately, statistics on the fates of duds are difficult to obtain. Consequently, many of the fate probabilities used here are order-of-magnitude estimates based on limited data or subjective reasoning; they necessarily include large uncertainties. For now, they serve to indicate the relative significance of the fates of UXO and which fates warrant more detailed investigation.

Dud rounds may either penetrate into the soil or remain on the surface, depending on the type of round, its impact velocity and angle, and the soil conditions. Data on the burial depths of 7299 UXO that had been fired into 11 different impact areas (UXO database) indicate that about 5% of duds remain on the surface weighted by the total masses of HE for the five most significant munitions (see Fig. 7). We will use this value as an approximation for all locations and munitions. This is roughly consistent with the value determined for the MMR HUTA (4/116 = 3%, see Section 4.23).

Whether on the surface or buried, one of five fates might befall a UXO: blow-in-place detonation (HO or LO), sympathetic detonation from a nearby explosion of a round, splitting of the shell casing, or corrosive perforation of the shell casing (Fig. 27). We list these roughly in order of increasing time scale for the release of the HE charge in the UXO. Because sympathetic detonations are triggered by uncontrolled processes, which bypass the rounds' detonation chain (a shock wave or frag. impact), we assume they would produce low-order detonations and scatter HE particles similar to BIP low-order detonations. For the split-casing and corrosive-perforation cases, we assume the HE charges remain intact. Note that the relative proportions for each fate vary depending on whether the UXO lies on the surface or is buried.

Surface UXO. The Army has no standard policy to blow UXO for range maintenance. The only routine BIP operations are those used to clear access roads to targets. We therefore estimate that only 1% of surface UXO are blown in place. We further assume that 90% of these operations produce HO detonations and 10% produce LO detonations (to allow for poor access to the round or a malfunctioning C4 charge). At MMR, two of the four surface UXO had split casings. This proportion is high compared with anecdotal evidence that suggests split-casing UXO are rare. We, therefore, use 1% as our order-of-magnitude estimate. Any estimate of the probability of sympathetic detonations is also highly uncertain because little direct evidence remains and LO live-fire detonations produce similar debris. At a 10% level, one sympathetic detonation would occur for every ~300 HO live-fire detonations. We use this as our order-of-magnitude estimate

for sympathetically detonated surface UXO. The remaining surface UXO (88%) undergo long-term corrosion.

Buried UXO. We know of no routine BIP operations to clear buried UXO, and we, therefore, assign zero probability to that fate. As with surface UXO, we assume 1% of the buried UXO have split casings. This is consistent with the data from the MMR HUTA, where 1 of the 112 buried UXO had split casings. It also appears that three of the buried rounds had detonated sympathetically because they looked like LO detonations but were at least 0.25 m below the surface. This high-use area should experience higher-than average sympathetic detonations rates. Therefore, we estimate that 1% of all buried UXO undergo sympathetic detonation on average. At a 1% level, one sympathetic detonation would occur for every ~3000 HO live-fire detonations. The remaining rounds eventually experience corrosive perforation. Some UXO have been corroding for decades, so that some proportion could already be quite permeable to water flow. For example, corrosion rates of 0.1 mm/yr are possible in aerated or saline soils and 1.5 mm/yr in flooded soils (see Table 6). In such locations, complete corrosion of UXO casings could occur within 10–100 years. We, therefore, use 1% as our order-of-magnitude estimate for currently buried UXO that are fully permeable to flow and consequently undergoing neat dissolution. The remaining 97% are developing pinhole perforations and at most are leaking HE at the pinhole rate. We use two fates for corroding buried UXO because the applicable dissolution rates are vastly different.

Clearly, the uncertainty in all of these estimates could be reduced with further study. EOD records could form the basis for improved estimates of BIP rates and the proportion of HO and LO outcomes. Likewise, estimates for sympathetic detonations could be based on observations or derived from UXO areal densities and crater diameters from HO live-fire rounds. Similarly, case-splitting rates could be obtained from data on recovered UXO or models similar to those used to estimate UXO penetration depths. Also, the condition of corroded UXO could be more thoroughly investigated to assess the proportion that is essentially impermeable to water flow. All such efforts, however, are beyond the scope of this work.

8.1.6 Dissolution Times for each Munition Fate

The time estimates for dissolution of HE particles, based on available information, vary significantly (Table 13). Nevertheless, we may make order-of-magnitude estimates that pertain to the fates of munitions fired on training ranges (Table 14). Note that if the dissolution time, τ, for a given fate is less than 50 years (the assumed period of training use), then the annual occurrence rate for

that fate governs its contribution to present-day dissolved HE flux. For example, if τ = 10 years, only 10 years of munitions experiencing that fate will be present, and each year's mass will dissolve by $1/10^{th}$. Conversely, if τ is greater than 50 years, present-day dissolution will operate on the total mass contributed by that fate, M_f. The present-day dissolved HE flux will thus be M_f/τ.

Particles scattered on the surface by live-fire high-order detonations (where most of the mass consists of particles << 1 mm) should dissolve within a year. Blow-in-place HO detonations produce larger particles (up to a few millimeters) but these should dissolve in less than 50 years. Thus, for both types of HO detonations, their annual occurrence rates govern their contribution to training-range dissolved HE flux.

The dissolution time for particles scattered on the surface by low-order detonations (live-fire or BIP) is more uncertain. Most of the scattered mass consists of particles smaller than a few centimeters. Simple dissolution could require hundreds of years, but the particles are friable and likely to break apart under the action of weathering and mechanical agitation from subsequent detonations. We will therefore use τ = 100 years as an estimate for particles from all LO detonations (live-fire, surface BIP, and buried BIP). We will also use this value for mass scattered by sympathetic detonations of UXO (surface or buried) because these detonations are probably low order.

We assume that a split-shell UXO has its entire HE charge exposed to dissolution. Clearly, the degree of damage to the casing will influence its role in impeding water flow. However, corrosion of the casing will probably accelerate, so the impediment to flow will likely be temporary. For simplicity, we assume that if the split-shell UXO is buried, the shell does not impede dissolution by advection, and, thus, the HE mass will undergo "neat" dissolution with τ = 10,000 years. On the surface, such a round might not be fully wetted. Nevertheless, we will assume that it also undergoes dissolution at the neat rate. These assumptions probably cause our results to over-estimate somewhat the contribution of HE contamination from split-shell UXO.

Intact UXO, either surface or buried, will not begin to release HE until corrosion perforates the shell casing. This process can take decades to centuries. Buried UXO would then undergo pinhole dissolution as modeled by Matyskiela (2003). The dissolution rate is about 10^{-7} times smaller than the neat rate based on annual average rainfall rate; that is $\tau \sim 10^{10}$ years for pinhole dissolution. For a surface UXO with a pinhole perforation, water might not completely saturate the HE-to-casing gap, and dissolution would be slower than the pinhole rate. To be conservative, we will neglect the time needed for pinhole corrosion and assume that present-day surface intact UXO and most buried intact UXO release

HE at the pinhole dissolution rate. For UXO buried, we have assumed that a small proportion (1%) of shell casings might already be fully permeable to water flow. For this fate we assume that the much shorter neat dissolution time applies (τ = 10,000 yr).

8.2 Estimated Dissolved HE Flux

Table 14 summarizes our model estimates for the relative contribution of each munition fate to annual dissolved HE on training ranges. These results must be treated cautiously owing to the high uncertainties in many input parameters.

Generally, detonations that release explosives at percent levels as particles will deliver significant fluxes of dissolved HE to the soil. This includes LO live-fire and sympathetic detonations of surface and buried UXO. Also, HO live-fire produces a fairly significant HE flux, despite the low mass released per round, because it's by far the most common fate. Neat dissolution of buried UXO, with split or fully corroded casings, collectively contribute about 1% of the annual dissolved HE.

The model predicts a total HE dissolved flux of ~ 10^3 kg/yr for all training use of munitions. About 60% of this flux is from live-fire, primarily LO, detonations (Fig. 28). UXO of all fates account for the other 40%, most of which derives from sympathetic detonations of surface and buried UXO. The importance of sympathetic detonations hinges on the highly uncertain assumptions that 10% of the surface and 1% of the buried UXO will detonate sympathetically from nearby live-fire detonations. These probabilities correspond to ratios of 1:300 and 1:3000 sympathetic detonations to HO live-fire detonations.

Not surprisingly, the model indicates that the flux of HE released through pinhole corrosion of UXO is insignificant compared with other fates, even neglecting the time needed for corrosion to produce a pinhole perforation. This is because dissolution at the pinhole rate is extremely slow. However, for soils where corrosion removes the casing as an impediment to water flow, the neat dissolution rate will prevail, and it is 10^6 times higher. Figure 28 illustrates the relative HE contamination if 1% of the buried UXO are dissolving at the neat rate. However, if 10% of buried UXO are sufficiently corroded to allow dissolution at the neat rate, their dissolved HE flux will exceed that produced by live fire HO detonations (Fig. 29). Furthermore, because the neat dissolution rate increases strongly with decreasing particle size, nearby detonations that cause HE blocks to fragment (but not detonate) will significantly increase the contribution of this fate.

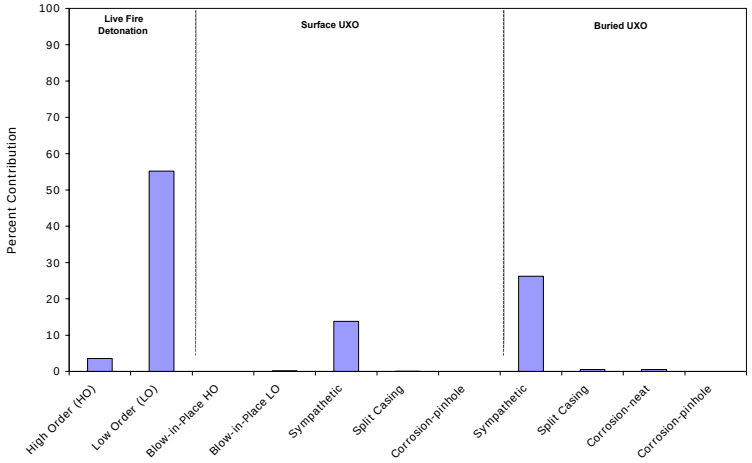

Figure 28. Estimated contamination rate by fate of the munition. Here 1% of the UXO are fully corroded and undergoing neat dissolution.

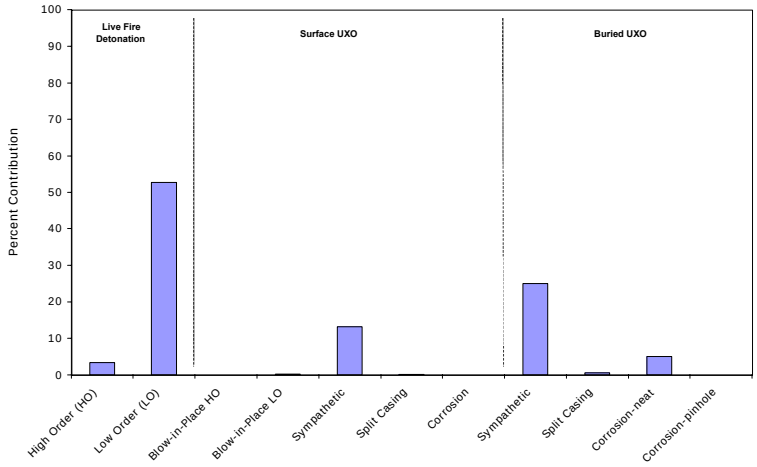

Figure 29. Estimated contamination rate by fate of the munition with 10% fully corroded and undergoing neat dissolution.

Clearly, corrosion will steadily increase the proportion of existing UXO with fully corroded casings and, thus, will increase the dissolved HE flux from this fate. Furthermore, whenever training ranges are no longer subject to live fire (e.g., BRAC, range abandonment), particulate HE will not be replenished as it dissolves, and dissolution of corroded UXO will grow in importance with time;

eventually, it will predominate the dissolved HE flux. That is, the low present-day ranking of corroding UXO as contaminant sources does not imply that UXO should remain in the ground indefinitely to corrode. It simply means that compared with on-going detonations, corroding UXO are only a small contribution to the overall dissolved HE flux.

The model necessarily approximates many processes, and the results will change depending on the parameters chosen. Insofar as possible, we have tried to justify our choices. Listed here are the most significant uncertainties associated with the model:

- The ASRP data (Dauphin and Doyle 2000) may underestimate the dud and low-order probabilities for munitions fired during training by inexperienced crews. Also, impacts into hard soils or rock on training ranges could trigger LO detonations from what would otherwise be dud rounds. Because HO detonations produce much lower dissolved HE flux, any increase in dud or LO probabilities is significant.
- High-order detonations would increase in significance if current measures of HE mass-release omit scarce millimeter-sized particles thrown outside the soot plume or area sampled. Also, the ASRP test firings are classified as high order by sound and the absence of LO debris. Detonations that produce yields greater than 90% would probably be classified as high order yet would scatter percent-level explosives as fine particles. The small number of high-order live-fire rounds sampled to date for HE residues would be unlikely to have captured this effect, if it occurs. Because live-fire HO detonation is the most likely fate, any increase in the mass released by these detonations would be significant.
- The proportion of UXO likely to detonate sympathetically is unknown at this time. We chose probabilities of 1% for buried UXO and 10% for surface UXO, and the model then ranks these fates as the second and third highest contributors to dissolved HE flux. These results highlight the potential importance of sympathetic detonations and the need to quantify their probabilities more reliably.
- Time scales for HE particle dissolution are uncertain and more work is needed to constrain them. In addition, the action of weather and mechanical agitation to break large particles into small ones needs investigation because the resulting small particles dissolve quickly. This includes the effect of nearby detonations that could fragment an HE block (even without causing sympathetic detonation).
- Buried UXO with split casings are potentially important sources of dissolved HE flux. We chose a 1% probability for both surface and buried

UXO. Whether this number is a good national average is uncertain. Also, our definition implies that the split casing offers no impediment to flow. We do not know whether this definition is consistent with that used to categorize inspected UXO. However, a damaged casing should corrode open rapidly and consequently become consistent with our definition within a short time. Because corrosion of an intact casing is so slow, some effort is warranted to quantify numbers and types of split casings and the rates at which they corrode.

- The proportion of buried UXO that is fully corroded is highly uncertain. In this context, fully corroded implies that the casing does not significantly impede water flow, and the HE fill dissolves at the neat rate. We used 1% as an order-of-magnitude estimate for this fate, but regardless of its current value, the importance of this fate will increase with time as older UXO more fully corrode.
- The model used here does not account separately for TNT and Comp B (i.e., RXD and TNT) rounds. However, only RDX is found in appreciable quantities in groundwater because it does not readily break down. Our HE flux estimates should not be used to estimate RDX input unless they are corrected for the relative proportion of TNT- and Comp B-filled rounds.
- The model input parameters are estimates based on average conditions across all Army training ranges. Local variations could be significant owing to soil types, rainfall rates, munitions fired, training practices, etc.

9 SUMMARY

A fired munition can suffer one of many fates. Using data on the relative rates of the different outcomes suggests that various types of LO detonations (live fire and sympathetic detonations), where a significant amount of the explosive filler is released, are the largest contributors to dissolved HE flux on training ranges. Also, HO live-fire produces a fairly significant HE flux, despite the low mass released per round, because it is by far the most common fate. The significance of neat dissolution from fully corroded rounds will increase with time and, when about 10% of the current UXO corrode to the point where they are permeable to water flow, UXO will rival HO detonations as a source of dissolved HE flux. At present, however, the available information on corrosion rates, measured leak rates of corroded ordnance, and the dissolution rates for bulk explosive masses suggest that UXO are not currently a source of widespread HE flux on our ranges.

We find that corrosion of low-carbon steel, the most commonly used steel in UXO, probably occurs at about 0.025 mm per year. Interestingly, variations in corrosion rate attributable to soil conditions and the casing alloy are within a factor of 5. This suggests that most UXO, which have a minimum wall thickness between 2 and 10 mm, will corrode within 80 to 400 years in aerated soils. Under reducing conditions similar to those encountered in wetlands and other anaerobic and flooded environments, sulfide production accelerates corrosion by about a factor of 10 (with considerable variability), resulting in perforation of the round after approximately 10–40 years. Pit corrosion is also common in soil environments and results in deep, small perforations that leak HE at a very slow, pinhole rate. An intriguing possibility is that the reactive intermediates formed during metal corrosion may facilitate the degradation of RDX, TNT, and other explosives as they leak from the UXO casing. More work is warranted in this area, although the first-order questions of the number, type, and distribution of UXO at ranges need to be addressed before these secondary effects can be quantified.

Future studies would benefit from accurate, long-term range firing records. Such records could be obtained if the Army developed and implemented an easy to use method for recording, transferring, and saving firing records. Possibly seismic arrays, acoustic sensors, or other methods could be developed to automatically keep track of the number of rounds fired and their fate. Currently, only order-of-magnitude estimates of HE release are possible owing to a lack of information on the number and actual fates experienced by different types of fired munitions.

Currently, LO detonations appear to be the main source of HE release on training ranges. Therefore, any action that decreases the rate of LO detonations, either live fire or sympathetic, is important, for example, improving the reliability of munitions and fuzes, incorporating tags into rounds so that duds and LO can be found, and removing low-order rounds while their positions are known and before their HE is scattered by subsequent detonations.

Because all UXO will eventually corrode if left in place and release their contents into the ground, it is advisable to 1) remove as many UXO as possible before they perforate, and 2) minimize the number of new UXO. This is especially important for ranges overlying important aquifers or where soil conditions are known to accelerate corrosion (wetlands). Priority items would be those that contain a lot of HE or those that contain explosives known to migrate to the groundwater (primarily RDX).

It is preferable to destroy all movable UXO in a blast chamber where the residues are contained. The residues from the blast chamber along with any chunk explosives found on the range could then be destroyed in a non- contaminating manner, such as dissolution followed by chemical or thermal destruction (e.g., Thorne 2003). If some rounds have to be blown-in-place, techniques that produce a high-order detonations are preferable. Also an alternative to C4, which is mostly RDX and does not always fully detonate, could be considered. Its replacement with a non-contaminating explosive that is highly efficient in producing high-order detonations would decrease the release of RDX.

Because each installation is unique, range management and practices could be tailored to sustain training activities and avoid offsite contamination given the ranges' geologic and climactic setting. For example inert rounds could be used for training on ranges that have high rainfall and shallow water tables and HE rounds reserved for ranges where the transport of HE to groundwater is slow (low rainfall, deep groundwater table). Good stewardship of the training lands improves the Army's relationship with residents living near the installations, extends the life of the ranges, and lowers costs if and when the installation is closed.

REFERENCES

Adams, J.B. (2001) Modeling the corrosion rate of unexploded ordnances. Session 48, *Geological Society of America Annual Meeting, 5–9 November 2001*.

Adams, J.B. (1999) Unexploded ordnance recovery depth database. Abstract in *UXO Forum*.

Adley, M.D, R.P. Berger, J.D. Cargile, H.G. White, and D.C. Creighton (1997) Three-dimensional projectile penetration into curvilinear geologic / structural target: User's guide for PENCRV3D. U.S. Army Waterways Experiment Station, Vicksburg, Mississippi.

AMEX (in review) Link between military training activities and grounwater contamination of propellant, explosive, and pyrotechnic (PEP) compounds. USACE Report MMR-6810, pp. 1–165.

Ampleman G., S. Thiboutot, S. Désilets, A. Gagnon, and A. Marois (2000) Evaluation of the soils contaminated by explosives at CFB Chilliwack and CFAD Rocky Point. DREV Report TR-2000-102.

Ampleman G., S. Thiboutot, J. Lewis, A. Marois, A. Gagnon, M. Bouchard, R. Martel, R. Lefebvre, C. Gauthier, J.M Ballard, T.A. Ranney , T.F. Jenkins, and J. Pennington (2003a) Evaluation of the impacts of live fire training at CFB Shilo. Final Report. Defense R&D Canada—Valcartier, TR 2003-066.

Ampleman G., S. Thiboutot, J. Lewis, A. Marois, A. Gagnon, M. Gagnon, S. Jean, T.F. Jenkins, A. Hewitt, J. Pennington, and T.A. Ranney (2003b) Evaluation of the contamination by explosives in soils, biomass and surface water at Cold Lake Air Weapons Range (CLAWR), Alberta. Phase I Report, Defense Research Establishment, Department of National Defense, Canada.

Arshed, M., M. Anwarulislam, M. Siddique, and N.M. Butt (1993) Study of the corrosion of mild-steel due to prolonged immersion in deionized water. *Journal of Radioanalytical and Nuclear Chemistry-Letters*, **175**(6): 467–472.

Arshed, M., N.M. Butt, M. Siddique, and M. Anwarulislam (1992) Study of corrosion of ss-304 exposed to sea-water. *Journal of Radioanalytical and Nuclear Chemistry-Letters*, **165**(2): 107–113.

Booth, G.H., and A.K. Tiller (1968) Cathodic characteristics of mild steel in suspensions of sulphate-reducing bacteria. *Corrosion Science*, **8**(8): 583.

Bucci, J.E., and P. F. Buckley (1998) Modeling the degradation of unexploded ordnance (UXO) and its use as a tool in the development of risk assessments. (https://www.denix.osd.mil/denix/Public/News/OSD/UXO/Conferences/Forum/Bucci.pdf)

Buttle, J.M. (1994) Isotope hydrograph separations and rapid delivery of pre-event water from drainage basins. *Progress in Physical Geography*, **18**: 16–41.

California Department of Transportation (1999) Method for estimating the service life of steel culverts. California Test Method 643. Engineering Service Center, California Department of Transportation, Sacramento.

Clausen J, J. Robb, D. Curry and N. Korte (2004) A case study of contaminants in military ranges: Camp Edwards, Massachusetts, USA. *Environmental Pollution*, **129**: 13–21.

Collins, C.M., and D.J. Calkins (1995) Winter tests of artillery firing into Eagle River Flats, Fort Richardson, Alaska. U.S. Army Cold Regions Research and Engineering Laboratory, Special Report 95-2.

Craig, B.D. (ed.) (1989) *Handbook of Corrosion Data*. Metals Park, Ohio: ASM International.

Crull, M., L. Taylor, and J. Tipton (1999) Estimating ordnance penetration into earth. *UXO/Countermine Forum*. Atlanta, Georgia.

Darrach, M.R., A. Chutjian, and G.A. Plett (1998) Trace explosive signatures from World War II unexploded undersea ordnance. *Environmental Science and Technology*, **32**: 1354–1358.

Dauphin, L., and C. Doyle (2000) Study of ammunition dud and low order detonation rates. U.S. Army Defense Ammunition Center—Technical Center for Explosives Safety. Technical Report written for U.S. Army Environmental Center, Aberdeen Proving Ground, Maryland.

Dauphin, L., and C. Doyle (2001) Phase II study of ammunition dud and low order rates. U.S. Army Defense Ammunition Center—Technical Center for Explosives Safety. Technical Report written for U.S. Army Environmental Center, Aberdeen Proving Ground, Maryland.

Davalos, J., J.F. Marco, M. Gracia, and J.R. Gancedo (1991) The corrosion products of weathering steel and pure iron in simulated wet-dry cycles. *Hyperfine Interactions*, **66**(1–4): 63–70.

Delaney W.P., and D. Etter (2003) *Unexploded Ordnance (UXO).* Report of the Defense Science Board Task Force, Office of the Under Secretary of Defense for Acquisition, Technology and Logistics, Washington DC. http://www.acq.osd.mil/dsb/uxo.pdf

Department of Commerce (1968) *Climatic Atlas of the United States*.

Doyle, G., M.V. Seica, and M.W.F. Grabinsky (2003) The role of soil in the external corrosion of cast iron water mains in Toronto, Canada. *Canadian Geotechnical Journal*, **40**(2): 225–236.

Drissi S.H., P. Refait, M. Abdelmoula, and J.M.R. Genin (1995) The preparation and thermodynamic properties of Fe(II)-Fe(III) hydroxide-carbonate (green-rust-1) - pourbaix diagram of iron in carbonate-containing aqueous-media. *Corrosion Science*, **37**(12): 2025–2041.

Dube P., G. Ampleman, S. Thiboutot, A. Gagnon, and A. Marois (1999) Characterization of potentially explosives-contaminated sites at CFB Gagetown, 14 Wing Greenwood and CFAD Bedford. Defense Research Establishment, Valcartier, Quebec, DREV-TR-1999-137.

Edyvean, R.G.J., and H.A. Videla (1991) Biological corrosion. *Interdisciplinary Science Reviews*, **16**(3): 267–282.

Fabian, G.L., and S. Ostazeski (2002) Corrosion of unexploded ordnance (final report). U.S. Army Environmental Center Report SFIM-AEC-PC-CR-2002041.

Foster, J. (1998) Report of the Defense Science Board Task Force on Unexploded Ordnance (UXO) Clearance, Active Range UXO Clearance, and Explosive Ordnance Disposal (EOD) Programs.

Frankel, G.S. (1998) Pitting corrosion of metals—A review of the critical factors. *Journal of the Electrochemical Society*, **145**(6): 2186–2198.

Fry, M.A., R.E. Durrett, G.P. Ganong, D.A. Matuska, and M.D. Stucker (1976) The HULL Hydrodynamics computer code. Air Force Weapons Laboratory, Kirtland Air Force Base, New Mexico, AFWL-TR-76-183.

Ge, H.H., D.D. Zhou, and W.Q. Wu (2003) Passivation model of 316 stainless steel in simulated cooling water and the effect of sulfide on the passive film. *Applied Surface Science*, 211(1-4): 321–334.

Genin, J.M.R., G. Bourrie, F. Trolard, M. Abdelmoula, A. Jaffrezic, P. Refait, V. Maitre, B. Humbert, and A. Herbillon (1998) Thermodynamic equilibria in aqueous suspensions of synthetic and natural Fe(II)-Fe(III) green rusts: Occurrences of the mineral in hydromorphic soils. *Environmental Science and Technology*, **32**(8): 1058–1068.

Grant, D.E., and M. Crull (1999) Evaluation of PENCRV3D for determination of ordnance ground penetration. *UXO/Countermine Forum*. Atlanta, Georgia.

Gu, B.H., D.B. Watson, L.Y. Wu, D.H. Phillips, D.C. White, and J.Z. Zhou (2002) Microbiological characteristics in a zero-valent iron reactive barrier. *Environmental Monitoring and Assessment*, **77**(3): 293–309.

Hamilton, W.A. (1983) The role of sulfate-reducing bacteria in anaerobic corrosion. *Journal of Applied Bacteriology*, **55**(3): R3–R3.

Hamilton, W.A. (1985) Sulfate-reducing bacteria and anaerobic corrosion. *Annual Review of Microbiology*, **39**: 195–217.

Hamilton, W.A. (1998) Bioenergetics of sulphate-reducing bacteria in relation to their environmental impact. *Biodegradation*, **9**(3–4): 201–212.

Hamilton, W.A. (2003) Microbially influenced corrosion as a model system for the study of metal microbe interactions: A unifying electron transfer hypothesis. *Biofouling*, **19**(1): 65–76.

Hewitt, A.D., T.F. Jenkins, T. Ranney, D. Lambert, and N. Perron (2004) Characterization of energetic residues at military firing ranges: Scholfield Barracks and Pohakuloa Training Area. Chapter 3, Distribution and fate of energetics on DoD test and training ranges: Interin report 4. U.S. Army Research and Development Center, ERDC TR-04-4.

Hewitt, A.D., T.F. Jenkins, T. Ranney, J. Stark, M.E. Walsh, S. Taylor, M. Walsh, D. Lambert, N. Perron, N. Collins, and R. Karn (2003) Estimates for explosive residue deposition from the detonation of army munitions. U.S. Army Engineer Research and Development Center, Cold Regions Research and Engineering Laboratory, Technical Report ERDC/CRREL TR-03-16.

Hundal, L.S., J. Singh, E.L. Bier, P.J. Shea, S.D. Comfort, and W.L. Powers (1997) Removal of TNT and RDX from water and soil using iron metal. *Environmental Pollution*, **97**(1–2): 55–64.

Isaksen, K., and J.L. Sollid (2002) *Losavleiringer og permafrost i Hjerkinn skytefelt, Dovrefjell.*

Ishikawa, T., T. Ueno, A. Yasukawa, K. Kandori, T. Nakayama, and T. Tsubota (2003) Influence of metal ions on the structure of poorly crystallized iron oxide rusts. *Corrosion Science*, **45**(5): 1037–1049.

Jenkins, T.J., C.L. Grant, G.S. Brar, P.G. Thorne, T.A. Ranney, and P.W. Schumacher (1996) Assessment of sampling error associated with collection and analysis of soil samples at explosive-contaminated sites. U.S. Army Cold Regions Research and Engineering Laboratory, Special Report 96-15.

Jenkins T.J., M.E Walsh, P.G. Thorne, S. Thiboutot, G. Ampleman, T.A. Ranney, and C.L. Grant (1997) Assessment of sampling error associated with collection and analysis of soil samples at a firing range contaminated with HMX. U.S. Army Cold Regions Research and Engineering Laboratory, Special Report 97-22.

Jenkins T.J., M.E Walsh, P.G. Thorne, P.H Miyares, T.A. Ranney, C.L. Grant, and J.R. Esparza (1998) Site characterization for explosives contamination at a military firing range impact area, U.S. Army Cold Regions Research and Engineering Laboratory, Special Report 98-9.

Jenkins, T.J., T.A. Ranney, M.E. Walsh, P.H. Miyares, A.D. Hewitt, and N.H. Collins (2000) Evaluating the use of snow-covered ranges to estimate the explosives residues that result from detonation of Army munitions. U.S. Army Engineer Research and Development Center, Cold Regions Research and Engineering Laboratory, Technical Report ERDC/CRREL TR-00-15.

Jenkins, T.J., J.C. Pennington, T.A. Ranney, T.E. Berry Jr., P.H. Miyares, M.E. Walsh, A.D. Hewitt, N.M. Perron, L.V. Parker, C.A. Hayes, and E.G. Wahlgren (2001) Characterization of explosives contamination at military firing ranges. U.S. Army Engineer Research and Development Center, Cold Regions Research and Engineering Laboratory, Technical Report ERDC/CRREL TR-01-5.

Jones D.A. (1996) *Principles and Prevention of Corrosion*. Prentice Hall.

Kajiyama, F., and K. Okamura (1999) Evaluating cathodic protection reliability on steel pipe in microbially active soils. *Corrosion*, **55**(1): 74–80.

Kholodenko, V.P., S.K. Jigletsova, V.A. Chugunov, V.B. Rodin, V.S. Kobelev, and S.V. Karpov (2000) Chemicomicrobiological diagnostics of stress corrosion cracking of trunk pipelines. *Applied Biochemistry and Microbiology*, **36**(6): 594–601.

Kingery, C.N, and G. Bulmash (1984) Airblast parameters from TNT spherical air burst and hemispherical surface burst. U.S. Armament Research and Development Center, Ballistics Research Laboratory, Aberdeen Proving Ground, Maryland. Technical report ARBRL-TR-02555.

Kloppel, H., A. Fliedner, and W. Kordel (1997) Behavior and ecotoxicology of aluminum in soil and water—Review of the scientific literature. *Chemosphere*, **35**(1–2): 353–363.

Kuznetsova, A., T.D. Burleigh, V. Zhukov, J. Blachere, and J.T. Yates (1998) Electrochemical evaluation of a new type of corrosion passivation layer: Artificially produced Al_2O_3 films on aluminum. *Langmuir*, **14**(9): 2502–2507.

Lee, A.K., and D.K. Newman (2003) Microbial iron respiration: impacts on corrosion processes. *Applied Microbiology and Biotechnology*, **62**(2–3): 134–139.

Lee, J.H., and J.E. Atkins (1995) Performance Assessment 1995. Chapter 5, Waste Package Degradation. Office of Civilian Radioactive Waste Management, Department of Energy, pp. 5-1 to 5-17.

Lever J., S. Taylor, L. Perovich, K. Bjella, and B. Packer (in prep) Dissolution of Composition B. U.S. Army Engineer Research and Development Center, Cold Regions Research and Engineering Laboratory

Levlin, E. (1996) Aeration cell corrosion of carbon steel in soil: In situ monitoring cell current and potential. *Corrosion Science*, **38**(12): 2083–2090.

Lewis J. S. Thiboutot, G. Ampleman, S. Brochu, T. Ranney, and S. Taylor (2002) Open detonation of military munitions on snow: An investigation of the quantities of energetic material residues produced. RDDC-DRDC—Valcartier.

Li, S.Y., Y.G. Kim, K.S. Jeon, Y.T. Kho, and T. Kang (2001) Microbiologically influenced corrosion of carbon steel exposed to anaerobic soil. *Corrosion*, **57**(9): 815–828.

Linhardt, P. (1997) Corrosion of metals in natural waters influenced by manganese oxidizing microorganisms. *Biodegradation*, **8**: 201–210.

Little B., P. Wagner, and F. Mansfeld (1991) Microbiologically influenced corrosion of metals and alloys. *International Materials Review*, **36**(6): 253–272.

Little, B., P. Wagner, K. Hart, R. Ray, D. Lavoie, K. Nealson, and C. Aguilar (1998) The role of biomineralization in microbiologically influenced corrosion. *Biodegradation*, **9**(1): 1–10.

Little, B., R. Ray, and R. Pope (2000) Relationship between corrosion and the biological sulfur cycle: A review. *Corrosion*, **56**: 433–443.

Lyman, T. (1961) *Metals Handbook*.Volume 1. *Properties and Selection of Metals*. Metals Park, Ohio: ASM International.

Lynch, J.C, J.M. Brannon, and J.J. Delfino (2002) Dissolution rates of three high explosive compounds: TNT, RDX and HMX. *Chemosphere*, **47**: 725–734.

Matyskiela (2003) Modeling of chemical transport from UXO to surrounding soil. Final Report submitted to Praxis Environmental Technologies, Burlingame, California.

Murad, E., and U. Schwertmann (1980) The Mossbauer spectrum of ferrihydrite and its relations to those of other iron-oxides. *American Mineralogist*, **65**(9–10): 1044–1049.

Music, S., D. Dragcevic, I. CzakoNagy, and S. Popovic (1997) FT-IR and Mossbauer study of corrosion of steel in tap and mineral water. *Croatica Chemica Acta,* **70**(2): 689–702.

Music, S., M. Gotic, and S. Popovic (1993) X-Ray-diffraction and Fourier-transform infrared-analysis of the rust formed by corrosion of steel in aqueous-solutions. *Journal of Materials Science,* **28**(21): 5744–5752.

Naval Explosive Ordnance Disposal Technology Division (1996) Unexploded Ordnance (UXO): An overview. (https://www.denix.osd.mil/Pubilc/Library/Explosives/uxo/uxo.html#for)

NDCEE (2003) Unexploded Ordnance (UXO) Task 307; Subtask 4: UXO Recovery Database [Computer Software]. Limited-access Online database. 10 January 2004. http://uxords.ctcgsc.org.

Nordstrom, D.K., and C.N. Alpers (1999) Negative pH, efflorescent mineralogy, and consequences for environmental restoration at the Iron Mountain Superfund site, California. *Proceedings of the National Academy of Sciences of the United States of America*, **96**(7): 3455–3462.

Nordstrom, D.K., C.N. Alpers, C.J. Ptacek, and D.W. Blowes (2000) Negative pH and extremely acidic mine waters from Iron Mountain, California. *Environmental Science and Technology*, **34**(2): 254–258.

Nore, R. (1994) Report on selected ordnance removal projects. *Proceedings, Twenty-Sixth, DoD Explosives Safety Seminar. Alexandria, Virginia*. Department of Defense, Explosives Safety Board, 1997, CD-ROM.

Norin, M., and T.G. Vinka (2003) Corrosion of carbon steel in filling material in an urban environment. *Materials and Corrosion—Werkstoffe Und Korrosion*, **54**(9): 641–651.

Ogden Environmental and Energy Services (2000) Client draft IAGS Technical Team Memorandum 00-3: Evaluation of gun and mortar firing positions for the Camp Edwards impact groundwater quality study, MMR, Cape Code, Massachusetts. Nashville, Tennessee.

Papadopoulos, J.A. (2003) Munition metal parts manufacturing changes, 1920 to present, for unexploded ordnance database. U.S. Army Armament Research, Development, and Engineering Center, Picatinny Arsenal, New Jersey, Special Publication ARWEC-SP-02001.

Pedersen M.A., J. Nokes and D. Wardlaw (2002) Low-order, underwater detonation. Environmental Security Technology Certification Program, ESTCP Report UX-0104.

Penhale, H.R. (1971) Corrosion of mild steel plates in some New-Zealand soils, *New Zealand Journal of Science*, **14**(2): 336–337.

Pennington, J.C., T. F. Jenkins, J.M. Brannon, J. Lynch, T.A. Ranney, T.E. Berry, Jr., C.A. Hayes, P.H. Miyares, M.E. Walsh, A.D. Hewitt, N. Perron, and J.J. Delfino (2001) Distribution and fate of energetics on DoD test and training ranges: Interim Report 1. U. S. Army Engineer Research and Development Center, ERDC TR-01-13.

Pennington, J.C., T.F. Jenkins, G. Ampleman, S. Thiboutot, J.M. Brannon, J. Lynch, T.A. Ranney, J.A. Stark, M.E Walsh, J. Lewis, C.A. Hayes, J.E. Mirecki, A.D. Hewitt, N.M. Perron, D. Lambert, J. Clausen, and J.J. Delfino (2002) Distribution and fate of energetics on DoD test and training ranges: Report 2. U.S. Army Engineer Research and Development Center, Environmental Laboratory Technical Report, ERDC/EL TR-01-13.

Pennington, J.C., T.F. Jenkins, G. Ampleman, S. Thiboutot, J.M. Brannon, J. Lewis, J.E. Delaney, J. Clausen, A.D. Hewitt, M.A. Hollander, C.A. Hayes, J.A. Stark, A. Marois, S. Brochu, H.Q. Dinh, D. Lambert, R. Martel, P. Brousseau, N.M. Perron, R. Lefebvre, W. Davis, T.A. Ranney, C. Gauthier, S. Taylor, and J.M. Ballard (2003) Distribution and fate of energetics on DoD test and training ranges: Report 3. U. S. Army Engineer Research and Development Center, Environmental Laboratory Technical Report, ERDC/EL TR-02-EL-191.

Phambu, N. (2003) Characterization of aluminum hydroxide thin film on metallic aluminum powder. *Materials Letters*, **57**(19): 2907–2913.

Phelan J.M., S.W. Webb, J.V. Romero, J.L. Barnett, F. Griffin and M. Eliassi (2003) Measurement and modeling of energetic material mass transfer to soil pore water—Project CP-1227. Sandia Report 2003-0153.

Pitard, F.F. (1993) *Pierre Gy's Sampling Theory and Sampling Practice: Heterogeneity, Sampling Correctness, and Statistical Process Control*. Boca Raton, Florida: CRC Press.

Prakash, N., K. Srivastava, and S.B. Gupta (1988) Corrosion of mild-steel by soil containing sulfate reducing bacteria. *Journal of Microbial Biotechnology*, **3**(2): 79–84.

Praxis (2004) UXO Corrosion in soil, SERDP final technical report prepared for U.S. Army Environmental Center. Burlingame, California.

Pruppacher, H.R., and J.D. Klett (1997) *Microphysics of Clouds and Precipitation*. Boston: D. Reidel.

Racine, C.H, M.E. Walsh, C.M. Collins, D.J. Calkins, B.D. Roebuck and L. Reitsma (1992) Waterfowl mortality in Eagle River Flats, Alaska: The Role of munition residues. U.S. Army Cold Regions Research and Engineering Laboratory, CRREL Report 92-5.

Radtke, C.W., D. Gianotto, and F.F. Roberto (2002) Effects of particulate explosives on estimating contamination at a historical explosives testing area. *Chemosphere*, **46**: 3–9.

Refait, P.H., M. Abdelmoula, and J.M.R. Genin (1998) Mechanisms of formation and structure of green rust one in aqueous corrosion of iron in the presence of chloride ions. *Corrosion Science*, **40**(9), 1547–1560.

Romanov, M. (1957) *Underground Corrosion*. National Bureau of Standards Circular 579, US Government Printing Office, Washington, DC.

Scherer, M.M., S. Richter, R.L. Valentine, and P.J.J. Alvarez (2000) Chemistry and microbiology of permeable reactive barriers for in situ groundwater clean up. *Critical Reviews in Microbiology*, **26**(4): 221–264.

Scherer, M.M., K.M. Johnson, J.C. Westall, and P.G. Tratnyek (2001) Mass transport effects on the kinetics of nitrobenzene reduction by iron metal. *Environmental Science and Technology*, **35**(13): 2804–2811.

Schutt, H.U., and P.R. Rhodes (1996) Corrosion in an aqueous hydrogen sulfide, ammonia, and oxygen system. *Corrosion*, **52**(12): 947–952.

Simon, L., J.M.R. Genin, and P.H. Refait (1997) Standard free enthalpy of formation of Fe(II)-Fe(III) hydroxysulphite green rust one and its oxidation into hydroxysulphate green rust two. *Corrosion Science*, **39**(9): 1673–1685.

Stumm, W. (Ed.) (1987) *Aquatic Surface Chemistry: Chemical Processes at the Particle-Water Interface*. Wiley.

Talbot D.D., and E.J. Talbot (1998) *Corrosion Science and Technology*. Boca Raton, Florida: CRC Press.

Taylor S., J. Lever, L. Perovich, E. Campbell, and J. Pennington (2004b) A study of Composition B particle from 81-mm mortar detonations. *Sustainable Range Management Conference.*

Taylor, S., A. Hewitt, J. Lever, C. Hayes, L. Perovich, P. Thorne, and C. Daghlian (2004a) TNT particle size distributions from detonated 155-mm howitzer rounds. *Chemosphere*, **55**: 357–367.

TetraTech (2002) Draft, final high use target area investigation report. Phase II (HUTA II). Massachusetts Military Reservation Camp Edwards. (MMR-6900), November, Tetra Tech Inc. Brookfield, Wisconsin.

Thiboutot, S., G. Ampleman, A. Gagnon, A. Marois, T.F. Jenkins, M.E. Walsh, P.G. Thorne, and T.A. Ranney (1998) Characterization of antitank firing ranges at CDB Valcartier, WATC Wainwright, and CFAD Dundrum. Defense Research Establishment, Department of National Defense, Canada.

Thiboutot, S., G. Ampleman, J. Lewis, D. Faucher, A. Marois, R. Martel, J.M. Ballard, S. Downe, T.F. Jenkins, and A. Hewitt (2003) Environmental conditions of surface soils and biomass prevailing in the training area at CFB Gagetown, New Brunswick. Defense Research Establishment, Department of National Defense, Canada, TR 2003-152.

Thorne, P. (2003) On-range treatment of ordnance debris and bulk energetics resulting from low-order detonations. SERDP project CP-1330.

USA Environmental, Inc. (2001) 100% grid sampling and 4-ft OE removal after action report. Inland Range contract report, former Fort Ord, California, site OE-50. Prepared for U.S. Army Engineer District, Sacramento.

U.S. Army (1981) Army ammunition data sheets—Rockets. Technical Manual 43-0001-30.

U.S. Army (1994) Army munitions data sheets for artillery ammunition: Guns, howitzers, mortars, recoilless rifles, grenade launchers, and artillery fuzes. Department of the Army Technical Manual TM 43-0001-28.

U.S. Army (1998) Design and analysis of hardened structures to conventional weapons effects. Technical Manual 5-855-1.

U.S. Army (1999) Establishing a temporary open burn and open detonation site for conventional ordnance and explosives projects. Technical Manual 60A-1-1-31.

U.S. Army (undated) Army active/inactive range inventory (managed by AEC—Lisa Greenfeld).

U.S. Army Center for Health Promotion and Preventive Medicine (2000) Training range site characterization and risk screening, Camp Shelby Mississippi, 7–23 September 1999. USACHPPM, Aberdeen Proving Ground, Geohydrologic study No. 38-EH-8879-99.

U.S. Government Printing Office (1989) *Department of Defense Dictionary of Military and Associated Terms*. Joint Pub 1-02.

USAMC (1985) Complete round charts—Artillery ammunition, U.S. Army Materiel Command Pamphlet AMC-P 700-3-3

UXO Corrosion, Annual report to SERDP—CP1226

UXO Recovery Depth Database (unpublished) provided by R.Young, USACE, Huntsville.

Veleva, L., P. Castro, G. Hernandez-Duque, and M. Schorr (1998) The corrosion performance of steel and reinforced concrete in a tropical humid climate. A review. *Corrosion Reviews*, **16**(3): 235—–284.

Videla, H.A. (2000) An overview of mechanisms by which sulphate-reducing bacteria influence corrosion of steel in marine environments. *Biofouling*, **15**(1–3): 37–47.

Videla, H.A. (2002) Prevention and control of biocorrosion. *International Biodeterioration and Biodegradation*, **49**(4): 259–270.

Virtanen, S., and M. Buchler (2003) Electrochemical behavior of surface films formed on Fe in chromate solutions. *Corrosion Science*, **45**(7): 1405–1419.

Walsh M.E., C.M. Collins, C.H. Racine, T.F. Jenkins, A.B. Gelvin, and T.A. Ranney (2001) Sampling for Explosive Residues at Fort Greely, Alaska. U.S. Army Engineer Research and Development Center, Cold Regions Research and Engineering Laboratory, Technical Report ERDC/CRREL TR-01-15.

Walsh, M.E., C.A. Ramsey, and T.F. Jenkins (2002) The effect of particle size reduction by grinding on sub-sampling variance of explosives residues in soil. *Chemosphere*, **49**: 1267–1273.

Walsh, M.E., C.M. Collins, T.F. Jenkins, A.D. Hewitt, J. Stark,, and K. Myers (2003) Sampling for explosives at Fort Greely, Alaska. *Soil and Sediment Contamination*, **12**: 631–645.

Walsh, M.E., C.M. Collins, A.D. Hewitt, M.R. Walsh, T.F. Jenkins, J. Stark, A. B. Gelvin, T. Douglas, N. Perron, D. Lambert, R. Bailey, and K. Myers (2004) Range characterization studies at Donnelly training area, Alaska 2001 and 2002. U.S. Army Engineer Research and Development Center, Cold Regions Research and Engineering Laboratory, Technical Report ERDC/CRREL TR-04-5.

Wexler, R.L. (1991) Hourly and daily precipitation frequencies for the United States. Engineering and Topographic Laboratory.

Wildman, M.J., and P.J.J. Alvarez (2001) RDX degradation using an integrated Fe(0)-microbial treatment approach. *Water Science and Technology*, **43**(2): 25–33.

Yfantis, D.K., A.D. Yfantis, and I. Anastassopoulou (1998) Biological corrosion of metallic parts in underground irrigation system: study of alternative materials. *British Corrosion Journal*, **33**(3): 237–240.

Zhang, X.G.(1999) Corrosion ratios of steel to zinc in natural corrosion environments. *Corrosion*, **55**(8): 787–794.

APPENDIX A: CORROSION OF UXO

Thermodynamics of Corrosion

Unexploded ordnance contain explosives, a metal casing and other components. Initially, neither the explosives nor the metals are soluble; thus, they pose only moderate environmental risk. However, following corrosion of the metal casing, toxic explosives and metals may be leached from UXO, potentially contaminating soils and groundwater. Additionally, corrosion may lead to either catastrophic failure of the casing or to the development of small holes (pinholes), processes that may release explosives into the environment. Consequently, an understanding of the mechanism of UXO corrosion in soils is needed to ascertain the risks associated with their presence in the environment.

Most corrosion processes are highly favored thermodynamically as the oxidation of metals is highly exergonic. For example, the corrosion of iron (the main constituent in steel) proceeds according to the following chemical reaction:

$$2\mathrm{Fe} + \frac{3}{2}\mathrm{O_2} \Leftrightarrow \mathrm{Fe_2O_3}\ \Delta G_{rxn}{}^{0} = -742\ \mathrm{kJ/mol} \qquad \text{(A1)}$$

The release of free energy is typical of other corrosion processes and shows the drive for metals to dissolve to form other phases. In fact, iron is not stable under any typical soil water pH-E_h conditions (Fig. A1). Other metals and alloys, including steel, the most common casing for munitions, are similarly unstable under commonly encountered thermodynamic conditions.

Reaction A1 shows the production of a solid phase, Fe_2O_3. When conditions of pH and E_h change, solution phases such as dissolved Fe(II) and Fe(III) also may form (Fig. A1). Generally, it is desirable from a remediation standpoint to produce solid phases during corrosion—they are more stable, less prone to transport, they react with potential contaminants (both inorganic and organic species adsorb strongly to iron oxides), and some oxidation products protect the metal surface from further oxidation (Kuznetsova et al. 1998, Ge et al. 2003, Virtanen and Buchler 2003). The protection of the surface is called passivation. Passivation is seen graphically in the case of aluminum corrosion. Aluminum is a highly reactive metal that is susceptible to corrosion. However, Al corrosion is actually quite slow under normal soil conditions (near neutral pH, low ionic strength). Aluminum corrodes through the formation of Al_2O_3 on the metal surface, which protects it from further oxidation or deterioration (Kloppel et al. 1997, Kuznetsova et al. 1998, Phambu 2003). This protection is a kinetic effect, in that

the thermodynamic driving force for corrosion remains, but the surface oxidation is slowed by the presence of a passivating oxide. Passivation is discussed in detail below.

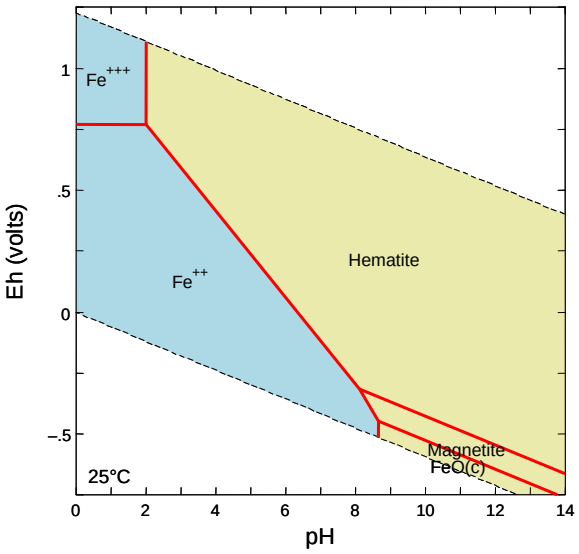

Figure A1. Fe phase diagram for Fe-O_2 system at 25ºC. The diagram is derived using a dissolved Fe concentration of 1 µM. Dark shaded phases are aqueous, while lighter phases are solids. The diagonal dotted lines show boundaries for the stability of water; the vertical dotted line shows the change in carbonate speciation. Hematite is α-Fe_2O_3 (s).

The presence of other species, as occurs in soils and sediments, strongly impacts corrosion and may also affect the formation of corrosion products (Kajiyama and Okamura 1999, Kholodenko et al. 2000, Li et al. 2001). In the case of iron, many soil species, including sulfate, phosphate, and dissolved silica, affect mineral formation (Fig. A2). Iron may form stable solid phases with Si, P, and other phases in this system; thus, knowing the solution composition is critical to understanding the products of steel and iron within soil. These precipitated solids may also form on the metal surface, thereby influencing corrosion. Conversely, some species (e.g., chloride) in solution may help to dissolve passivating oxides, thereby accelerating corrosion.

The thermodynamic effects described above focus on the corrosion of Fe. Steel corrosion has been studied in detail (Zhang 1999), and is analogous to Fe corrosion. One important difference between iron and steel is the chemical addi-

tives (e.g., Cr, C, and Mn) present in steel. These additives are minor, and do not typically influence the phase diagrams for steel relative to iron corrosion; however, additives strongly alter the kinetics of chemical corrosion. Limited attention has been devoted to the specific mechanism of UXO corrosion (Bucci and Buckley 1998, Fabian and Ostazeski 2002, Praxis 2004, AMEX, in review); we focus on mechanistic studies that examine steel and iron corrosion, and apply these mechanistic studies to our understanding of the processes by which UXO corrode and perforate.

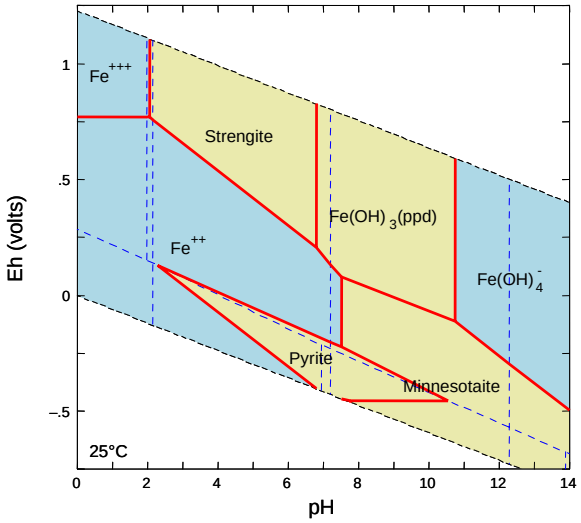

Figure A2. Fe phase diagram for Fe-O_2-S-PO_4-CO_3-H_2O system at 25ºC. The diagram is derived using a dissolved Fe concentration of 1 µM, a total CO_3^{2-} of 0.1 mM, total PO_4^{3-} and SO_4^{2-} of 1 µM, and SiO_2 of 50 µM, similar concentrations to those found in soils. Darker shaded phases are aqueous, while lighter phases are solids. The diagonal dotted lines show boundaries for the stability of water; the vertical dotted lines show the change in carbonate, phosphate, and sulfur speciation. Minnesotaite is an iron-containing phyllosilicate, and strengite is hydrated $FePO_4$.

Kinetics of Corrosion

Although thermodynamic (energetic) considerations indicate that corrosion is favored under the most commonly encountered soil conditions, kinetic factors ultimately determine the *extent* to which this oxidation occurs, the ultimate reac-

tion products of oxidation, and the distribution of these reaction products (e.g., whether they are attached to the surface). The most stable reaction products thermodynamically are often not formed during metal corrosion in soils because of sluggish reaction kinetics, instead leading to the formation of other, metastable, reaction products. For example, magnetite (Fe_3O_4) and maghemite (γ-FeOOH) production usually is favored over minnesotaite or other ferrous silicates under slightly reducing, sulfide deficient pH-E_h conditions. Similarly, ferrihydrite [$Fe(OH)_3$], lepidocrosite (γ-FeOOH), or green rusts [mixed Fe(II)/Fe(III) hydroxides] usually are produced instead of hematite (Fe_2O_3), the most stable ferric mineral, during iron oxidation (Murad and Schwertmann 1980; Davalos et al. 1991; Arshed et al. 1992, 1993; Music et al. 1993, 1997). These metastable products may be somewhat resistant to further chemical reaction; however, others, such as green rust, are highly reactive and may be important in other chemical processes. Below we discuss two important aspects of corrosion kinetics: passivation of metal surfaces and biologically mediated metal corrosion.

Fundamentals of Corrosion Kinetics

The most important means of quantifying the rate of chemical corrosion is using the corrosion potential and current. As corrosion involves disequilibrium, the corrosion potential reflects the E_h at which corrosion occurs, while the corrosion current indicates the rate of electron transfer. The extent of electrochemical reactions is determined by the rate of electron transfer; understanding this corrosion current is vital to estimate the rate of chemical corrosion. For a more complete discussion of these principles, consult one of many excellent reviews of the subject (Jones 1996, Talbot and Talbot 1998).

For understanding corrosion kinetics, it is useful to describe the electrochemical reactions that occur during corrosion in terms of their half reactions. For example, the corrosion of iron in hydrochloric acid solution can be described using the following set of half reactions, which sum to a complete expression of the total reaction:

Oxidation (at anode)	$Fe^0 \rightarrow Fe^{2+}(aq) + 2e^-$	(A2)
Reduction (at cathode)	$2HCl + 2e^- \rightarrow 2Cl^-(aq) + H_2(g)$	(A3)
Net Reaction	$Fe^0 + 2HCl \rightarrow Fe^{2+}(aq) + 2Cl^-(aq) + H_2(g)$	(A4)

Both the oxidation and reduction reactions occur at the surface of the corroding metal; however, the anode (where oxidation occurs) and cathode (where

reduction occurs) are separated on the metal surface (Fig. A3). Consequently, both chemical species and electrons flow from the anode to the cathode during oxidation. The rate of both half reactions must be equal so as to maintain electrical and charge neutrality. Thus, if either the anodic or cathodic reaction proceeds very slowly, the net rate of corrosion also will be slow.

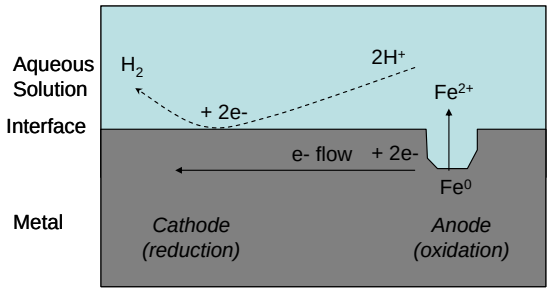

Figure A3. Corrosion of iron in an aqueous solution of HCl. The anodic reaction generates the dissolved metal and electrons, which are transferred to the cathode, where they are used to reduce protons in solution. The extent of proton transfer is equal to the electron flow, a condition required to maintain charge neutrality.

Because the rate of corrosion depends on the rate of the anodic (oxidation) and cathodic (reduction) reactions, it is necessary to identify the dominant half reactions to estimate the rate of oxidation. When alloys such as steel corrode, several anodic (oxidation) reactions may occur, each of which liberates a cation and electrons. For example, a Cr and Mn-containing steel could undergo the following anodic reactions:

$$Fe^0 \rightarrow Fe^{2+}(aq) + 2e^- \quad \text{(A5)}$$

$$Cr^0 \rightarrow Cr^{3+}(aq) + 3e^- \quad \text{(A6)}$$

$$Mn^0 \rightarrow Mn^{2+}(aq) + 2e^- \quad \text{(A7)}$$

In the case of carbon steel, the oxidation of elemental carbon to $CO_2(g)$ also may occur at the anode. As CO_2 is soluble and diffuses away quickly relative to

ions, carbon steels are more easily corroded than other steels. Anodic reactions are usually straightforward to predict; however, iron and some other metals may form multiple oxidation states, and therefore be oxidized through multiple anodic reactions. For example, iron may also be oxidized to the trivalent state:

$$Fe^0 \rightarrow Fe^{3+}(aq) + 3e^- \quad \text{(A8)}$$

Each of the thermodynamically viable reactions contributes to the overall rate of corrosion; however, the relative contribution of each depends on the rate of each process. Slow reactions contribute little to the total reaction rate; thus, the fastest reactions will predominate when multiple oxidation reactions occur.

Cathodic reactions are somewhat more complex in that many possible reactions may occur, depending on the solution conditions. For example, hydrogen may be evolved from an acidic solution as in the above example:

$$2H^+ + 2e^- \rightarrow H_2(g) \quad \text{(A9)}$$

Alternatively, oxygen may, when present, be reduced in acidic solutions:

$$O_2 + 4e^- + 4H^+ \rightarrow 2H_2O \quad \text{(A10)}$$

Oxygen reduction may also occur in neutral or alkaline solutions through a different pathway:

$$O_2 + 4e^- + 2H_2O \rightarrow 4OH^- \quad \text{(A11)}$$

Other reactions, including the reduction of a solution species (such as Fe^{3+} or NO_3^-), may occur simultaneously. Complications also may arise if solid phases (e.g., ferrihydrite during iron or steel corrosion) are produced directly during corrosion. As these products are quite stable, their formation influences the thermodynamics of corrosion, but their presence also can influence the rate of corrosion because solid phases may block surface sites reactive towards oxidation.

Mixed potential theory provides a basis for determining electrochemical reaction rates. This theory is based on two principal assumptions. First, the theory assumes that the anodic current and the cathodic current are equal and opposite. In fact, the number of electrons transferred in each must be equal to maintain charge neutrality. The second assumption is more tenuous and depends on the assumption that electrochemical oxidation and reduction processes occur inde-

pendently and that they can be separated into distinct processes. This is precisely what we have done in the above example of iron corrosion in HCl, and it is a generally good approximation for many systems; however, care must be taken to avoid applying this theory to systems that have dependent cathodic and anodic processes.

Mixed potential theory is grounded in transition state theory, which assumes that the rate of a chemical reaction depends on the activation energy, and the thermodynamic driving force for the chemical reaction is described by change in free energy of the system (Fig. A4). The net change in free energy can also be related to a net change in potential, called an overpotential (η_{anodic}) by the expression $\Delta G = -nF\eta$. The current (which is proportional to rate) of the resulting chemical reaction can then be expressed using conventional theory as:

$$\text{Current} = \text{A}\exp\left[\frac{-\Delta G}{\text{R}T}\right] = A\exp\left[\frac{-n\text{F}\eta}{\text{R}T}\right] \tag{A12}$$

Where A is a proportionality constant, ΔG is the change in free energy, R is the Ideal Gas Constant, T is the temperature in K, n is the number of electrons in the half reaction, and F is Faraday's constant. Note that this expression implies that the voltage of the over-potential is proportional to the log of the current ($\eta \propto \log i$). Thus, as the thermodynamic driving force increases, so does the rate of corrosion. This can be expressed for both the anode and cathode using the following expressions:

$$\eta_a = \alpha_a + \beta_a \log i_a \tag{A13}$$

$$\eta_c = \alpha_c + \beta_c \log i_c \tag{A14}$$

Where α and β are Tafel constants for the anodic (a) and cathodic (c) reactions. Note that the current i is the same for both anodic and cathodic processes.

The aforementioned kinetic control is called *activation polarization*, and occurs when chemical processes control reaction rate. Activation potential can easily be identified in Tafel plots (Fig. A5). In such cases, the rate of the anodic reaction current (rate) increases with increasing potential (oxidation is favored under increasingly high potential), and the cathodic reaction current increases as the potential drops, as reduction is favored under negative relative potentials.

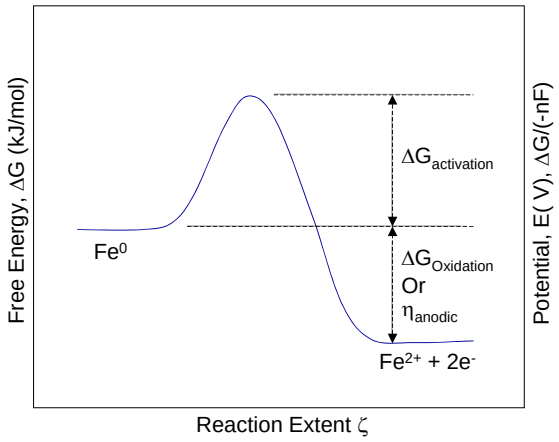

Figure A4. Coordinate diagram for an activation controlled (chemically controlled) reaction. The reaction extent describes the conversion of reactants at the left, to products at the right. The reaction rate is proportional to current, and depends on the fraction of the population that has energy in excess of the free energy of activation (which is determined by Boltzmann's distribution).

Under extremely rapid reaction rates, concentrations of either reactants or products may build up (or be depleted) at the surface of the corroding metal. In such cases, the reaction rate depends on the concentration of these species and the electrochemical reaction is controlled by *concentration polarization* (Fig. A6). Under conditions of concentration polarization, the current drops sharply at a limiting current (i_L), which is determined by the diffusion constant (D) and concentration (C) of the diffusing species and thickness d of the diffusion layer:

$$i_L = \left(\frac{DnF}{\delta} \right) C \qquad \text{(A15)}$$

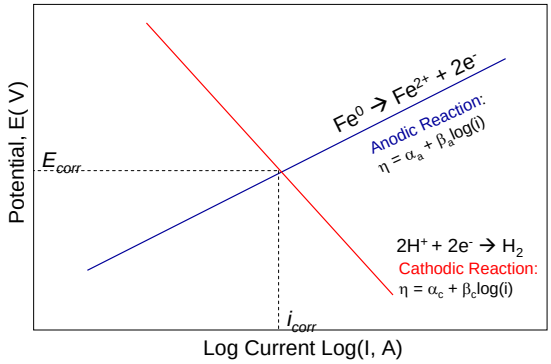

Figure A5. Activation polarization curves for both anodic and cathodic reactions of Fe corrosion in dilute acid. The point at which the currents are equal defines the corrosion potential and current for the system. The curve with the steepest slope ultimately controls the corrosion potential as small changes in its slope or position significantly change the corrosion current.

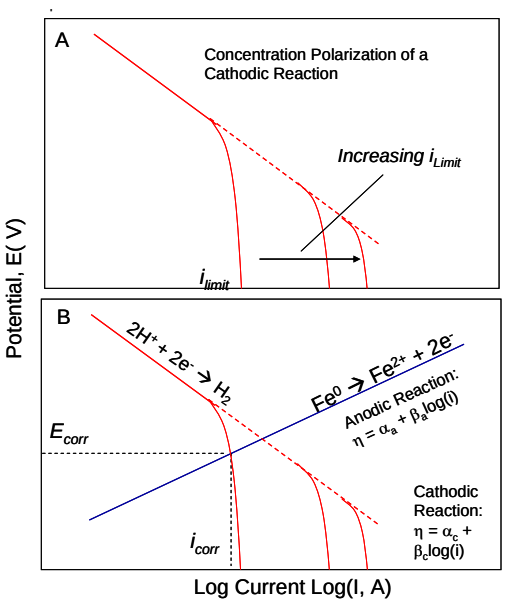

Figure A6. Effect of concentration polarization on the current of corrosion. The limiting current (i_{limit}) depends on diffusion through a surface layer (A); increasing the velocity of agitation, temperature, or concentration will increase i_{limit}. As the corrosion of the anodic reaction is equal to that of the cathode, the corrosion potential and voltage are decreased by concentration polarization relative to activation polarization. At currents below that of the limiting current, corrosion occurs through conventional, activation polarization conditions.

For example, in the case of steel corrosion, the cathodic reaction may be limited by the diffusion of H^+ to the surface to be reduced to H_2.

The overall rate of an electrochemical reaction is determined by the potential at which the anodic and cathodic currents are equal (Fig. A5 and A6). Conceptually, this crossover results in a set potential (E_{corr}) and current (i_{corr}) at which corrosion proceeds. This current is essentially constant; thus, neither corrosion rates nor corrosion potentials change during electrochemical corrosion unless reaction products form that induce concentration polarization. This leads to an effective electrochemical buffer in which the redox status of the system is maintained over extended periods. This electrochemical buffer is referred to as *apoise*. For systems in which the anodic and cathodic reactions are known, the Tafel constants can be used to determine the corrosion potential and rate. Under diffusion-limited conditions, i_L will determine the overall corrosion rate.

In many laboratory systems, stirring limits the diffusion layer thickness, thereby increasing i_L so that concentration polarization may not be observed; however, concentration polarization occurs more often in soil systems. Water is frequently immobile and poorly mixed in soil systems, leading to diffusional limitations and concentration polarization. Slow diffusion also can lead to the build-up of oxidation products locally at the metal surface, which may lead to the precipitation of an insoluble surface layer that will decrease the overall reaction rate. Thus, corrosion rates estimated from Tafel constants alone represent high estimates of corrosion rates in soil systems. Similarly, care must be exercised when extrapolating corrosion rates determined for steel in aqueous solutions to complex soil matrices.

For poorly conducting solids, ohmic polarization, which limits the flow of electrons from the anode to the cathode, may limit corrosion rates. Ohmic polarization is caused by the formation of a potential difference between the anode and cathode (under non-ohmic conditions, the potential of the anode and cathode are equal and set by the corrosion potential). Although ohmic polarization results in unequal potentials at the anode and cathode, the current is the same at both the anode and cathode. Ohmic polarization is observed in systems where charge is transferred via ion transport because solutions are not conductive; however, it seldom is limiting for metal corrosion.

Changing the composition of the solution changes the driving force for corrosion by changing the value of the Tafel constants α or β. This can be seen graphically in Figure A7, which shows the effect of changing pH on the cathodic reaction. As the acidity increases (as the pH drops), so does the hydrogen ion concentration. The resulting increase in hydrogen ion activity enhances the reduction of hydrogen ions to hydrogen gas, increasing the cathodic current at all

potentials. This shift in the cathodic polarization curve leads to a different cross-over point with the anodic reaction (which is not affected by pH in this simplistic system); thus, the corrosion current and potentials increase. Often both the cathodic and anodic polarization curves are affected by a change in solution composition. For example, in the case of the corrosion of a passivating metal, both the cathodic and anodic polarization curves will shift, also causing the corrosion potential and current to change.

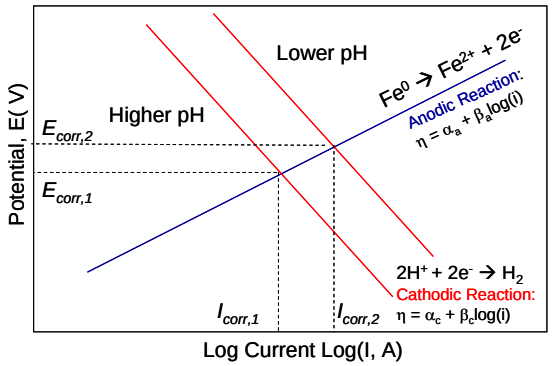

Figure A7. Influence of pH on the corrosion rate of an active metal. The example would apply for the acidic corrosion of Fe metal. The corrosion current and potential at the lower pH ($i_{corr,2}$, $E_{corr,2}$) is higher than at higher pH. It is fairly straightforward to predict which reactions will be impacted by changes in solution composition. As only the cathodic reaction involves H^+, it is the only reaction affected by changes in pH (unless the pH is high enough to induce Fe^{2+}hydrolysis). Similarly, complexation of Fe(II) by citric acid would change the pH and Fe(II) activity, changing both the anodic and cathodic polarization curves.

Passivation of Metal Surfaces

Corrosion processes are ultimately dependent on surface mediated processes. In metal corrosion, the metal surface corrodes through the chemical reaction of a dissolved solute (e.g., oxygen) with a reactive metal surface. Consequently, the rate of the reaction depends in some manner on the reactive surface area of the metal. Frequently, passivation occurs through the formation of an insoluble metal oxide film that blocks the metal surface from oxidants in solution (Fig. A8).

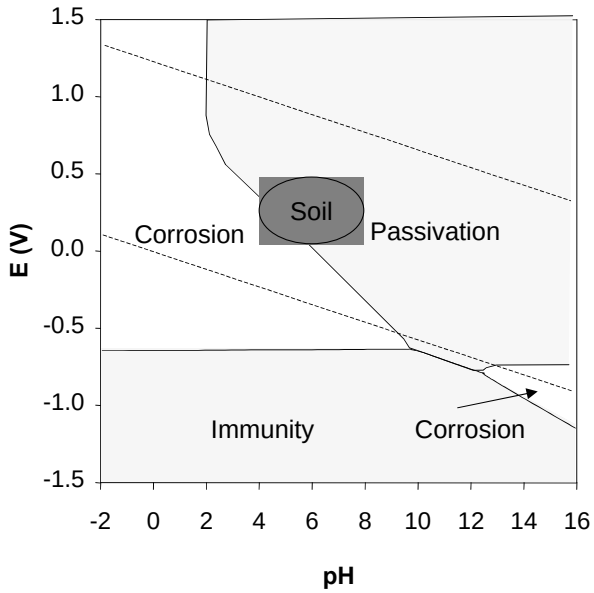

Figure A8. Domains in which passivation of iron can occur. Note that these domains are very similar to those in which solid phases are formed. Immunity occurs in E-pH domains where there is no thermodynamic driving force for corrosion. The dotted lines indicate the stability zone of water and the shaded oval is the domain in E-pH space that is most prevalent in soils.

Such films are only effective in passivating surfaces if they form effective two-dimensional arrays on the surface; thus, the microstructural compatibility of the interface between the surface and the overlying oxide film is important. This compatibility can be expressed using the following expression (Stumm 1987):

$$\Delta G_{\text{interface}} = \overline{\delta}_{\text{NW}} S_{\text{NW}} + (\overline{\delta}_{\text{NS}} + \overline{\delta}_{\text{SW}}) S_{\text{NS}} \quad \text{(A16)}$$

Where the $\overline{\delta}$ refers to the surface free energy of the given surface, and *S* is the surface area, and *NW*, *NS* and *SW* refer to the nuclei (of the metal oxide)–water, nuclei–substrate, and substrate (the metal)–water interactions. Passivation occurs under the specific case that the lattice of the metal oxide has attractive and comparable surface energy and similar lattice dimensions (implying that $\overline{\delta}_{\text{NW}} \approx \overline{\delta}_{\text{SW}}, \overline{\delta}_{\text{NS}} < \overline{\delta}_{\text{NW}}$):

$$\Delta G_{\text{interface}} = \overline{\delta}_{\text{NW}} (S_{\text{NW}} - S_{\text{NS}}) \quad \text{(A17)}$$

Under these conditions, the surface oxide can effectively cover the surface with a passivating layer, thereby preventing further oxidation (Fig. A9). However, if the corroding metal substrate and the oxide have dissimilar energies, then the surface coating will not develop into a crystalline solid, nor will it effectively protect the surface from further oxidation.

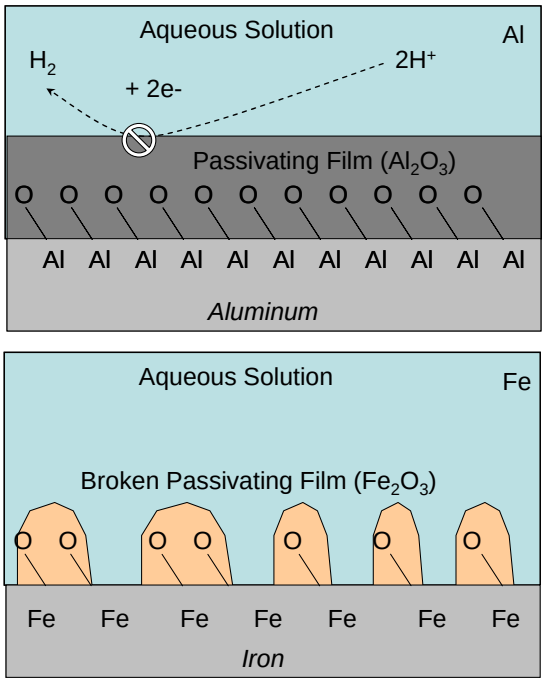

Figure A9. Formation of passivation layers during the corrosion of iron (Fe) and aluminum (Al). The passivation layer on Al is complete because the Al oxide forms a compatible passivating film. As drawn, the passivation occurs by blocking the cathodic reaction; however, anodic passivation is also possible. In contrast, the Fe oxide film is not compatible and forms oxides that are ineffective at blocking the surface.

Most UXO are composed of carbon steel, though a limited number of aluminum grenades also have been used. Aluminum is effectively passivated by the formation of Al_2O_3 films, which are highly compatible with Al surfaces (Fig. A9). This passivation leads to fairly corrosion resistant aluminum surfaces except

in chloride containing solutions. This protection occurs despite aluminum metal being sufficiently reactive that fine Al powders oxidize sufficiently rapidly to induce explosions. In contrast, steel UXO corrode to ferric (hydr)oxides, which do not bond strongly to the metal surface and consequently have only limited potential to passivate the metal surface (Fig. A9). This weak bonding is caused by unfavorable interactions between Fe at the surface and the oxide over layer. Stainless steels, however, are frequently passivated though the addition of chemical modifiers that can form compatible oxide films. For example, Cr in stainless steel forms passivating Cr_2O_3 films on steel. Thus, knowing the type of material composing the UXO shell is important for understanding its overall corrosion rate.

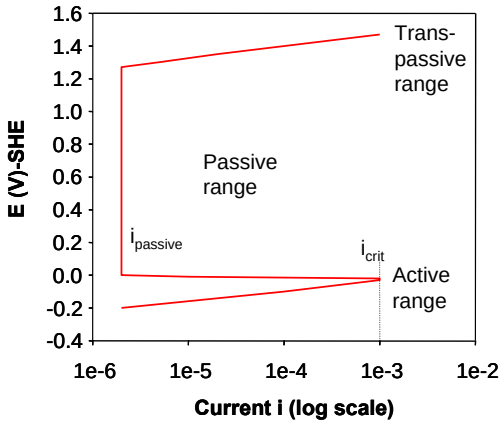

Figure A10. Passivation influences on corrosion current for stainless steel corrosion. Anodic polarization for AISI304 Stainless Steel in 0.05 M H2SO4 (pH 1.2). In the active range, corrosion increases with overpotential, in the passive region, the production of an oxide overgrowth at i_{crit} limits corrosion currents to a constant value ($i_{passive}$), and in the transpassive region, this overlayer breakdown permits increased reaction rates. Based on data from Talbot and Talbot (1998).

Passivation influences both the corrosion potential and current. For stainless steel, the current of the anodic reaction changes rapidly as the potential increases (Fig. A10). This response is caused by sufficiently rapid corrosion to develop large surface concentrations of the dissolved ion, thereby inducing precipitation

of an insoluble metal hydroxide or oxide. In this passivated range of potentials, the current is limited by diffusion and is nearly independent of potential. At extremely high over potentials, however, the current again increases as there is sufficient driving force to overcome the passivation layer. In this high potential region, the passivation layer is breached, typically at the anode, resulting in rapid oxidation at a specific and small location. In this case, the resulting pitting may severely undermine the strength and integrity of the steel. In contrast, oxidation proceeds *uniformly* (equal rates across the surface) when the reaction is controlled by activation or concentration polarization. This pitting mechanism has been discussed at some length by Fabian and Ostazeski (2002), who also identify pitting corrosion as a potentially important mechanism of UXO failure. Unfortunately, the shape and depth of corrosion pits, and the rate of pitting corrosion, are very difficult to estimate as they vary with steel type, impact, and construction stresses, the extent of overpotential in the soil, and a variety of other factors.

Often, steels are treated with *inhibitors* to decrease the rate of corrosion by increasing passivation. One such inhibitor is dissolved chromate, which oxidizes any evolved ferrous iron to insoluble oxides, and also forms a passivating insoluble oxide:

Chromate reduction:	$2CrO_4^{2-} + 10H^+ + 6e^- \rightarrow Cr_2O_3(s) + 5H_2O$	(A18)
Fe oxidation:	$6Fe^{2+} + 9H_2O \rightarrow 3Fe_2O_3(s) + 18H^+ + 6e^-$	(A19)
Net Reaction:	$2CrO_4^{2-} + 6Fe^{2+} + 4H_2O \rightarrow Cr_2O_3(s) + 3Fe_2O_3(s) + 8H^+$	(A20)

This reaction is sufficiently favorable that even low concentrations of chromate can help to form insoluble oxides on the metal surface that are sufficiently thick and uniform to slow corrosion. There are also many elements found in soil that may passivate the metal surface. One possible soil oxidant is manganese (III, IV) oxides, which are ubiquitous in soils (average concentrations in soil of about 0.1–0.2%).

$$MnO_2 + 4H^+ + 2e^- \rightarrow Mn^{2+} + 2H_2O \quad \text{(A21)}$$

Manganese(IV) reduction itself does not passivate the metal; rather, manganese oxides react with reduced ferrous iron produced at the anode to form iron oxide films.

Biologically Mediated Metal Corrosion

Biological reactions are ubiquitous in soil systems. Frequently, biological processes accelerate corrosion through a variety of processes (Prakash et al. 1988, Kloppel et al. 1997, Yfantis et al. 1998, Kajiyama and Okamura 1999, Li et al. 2001, Gu et al. 2002, Doyle et al. 2003). One of the most obvious and most important means by which biological organisms accelerate corrosion is through the secretion of acid, directly as small organic acids, into the soil solution. Acid is released into soils by organisms as a result of nutrient uptake (cation uptake is balanced by excretion of H^+) and as a means of regulating their environment. Acidity is also generated by the excretion of respiratory carbon dioxide. Upon dissolution, this CO_2 forms carbonic acid, which is a weak acid:

$$CH_2O+O_2 \xrightarrow{respiration} H_2O + CO_2(g) \rightarrow H_2CO_3(aq) \Leftrightarrow H^+ + HCO_3^- \quad \text{(A22)}$$

Some metabolic processes involve the direct production of acid; sulfur oxidizers such as *Thiobacillus spp*. oxidize inorganic sulfide and elemental sulfur to sulfate, producing considerable acidity.

$$HS^- + 4H_2O \rightarrow SO_4^{2-} + 9H^+ + 8e^- \quad \text{(A23)}$$

Such acid generation can be severe—the pH of soil pore waters at Iron Mountain, California, have decreased to negative values as a result of such oxidative processes (Nordstrom and Alpers 1999, Nordstrom et al. 2000). As metal passivation does not occur under acidic conditions, chemical oxidation is typically enhanced in acidic soils and other environments.

Organic acids such as oxalic acid ($H_2C_2O_4$) also influence corrosion by complexing metal ions. For example, aluminum is complexed by oxalate through the following reaction:

$$AlOOH + 3C_2O_4^{2-} + 3H^+ \rightarrow Al(C_2O_4)_3^{3-} + 2H_2O \quad \text{(A24)}$$

Such reactions are important because they prevent passivation by oxide minerals such as AlOOH, and may even dissolve oxidized layers formed prior to their introduction. Consequently, complexation by oxalate and other biologically produced chemical species (e.g., citrate, soil organic matter) also increases corrosion rates.

In a given environment, specific metabolites may exert considerable influence on corrosion rates. In particular, the excretion of hydrogen sulfide by sulfate

reducing bacteria (SRB) can contribute to corrosion in anaerobic environments (Booth and Tiller 1968; Edyvean and Videla 1991; Hamilton 1985, 1998; Videla 2002). SRBs reduce sulfate to hydrogen sulfide, usually using a carbon source as the electron donor (the reverse reaction to eq A9). Hydrogen sulfide then can be re-oxidized through chemical or biological processes, producing sulfuric acid. Alternatively, it can precipitate out with iron or other cations to make sulfide minerals such as mackinawite (FeS_{1-x}). These solids reduce the polarization resistance for cathodic (reductive) corrosion, thereby increasing the corrosion rate by as much as an order of magnitude (Kajiyama and Okamura 1999, Li et al. 2001). Ammonia and other nitrogen oxoanions also are produced through biological processes and influence corrosion.

Bacteria also may accelerate steel and iron corrosion by changing the concentration of dissolved iron (Hamilton 1985, 2003; Little et al. 1991, 1998; Lee and Newman 2003). This effect is limited to anaerobic soils and sediments where dissimilatory (metabolic) iron reduction is favored, as assimilatory pathways (those used for cellular incorporation) typically require little Fe and do not change the dissolved concentration appreciably. Dissimilatory iron reduction involves the reduction of insoluble iron oxides to Fe(II) either through direct contact or via a solution-phase electron shuttle or extracellular protein. Under static conditions in which iron reducing bacteria are actively reducing suspended Fe(III), the corrosion rate may actually be slowed as their metabolic processes consume oxygen in the system that would otherwise attack the metal. However, bacteria in a flowing, slightly aerated environment would reduce passivating Fe(III) oxide films, while flow would facilitate reactant transport, increasing corrosion rates. More research is needed to determine the interplay between these two possibilities.

It should be noted that biologically facilitated reactions do not change the energetics (thermodynamics) of corrosion, rather they change the mechanism by which corrosion occurs and, thereby, potentially, the rate of corrosion and the phases that are formed through corrosion. Biological corrosion reactions often result in the production of unique, metastable solid phases with different stability than chemically produced solid phases. In some cases, corrosion can lead to the formation of metastable reaction products, such as magnetite, that have unusually stable structures and low reactivity (Veleva et al. 1998, Ishikawa et al. 2003). However, reactive phases, such as green rust, may also be formed through a combination of biological and chemical processes (Drissi et al. 1995, Simon et al. 1997, Genin et al. 1998, Refait et al. 1998). These solid phases are highly reactive, and may in fact react strongly with contaminants such as RDX and TNT that have been released from leaking UXO (Hundal et al. 1997, Scherer et al. 2001, Wildman and Alvarez 2001). These compounds also are formed primarily in an-

aerobic soils and wetlands, environments that likely contain a large number of corroded UXO.

UXO Corrosion Rates in Soils

Under typical soil conditions (near neutral pH, moderately oxidizing conditions), iron, various alloys of steel, and aluminum are chemically unstable. Despite this instability, UXO and other metallic objects are often stable in soil environments over long periods. This is easily explained using the equations given here. Aerated soils are typically close to neutral with redox potentials of about 0.5 V. Under such conditions, passivation films are formed (Fig. A8) that can slow the corrosion rate by about three orders of magnitude (Fig. A10). Slow diffusion and near neutral pH in soils enhance the production of passivating oxides in soils, further slowing the corrosion rate.

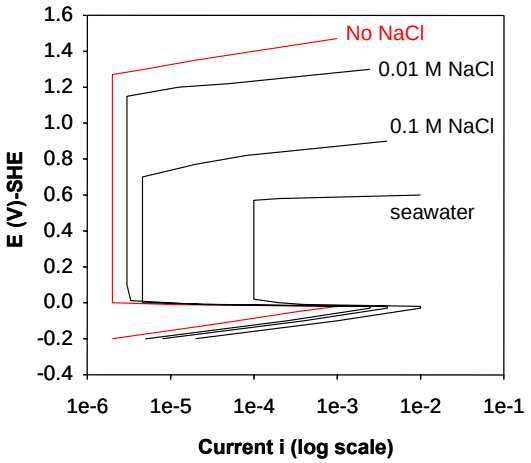

Figure A11. Effect of added chloride on steel corrosion. Anodic polarization for AISI304 Stainless Steel in 0.05 M H_2SO_4 and varying concentrations of NaCl. Salt changes the corrosion current in the active region to some extent, but it appreciably alters the passive corrosion current, and lowers the potential of the transpassive region, where pitting occurs. Thus, pitting is the dominant form of corrosion in oxygenated waters (E ~ 0.55 V) under these conditions. Based on data from Talbot and Talbot (1998).

Often, corrosion in soils occurs at a different rate than is predicted on the basis of laboratory studies. Many of these differences are ascribable to differences

in chemical composition in soils from experimental conditions. For example, changes in pH or dissolved ions result in significant changes in the anodic or cathodic polarization curves and in secondary mineral precipitation, thereby influencing the corrosion rate (Fig. A11). As a result, the corrosion rate of steel in soil systems is often determined empirically by measuring a loss in weight over time, or by measuring the thickness change over time (Romanov 1957). This approach works well for active materials (those that do not form surface coatings) that corrode uniformly with little pitting, and rapidly enough to ensure accurate measurements. It is problematic for stainless steels and other resistant alloys, which react slowly enough that there is appreciable error in the measurements. The principal model for UXO corrosion estimates corrosion rates based on an empirical study of galvanized steel (Bucci and Buckley 1998, AMEX, in review). Although useful, estimates based on galvanized metals may be grossly in error, as galvanization is designed to protect the steel by coating the metal with zinc that corrodes preferentially. However, once this coating corrodes, the steel corrodes in much the same way as ungalvanized steel. Despite these limitations, empirical corrosion rates of many steels have been estimated in a wide range of media (see the *Handbook of Corrosion Data* [Craig 1989]). For the steel alloys commonly used in UXO production, the corrosion rates in a variety of media are shown in Table 6.

It is clear from Table 6 that corrosion of steels in soil varies significantly, depending on the alloy type and reaction conditions. In each case, corrosion is fastest in acidic conditions, where passivation is less pronounced, or in saline environments, where the dissolved salts increase the conductivity of the solution and chloride complexes of Al and Fe increase their solubility. Most munitions have been produced from low to moderate carbon content steels, as carbon steels have the highest strengths. This carbon steel is highly reactive, corroding more rapidly than other steels and also undergoing extensive pit corrosion. In contrast, the most stable alloys of stainless steel (e.g., Alloy 316) are nearly 100 times less reactive. Thus, munitions made with recalcitrant alloys are much less likely to fail through corrosion. Unfortunately, few munitions are constructed of such alloys; only a few types of grenades are constructed of resistant Al alloys, and none of the steel alloys used in munitions are stainless, as it has less desirable mechanical properties.

Empirical corrosion rates for steel and other metals in soils have also been determined, but relatively little work has been done to create general expressions that relate soil chemical characteristics to corrosion rates. In general, corrosion in soils occurs more rapidly than in solutions of a single constituent composition (e.g., NaCl). For most corroding low-carbon steels, the corrosion of carbon steels occurs at about 0.02–0.1 (average of 0.025) mm/year (Penhale 1971, Levlin

1996, Norin and Vinka 2003) in oxidizing soil environments. This rate is at least 10× slower for stainless steels, which corrode at less than 0.01 mm/year (Kajiyama and Okamura 1999). Steel corrosion is accelerated in sulfidic anaerobic environments, often corroding up to 1 mm/year (Hamilton 1983, 1985, 2003; Little et al. 1991; Schutt and Rhodes 1996; Kajiyama and Okamura 1999; Li et al. 2001; Videla 2000). These rates are similar to those calculated using the UXO corrosion model of Garber and Adams (included in Fabian and Ostazeski 2002), although our estimates are somewhat more general and require much less input information.

The rates of corrosion in aerated soils shown in Table 6 are not particularly rapid, and would lead to the uniform failure of small munitions (grenades, etc., with minimum wall thicknesses of 2–5 mm) in about 80–200 years. Larger munitions with thicker walls (5–10 mm walls) would fail in 200–400 years. Pitting corrosion is more prevalent than uniform corrosion in soils (Frankel 1998, Doyle et al. 2003, Norin and Vinka 2003) and also results in much deeper corrosion, potentially decreasing the time required to perforate the UXO to about 20 and 50 years for small and larger munitions, respectively. In reducing soils, munitions could corrode much more rapidly, in as little as a few years; consequently, the casings of munitions in wetlands likely have corroded through to the HE fill. Saline environments, such as those encountered in proving grounds in arid basins such as China Lake, California, also may have saline soil chemical conditions favorable for enhanced corrosion.

The above estimated corrosion rates should be viewed with some caution, as it is difficult to determine precisely the rate of corrosion in soils, in part because of variation in soil pH, salinity (conductivity), moisture, and age. In general, more acidic soils will corrode steel more readily than alkaline soils because of increasing passivation, and soils with high concentrations of dissolved salts cause rapid corrosion because of complexation of oxidation products with dissolved ions, improved diffusion (which increases limiting currents), and other factors. Soil organic matter (and other organic molecules) also may influence corrosion through adsorption and blocking of active sites. Fortunately, the corrosion rate of steel in a broad variety of soils apparently only varies by a factor of 2 to 5.

The effect of increasing soil water content on corrosion is more complex. In aerated soils, increasing the water content leads to increased corrosion rates as the oxidation products are more easily removed from the surface under conditions of flow; however, under anaerobic conditions, which occur in many flooded soils, microbial processes may lead to the reduction of iron(III) hydroxides and sulfate, preventing passivation and also activating the cathode for further oxidation. These biological effects can be quite significant, increasing the corrosion

rate by an order of magnitude or more, but more work is needed to better understand and quantify the processes by which biological corrosion occurs in soils.

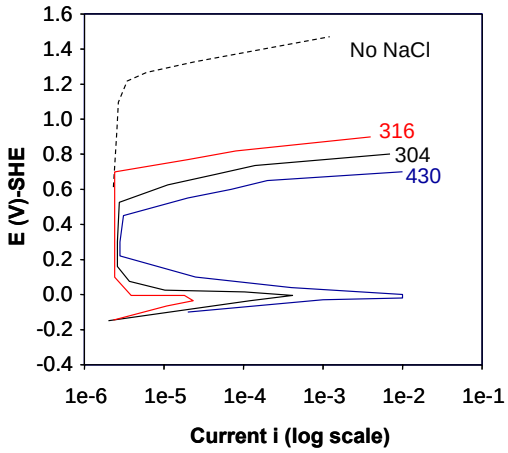

Figure A12. Effect of alloy composition on steel corrosion. Anodic polarization for Stainless Steels of various composition (316, 304, and 430) in 0.05 M H_2SO_4 and 0.01 M NaCl. The steel allow changes the corrosion in the active region, and influences the potential of the transpassive region, where pitting occurs. The dotted line shows the anodic polarization curve for all steels in the absence of NaCl. Based on data from Talbot and Talbot (1998).

Some dissolved soil constituents (e.g., phosphate) may react with corrosion products (e.g., Fe^{3+}) to form precipitates that are effective in slowing corrosion. Such approaches are commonly used to regulate the oxidation of buried metals and other oxidation sensitive materials (e.g., sulfide minerals). Additionally, the alloy of steel also influences the overpotential required for pitting (Fig. A12). In the case of carbon steels (the form of steel in most UXO), the overpotential required for transpassive corrosion is low, and thus they are commonly corroded through rapid pitting. Although the chemical conditions present in the soil may accelerate corrosion relative to the rate predicted for simple passivated metals, the extent and depth of pitting are difficult to quantify.

Pitting corrosion is especially pertinent for UXO and the soil solutions in which they are found. Stainless steels (although not all steels) are normally passivated under typical redox potentials. However, soil solutions contain apprecia-

ble solutes, which can influence the overpotential required for transpassive corrosion and induce pitting corrosion (Fig. A11). Such pitting may result in pinhole failures in the UXO, which may release small volumes of explosives contained within them. Pinholes also provide an additional avenue for corrosion (corrosion can then occur from within), thereby increasing the rate of catastrophic failure. Pitting also influences UXO integrity and strength, potentially destabilizing the UXO to mechanical breakdown.

Summary of UXO Corrosion Data

The mechanism of metal corrosion can have a profound impact on explosives ultimate release; however, little specific work has been done on the corrosion of UXOs in the environment. Here, we report theoretical and empirical (experimentally determined) corrosion rates for steel in soil. In general, we find that steel corrosion will eventually lead to the failure of UXOs and other munitions, with failure taking between 10 years for some thin-walled munitions in wetlands and other flooded environments, and up to a few hundred years for larger munitions in aerated environments. Pitting corrosion is much more rapid, potentially leading to failure 5 to 15 times more rapidly than the uniform corrosion rates stated above. There are many approximations in this work. The most significant approximation involves the use of a single corrosion rate for all soils and alloys. This is clearly not the case; UXOs are found in soils with a wide variety of water contents, salinities, compositions, and pH. While more research is needed to refine our understanding of UXO corrosion in environments such as firing ranges that are contaminated with UXOs, the rate estimation is justified in that most empirical corrosion rates are within a factor of 2 to 5 from this rate, and most of the alloys used in the production of UXOs are low carbon steel with similar corrosion characteristics. It should be noted that these corrosion rates are sufficiently slow that corrosion of UXOs in most soil environments is limited, primarily because of passivation. Exceptions arise when evaluating corrosion rates in marine environments and poorly aerated (flooded) soils, where corrosion may occur much more rapidly and lead to pitting. Previous studies on UXO corrosion have implied that corrosion in soils is slowed by passivation, and thus not a major concern (Bucci and Buckley 1998, AMEC, in review). While our results are not inconsistent with these findings, the presence of dissolved solutes and lower pH in some soils may prevent passivation and lead to considerably increased corrosion rates. Thus, site-specific evaluations of corrosion rates (or potential corrosion rates) should be performed prior to extrapolating to UXOs in all soil environments.

The observed reaction rates are sufficiently rapid that some fraction of the UXO are corroded sufficiently to release explosives and other contaminants into

soils and sediments. There are limited reports in the literature of the detection of organics associated with UXO failure, although the concentrations are typically small and it is difficult to know whether corrosion or physical damage to the munitions caused their release. A quantitative assessment of the number of failing UXO also is not possible given the uncertainty in UXO distribution, coverage, age, and dud rates (estimated at 1 to10%), each of which affects their number and corrosion characteristics. The physical condition of UXO in the field is also not well known; stresses applied to UXO during fabrication, launch, and impact are important as stresses can facilitate corrosion through metal activation. Furthermore, a quantitative estimate of the number of UXO buried in unusually corrosive (anaerobic and saline) environments is also poorly constrained. Thus, it is difficult to determine both the number of UXO, and their corrosion rate, particularly for corrosion in sensitive areas.

Many of the perforations in UXO are probably limited to relatively small holes formed as a result of pitting corrosion, but some small munitions, particularly in flooded soils and sediments with low hydrologic gradients, may also have failed through anaerobic corrosion induced by sulfate reducing bacteria. However, there are major questions about the extent to which these pinholes will release these toxins, and the interactions of these toxins with the corroding metals and soil microbial populations. One intriguing possibility is that the reactive intermediates formed during metal corrosion may facilitate the degradation of RDX, TNT, and other explosives during discharge from the UXO hull (Hundal et al. 1997, Scherer et al. 2000). More work also is warranted in this area, although the first-order questions of the characterization and distribution of UXO at a variety of different locations needs to be addressed before the effects of such secondary reactions can be quantified.

REPORT DOCUMENTATION PAGE

Form Approved
OMB No. 0704-0188

1. REPORT DATE *(DD-MM-YYYY)*	2. REPORT TYPE	3. DATES COVERED *(From - To)*
December 2004	Final Technical	2003-2004

4. TITLE AND SUBTITLE

Underground UXO: Are They a Significant Source of Explosives in Soil Compared to Low- and High-Order Detonations?

5a. CONTRACT NUMBER

5b. GRANT NUMBER

5c. PROGRAM ELEMENT NUMBER

6. AUTHOR(S)

Susan Taylor, James Lever, Michael Walsh, Marianne E. Walsh, Benjamin Bostick, and Bonnie Packer

5d. PROJECT NUMBER
T03-006

5e. TASK NUMBER

5f. WORK UNIT NUMBER

7. PERFORMING ORGANIZATION NAME(S) AND ADDRESS(ES)

Cold Regions Research and Engineering Laboratory
U.S. Army Engineer Research and Development Center
72 Lyme Road
Hanover, NH 03755

8. PERFORMING ORGANIZATION REPORT NUMBER

ERDC/CRREL TR-04-23

9. SPONSORING / MONITORING AGENCY NAME(S) AND ADDRESS(ES)

USAEC
ATTN: SFIM-AEC-PCT
Aberdeen Proving Ground, MD 20101-540

10. SPONSOR/MONITOR'S ACRONYM(S)

USAEC

11. SPONSOR/MONITOR'S REPORT NUMBER(S)

SFIM-AEC-AT-CR-2004022

12. DISTRIBUTION / AVAILABILITY STATEMENT

Approved for public release; distribution is unlimited

13. SUPPLEMENTARY NOTES

Project participants/contributors included: Dartmouth College and AEC

14. ABSTRACT

Are the amounts of explosives leaking from UXO significant compared to other sources? To answer this question we compiled data on the contamination released by above ground detonations of different order and by the rupture or corrosion of UXO. The results indicate that low-order detonations, be they from malfunctioning munitions or sympathetic detonations, are currently the largest contributors to range contamination. Also, dissolution of the explosive charge from heavily corroded UXO is significant and will increase in importance with time. Unfortunately, only order-of-magnitude estimates are possible due to shortage of data on the actual fates experienced by different types of munitions. However, the framework used here for compiling and ranking the explosive sources canhelp guide policy-making and future research activity to reduce range contamination.

15. SUBJECT TERMS

Corrosion
Explosives transport
Low-order detonations
Munition fate
UXO (Unexploded Ordnance)

16. SECURITY CLASSIFICATION OF:			17. LIMITATION OF ABSTRACT	18. NUMBER OF PAGES	19a. NAME OF RESPONSIBLE PERSON
a. REPORT	b. ABSTRACT	c. THIS PAGE			19b. TELEPHONE NUMBER *(include area code)*
U	U	U	U	129	

DEPARTMENT OF THE ARMY
ENGINEER RESEARCH AND DEVELOPMENT CENTER, CORPS OF ENGINEERS
COLD REGIONS RESEARCH AND ENGINEERING LABORATORY
72 LYME ROAD
HANOVER, NEW HAMPSHIRE 03755-1290

REPLY TO
ATTENTION OF

Lisa Hoffmeister
Librarian
ERDC
72 Lyme Rd
Hanover NH 03755-1290

March 3, 2015

Defense Technical Information Center
8725 John J. Kingman Rd
Fort Belvoir VA 22060-6218

To Whom It May Concern:
It has come to my attention that one of our reports in your database has the wrong distribution statement. The report, "Underground UXO: are they a significant source of explosives in soil compared to low-and high-order detonations?", by Susan Taylor, et al. has the distribution as "authorized to the Department of Defense and US DoD contractors..." (ADB308065). This report should be approved for public release; distribution unlimited. An electronic copy of the unlimited report can be found at http://acwc.sdp.sirsi.net/client/search/asset/1005360 . Please let me know if you have any questions. Thank you.

Sincerely,

Lisa Hoffmeister

Lisa Hoffmeister
Elizabeth.r.hoffmeister@usace.army.mil
603-646-4338